The Development of Novel Surface Modifications for use in a Skeletal Regeneration System

Thesis submitted in accordance with the requirements of the University of Liverpool for the degree of Doctor in Philosophy by

Sandra Fawcett

September 2013

Acknowledgements

I would like to thank my supervisors:
Prof. John Hunt, for allowing me to pursue this PhD and being sufficiently tough on me to make me able to achieve my goal.
Dr Judith Curran for everything from day to day supervision and confocal microscopy to shopping trips!
Dr Nick Rhodes for our last minute meetings and guidance with my write up, and interesting chats. Their help, support and guidance, during this work has been essential and I really can't express my gratitude.

I would like to thank Prof. Gallagher, and his team Jane, Pete and Craig for allowing me to use their laboratory and sourcing some primary tissue for cell isolation. Thanks!

I would like to thank my collaborators Dr.Lloyd Hammilton, and Prof.Kevin Shakeshef and Prof. Alexander Morgan for all the help regarding the plasma modifications and injectable system.

I also need to thank Dr Mark Murphey for help with AFM.

I have a lot of people to thank, my friends from clinical engineering past and present, Katie, Fiona, Shirl, Lyndsey, Nick, Theun, Mick, Rui, Fanrong....thanks for being encouraging and wonderful people to work with. This whole thing was so much more fun because of you all.

I would also like to thank my new colleges in Clinical and Molecular Pharmacology.

To my emergency support team (Mum, Dad, Jenny and Bill) for being there to offer love support and emergency child care!

To the people who I did this for (and who I couldn't have possibly have done this without), Stephen, for everything that you have done, so that I could do this, all the support, love and encouragement I can't even begin to thank you for, supporting me through not just the last four years but since we met and finally this is for this my amazing wonderful fabulous boys, Dylan and George who's pride in their Mum made me continue when things got difficult.

Contents

Chapter 1 Introduction

Chapter 2 Methods and Materials

Chapter 3 Plasma Modification Results

Chapter 4 Silane Modifications on Glass Substrate

Chapter 5 Results: Mesenchymal Stem Cell Response to the Silane Modification of PLGA Films and Injectable 3D System

Chapter 6 Summary Discussion and further work

Chapter 7 Conclusion

List of Figures

3.6 LDH assay analysis of cell number on modified scaffolds. Scaffolds were seeded with MSC for 14 and 28 days, and an LDH assay was conducted on the modified and untreated scaffolds after maceration at these timepoints

3.7 :Histological analysis of allyl amine-treated scaffolds. Scaffolds were cultured with MSCs for 28 days, histologically processed and stained with (a) Von Kossa for mineralization, (b) Alizarin red for mineralization, (c) Van Geison for collagen, (d)H and E for cellular morphology and density and (e)Alcian blue for gylosaminoglycan

3.8 Histological analysis of hexane-treated scaffolds. Scaffolds were cultured with MSCs for 28 days, histologically processed and stained with (a) Von Kossa for mineralization, (b) Alizarin red for mineralization, (c) Van Geison for collagen, (d)H and E for cellular morphology and density and (e)Alcian blue for gylosaminoglycan3.9 Histological analysis of acrylic acid-treated scaffolds. Scaffolds were cultured with MSCs for 28 days, histologically processed and stained with (a) Von Kossa for mineralization, (b) Alizarin red for mineralization, (c) Van Geison for collagen, (d)H and E for cellular morphology and density and (e)Alcian blue for gylosaminoglycan

3.10 : Histological analysis of allyl alcohol-treated scaffolds. Scaffolds were cultured with MSCs for 28 days, histologically processed and stained with (a) Von Kossa for mineralization, (b) Alizarin red for mineralization, (c) Van Geison for collagen, (d)H and E for cellular morphology and density and (e)Alcian blue for gylosaminoglycan

3.11 Histological analysis of untreated scaffolds. Scaffolds were cultured with MSCs for 28 days, histologically processed and stained with (a) Von Kossa for mineralization, (b) Alizarin red for mineralization, (c) Van Geison for collagen, (d)H and E for cellular morphology and density and (e)Alcian blue for gylosaminoglycan3.12Images from dual and triple scaffold modifications. Allyl amine and allyl alcohol modified spheres were compacted in two layers of the same

scaffold (dual modification) and allyl amine, hexane and allyl alcohol were compacted into three layers of the same scaffold (triple modification). The scaffolds were processed and stained using alizian red and alcian blue. (a)Alcian blue stain of triple modification scaffold, (b) Alizian red of triple modification scaffold, (c) Alcian blue of dual modification, (d) Alizarin red of dual modification, (e) Alizarin red stain of single allyl amine modified scaffold, (f) Alcian blue stain of single allyl amine modified scaffold, (g) Alizarin red of single allyl alcohol modified scaffold, and (h) Alcian blue single modification allyl alcohol scaffold

4.1.1 AFM micrograph of untreated borosilicate glass. 12mm diameter glass coverslips were cleaned as stated in protocol. AFM images taken from 5 areas per sample, representative image shown

4.1.2 AFM image of borosilicate glass treated with CL3. 12mm diameter glass coverslips were cleaned as stated in protocol, and modified using oxygen plasma, then the CL3 silane. AFM images taken from 5 areas per sample, representative image shown

4.1.3 AFM micrograph or borosilicate glass treated with CL4. 12mm diameter glass coverslips were cleaned as stated in protocol, and modified using oxygen plasma, then the CL4 silane. AFM images taken from 5 areas per sample, representative image shown4.1.4 AFM micrograph of borosilicate glass treated with CL6. 12mm diameter glass coverslips were cleaned as stated in protocol, and modified using oxygen plasma, then the CL6 silane. AFM images taken from 5 areas per sample, representative image shown

on silane modified glass for 7 days and stained with collagen I, DAPI and Oregeon green. Blue staining shows nuclei, green staining shows actin filaments and red staining shows presence of collagen I (a)untreated control, (b) CL3 (c) CL4, (d) CL6, (e) CL7 and (f)

4.22 Immunostaining of MSCs cultured on modified glass at 7 days. MSC were cultured on silane modified glass for 7 days and stained with osteocalcin, DAPI and Oregeon green. Blue staining shows nuclei, green staining shows actin filaments and red staining shows presence of osteocalcin (a)untreated control, (b) CL3 (c) CL4, (d) CL6, (e) CL7 and (f) CL11

4.23 Osteoblast-like cells cultured on silane modified glass for 7 days. Osteoblast like cells were cultured on the silane modified glass (and an untreated control) for 7 days, then stained with Von Kossa's stain for mineralisation (a) untreated glass control, (b) CL3, (c) CL4, (d) CL6, (e) CL7 and (f) CL114.24 , Osteoblast-like cells cultured on silane modified glass for 14 days. Osteoblast like cells were cultured on the silane modified glass (and an untreated control) for 14 days, then stained with Von Kossa's stain for mineralisation (a) untreated glass control, (b) CL3, (c) CL4, (d) CL6, (e) CL7 and (f) CL114.25 25 Osteoblast-like cells cultured on silane modified glass for 28 days. Osteoblast like cells were cultured on the silane modified glass (and an untreated control) for 28 days, then stained with Von Kossa's stain for mineralisation (a) untreated glass control, (b) CL3, (c) CL4, (d) CL6, (e) CL7 and (f) CL11

4.26 Quantity of nodules formed on the modified surfaces. The nodules were counted using a light microscope. (N=16) Seris 1,2 and 3 correspond to 7, 14 and 28 days, results show avage and error bars show standards deviation from the mean

4.27 Size of nodules on the modified surfaces Nodules on surfaces treated with CL3 and CL4 were measured after after 7,14 and 28 days results show avage and error bars show standards deviation from the mean

4.28 SEM micrographs of Osteoblast-like cells cultured on silane modified glass after 7 days incubation. Osteoblast –like cells were isolated from human trabecular bone and seeded onto the silane modified surfaces. (a) untreated glass, (b) CL3, (c) CL4, (d) CL6 , (e) CL7 and (f) CL11. White arrows indicate nodules, green arrow indicates production of ECM on CL11 and red arrow shows very rounded cells on CL6 modification

4.29 SEM micrographs of Osteoblast-like cells cultured on silane modified glass after 14 days incubation. Osteoblast –like cells were isolated from human trabecular bone and seeded onto the silane modified surfaces. (a) untreated glass, (b) CL3, (c) CL4, (d) CL6 , (e) CL7 and (f) CL11. White arrows indicate nodules, green arrow indicates production of ECM on CL11 and red arrow shows very rounded cells on CL6 modification 4.30 , SEM micrographs of Osteoblast-like cells cultured on silane modified glass after 28days incubation. Osteoblast – like cells were isolated from human trabecular bone and seeded onto the silane modified surfaces. (a) untreated glass, (b) CL3, (c) CL4, (d) CL6 , (e) CL7 and (f) CL11. White arrows indicate nodules, green arrow indicates production of ECM on CL11 and red arrow shows very rounded cells on CL6 modification

4.31 SEM micrographs of Osteoblast-like cells cultured on silane modified glass after 7 days incubation. Osteoblast –like cells were isolated from human trabecular bone and seeded onto the silane modified surfaces Image taken from surface of nodule formed at 7 days incubation on CL3. White arrows highlight the fiberous nature of the matrix, and green arrows show areas of smooth mineralisation

4.32 SEM micrographs of Osteoblast-like cells cultured on silane modified glass after 7 days incubation. Osteoblast –like cells were isolated from human trabecular bone and seeded onto the silane modified surfaces. High magnification image of cells after 7 days incubation on CL11. Highlighting the output of matrix by the cells, while cells remain in monolayer

4.33 Expression of osteopontin in human osteoblast like cells after 7, 14 and 28 day incubation with silane modified glass. Osteoblast like cells were isolated from human trabecular bone and processed for rtPCR. Expression of osteopontin was measured and normalised to expression of B-Actin and unmodified scaffold. Data shown is average expression and standard deviation from mean. *=p<0.10, **=p<0.05, ***=p=<0.01

4.34 Expression of osteocalcin in human osteoblast like cells after 7, 14 and 28 day incubation with silane modified glass. Osteoblast like cells were isolated from human trabecular bone and processed for rtPCR. Expression of osteopontin was measured and normalised to expression of B-Actin and unmodified scaffold. Data shown is average expression and standard deviation from mean. *=p<0.10, **=p<0.05, ***=p=<0.01

4.35 Expression of osteonectin in human osteoblast like cells after 7, 14 and 28 day incubation with silane modified glass. Osteoblast like cells were isolated from human trabecular bone and processed for rtPCR. Expression of osteopontin was measured and normalised to expression of B-Actin and unmodified scaffold. Data shown is average expression and standard deviation from mean. *=p<0.10, **=p<0.05, ***=p=<0.01

4.36 Expression of collagen I in human osteoblast like cells after 7, 14 and 28 day incubation with silane modified glass. Osteoblast like cells were isolated from human trabecular bone and processed for rtPCR. Expression of osteopontin was measured and normalised to expression of B-Actin and unmodified scaffold. Data shown is average expression and standard deviation from mean. *=p<0.10, **=p<0.05, ***=p=<0.01

4.37 Expression of CBFA1 in human osteoblast like cells after 7, 14 and 28 day incubation with silane modified glass. Osteoblast like cells were isolated from human trabecular bone and processed for rtPCR. Expression of osteopontin was measured and normalised to expression of B-Actin and unmodified scaffold. Data shown is average expression and standard deviation from mean. *=p<0.10, **=p<0.05, ***=p=<0.01

List of tables

Abstract

Non-union fractures are defined as fractures that do not heal after 6 months of conventional treatment. They usually require multiple surgical treatments, autologous bone grafts or treatments with growth factors or Bone morphogenetic proteins (BMPs). There is a clinical need for a material which can be used to replace autologous bone transplantation in the treatment non-union fractures that negates the problems associated with autologous grafts.

This thesis aims to consider and develop a coating that can be used on a readily available polymer biomaterial to induce a response from mesenchymal stem cells, which are found in abundance at fracture sites, and facilitate repair by their differentiation into osteogenic cells. The use of a synthetic chemical coating rather than a growth factor or peptide aims to cause similar effects at a greatly reduced cost

Plasma application techniques were used initially to screen potential terminal groups on a 3D system. Amine groups were found to be osteogenic (which was confirmed by positive Von Kossa and Alizarin red staining), and hydroxyl groups were found to be chondrocytic (which was confirmed by positive Van Geison and Alcian blue staining). The osteogenic effect of the amine group was investigated further, but in the form of silane SAMs, which were more easily definable. The presentation of the terminal group was investigated using varying carbon chain length, to see if this had an effect on osteogenicity) This was explored using both MSC and primary osteoblast-like cell models on glass initially, then on PLGA films and finally a 3D PLGA system.

The results of this showed positive expression of osteogenic markers for the MSC and osteoblast-like cells when on glass and PLGA films. There was an expression of the osteogenic marker osteocalcin and a positive mineralisation stain (Von Kossa) at 7 days. This effect however was not transferred to a 3D platform as further optimisation will be required to achieve this goal-an essential progression on the way to the development of an injectable 3D system suitable for clinical application.

Chapter 1:Introduction, Literature Review and Hypothesis

1.1 The Principles of Regenerative Medicine

The primary purpose of regenerative medicine is to provide strategies to replace tissue when injury, disease or congenital defect causes it to be missing[1]. This is becoming more and more important. Therapies that enable people to retain their healthy bodies beyond what is experienced today, in this changing economic climate with an aging population, will become more relevant.

The natural response to injury, depending on the location, is to fill the space created by degraded tissue with scar/fibrous tissue. This often has insufficient mechanical and functional properties to provide the full functionality of the tissue lost and can lead to severe complications. The core principle of regenerative medicine is to guide the healing process using a range of signals to improve the quality of the repair, achieving more natural tissue faster, hence providing improved functionality more quickly. This principle in its broadest sense can be applied to any aspect of regenerative medicine, but for the purposes of this thesis, the issues surrounding skeletal regeneration will be the main focus.

1.2 Bone Fracture

Most uncomplicated bone fractures will heal after 3-4 months of conventional treatment. There is a little variation depending on the site of the fracture, but as a general rule, this is considered to be correct. Clinicians will use X-rays to determine the normal physiological anatomy of the bone has been restored. There are also a few physiological tests that are carried out to determine if a fracture has healed sufficiently and these are the absence

of pain with movement, and ability to bear weight. When the normal pathway of treatment is not effective, the fracture is defined as being non-union[2].

1.3 Non Union Bone Fracture

A non-union bone fracture is defined as a bone injury that fails to heal after six months - when conventional treatments have been applied, or a fracture that has shown no progression of healing for 3 months[2]. There is some debate about this figure as some delayed unions can occur after the 6 month period has passed, particularly if there have been complications such as infection in the site, but as a general rule, the 6 month period is the guideline most clinicians use[2]. The repercussions of non-union bone fractures for the patient can be impaired function and skeletal deformity. It is expensive to treat, and often causes the patient to have numerous surgical procedures[3]. The root cause of why some patients experience this failure to heal is not well documented, however there are some indications in the literature that the initial cellular response is considerably different in patients suffering from non-union fractures[4].

Webber defined two types of non-union fracture, depending on the viability of the fragments of bone present. The first classification is called the hyper-vascular or hypertrophic non-union. In this presentation of the non-union fracture, the bone ends are still biologically active and have a functioning blood supply. A light callus forms because there is slight movement in the joint around the fracture site, which is not detectable until the patient is in surgery, but the callus prevents the fracture ends from joining. It is a well-established fact that the bone ends need to be totally immobilised to fully join, and even slight motion can be responsible for non-union fracture. Hyper-vascular non-union fractures have been defined as taking three different presentations. The first presentation is the “elephant foot” morphology, which is named because the ends of the bone are covered with a highly vascular

callus that broadens at the fracture site. The reason for this presentation varies, but can be linked to poor fixation, the join being too mobile, or due to premature loading of weight, which can lead to peudoarthrosis. The second presentation contains less callus and is named, "horses foot" which is less hypertrophic. This presentation is more common if the fixation of the bone has been slightly unstable and is more likely to spontaneously join, as the callus forms and stabilises the fracture. The third presentation is oligotrophic, and contains no callus and is referred to as a lax non-union fracture[2].

The second classification is avascular non-union bone fracture. In this class the bone fractures are avascular or atrophic and not able to form callus. These are the more problematic fractures as they show no changes over long periods of time, and require sustained surgical intervention as immobilisation will not allow the bone ends to heal as they are no longer vital. Avascular non-union is defined by one of four presentations. The torsion wedge non-union is defined as a fragment of non-viable bone which has fused onto one of the viable ends. The comminuted non-union occurs if the fragments are necrotic. Defect non-unions occur if a piece of the bone has been lost, during an accident, or because of infection. In these cases the ends can still be viable but the distance between them is too large to bridge, and because of this the ends become atrophic. Lastly there are the atrophic non-unions, which usually start out as one of the other classifications and are the end point of the non-union[2].

If left untreated the medullary canals become blocked, and the bone ends become joined by fibrous tissue. Pseudoarthrosis can form, which takes either a stiff or lax form. Treatments for this condition vary from compression[5] and distraction, to dissection and the grafting of new autologous bone[6]. This is a long and complicated process, and there is a significant clinical need for a system that can be used to treat it without the need for the use

of autologous tissue. One possible solution is the application of a material to support stem cell growth and differentiation. Increasing and enhancing the healing process between the non-union ends of the bone, with an aim to regenerate functional and calcified bone in the void rather than fibrous tissue that can lead to pseudoarthrosis.

1.4 Normal Bone Healing Pathway

The sequence of events after a bone fracture has occurred starts with the formation of a haematoma. Injury incurred to the vascular system causes the clotting cascade to be stimulated and haematoma formation. The haematoma contains large volumes of platelets and releases cellular signals. Inflammation is initiated with an increase in localised blood flow and permeability of the blood vessels. There is a migration of leukocytes to the injury site stimulates more cytokines to be released, recruiting mesenchymal stem cells (MSC) to the site of injury. MSC proliferate and differentiate into osteoblast-like cells and there is increased angiogenisis. Ossification then occurs, where the osteoblasts start to lay down a collagen network, which then ossifies to form a callus capable of bridging the gap between bone ends. At this point the callus is named lamellar bone. The last phase is remodelling which is orchestrated by osteoclasts and results in the woven bone formation, which has better mechanical properties than lamellar bone[7].

There are four major populations of cells responsible for the regeneration of bone:

- Osteoblasts, which have a regenerative role, and originate from MSC and are the main producers of the extracellular matrix that comprises bone.

- Osteoclasts, which are the enzyme producing cells that can dissolve collagens and are the key to bone remodelling, originate from the haemopoteitic stem cell fraction of bone marrow.
- Osteocytes, which are differentiated osteoblasts, and have a less productive and more regulatory role.
- Bone lining cells, which are osteocytes which are not embedded in the bone matrix, line the bone surface, remaining inactive until they are stimulated to change[8].

During fracture healing the role of MSC is vitally important. They are the essential player in the bone regeneration process, and it has been shown that the bone morphogenetic proteins (BMPs) play key roles in mesenchymal stem cell recruitment in vivo[9]. There is also some evidence to suggest that stromal cell derived factor -1 (SDF-1) plays a role in regulating the recruitment of MSC to the site where they are required[9].

1.5 The Formation of a Cartilaginous Callus

The formation of a cartilaginous callus is the result of initial stem cell differentiation, which later will be mineralised and remodelled. This cartilaginous callus is the blueprint for the formation of bone, and provides many of the raw materials required. The ossification of the callus occurs at the bone ends before it bridges into the central portion of the callus. This causes the initial stabilisation phase.

On a molecular level, it is at this point collagen I and II are produced in abundance, and the transforming growth factor beta (TGF-B) peptides are involved in endochondral ossification. The BMPs are also involved in the ossification process[10]. The vascularisation of the site is a necessity if the callus is to lead to full bone repair. There is a fine balance required to instigate the required angiogenesis, alongside the removal of cartilaginous tissue

to make way for it. Vascular endothelial growth factor (VEGF) plays a principle role in the angiogenesis of the fracture site.

After angiogenesis has occurred the cartilaginous callus should be resorbed and replaced by a bony callus which has greater mechanical properties. The number of cells in the bone fracture site increases as they are switched into a proliferative state, allowing more extracellular matrix to be produced. The Wnt family of molecules is likely to be key facilitators in this in the differentiation of MSCs to osteoblasts, which is required for this step in fracture healing to occur. Chondrocytes from the callus proliferate quickly during this phase of the healing process and can become hypertrophic which can lead to the extracellular matrix becoming calcified. When this occurs there is a cascade of inflammatory cytokines including macrophage-colony stimulating factor (M-CSF), receptor activator of nulear factor kappa B ligand (RANKL) osteoprotegrin (OPG) and tissue necrosis factor alpha (TNFa). This cascade allows the recruitment of more osteoblasts and osteoclasts which promotes chondrocyte apoptosis. Calcium accumulates in the mitochondria of the chondrocytes in this hypoxic environment. Calcium is transported though the cytoplasm and is deposited in the extracellular matrix (ECM), where they can precipitate with phosphate and start the mineralisation process. These initial deposits nucleate and form apatite crystals, which are carried to the nucleation point in microvesicles[11], forming the hard callus. As the calcified cartilage is mineralised it becomes woven bone[9]. The growth factors that are responsible for this phase of osteoblastic activity have been studied extensively and it has been determined that there is a balance required of several growth factors including transforming growth factors (TGF-B1, TGF-B2 and TGF-B), vitamin D and fibroblast growth factor (FGF-2) which are key players in maintaining osteoblast function and establishing a mineralisation pathway. None of these factors in isolation can cause mineralisation from osteoblasts[12].

The next phase is the remodelling of the woven bone so that it can become lamellar bone with a medullary cavity. Again, the inflammatory cytokines interleukin 1(IL-1) and tumour necrosis factor alpha (TNF alpha) have a role to play in the second reabsorption phase. The BMPs also have roles to play in this phase, especially bone morphogenetic protein 2 (BMP-2). During this phase it is the role of osteoclasts to reabsorb the woven bone, and the job of the osteoblasts to extrude correctly structured lamellar bone. This is a process which can take years to be fully achieved, and requires specific environmental conditions, creating an inductive electrical polarity, by the correct amount of pressure being loaded onto the micro-crystalline environment.

1.6 The *in vivo* Osteogenic Differentiation Pathway of Mesenchymal Stem Cells

Bone formation is a complex morphological process that results in complete differentiation of MSCs, at a temporally correct point within a constantly fluxing system, and at the correct location.

Multiple local and systemic factors play a role in this differentiation. The local factors that instigate and maintain osteogenic differentiation of MSCs include transforming growth factor beta (TGF-B), core binding factor alpha-1 (CBFA-1), alkaline phosphtase (ALP), collagen I, osteopontin (OP), osteonectin (ON), bone sialoprotein (BSP), apoptosis mediating surface antigen (Fas), the interleukins (IL), and the apoptosis regulating Bd-2-associated X protein (BAX). These local factors however do not work in isolation and there are also some systemic factors that stimulate the osteogenic response, including parathyroid hormone, vitamin D, leptin, calcitonin, somatotropin, thyroxine, estrogens, androgens and glucocorticoids. All of these factors play their part in the mesenchymal response in vivo, and

help to support the pathway of the MSC, to pre-osteoblast, to mature osteoblast and all the mineralisation phases, and ultimately to apoptosis or maturation into osteocyte morphology[13].

To highlight just a few of these factors in a little more detail, the role of CBFA-1 is vital to the osteogenic process, and is considered a key marker of osteogenesis. It is a member of the runt-related transcription factor (RUNX) family of transcription factors, and has demonstrated an important regulatory role where it stimulates the up-regulation of osteoblast genes such as osteocalcin. It could be described as the corner pin of the osteogenic response and this is one reason why this marker is used so frequently as a marker of osteogenesis[14],[15]. Caution should be taken however when using CBFA-1 as a marker of the osteogenic differentiation of MSCs, as it is a transcription factor, and will only be present in the early phases of differentiation, for short periods of time, so it is not a marker that could be used alone, but would add weight to a panel of markers for osteogenesis.

Osteonectin is expressed in pre-osserous cells, as well as osteoblasts and is one of the first indicators of osteogenic differentiation. However is is not specific to osteogenic differentiation as it can also be expressed by cells undergoing a chondrogenic lineage differentiation[16]. Osteopontin is expressed during the mineralisation process, and is only present when mineralisation is occurring. It has been shown to be present in cells found adjacent to mineralised matrix[16]. Osteocalcin is a marker of bone metabolism, and has been used extensively as a marker of new bone formation[17]. It could be described as a bone-specific protein which consists of a sequence 49 amino acids[18]. Osteocalcin is only secreted by osteoblasts that have been in contact with an established mineralised matrix and so is a very specific marker of functioning cells.

The TGF B super-family contains all the BMPs and are involved in many regenerative and developmental processes, not just bone regeneration. BMP 2 is specific to

bone regeneration, as is BMP 7[10]. TGF-beta itself has been shown to increase bone formation *in vitro*, by allowing osteoblasts to expand in culture more readily, but seems to retard the mineralisation effect[12].

1.7 Current Therapy for Bone Loss in Non Union Fracture

Autologous bone grafts are the gold standard for the treatment of non- union bone fractures. There are many reasons why autologous bone grafts are the treatment of choice. The bone harvested can be classified as osteoinductive, as it contains viable MSCs and osteoblasts in addition to the molecules that are necessary to induce undifferentiated cells along an osteogenic lineage, such as BMPs and members of the TGF B super family. It can also be classified as osteoconductive, because its structure (particularly if it is cancellous bone), will allow the in-growth of cells from the adjacent bone ends of the fracture site. All the factors required to achieve a repair are present, because the bone taken from a donor site in the patient's body is ideally suited for the purpose of filling a non-union fracture void[19]. The type of bone harvested does influence the success and the mechanical stability of the repair. Cancellous bone, as described above has lots of properties that influence and bring about a good repair, but initially it has no mechanical strength, and it takes approximately 12 months for the repair to be as mechanically sound as normal bone. Conversely, cortical bone has better mechanical properties but because of its dense structure, is less effective at delivering the appropriate factors to the site[19]. But, removing bone from another area of the patient's body to use in the fracture site is not always possible, depending on the size of the defect, can cause further complications.

Donor site morbidity is a serious problem, and the use of the fibula as a harvesting site can lead to pain, muscle weakness, nerve damage, infection, stress fractures and joint instability. It is thought that up to 57.7% of patients experience some of these complications[20]. Short term complications such as muscle weakness, do improve over a short period of time, but pain can last in excess of 12 months in some patients[20]. The quality of the autologous bone graft also reduces with the age of the patient[21].

Bone marrow aspirates are used to treat non-union fractures in some instances, where relatively large quantities of bone marrow are used and where stem cells are added back into the site. There are several problems associated with this technique, one being that there is no means of keeping the cells in the intended location if no scaffold is used. The quantity of bone marrow required to do this procedure could cause other complications[20].

Allografts are the next option for treatment after the other possibilities have been explored. Allografts use de-cellularized bone from human cadavers or live donors. They are less effective than autografts as the processing used to make them safe to use in other patients, strip them of many of the factors that make the graft osteoinductive, and mean that only their osteoconductive properties remain, loosing many of the osteogenic properties[20]. Complications from using donor tissue like this include transmission of viruses, including very rarely human immunodeficiency virus (HIV). Bacterial infection is also more likely, with some reports suggesting that these rates are as high as 12.8%, but this is variable in the literature[20],[21].

The use of bone morphogenetic proteins (BMPs) as a therapy greatly increases the healing potential of non-union fractures[22], as an overview of the studies conducted into the use of BMPs states that success rate in patients who were treated for pseudoarthrosis was around 75%. This still does not quite meet the 84% success rate of autologous bone, but was

seen to be a good substitute[21],[22]. Initially it was thought that BMP2 was completely safe for human use, as initial studies undertaken in 2002 showed no complications arising from its use for bone regeneration. This, however, was not the case and initial studies have been discredited. Later studies, when rhBMP2 was in general use in several countries, found that there were severe complications, including overgrowth of bone, osteoclast stimulation and activity leading to graft failure, local wound problems, including inflammation, neurological complications and carcinogenic properties[23]. Treatment using BMP 7 seems to be showing some promise to date[24].

There are incidences where a synthetic bone regeneration system, which has osteoinductive, osteoconductive and osteogenic potential and is close to the gold standard of autologous bone, would be clinically-relevant and aid the recovery of patients with severe and often life-threatening injury. The direction of the work undertaken in this thesis is influenced heavily by this aim.

1.8 Synthetic Bone Grafts

Of the synthetic bone grafts, the ceramic-based materials are the most commonly used. Hydroxyapatite and B-tricalcium phosphate are the most common of this subset. There are a few advantages to these materials over allogeneic bone, as there is no risk of virus transmittance, and they have a very long shelf life. They are osteoconductive but not osteoinductive when used in their unmodified states[21]. To fully integrate they are reliant on bone in-growth, and need to be stable under physiological conditions to last long enough for this to occur. One disadvantage of hydroxyapatite is that there is no reabsorption by osteoclasts, unlike allografts, which are eventually reabsorbed. Conversely, the material will be *in situ* long enough to be integrated by the in-growth of bone if the porous structure of the scaffold is sufficient.

1.9 The Ideal Bone Biomaterial

The ideal bone biomaterial would have all of the properties of an autologous graft. It would have the capability to be osteoconductive, osteoinductive and osteogenic. It would be osteoconductive to allow full integration with the host skeletal tissue, it would be osteoinductive to the cells that migrate into the material from the host, but ideally it would also be osteogenic as it could be used as a carrier or delivery system for the patient's own therapeutic MSC. The material would have mechanical properties similar to the tissue it intends to replace and, ideally if used in conjunction with cells, be degradable at the same rate as cells can mineralise the scaffold. If this was incorporated into an easy to use injectable system that could bridge gaps of any shape or size it would be both clinically useful, and remove the requirement for autologous bone harvesting, thus improving the health of the patient.

During this work, we have taken an injectable polymer system which already has osteoconductive properties, and mechanical strength similar to trabecular bone, and changed its surface chemistry to boost its osteoinductive properties, while testing its osteogenic potential using an *in vitro* MSC model.

1.10 Mesenchymal Stem Cells (MSCs)

It has already been stated that MSCs play a crucial role in the normal healing pathway of bone fracture injuries. Undifferentiated stem cells migrate to the area where they are required and are stimulated by BMPs and regulatory cytokines to proliferate and differentiate into chondrocytes and osteoblasts, allowing osteogenic regeneration to occur[25]. Much of the

current bone regeneration research has concentrated on using BMPs in their various forms to stimulate this natural healing response[26]. Mimicking and enhancing this response should lead to a successful therapy. This is one of the reasons why adult MSCs are ideal candidates for autologous bone regeneration.

There are multiple sources of MSCs within the body[27]. Most tissues contain their own source of cells, but their potency and their niche varies between tissues. It is the current opinion that a stem cell isolated from adipose tissue will not be capable of achieving the same fate as a stem cell derived from blood. While there may be a small degree of overlap, there is a fundamental difference in their differentiation capability. Bone marrow derived MSCs are considered to be more potent than stem cells derived from other adult tissues[25]. There are two populations of stem cells found in the bone marrow, these are MSCs and hematopoietic stem cells. Hematopoietic stem cells have a very specific niche where they produce blood cells and osteoclasts. Hematopoietic stem cells are unlikely to be used as a cell for bone regeneration which is regulated by the osteoblastic lineage. However, bone marrow derived MSCs are likely to be very useful for this task.

It is currently considered that bone marrow derived mesenchymal stem cells (BM-MSCs) are pluripotent, rather than multipotent[28] as they can, and have been stimulated to differentiate into cells that derive from each of the germ layersfor example they can be pushed down osteogenic and chondrogenic [29] pathways from the mesoderm, neurons which originate from the ectoderm [30], and pancreatic cells and hepatocytes from the endoderm[31,28].

BM-MSCs are ideal for any osteogenic lineage induction as this cell type plays a role in the healing response of bone *in vivo*. It is well documented that this cell type has the potential to be used in bone regeneration therapies, under the correct conditions[32],[33]. These cells are donor specific, ideally cells can be taken from bone marrow aspirates and cultured to

increase cell number until enough of the patients own cells are available to perform a regeneration procedure. Another advantage is the isolation techniques are relatively simple, and exploit the cells inherent ability to adhere to plastic when cultured. The bone marrow aspirate, usually taken from the iliac crest, is first subjected to sorting of nucleated cells from other material via a density gradient. Then the nucleated cells are cultured for 24 hours in an appropriate media, and all non-adherent material is removed[34].

The lack of standardization in the initial isolation, characterisation of the cell population, and culture methodology can be problematic. There is variation between techniques used to isolate and culture MSCs, and these subtle variations could be responsible for some of the conflicting results seen in some studies. It is for this reason it is often unreliable to compare results obtained from different research groups, and it could explain some of the discrepancies seen[35]. Therefore there is a need for standardization of isolation protocols, characterization of resultant cell populations and expansion techniques.

There is patient variability in these cells and often the age and general health of the patient can affect how these cells proliferate *in vitro*. Any work undertaken with primary MSCs should consider donor variation[36]. There was considerable donor variation demonstrated by Zhukareva *et al*[36], when MSC response to pro-inflammatory cytokines was measured using a panel of markers. This study exemplifies how the patients' cells will behave differently when exposed to exogenous stimuli. This however, does not detract from the positive aspects of adult human MSCs, but must be considered when any research involving these cells is undertaken in respect of the number of repeats necessary to validate a given response[36].

One of the most remarkable advantages of using MSCs relates to their immunological profile and how they can be classed as non-immunogenic. They are essentially

immunologically privileged because they express major histocompatibility complex I (MHC I) but not major histocompatibility complex II (MHC II). They do not express the cluster of differentiation antigens (CD antigens) CD40, CD80 or CD86 which stimulate an immune response. These cells will evade the immune system of the host, and there is some evidence to suggest that the MSCs can suppress T cell proliferation[37].

1.11 The Identification and Profile of Mesenchymal Stem Cells

The definition of the BM-MSC has been problematic. The answer to that issue is not simple, because the defining feature of a stem cell is that it has the potential to change into any number of other cells, all of which will present markers the BM-MSC may also present. A panel of positive and negative markers is therefore the way they are defined, and should be defined periodically throughout the lifespan of the culture. This brings together a profile of the cell that a potential BM-MSC has to meet. Positive markers of BM-MSCs include CD73, CD90, CD105. BM-MSCs should also be CD34, CD45, CD14 or CD11b, CD79 or CD19 and HLA-DR negative. The minimum number of cells expressing CD73, CD105 and CD90 in a population should be 95%. The maximum number of cells expressing the negative markers should be 2%[38]. If this profile is used universally by researches it may go some way towards creating a standardized profile by which MSCs are defined and creating a cohesive methodology.

There is also a physical requirement that needs to be met, when defining BM-MSCs, which is their ability to adhere to plastic in culture. If they do not adhere to plastic they are not MSCs. The cells also need to have at least a multipotent differential potential. They must be capable of differentiation into osteoblasts, chondrocytes and adipocytes as a minimum requirement, under the appropriate stimuli. Histological stains can be used as evidence of this; osteoblasts can be stained by Von Kossa for calcification or Alizarin Red for

mineralization, chondrocytes using Alcian blue for glycos-amino-glycan (GAG) and adipocytes can be stained with Oil red O for lipids[38].

Another problem that researchers face when using BM-MSCs is that of senescence. Embryonic stem cells (ESC) go through many passages, and remain phenotypically correct, where BM-MSCs will only passage a relatively small number of times before they lose their stem markers and become senescent. This creates problems when it is necessary to achieve the large cell numbers required for cell therapies[39]. Senescence is thought to occur due to shortening of telomere length during cell division, and as this is also a phenomenon observed during the natural ageing process, it also suggests that stem cells from older patients will be more prone to senescence[40]. It is necessary to use MSCs before they get to the point of senescence. It is important before undertaking any experiment with cultured mesenchymal stem cells that they are tested to express the panel of stem cell markers mentioned previously, as senescence halts their expression[40]. The characterisation of MSC populations will ensure the cells used in any experiment or therapy are a homogeneous population most likely to behave in a predictable way, being more predisposed to differentiate.

1.12 Differentiation of Mesenchymal Stem Cells

The aim of differentiating MSCs is to create terminally differentiated cells that have applications for treating disease or injury. The ultimate goal is to be able to put MSCs into the body, either on a scaffold or on their own. They get their cues from the physical and chemical properties of the scaffold, either prior to implantation or after. Alternatively, the scaffold can create a host response that cues the differentiation required.

There is evidence to suggest that MSCs have been differentiated into many different cells and tissues. Adipogenic differentiation of MSCs would potentially be very useful for producing a filler material for reconstructive surgery [41]. Chondrogenic differentiation is leading to the growth of new cartilage that would represent a significant advance for the treatment of sports injuries [42]. Osteogenic differentiation could help surgeons repair non-union bone fractures[43] and the production of nervous tissue through neural differentiation would help many people who are paralysed with spinal injuries[30]. Differentiation of MSCs into pancreatic islet cells may be an avenue to explore for type 1 diabetes mellitus[31]. The underlying fundamental science of the cell differentiation pathways is not yet fully understood. It is possible to promote differentiation *in vitro* using a wide range of stimuli using many different physical factors, exogenous growth factors supplied via culture media, or the interactions of cells with a surface.

1.13 Cell Delivery Systems for Bone Regeneration

Stem cell therapies undoubtedly have a lot of potential in regenerative medicine. Seeding MSCs at the area where the regeneration is required to occur, is more problematic than first anticipated. A quantitative study of the delivery of MSCs into a rat model by two intravascular routes (the coronary artery and directly into the myocardium) demonstrated this particularly well. The cells injected were labelled and it was shown that none of the cells injected into the coronary artery were found in the myocardial tissue, and only 15% of the cells injected directly into the myocardium were found to have been retained. This example highlights the extent to which stem cells will migrate if introduced by the vascular system, as

the cells were found in the spleen, liver and lungs of the rat model[44]. The small retention rate highlights the necessity of a delivery system that will retain the appropriate number of cells in the designated area of application.

As stated above, a major obstacle in the development of a stem cell-based therapy is the delivery of the cells to the required location. A delivery system is needed that fulfils the requirements of being both conducive to MSC proliferation and differentiation but also degradable at a rate that allows tissue regeneration to occur, and has the correct mechanical properties to substitute bone whilst regeneration occurs. There are a few studies (outlined below) that are working towards some of these properties.

Some injectable hydrogels show promise for the stimulation and delivery of bioactive compounds to a site of injury, but struggle to match up to the mechanical properties required for bone replacement, particularly if the replacement has to bear weight[45]. Injectable systems that would bear weight such as foamed injectable hydroxyapatite scaffolds, require exact timing of the injection to retain their pore structure which is vitally important for the osteoconductivity of the material, and the application of this in surgery would be impractical[46]. Some studies have tried to combine the two techniques, using a hydrogel to encapsulate umbilical cord stem cells prior to incorporation into a calcium phosphate paste[47]. While this study has showed some positive results, there is still the question of how this technique could be used in a clinical setting. Putting aside the issues regarding using umbilical cord stem cells and the risks of viral transmission that come into play when using donor cells, the encapsulation process requires specialised equipment to achieve the size of spheres required to maintain the mechanical strength required for bone applications. Several other studies have used hydrogels in various forms[48],[49],[50] but some of these studies were very preliminary, and will require further investigation before they would be used in a clinical

setting. Detection of ectopic bone formation has proven to be a good model for proof of principle systems, in terms of observing how the materials will react in the *in vivo* environment. Some of the calcium phosphate/hydrogel biphasic injectable systems have showed very promising results under these experimental conditions[51]. But there is some way to go, before these systems have the correct load bearing mechanical strength for applications in real non-union bone fracture environments. It seems a simple yet effective system that meets all the requirements is, as yet, unavailable. Hydrogel and calcium phosphate injectable systems may not be appropriate bone regeneration biomaterials and novel degradable polymers could be good candidates for the next phase of research into injectable bone regeneration systems.

1.14 Polymers as Cell Delivery Systems

Polymers can be designed to have properties which are desirable for tissue engineering processes. Elasticity, strength, and the ability to degrade at a controlled rate are just a few of the possibilities that make them very versatile and applicable for the generation of new tissues. The molecular structure of a polymer includes repeating units, which form long chains that can have cross linkages. The presence or absence of these cross linkages are responsible for many of the physical properties of polymers that provide their versatility for regenerative medicines purposes. The poly(α-hydroxyacids) are particularly useful for the purposes of tissue engineering, this group includes poly(lactic acid) (PLA), poly(glycolic acid)(PGA), poly (lactic-co-glycolic acid) (PLGA) and poly(carpolactone) (PCL). These polymers have been used extensively in the tissue engineering field [52,53].

The physical properties of polymers are temperature dependant, and polymers can change state at certain temperatures. When a polymer is in a liquid, or melt, state it has enough thermal energy to allow long free chains of molecules to move around randomly.

During this phase the polymer is elastic and flexible. When cooled a polymer passes through its glass transition temperature (Tg), which varies between polymers and occurs when the long free chain molecules cease to move and the polymer will then become hard and stiff, like glass. This explains why some polymers are flexible or stiff, the temperature the individual polymer is used at, whether below or above its Tg value, determines its physical properties. In applications for regenerative medicine the temperature that the polymer will be used at is 37 ^{o}C. Therefore the physical properties of the polymer must be appropriate for its intended end use at 37 ^{o}C, if it is required to be flexible, for example, in the case of a blood vessel, the polymer must be in its melt phase. If the purpose it bone regeneration, it is more likely that the polymer must be more rigid, and should be used below its Tg value[54]. Although 37 ^{o}C is the temperature at which the polymer will function, it should also be stated that initially the material will cause an inflammatory response, which will increase the localised temperature to a small degree and it must be capable of withstanding some temperature tolerance without changing its structural integrity[55].

The aliphatic polyesters PGA and poly-L-lactide (PLLA), are used heavily in tissue engineering and regenerative medicine applications. The copolymer of these two polymers (PLGA) has shown to be particularly versatile in this area of research because its degradation products are glycolic acid and lactic acid, which are easily metabolised[56]. PLGA is seen to be biocompatible, as it has been used with many different cell types, including MSC[52]. PLGA in its bulk form has got some limitations due to its hydrophobic nature and the released metabolic products can cause an acidic environment[56,57]. Its capacity for variable degradation rate however is a benefit, which has led to further work being conducted to try to make use of this polymer in the tissue engineering and regenerative medicine field.

PLGA is a good candidate for an injectable system, as it can be used in a Tg phase that is conducive to bone regeneration[58]. The degradation profile of PLGA it has been exploited when used in conjunction with calcium phosphate scaffolds to allow the degradation of the osteoinductive calcium phosphate structure[59]. This work is starting to show some promise as the PLGA improves the osteoconductivity of the injectable calcium phosphate by degrading and leaving a pourous structure behind. This technique has been employed in other studies[60], and the resulting biomaterial has been shown to have load bearing qualities after 8 weeks of implantation. To make a fully degradable system is the ultimate goal, and using PLGA alone may be a way to execute this. The bulk qualities of PLGA have many advantages. A material that can degrade in a controllable manner has mechanical properties which are desirable for the purpose of bone tissue engineering and which can be manufactures to form spheres or particles that are injectable has many benefits for this application. In its standard form, the surface properties are not as desirable as the bulk qualities (i.e, it controllable degradation rate). Several studies have been conducted to test the effects of making the surface of PLGA more biocompatible and less hydrophobic, ranging from bulk coatings of gelatin[61], to the addition of peptides and surface chemistries[62] in order to support cell growth[62], proliferation and differentiation, and so create a material that is osteoinductive in addition to being osteoconductive[63,57]. There are many appealing surface modification methods that have attempted improve the biocompatibility of PLGA, outlined below.

1.15 Surface Modifications

Modifying the surface of a currently available and approved material is a method of retaining the desirable bulk qualities of an established biomaterial while enhancing the surface properties. As discussed earlier, the use of whole proteins and peptides is a stage along a route to discovering the factors that influence the differentiation of stem cells. Breaking the idea down to basic interactions, the next logical progression of the idea that stem cell fate can be influenced by ECM is to look at the basic chemical composition of the ECM and to investigate if it can be copied to some extent by the addition of synthetic chemicals onto a biomaterial surface. This technique is a relatively inexpensive way of broadening the applications in which approved biomaterials can be used, which reverses the significant downside of applying very expensive and complicated to produce peptides to the biomaterials surface.

In the case of stem cell interactions it is desirable to induce a differentiation response from the cells via interactions with applied chemical groups on the surface of the material[62, 64, 65, 66].

1.16 Modifications for Cellular Interactions to Mimic the Extracellular Matrix (ECM).

The main aim of modifying a surface is to make it more conducive for regenerative medicine/tissue engineering purposes. The ideal scenario is to mimic the extracellular matrix. The extracellular matrix is the overall term for the extruded proteinacious matrix that is produced by cells to provide a scaffold with the architecture required for a particular tissue. Many different cells are responsible for the different extracellular matrix profiles of different tissues, for example, chondrocytes are responsible for the ECM in cartilage which is rich in glycos-amino-glycans (GAG) and specific to that tissue, and bone matrix is excreted by osteoblasts and consists of the proteins collagen I, osteocalcin, osteonectin and osteopontin to give just a few examples[11]. The function of the extracellular matrix varies between tissues,

but it always acts as a structural material for the tissue it constitutes. However it is not merely a structural protein network, the some of the effects of the ECM are much more subtle. ECM also influences the cells that are recruited to its location by inducing undifferentiated cells such as MSC, along a particular lineage. Cells use the signals given to them by the structure of the ECM to reorder their cytoskeleton and take on different morphologies, which ultimately leads to different phenotypes[67]. There is currently some debate as to whether it is the surface topography that influences cell fate, or the surface chemistry[62]. Both these factors likely influence cell-matrix interactions. Both topography and surface chemistry of ECM have been taken forward as approaches to create smart materials that can influence cell fate, essentially mimicking the ECM, in either its physical or chemical properties.

Initial studies in this area demonstrated the concentration of specific proteins, (*i.e.* fibronectin and laminin) and their subsequent concentrations on a 3D collagen scaffold could influence embryonic stem cells to differentiate into specific lineages (smooth muscle and cardiac cells)[68]. This bulk coating of protein however could be refined, so that specific active pieces of the proteins could be used to influence stem cell fate in a very targeted and accurate way.

1.17 Peptide Modifications

Peptides are the next step along this surface chemistry driven pathway, allowing biomaterials to mimic natural ECM, avoiding some of the risk factors of using whole proteins from either xenological or human sources. This work has enabled researchers to establish the origins of important signals in the differentiation pathway of stem cells. This is being conducted using several novel screening methods, including the expression of peptides in a

bacterial model where the bacterium are transfected with a plasmid containing the coding for different peptides, which are then expressed in the bacteria[69].

Peptides that are engineered synthetically are very useful as a research tool as they simulate the ECM in a controllable manner. It is possible to distinguish the differing roles of the various molecules in ECM by engineering the individual peptides and testing them in isolation[70]. Isolating the peptides was an important step towards determining the individual capacity of the peptides and the peptides which were relevant for the osteogenic lineage. More established RGD and BMP were determined to be very relevant for the osteogenic lineage. During one study peptide amphiphiles were functionalised with RGD and DGEA which were seen to be osteoinductive in their properties[71]. Both of the peptides showed an increase in osteoinductivity when cultured with media containing growth factors, whilst RGD showed a degree of phenotypic change when cultured in the absence of growth factors. This demonstrated very clearly the RGD has osteoinductive qualities that may be used to functionalise biomaterial surfaces[71].

The osteoinductive properties of the RGD peptide are difficult to deny. The only foreseeable problems (which are considerable) with the use of peptides on a large scale is cost and availability. It is very expensive and time consuming to produce peptides, and if they were to be used commercially would be required in large volumes. The expense of using peptides is their limiting factor, and for this reason, identifying active molecules to bind material surfaces is progressing as the analytical techniques have improved. Isolating the chemical groups active from within the peptide, and applying them to biomaterial surfaces is a new strategy within the field. This is more cost effective than using peptides, and is starting to yield similar results, *in vitro.*

1.18 Chemical Modification

There are many methods of modifying a polymer surface[72]. A polymer surface usually needs to be functionalised before the application of an active chemical group. There are several ways to do this depending on the outcome that is required. To achieve maximum functionalization, a polyfunctional agent can be grafted to the surface of the polymer. This allows the more functional units to be available and effectively increases the functional units per given unit of surface area compared to that of using a single function molecule. However, there can be problems with steric hindrance when functional groups are tightly packed together on a surface. One way to overcome this difficulty is to use a spacer molecule, which allows movement and often acts as a protective layer to keep the active chemical group away from hydrophobic surfaces, which can denature some bioactive compounds[73]. The chain length of these spacer molecules is variable, and finding an optimum chain length for a particular chemical group is important and could be a reason for the conflicting results reported in the literature where surface modifications appear to have the same chemical terminal group but induce different differentiation pathways in stem cells[74].

By using combinations of functional groups arranged in different ways it is possible to mimic the natural ECM in various tissues. The chemical groups that are of particular interest for skeletal regeneration are $-NH_2$, CH_3, -OH and –COOH as all these groups are found on bone ECM.

1.19 Amine Groups

Amine groups have been shown to play an active role in the immobilisation of proteins, because of their positive charge and it is thought that the amine groups have the capacity to attract and interact with proteins on the surface of a biomaterial[75]. However there have been some variable results reported in terms of the effects observed on MSCs exposed to these modifications, in some cases have been directly contradictory. Amine rich surfaces have been reported to be osteogenic,[62] chondrogenic[65] and non-differentiating[75]. Clearly the reaction of the cells to the terminal groups is only part of the differentiation and presentation of the modification is likely to also play a role. Interestingly, there have been differences seen when the same chemical is deposited onto a biomaterials surface in different ways (*e.g.* APTES). APTES was deposited using a Plasma technique[76] showed no significant increase in osteogenic response with a pre-osteoblastic cell line compared to a control untreated substrate, where-as APTES applied using a wet chemical technique caused an osteogenic effect from MSCs[62]. This contradictory data merits further investigation, as it appears that amine groups if presented in the correct way could have powerful osteogenic properties. It is essential to isolate the parameters that affect the presentation of the amine and determine which of the many possible modification techniques will have the most clinical relevance.

Clearly there is need for clarification of the surface modifications at a molecular level. Clarification may come from varying presentation of the terminal groups to achieve an optimised and reproducible response from the cells.

1.20 Methyl Groups

The addition of methyl groups to a surface has also shown mixed results. There is evidence to show that this is due to several different factors. The addition of methyl groups

to a surface has been shown in some studies to cause a chondrogenic response in MSC[65], whilst others have shown that specific hydrocarbon chain lengths can maintain the MSC phenotype[74]. The different results seen when the chain length is varied could offer some explanation for the variance in the results seen in the literature from studies where the presentation of the chemical group has not been considered to be a factor.

1.21 Hydroxyl Groups

Hydroxyl groups have been used quite extensively in biomaterials applications and have been shown to induce and maintain chondrogenic in chondrogenic phenotype [77]. However they have also demonstrated that they have the ability to form apatite surfaces when in contact with calcium rich solutions[78], which would indicate that the surface chemistry would induce an osteogenic response. So again there seems to be more factors involved in the differentiation of the cells than purely the terminal group, and it may be that again it is the presentation of the end group that is the key to its effect on cell populations.

1.22 Carboxyl Groups

Carboxyl groups have also demonstrated varying results in the literature. There is some evidence to suggest that carboxyl groups can cause an osteogenic response from mesenchymal stem cells[65], whilst other studies show that there is a chondrogenic response[62]. These conflicting results require further investigation.

1.23 Plasma Modification Techniques

The use of plasma to introduce different surface chemistries to a substrate is widely reported. [66],[79],[80]. Plasma is considered to be the fourth state of matter and can be produced

when gases are excited into high energy states with either an electron source such as a hot filament, micro-waves or radio- waves. When plasma is in this state ions and molecules of various different can be deposited onto a surface. One advantage to this technique is that it can be used on 3D shapes, as it does not require a line of sight. This is particularly useful for complex tissue engineering scaffolds. An example of this which has been used clinically is the coating of calcium ions onto a titanium bone implant to increase bone adhesion[79].

Plasma deposition has several other advantages when used to coat a 3D object, which is likely to be a considerable advantage when applying surface chemistries to biomaterials suitable for bone regeneration. It can graft surface discrete chemistries onto polymers without the need for prior functionalization, even when using polymers.

The main disadvantage to using plasma coating is that there is no way to control the order of the deposition. It is completely random and there is no way of controlling the distance between the surface chemistries. In addition it can be very difficult to quantify the concentration of the groups deposited. This is problematic as the characterisation of the surfaces is vitally important when it comes to transferring the optimal concentration onto different substrates. Defining the concentration of a chemistry on a surface is much simpler if you are using a wet chemical technique, where a known concentration can be measured at the start of the coating reaction and at the end of the coating reaction, allowing quantification of the deposited chemical.

1.24 Silane Modification Techniques

Surfaces can be modified using a silanisation technique. It has successfully been used on an array of polymer substrates to introduce $–CH_3$, $-NH_2$, -OH and –COOHgroups[62].

Silanisation of a polymer first requires it to be functionalised, usually via the addition of oxygen groups to the surface. This is usually done using an oxygen plasma technique. When the oxygen groups have been attached to the surface of the polymer, a silane group can bond. Silanes are remarkable molecules for several reasons. There have a reactive silane body, a hydrocarbon chain and an end group. The chain length can be varied as can the end group, while the silane group remains able to bind free oxygen molecules on a surface. It is also a non toxic molecule that is suitable for cellular interaction.

The most useful feature of silane molecules however is their ability to form self-assembled monolayers (SAMs)[81],[82]. The formation of silane SAMs includes a step which involves an irreversible covalent which makes them particularly stable[81]. They do however, need surface oxygen or –OH groups on the substrate with which to form hydrolytic bonds, so the layer can be bonded to the substrate at anchor points. The packing density is controlled ultimately by the formation of a siloxane network [81] so there is more control of this parameter using silane modification compared to a plasma coating method. This may be useful for determining the optimum concentration of a given surface modification.

1.25 The Characterisation of Surface Modifications

It is particularly difficult to define the specific concentration of some surface chemistries on a modified surface. Most techniques used to characterise a surface characterise one particular parameter a modification has brought about. No one technique fully characterises all of the properties of a surface so it is always necessary to use a panel of techniques to comprehensively characterize a surface.

1.26 Water Contact Angle

Water contact angle (WCA) is generally the first technique that is performed to determine the likely surface energy of a modified surface, and is has the advantage of being relatively simple and quick to perform. Surface energy can predict the wettability of a surface (hydrophilic or hydrophobic) which can be a direct predictor of its ability to interact with cells. The use of WCA is a long established[83],[84] indication of surface energy and a core test for the assessment of a biomaterial and is often the first test done to evaluate the suitability of a surface for further research.[85],[86].

1.27 Scanning Electron Microscopy(SEM)

SEM is used to examine surface topography. An electron beam passes across a surface and bounces secondary electrons from the surface into a detector. From the energy patterns of these secondary electrons, an image on a surface is displayed in incredible detail in gray-scale. Until recently, this technique was reserved for conductive samples as any charge that built up on the surface as a result of the electron beam distorted the image. However the field has advanced sufficiently to provide instruments capable of imaging at low accelerating voltages, which do not require the samples to be fully conductive. This is combined with sputter coating, which ionises metal to form plasma which allows a very thin (10-20nm) coating of metal to be deposited on the samples surface. Thus the technique is suitable for the examination of polymer surfaces and macrotopographical features [87]. One drawback is that there is some loss of resolution when imaging at very high magnification. It is not possible to image nanoscale surface features on polymers where it would be entirely possible to observe these features on a very conductive sample such as a metal.

1.28 AFM (Atomic Force Microscopy)

To determine the topography of a polymeric surface at the nanoscale it generally requires use of an atomic force microscope (AFM).[88],[89],[90]. AFM uses a canter-lever to tap the surface and its attenuation determines the nanotopography of the surface. It has several advantages compared to SEM. It does not have to be conducted under a vacuum so it is not necessary to dry samples if they are wet, and it does not require the sample to be conductive. However, this technique is unsuitable for large areas as it is very time consuming. An area of $500nm^2$ can take several minutes to scan, so the technique is useful only on a nanoscale. Using this technique in conjunction with SEM builds up a comprehensive picture of the macro and nano topography of a surface[91]. Some drawbacks of using this technique include the aberration of some surface characteristics because of the tip. It is impossible to visualise overhanging features and spherical features will appear cone-like as the tip can not reach under them.

1.29 XPS (X-ray Photoelectron Spectroscopy)

The microscopy techniques discussed above are useful for defining the topography of the surfaces but do not reveal any differences in the chemical composition of the modification. One way to achieve a limited amount of information about the composition is to use X-ray photoelectron spectroscopy (XPS). This uses the element-specific pattern of photons and X-rays that are released when a surface is hit with an electron beam at a specific energy level[84],[92]. This gives the specific elemental composition of the surface, but is limited to any element higher on the periodic table than helium. Hydrogen and helium cannot be

measured using this technique because the as the diameter of the orbital is too small to facilitate the catch probability. This is a well established technique and is used routinely to determine the chemical composition of a biomaterials surface.[93],[94],[95].

1.30 Specific Chemical Assays - Ninhydrin

To determine a specific concentration of a particular terminal group, it is sometimes possible to use a specific chemical test such as Ninhydrin. Ninhydrin is a molecule which will react with free amine groups, to give a colorimetric change. This colour change can be quantified to determine changes in the amine concentration of a solution. It is possible then, to measure the depletion of an amine in a coating solution to determine quantity of amine deposited onto a surface.

Cellular interactions can only be accredited to surface modifications if they have been extensively characterised.

1.31 Topography vs Chemistry

The ability of surface topography to affect the fate of MSCs has been comprehensively researched in recent years. The size of surface features seems to be a factor in the stimulation of MSC differentiation. It has been shown in several publications that the grain size of titanium is particularly influential in the resulting stem cell neiche. Particle sizes smaller than 50nm appear to retain stem cell phenotype even in the presence of exogeneous stimulation from additional growth factors in the media. Conversely grain sizes larger than 200nm showed an increase in osteogenic markers, but only when stimulated to do so by

osteoinductive growth factors. In these examples it is not the chemistry of the surface that is responsible for this phenotypic change, as the surface chemistry is the same, it just differences in topography[96]. In another study, sub-nanoscale titanium surfaces could not sustain or increase differentiation from mouse MSC, but nanoscale surfaces did influence this significantly[97]. It appears that topography of titanium substrates in the range of 2-4nm causes osteogenic differentiation of human MSCs.

When the topographical stimulus is not sufficient to stimulate the cells to produce their own growth factors, topography to influence stem cell fate if the correct osteogenic stimulus is supplied in the media[62].

By increasing the stimulus, a nanotopography has been used to stimulate an osteogenic response from MSCs and osteo-progentitor cells, in the absence of differentiating media, using disordered nanolithography techniques up to 21 days[98].

To date there has been little research to determine what the effect of different chemistries on surface topography at a nano scale. It has often been shown that the chemistry enriched surfaces do not show any macro-topographical changes, but it is likely that significant changes do occur at a nano-topographical level. It may be that it is a combination of surface topography and chemistry that allows the powerful effects to be seen and it may here in this area of combining chemistry and topography will have the greatest results. It is at this point that it is worth mentioning that most of the research done in this area is conducted on a film or relatively flat substrate such as glass or gold add [62],[82]. Transferring the surface chemistries onto 3D substrates may not result in the same cell response, and this must be considered when taking a surface chemistry onto the 3D system.

1.31 2D to 3D

Base level cell reactions are assessed using the 2D substrates to observe how cells react to surface chemistries in the absence of other factors that inevitably require optimisation when cell culture is stepped up to 3D, such as the transportation of nutrient through a porous scaffold, oxygen gradient and the cell seeding density required to populate the scaffold. It is also important to determine if the modifications will produce a similar effect on a 3D substrate. The clinical applications for these chemistries would be in 3D systems, so it is important to demonstrate that it is possible and apply the fundamental theories to a usable clinical product.

1.32 Cell Responses in 3D Cultures

The 3D culture models that have been reported using osteoblasts suggest that they can be successfully cultured this way. In fact there have been reports that osteoblasts require no further exogenous growth factors to retain their phenotype when put into a 3D culture environment, although the cells were grown in sheets then bunched together in a spheroid like configuration[99].

In addition, 3D culture it is a well established chondrogenic differentiation tool. Pellet cultures allow cells to grow within a defined oxygen gradient. Any of the cells in the central portion of the cell pellet will experience a hypoxic environment which may be responsible for differentiation growth factors to be released.

1.33 The Ideal Bone Regeneration System

To summarise, an ideal bone regeneration system would be a degradable polymer, which could support active surface chemistries and could be used either as a carrier for the patients' own stem cells, or to stimulate the influx of MSCs and osteoblasts *in vivo*. The

material would have sufficient mechanical properties to withstand the forces inflicted upon it and mimic ECM to produce a response of sufficient power to allow the differentiation and mineralisation of the scaffold, at the same rate at which it degrades, in the absence of any cytotoxic degradation products. A porous, injectable PLGA system with an osteoinductive surface chemistry could meet all these demands and it is the development and optimisation of these surface chemistries on which this research will focus.

1.34 Hypothesis

Hypothesis 1

Surface chemistry can affect the phenotypical response of mesenchymal stem cells, when applied to a 3D polymeric bone regeneration system.

Hypothesis 2

The presentation of amine functional groups can have an effect of the cell response seen, when on a flat glass surface.

Hypothesis 3

The optimised amine modifications can be transferred to a polymeric surface, and a 3D injectable bone regeneration system, to give a unified cellular response.

1. Atala, A., Forest, W. Regenerative medicine strategies. *Journal of Pediatric Surgery* **47**, 17-28 (2012).

2. Frolke, J.P.M., Patka, P. Definition and classification of fracture non-unions. *Injury* **38S,** S19-S22 (2007).

3. Dahabreh, Z., Dimitriou, R. & Giannoudis, P.V. Health economics: A cost analysis of treatment of persistent fracture non-unions using bone morphogenetic protein-7. *Injury* **38,** 371-375 (2007)

4. Hofmann, A., Hofmann, A., Ritz, U., Hessmann,M.H., Schmid,C. Tresch,A. Cell viability, osteoblast differentiation, and gene expression are altered in human osteoblasts from hypertrophic fracture non-unions. *Bone* **42**, 894-906 (2008).

5. Ramoutar, D.N., Rodrigues, J., Quah, C., Boulton, C. & Moran, C.G. Judet decortication and compression plate fixation of long bone non-union: Is bone graft necessary? *Injury* **42**, 1430-4 (2011).

6. Wheeless Wheeless textbook of Orthopadics. www.wheelessonline.com/ortho/psedoarthrosis

7. Harwood, P.J. (ii) An update on fracture healing and non-union. *Orthopaedics and Trauma* **24**, 9-23 (2010).

8. Doblaré, M., García, J.M. & Gómez, M.J. Modelling bone tissue fracture and healing: a review. *Engineering Fracture Mechanics* **71**, 1809-1840 (2004).

9. Marsell, R. & Einhorn, T. A The biology of fracture healing. *Injury* **42**, 551-555 (2011).

10. Bragdon, B., Moseychuk, O. Saldanha,S. King.D. Bone morphogenetic proteins: a critical review. *Cellular signalling* **23**, 609-20 (2011).

11. Xiao, Z., Blonder, J., Zhou, M. & Veenstra, T.D. Proteomic analysis of extracellular matrix and vesicles. *Journal of proteomics* **72**, 34-45 (2009).

12. Bosetti, M., Boccafoschi, F., Leigheb, M. & Cannas, M.F. Effect of different growth factors on human osteoblasts activities: a possible application in bone regeneration for tissue engineering. *Biomolecular engineering* **24**, 613-8 (2007).

13. Blonder, J., Xiao, Z. & Veenstra, T.D. Proteomic profiling of differentiating osteoblasts. *Expert review of proteomics* **3**, 483-96 (2006).

14. Huang, L., Teng, X.Y., Cheng, Y.Y., Lee, K.M. & Kumta, S.M. Expression of preosteoblast markers and CBFA-1 and Osterix gene transcripts in stromal tumour cells of giant cell tumour of bone. *Bone* **34**, 393-401 (2004).

15. Makita, N. Makita, N. Suzuki,M. Asami,S. Takahata,R. Kohzaki. D. Two of four alternatively spliced isoforms of RUNX2 control osteocalcin gene expression in human osteoblast cells. *Gene* **413**, 8-17 (2008).

16. Nakase, T., Takaoka, K. Hirakawa,K. Hirota, S. Alterations in the expression of osteonectin, osteopontin and osteocalcin mRNAs during the development of skeletal tissues in vivo. *Bone and mineral* **26**, 109-22 (1994).

17. Theyse, L.F.H., Mol, J. A, Voorhout, G., Terlou, M. & Hazewinkel, H. A.W. The efficacy of the bone markers osteocalcin and the carboxyterminal cross-linked telopeptide of type-I collagen in evaluating osteogenesis in a canine crural lengthening model. *Veterinary journal* **171**, 525-31 (2006).

18. Lajeunesse, D., Kiebzak, G.M., Frondoza, C. & Sacktor, B. Regulation of osteocalcin secretion by human primary bone cells and by the human osteosarcoma cell line MG-63. *Bone and mineral* **14**, 237-50 (1991).

19. Dinopoulos, H., Dimitriou, R. & Giannoudis, P.V. Bone graft substitutes: What are the options? *The Surgeon* 1-10 (2012).

20. Nassr, A. Khan, MH Ali, M.H., Espiritu,M.T.,Hanks, S.E. Donor-site complications of autogenous nonvascularized fibula strut graft harvest for anterior cervical corpectomy and fusion surgery: experience with 163 consecutive cases. *The Spine Journal* **9**, 893-898 (2009).

21. Zimmermann, G. & Moghaddam, A. Allograft bone matrix versus synthetic bone graft substitutes. *Injury* **42**, S16-S21 (2011).

22. Eckardt, H. Eckardt, H. Christensen, K.S. Lind,M. Hansen, E.S. Recombinant human bone morphogenetic protein 2 enhances bone healing in an experimental model of fractures at risk of non-union. *Injury* **36** 489-494 (2005).

23. Carragee, E.J., Hurwitz, E.L. & Weiner, B.K. A critical review of recombinant human bone morphogenetic protein-2 trials in spinal surgery: emerging safety concerns and lessons learned. *The spine journal: official journal of the North American Spine Society* **11**, 471-91 (2011).

24. Zimmermann, G., Wagner, C., Schmeckenbecher, K., Wentzensen, a & Moghaddam, a Treatment of tibial shaft non-unions: bone morphogenetic proteins versus autologous bone graft. *Injury* **40 S3**, S50-3 (2009).

25. Undale, A.H., Westendorf, J.J., Yaszemski, M.J. & Khosla, S. Mesenchymal stem cells for bone repair and metabolic bone diseases. *Mayo Clinic proceedings. Mayo Clinic* **84**, 893-902 (2009).

26. Rengachary, S.S. Bone morphogenetic proteins: basic concepts. *Neurosurgical focus***13**, e2 (2002).

27. Park B.W., Kang ,E.J., Byun ,J.H., Son, M.G., Kim, H.J., Hah, Y.S., Kim, T.H., Mohana Kumar, B., Ock ,S.A., Rho and G.J. In vitro and in vivo osteogenesis of human mesenchymal stem cells derived from skin, bone marrow and dental follicle tissues. *Differentiation; research in biological diversity* **83**, 249-59 (2012).

28. Eckersley-Maslin, M. A., Warner, F.J., Grzelak, C. A, McCaughan, G.W. & Shackel, N. A. Bone marrow stem cells and the liver: are they relevant? *Journal of gastroenterology and hepatology* **24**, 1608-16 (2009).

29. Batorsky, A., Liao, J., Lund, A.W., Plopper, G.E. & Stegemann, J.P. Encapsulation of adult human mesenchymal stem cells within collagen-agarose microenvironments. *Biotechnology and bioengineering* **92**, 492-500 (2005).

30. Jung, D.-I. *et al.* A comparison of autologous and allogenic bone marrow-derived mesenchymal stem cell transplantation in canine spinal cord injury. *Journal of the neurological sciences* **285**, 67-77 (2009).

31. Limbert, C. & Seufert, J. In vitro (re)programming of human bone marrow stromal cells toward insulin-producing phenotypes. *Pediatric Diabetes* **10**, 413-419 (2009).

32. Marcacci M, Kon E, Moukhachev V, Lavroukov A, Kutepov S, Quarto R, Mastrogiacomo M, Cancedda R.. Stem cells associated with macroporous bioceramics for long bone repair: 6- to 7-year outcome of a pilot clinical study. *Tissue engineering* **13**, 947-55 (2007).

33. Hernigou, P., Poignard, a, Manicom, O., Mathieu, G. & Rouard, H. The use of percutaneous autologous bone marrow transplantation in nonunion and avascular necrosis of bone. *The Journal of bone and joint surgery. British volume* **87**, 896-902 (2005).

34. Sekiya, I., Vuoristo, J.T., Larson, B.L. & Prockop, D.J. In vitro cartilage formation by human adult stem cells from bone marrow stroma defines the sequence of cellular and molecular events during chondrogenesis. *Proceedings of the National Academy of Sciences of the United States of America* **99**, 4397-402 (2002).

35. Hwang, N.S., Varghese, S. & Elisseeff, J. Controlled differentiation of stem cells. *Advanced drug delivery reviews* **60**, 199-214 (2008).

36. Zhukareva, V., Obrocka, M., Houle, J.D., Fischer, I. & Neuhuber, B. Secretion profile of human bone marrow stromal cells: donor variability and response to inflammatory stimuli. *Cytokine* **50**, 317-21 (2010).

37. Chen, Y., Shao, J.-Z., Xiang, L.-X., Dong, X.J. & Zhang, G.-R. Mesenchymal stem cells: a promising candidate in regenerative medicine. *The international journal of biochemistry & cell biology* **40**, 815-20 (2008).

38. Dominici, M. , Le Blanc.K., Mueller, I., Slaper-CortenbachI. Minimal criteria for defining multipotent mesenchymal stromal cells. The International Society for Cellular Therapy position statement. *Cytotherapy* **8**, 315-7 (2006).

39. Vats, A., Bielby, R.C., Tolley, N.S., Nerem, R. & Polak, J.M. Stem cells. **366**, 592-602 (2005).

40. Ju, Z. Rudolph, L. Telomere dysfunction and stem cell aging. *Biochemie* **90**, 24-32 (2008).

41. Mandal, B.B. & Kundu, S.C. Osteogenic and adipogenic differentiation of rat bone marrow cells on non-mulberry and mulberry silk gland fibroin 3D scaffolds. *Biomaterials* **30**, 5019-30 (2009).

42. Hunziker, E.B. Articular cartilage repair: basic science and clinical progress. A review of the current status and prospects. *Osteoarthritis and cartilage / OARS, Osteoarthritis Research Society* **10**, 432-63 (2002).

43. Giannoudis, P.V. & Pountos, I. Tissue regeneration. The past, the present and the future. *Injury* **36 S4**, S2-5 (2005).

44. Hale, S.L., Dai, W., Dow, J.S. & Kloner, R.A. Mesenchymal stem cell administration at coronary artery reperfusion in the rat by two delivery routes: A quantitative assessment. **83**, 511-515 (2008).

45. Fu, S.Z., Ni,P.Y., Wang, B.Y., Chu,B.Y., Zheng,L., Luo,F. Injectable and thermo-sensitive PEG-PCL-PEG copolymer/collagen/n-HA hydrogel composite for guided bone regeneration. *Biomaterials* **33**, 4801-9 (2012).

46. Montufar, E.B.,Traykova,T. Gil,C. Harr,I. Almirall, A. Foamed surfactant solution as a template for self-setting injectable hydroxyapatite scaffolds for bone regeneration. *Acta biomaterialia* **6**, 876-85 (2010).

47. Zhao, L., Weir, M.D. & Xu, H.H.K. An injectable calcium phosphate-alginate hydrogel-umbilical cord mesenchymal stem cell paste for bone tissue engineering. *Biomaterials* **31**, 6502-10 (2010).

48. Payne, R.G., Yaszemski, M.J., Yasko, A.W. & Mikos, A.G. Development of an injectable, in situ crosslinkable, degradable polymeric carrier for osteogenic cell populations. Part 1. Encapsulation of marrow stromal osteoblasts in surface crosslinked gelatin microparticles. *Biomaterials* **23**, 4359-71 (2002).

49. Ji,Q.X., Deng,J., Xing, X.M., Yuan, C.Q., Yu, X.B., Xu ,Q.C., Biocompatibility of a chitosan-based injectable thermosensitive hydrogel and its effects on dog periodontal tissue regeneration. *Carbohydrate Polymers* **82**, 1153-1160 (2010).

50. Burdick, J. A and Anseth, K.S. Photoencapsulation of osteoblasts in injectable RGD-modified PEG hydrogels for bone tissue engineering. *Biomaterials* **23**, 4315-23 (2002).

51. Trojani, C., Boukhechba,F., Scimeca,J.C.& Vandenbos, F. Ectopic bone formation using an injectable biphasic calcium phosphate/Si-HPMC hydrogel composite loaded with undifferentiated bone marrow stromal cells. *Biomaterials* **27**, 3256-64 (2006).

52. Choi, Y.S., Park, S.-N. and Suh, H. Adipose tissue engineering using mesenchymal stem cells attached to injectable PLGA spheres. *Biomaterials* **26**, 5855-63 (2005).

53. Baker, S.C., Rohman, G., Southgate, J.& Cameron, N.R. The relationship between the mechanical properties and cell behaviour on PLGA and PCL scaffolds for bladder tissue engineering. *Biomaterials* **30**, 1321-8 (2009).

54. Ratner, B.D. *Biomaterials science: An introduction to materials in medicine*. (Elsevier Ltd: UK, 1996).

55. Xu, W. Instrumentation and experiment design for in-vitro interface temperature measurement during the insertion of an orthopaedic implant. *Control, Automation, Robotics and Vision* 1773-1778 (2008).

56. Sachlos, E. & Czernuszka, J.T. Making tissue engineering scaffolds work. Review: the application of solid freeform fabrication technology to the production of tissue engineering scaffolds. *European cells & materials* **5**, 29-39; discussion 39-40 (2003).

57. Wu, Y.C., Shaw, S.Y., Lin, H.R., Lee, T.M. & Yang, C.Y. Bone tissue engineering evaluation based on rat calvaria stromal cells cultured on modified PLGA scaffolds. *Biomaterials* **27**, 896-904 (2006).

58. Krebs, M.D., Sutter, K. A, Lin, A.S.P., Guldberg, R.E. &Alsberg, E. Injectable poly(lactic-co-glycolic) acid scaffolds with in situ pore formation for tissue engineering. *Acta biomaterialia* **5**, 2847-59 (2009).

59. Félix Lanao, R.P., Leeuwenburgh, S.C.G., Wolke, J.G.C. & Jansen, J. A Bone response to fast-degrading, injectable calcium phosphate cements containing PLGA microparticles. *Biomaterials* **32**, 8839-47 (2011).

60. Link, D.P., van den Dolder, J., Jurgens, W.J.F.M., Wolke, J.G.C. & Jansen, J. A Bone response to fast-degrading, injectable calcium phosphate cemesnts containing PLGA microparticles. *Biomaterials* **27**, 4941-7 (2006).

61. Meng, Z.X., Zeng, Q.T., Sun,Z.Z., Xu, X.X.& Wang, Y.S. Immobilizing natural macromolecule on PLGA electrospun nanofiber with surface entrapment and entrapment-graft techniques. *Colloids and surfaces. B, Biointerfaces* **94**, 44-50 (2012).

62. Curran, J.M., Chen, R. & Hunt, J. A. Controlling the phenotype and function of mesenchymal stem cells in vitro by adhesion to silane-modified clean glass surfaces. *Biomaterials* **26**, 7057-67 (2005).

63. Park, G.E., Pattison, M. A, Park, K. & Webster, T.J. Accelerated chondrocyte functions on NaOH-treated PLGA scaffolds. *Biomaterials* **26**, 3075-82 (2005).

64. Curran, J.M., Chen, R. & Hunt, J. A. The guidance of human mesenchymal stem cell differentiation in vitro by controlled modifications to the cell substrate. *Biomaterials* **27**, 4783-93 (2006).

65. Phillips, J.E., Petrie, T. A, Creighton, F.P. & García, A.J. Human mesenchymal stem cell differentiation on self-assembled monolayers presenting different surface chemistries. *Acta biomaterialia* **6**, 12-20 (2010).

66. Dawson, E., Mapili, G., Erickson, K., Taqvi, S. & Roy, K. Biomaterials for stem cell differentiation. *Advanced drug delivery reviews* **60**, 215-28 (2008).

67. Guilak, F. Cohen,D.M., Estes,B.T., Gimble,J.M.& Liedtke, W. Review Control of Stem Cell Fate by Physical Interactions with the Extracellular Matrix. *Stem Cell* **5**, 17-26 (2009).

68. Battista, S.Guarnieri,D., Borselli,C.& Zeppetelli, S. The effect of matrix composition of 3D constructs on embryonic stem cell differentiation. *Biomaterials* **26**, 6194-207 (2005).

69. Little, L.E., Dane, K.Y., Daugherty, P.S., Healy, K.E. & Schaffer, D.V. Biomaterials Exploiting bacterial peptide display technology to engineer biomaterials for neural stem cell culture. *Biomaterials* **32**, 1484-1494 (2011).

70. Lampe, K.J. & Heilshorn, S.C. Neuroscience Letters Building stem cell niches from the molecule up through engineered peptide materials. *Neuroscience Letters* **519**, 138-146 (2012).

71. Anderson, J.M. Vines,J.B., Patterson,J.L. Chen, H., Javed, A. . Osteogenic differentiation of human mesenchymal stem cells synergistically enhanced by biomimetic peptide amphiphiles combined with conditioned medium. *Acta Biomaterialia* **7**, 675-682 (2011).

72. Huang, N.,Huang, N., Yang, P., Leng, Y.X., Wang, J, & Sun H. Surface modification of biomaterials by plasma immersion ion implantation. *Surface and Coatings Technology* **186**, 218-226 (2004).

73. Goddard, J.M. & Hotchkiss, J.H. Polymer surface modification for the attachment of bioactive compounds. *Progress in Polymer Science* **32**, 698-725 (2007).

74. Curran, J.M., Pu, F., Chen, R. & Hunt, J. A. The use of dynamic surface chemistries to control msc isolation and function. *Biomaterials* **32**, 4753-60 (2011).

75. Mwale,F.Wang,H.T., Nelea,V., Luo,L.& Antoniou, J.. The effect of glow discharge plasma surface modification of polymers on the osteogenic differentiation of committed human mesenchymal stem cells. *Biomaterials* **27**, 2258-64 (2006).

76. Barradas, A.M.C., Lachmann, K.,Hlawacek, G., Frielink,C. Surface modifications by gas plasma control osteogenic differentiation of MC3T3-E1 cells. *Acta biomaterialia* **8**, 2969-77 (2012).

77. Ma, Z., Gao, C., Gong, Y. & Shen, J. Chondrocyte behaviors on poly-l-lactic acid (PLLA) membranes containing hydroxyl, amide or carboxyl groups. *Biomaterials* **24**, 3725-3730 (2003).

78. Kawashita, M. Nakao, M. Minoda, M Kim, H.M.& Beppu, T. Apatite-forming ability of carboxyl group-containing polymer gels in a simulated body fluid. *Biomaterials* **24**, 2477-2484 (2003).

79. Chu, P.K., Chen, J.Y., Wang, L.P. & Huang, N. Plasma-surface modification of biomaterials. *Materials Science and Engineering* **36**, 143-206 (2002).

80. Guo, L.Kawazoe,N., Fan,Y., Ito,Y., Tanaka,J.& Tateishi,T.. Chondrogenic differentiation of human mesenchymal stem cells on photoreactive polymer-modified surfaces. *Biomaterials* **29**, 23-32 (2008).

81. Schwartz, D.K. Mechanisms and kinetics of self-assembled monolayer formation. *Annual review of physical chemistry* **52**, 107-137 (2001).

82. Lee, M.H. Boettiger, D. Ducheyene, P.& Composto, R.J. Self-assembled monolayers of omega-functioal silanes: A platform for understanding cellular adhesion at the molecular level. *Silanes and other coupling agents* **4**, 1-16 (2007).

83. Xu, L.-C. & Siedlecki, C. A. Effects of surface wettability and contact time on protein adhesion to biomaterial surfaces. *Biomaterials* **28**, 3273-83 (2007).

84. Ratner, B.D. Characterization of Biomaterial Surfaces Measurement of Surface Properties **2**, (1993).

85. Groth, T. & Altankov, G. Studies on cell-biomaterial interaction: role of tyrosine phosphorylation during fibroblast spreading on surfaces varying in wettability. *Biomaterials* **17**, 1227-34 (1996).

86. Hook,A.L.,Anderson, D.G., Langer,R.& Williams,P. High throughput methods applied in biomaterial development and discovery. *Biomaterials* **31**, 187-98 (2010).

87. Zhao, C., Tan, A., Pastorin, G. & Ho, H.K. Nanomaterial scaffolds for stem cell proliferation and differentiation in tissue engineering. *Biotechnology Advances* 1-15 (2012).

88. Nozawa,J., Tsukamoto, K., Kobatake, H. J.& Yamada .J. AFM study on surface nanotopography of matrix olivines in Allende carbonaceous chondrite. *Icarus* **204**, 681-686 (2009).

89. Curtis, A.S.G., Casey, B. Gallagher, J.O.&Pasqui, D. Substratum nanotopography and the adhesion of biological cells. Are symmetry or regularity of nanotopography important? *Biophysical chemistry* **94**, 275-83 (2001).

90. Sawant, P.D. and Nicolau, D.V. Nano-topographic evaluation of highly disordered fractal-like structures of immobilized oligonucleotides using AFM. *Materials Science and Engineering: B* **132**, 147-150 (2006).

91. Morant, C., López, M., Gutiérrez, A & Jiménez, J. AFM and SEM characterization of non-toxic vanadium-free Ti alloys used as biomaterials. *Applied Surface Science* **220**, 79-87 (2003).

92. Ratner, B.D., Chilkoti, A. & Castner, D.G. Contemporary Methods for Characterizing Biomaterial Surfaces. 25-36 (1992).

93. McLeod, K., Kumar,S. Dutta, N.K. Smart,R.S.C.X-ray photoelectron spectroscopy study of the growth kinetics of biomimetically grown hydroxyapatite thin-film coatings. *Applied Surface Science* **256**, 7178-7185 (2010).

94. Hanawaa, T., Ukaib, H. & Murakamib, K. X-ray photoelectron spectroscopy of calcium-ion- implanted titanium. *Journal of electron spectroscopy and related phenomina* **63**, 347-354 (1993).

95. Davies, M.C., Khan, M. a, Lynn, R. a, Heller, J. & Watts, J.F. X-ray photoelectron spectroscopy analysis of the surface chemical structure of some biodegradable poly(orthoesters). *Biomaterials* **12**, 305-8 (1991).

96. Dulgar-tulloch, A.J., Bizios, R. & Siegel, R.W. Differentiation of human mesenchymal stem cells on nano- and micro-grain size titania. *Materials Science & Engineering C* **31**, 357-362 (2011).

97. Khang, D.Khang,D., Choi,J., Im,Y.M., Kim,Y.J., Jang,J.H.& Kang, S.S. Biomaterials Role of subnano- , nano- and submicron-surface features on osteoblast differentiation of bone marrow mesenchymal stem cells. *Biomaterials* **33**, 5997-6007 (2012).

98. Dalby, M.J.Gadegaard, N. Tare,R., Andar,A. & Riehle,M.O. The control of human mesenchymal cell differentiation using nanoscale symmetry and disorder. *Nature materials* **6**, 997-1003 (2007).

99. Ferrera, D. Poggi, S., Biassoni,C.& Dickson. G.R, Three-dimensional Cultures of Normal Human Osteoblasts: Proliferation and Differentiation Potential In Vitro and Upon Ectopic Implantation in Nude Mice. *Bone* **30**, 718-725 (2002).

Chapter 2: Materials and Methods

2.1 Methods for Chapter 3. PLGA scaffold construction and analysis

2.1.1 Manufacture of Materials: The two component injectable system.

The manufacture and plasma modification of the injectable system was conducted and supplied by Dr. Lloyd Hamilton, University of Nottingham. The basis of the injectable scaffold is a two part system; the PLGA sphere, which was the carrier component on which the modifications were made, and the adhesive component which was also PLGA but modified to change its glass transition temperature (Tg) temperature, which facilitated its adhesive properties.

2.1.2 Manufacture of PLGA sphere

1.2g of 85:15 PLGA (Lakeshore Biomaterials, UK) was dissolved in 6mL dichloromethane (Sigma, UK). This solution was pipetted drop by drop into a stirring solution of poly (vinyl alcohol) (PVA) 0.3% $^{w}/_{v}$ mw 23,000 (Sigma, UK). The solution was stirred constantly in a fume hood for 48 hours, spheres were recovered by filtration, and washed with distilled water and dried at room temperature under vacuum.

2.1.3 PLGA adhesive

The adhesive particles (component II) were manufactured by melt blending up to 15 wt% PEG (Mw 400) and PLGA and recovered as thin films. Polymer films were placed in

liquid nitrogen then ground and sieved into size fractions. The scaffold was composed of particles 100-300μm in diameter.

2.1.4 Material Modification of PLGA spheres

Plasma polymerisation was conducted on the PLGA spheres (method outlined in 2.1.2), in a custom built enclosed T-shaped borosilicate chamber system.(Lloyd Hamilton, University of Nottingham). Plasma was initiated via two external copper band electrodes secured to the borosilicate vessel and connected to a 13.56 MHz radio frequency power source (Coxial Power Ltd, UK). The power was adjusted to <1W and all substrates were exposed to an oxygen plasma (20W, 300mTorr) for 3 minutes. The thickness of the deposition process was monitored with a quartz crystal microbalance located within the reactor and coated to a thickness of 100 nm. The reactive monomers (allyl amine, hexane, acrylic acid and allyl alcohol) were deposited at 20W and 300mTorr.

Material characterisation:

2.1.5 Water contact angle measurement

The water contact angle is measured to determine the surface energy of a material, and when compared to other materials and controls is indicative of changes is surface energy, and in turn changes in surface properties and chemistry.

Water contact angle was measured using the PLGA spheres, compressed into cakes to enable the measurements to be taken. A total of 10 repeats were conducted, and the resulting means were analysed using ANNOVA to determine any statistical significance between the

values. Water contact angle measures the surface energy, and from this its hydrophobicity/hydrophlicity can be measured.

2.1.6 SEM of materials

SEM was conducted to determine what macro-topographical changes had occurred on the modified materials.

Dry films, glass or spheres were mounted onto aluminium SEM stubs (Agar scientific UK) using double sided carbon sticky tabs (Agar Scientific, UK). The samples were coated with 20nm of chromium using an EMTECH 575X sputter coater (Emtech, UK). The samples were then observed in a LEO 1550 FESEM (Zeiss, UK) using the secondary electron detector at 5kV accelerating voltage.

2.1.7 X-ray Photoelectron Spectroscopy (XPS)

XPS was conducted by Dr. Lloyd Hammilton, University of Nottingham. XPS is used to measure the elemental composition of a surface. XPS analysis was conducted with a Kratos Axis Ultra instrument equipped with a monochromated Al Kα X-ray source (1486.6 eV) at 15 mA emission current and 10 kV anode potential. The instrument was operated at fixed transmission mode and the take- off angle of 90° for the photoelectron analyser. All scans were charge-corrected to C 1s at 285eV. Data analysis was carried out with Casa XPS using the manufacturer's empirical sensitivity factors to quantify the elemental composition (in atomic %) from the spectra. The modified polymer spheres were fixed to a glass slide using double sided adhesive tape. The XPS spectra were taken from the surface of the spheres.

2.1.8. Culture of Mesenchymal stem cells (MSC)

Primary human MSC purchased from Lonza (UK), were defrosted rapidly in a 37^{o}C water bath. The vial was decanted into a T25 (Falcon, SLS UK) flask containing 5mL of HMSC culture media with 5% foetal calf serum (both Lonza UK). After 12 hours, the media was removed and replaced, to remove any traces of cryo-preservative that remained from the initial suspension solution. The cells were cultured until confluent, which typically was 1-2 days, and then passaged into a T75 culture flask (Falcon, SLS UK). The passaging process was as follows; all media was aspirated from the flask containing the MSC, and discarded. The adherent cells were washed with Dulbecco's PBS solution (Sigma, UK), for 1 minute and then aspirated off. Three mL of 10 % trypsin solution (Sigma UK) in Dulbecco's PBS (Sigma UK) were added and then incubated at 37^{o}C for 3-5 minutes, carefully noting the moment when the MSCs start to detach from the flask. Immediately 3mL of culture media containing serum was added to the flask to stop the enzymatic reaction. The cell suspension was then removed from the culture flask, and placed into a 15mL centrifuge tube (Falcon, SLS UK). The cell suspension was then centrifuged at 1500rpm for 5 minutes, to create a cell pellet. The supernatant was removed, and the pellet re-suspended in 1mL of fresh media containing 5% serum. The cells were seeded into a new T75 flask containing 10 mL of serum containing media. This flask was incubated at 37^{o}C with 5% CO_2 until confluent, with 5mL of old media removed and 5mL of new media added every 3-4 days.

When confluent, the media was removed, cells were washed with PBS for 1 minute, trypsinised using 5mL of trypsin (following the protocol above) and the reaction was stopped using 5 mL of serum containing media. The cells were pelleted (as described above) and re-suspended in 1.2 mL of media. 0.4mL of the cell suspension was then added to each of 3 T75 culture flasks containing 10 mL of media. These flasks were incubated at 37^{o}C with 5% CO_2

until confluent (as above). This process was repeated another 2 times, until passage 5 was reached, at which point the cells were used in the experiments outlined below.

2.1.9. Mesenchymal stem cell culture with 3D scaffolds.

MSCs were cultured in contact with modified PLGA spheres to determine the cellular response to the different surface chemistries. The PLGA system used consisted of two components, the PLGA sphere which act as a carrier for the surface chemistries (as introduced in chapter 3), and a PLGA adhesive which is temperature sensitive and cures at 37^{o}C binding the spheres. For this *in vitro* study the injectable system was cured into cylindrical scaffolds using a modified syringe. During the development of this technology the mechanical properties were examined and the ratio of adhesive to spheres was optimised for its suitability for bone regeneration. This optimised ratio was used in this work.

Modified beads (component 1) were mixed with the adhesive component (component 2) in a ratio of 1:3. They were sterilized by exposure to UV ozone for 10 seconds, and shaken. This was repeated three times, to ensure even exposure of beads to sterilizing environment.

A modified 1mL syringe was used to mould the scaffolds. The calibrations on the barrel of the syringe were used to measure the volume of the scaffold. The pr-mixed and optimised bead/adhesive mixture was packed into the syringe to a volume of 60µl. A previously optimised cell number of $0.5x10^{6}$ hMSCs was seeded onto the scaffold in a 100µl of serum free MSC media (Lonza, UK). The syringe mould was then incubated at 37^{o} C in 5% CO_2 for 30 minutes to cure. The cured scaffold was then ejected from its mould into a 6 well tissue culture plate and covered with 10 mL of basal MSC culture media with serum

(Lonza UK) placed on a shaker plate at 65rpm, and cultured at 37^{o} C in 5% CO_2 for 7, 14 and 28 days. Fresh media was added every 3 days.

2.1.10. Sample preparation for LDH Assay

LDH is an intracellular membrane bound marker which is released during cell lysis. The quantity of LDH that is released is consistent enough to aproximate the number of cells present using a serial dilution of cell lysates. A serial dilution of cells was made to create a standard curve of cells for the assay. Released LDH can be measured and related back to the standard curve of cells, to ascertain number on the scaffolds. The following concentrations of cells were prepared in 1mL of serum-free basal media (Lonza, UK); 0, $1x10^5$, $2.5x10^5$, $5x10^5$ and $1.2x10^6$. These tubes were then frozen at -80^{o}C until required for assay. Prior to assay samples were subjected to repeated freeze/thaw cycles to ensure complete release of LDH from all cells. All experiments were repeated 4 times.

At the 14 and 28 day time points, scaffolds were removed from their well and placed into a new 12 well tissue culture plate with 1 mL of serum free MSC media (Lonza, UK). As serum contains LDH, it should not be used with this assay. The scaffold was crushed, and placed in a -80^{o}C freezer. Samples were then subjected to the same freeze/thaw cycle described above to ensure complete release of LDH from all adhered cells throughout the scaffold.

2.1.11 LDH Assay

12mL of assay solution was added to 1 bottle of substrate mix (Promega, UK). 50µl of each of the test samples was added to a 96 well plate (SLS, UK). Each sample was run in triplicate. A standard curve was created using the positive LDH control in the kit (Promega,

UK). The following dilutions of units of LDH per mL were made; $6.6x10^{-4}$, $3.3x10^{-4}$, $1.65x10^{-4}$, $8.3325x10^{-5}$. These dilutions were made in PBS with 1% bovine serum albumin (BSA) (both Sigma, UK).50 µl of each of the dilutions were added to the empty wells on the 96 well plate. 50µl of standard cell solutions were added to empty wells. 50µl of assay buffer was added to all wells. After 30 minutes incubation in dark, 50µl of stop solution were added to the well plate. Each plate was measured on a plate reader at 492nm wavelength immediately. 4 separate repeats were conducted and data was analysed using standard deviations and ANNOVA to determine the variance of means and any statistical significance between the modifications.

2.1.12. Histology

The histological investigation of the 3D scaffolds was undertaken to examine the penetration of cells into the scaffold, and to ascertain if any of the cells had differentiated.

2.1.13. Fixation

Samples were removed from culture at 7, 14 and 28 day time points. They were fixed with a 2.5% solution of glutaraldehyde (Sigma, UK) for 48 hours, and dehydrated by 2 hour submersions in 70, 90 and 100% ethanol solutions.

2.1.14. Embedding of Samples in Glycolmethacrylate (GMA) Resin

Samples were embedded using Technovit 8100 (TAAB, UK) glycolmethacrylate (GMA) based resin. 100mL of base glycomethacrylate solution was mixed with 1 sachet of hardener 1. To 90mL of this solution 3mL of hardener 2 was added. Samples were then

placed into moulds and covered with the embedding solution and put in a vacuum on ice for 20 minutes. Samples were then removed from the vacuum oven, mineral oil was placed on top of the embedding solution, and then they were placed at -55^{o}C for 4 days, 4^{o}C for 6 hours prior to ejection from moulds.

2.1.15. Sectioning

Seven μm thick sections were taken from the resin blocks using a Polycut sledge microtome (Leica UK). These sections were floated in a water bath at room temperature and captured on a glass microscope slide pre-coated with aminopropyltriethyoxysilane (APTES) (Sigma UK).

2.1.16. Haematoxylin and Eosin stain

Haematoxylin and Eosin (H&E) stains the cell nucleus (blue) and cytoplasm (pink). This stain is useful for determining the extent of cellular infiltration throughout the scaffold.

Sections were taken through decreasing concentrations of ethanol (100%, 90% and 70%) for 2 minutes each then put into distilled water for 2 minutes. Sections were then stained with Harris's haematoxylin (Sigma, UK) for 5 minutes, washed in running alkali tap water for 5 minutes, differentiated using acid alcohol (100mL ethanol with 1mL of 1M hydrochloric acid (Sigma, UK)) for 2 seconds, washed with distilled water and stained with 1% Eosin (Sigma, UK) for 3 minutes. Sections were washed for 2 minutes in distilled water, followed by dehydration through increasing concentrations of ethanol (70%, 90% and 100%) for 2 minutes each, cleared in xylene (BDH, UK) for 2 minutes then mounted with glass coverslips in DPX (BDH, UK).

2.1.17. Van Gieson stain

Van Giesons' stain for collagen will show any of the multiple types of collagen that is produced by the cells in the scaffold. It does not differentiate between the different types of collagen and is a generic collagen stain. This is useful as an investigative stain to show the production of collagen by the differentiated stem cells, as the cells have to go down either an osteogenic or chondrogenic pathway to produce collagen.

Sections were taken through decreasing concentrations of ethanol (100%, 90% and 70%) for 2 minutes each then put into distilled water for 2 minutes. Sections were stained for 30 minutes with Weigerts' haematoxilyn (Sigma UK), then washed in running alkali tap water for 5 minutes. Samples were differentiated using 1% acid alcohol (100mL ethanol with 1mL of 1M hydrochloric acid (Sigma, UK)) for 2 seconds, and washed well with distilled water. Van Giesons stain (100mL of saturated picric acid solution) (Sigma, UK) was added to 5mL of 1% acid fuchsin solution (Sigma, UK). This solution was used to stain the sections for 5 minutes. Samples were blotted with filter paper and dehydrated through increasing concentrations of ethanol (70%, 90% and 100%) for 2 minutes each and cleared in xylene for 2 minutes followed by mounting with glass coverslips in DPX (BDH, UK).

2.1.18. Von Kossa stain

Von Kossa's stain for mineralisation is a standard test for osteogenic mineralisation. It only stains mineralised tissues and is a key indicator in the osteogenic differentiation pathway of MSCs.

Sections were hydrated using 3 submersions in distilled water for 2 minutes each, then covered with 2% silver nitrate solution (Sigma UK) and placed under a UV lamp for 1 hour. Samples were washed with distilled water and put in a 2.5% sodium thiosulphate solution (Sigma UK) for 3 minutes. Samples were washed with distilled water and counterstained using Harris's haematoxylin (Sigma UK) for 5 minutes, washed in running tap water for 5 minutes and differentiated in 1% acid alcohol for 2 seconds before being washed in distilled water. Samples were dehydrated through increasing concentrations of ethanol (70%, 90% and 100%) for 2 minutes each and cleared in xylene (BDH, UK) for 2 minutes prior to mounting with a glass coverslip in DPX (BDH, UK).

2.1.19. Alcian Blue stain

Alcian blue stains for glycosaminoglycan (GAG). GAG is a key marker for chondrogenic differentiation, there are many types of GAG, but Alcian blue is a generic stain for all GAG's, which are key proteoglycans in the chondrogenic differentiation pathway.

Sections were taken through decreasing concentrations of ethanol (100%, 90% and 70%) for 2 minutes each then put into distilled water for 2 minutes. Sections were stained for 30 minutes with alcian blue solution (1g of alcian blue 8GX (Sigma UK) dissolved in 3% glacial acetic acid (Sigma UK)). Samples were washed in running alkali tap water for 2 minutes then counterstained with nuclear fast red stain (Sigma UK) for 5 minutes and washed for 1 minute in running alkali tap water. Samples were then dehydrated through increasing

concentrations of ethanol (70%, 90% and 100%) for 2 minutes each and cleared in xylene for 2 minutes then mounted with glass coverslips in DPX (BDH, UK).

2.1.20. Alizarin Red stain

Alizarin red is a key histological stain for mineralised tissue, and an important marker for osteogenesis.

Samples were taken through decreasing concentrations of ethanol (100%, 90% and 70%) for 2 minutes each then put into distilled water for 2 minutes. 2% aqueous solution of Alizarin red (Sigma, UK) adjusted to pH to 4.1-4.3 with 10% ammonium hydroxide was applied to the sections for 5 minutes. Sections were blotted with filter paper. Samples were dehydrated through submersion for 2 minutes in increasing concentrations of ethanol (70%, 90% and 100%) and cleared by submersion in xylene for 2 minutes. Sections were then mounted with glass coverslips in DPX (BDH, UK).

2.1.21. Cryo SEM examination of cellular samples

Samples were removed from culture, washed with PBS and fixed in an aqueous solution of 2.5 % Glutaraldehyde (Sigma, UK) for 15 minutes. Samples were stored at 4^{o}C in Dulbecco's PBS (Sigma, UK).

Samples were prepared further immediately before examination by snap freezing in liquid nitrogen slush (BOC, UK) under vacuum using a Gatan Alto preparation station (Gatan, UK). Samples were transferred under vacuum to a Gatan Alto 2500 (Gatan UK) cryo transfer system which had been cooled to -190^{o}C with liquid nitrogen. The sample was sublimated by increasing the temperature of the chamber to -95^{o}C and held at that temperature for 15 minutes. The sample was then sputter coated with platinum, to a thickness of 20 nm and transferred under vacuum to the Gatan cold stage, which was chilled

to -190^{o}C with cooled nitrogen gas. The samples were examined using a LEO-1550 Field emission scanning electron microscope secondary electron detector at 5kV(Carl Zeiss SMT Ltd, UK).

2.1.22. MSCs on 3D scaffold prepared with multiple layers of modification

Beads modified with different chemistries were assembled to determine if a different response was observed when the chemistries varied across the scaffold. This aim would have implications in osteochondral regeneration, where a banded/zoned response would be necessary.

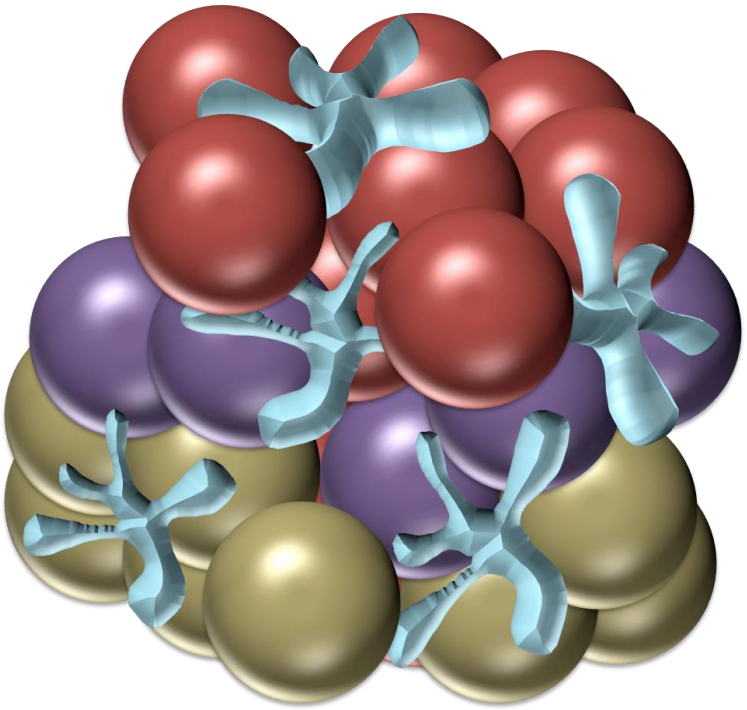

Figure 2.1: Diagram of layered surface modified spheres in scaffold, red spheres depict amine modified surface, purple spheres depict hexane modified surface and gold spheres depict allyl alcohol modified spheres.

The individual modifications were mixed with adhesive in 1:3 ratio. The total volume of the scaffolds was 120μl. The scaffold layers were prepared in the modified syringe (discussed earlier in this chapter) as described in the table below:

Scaffold Number	Total scaffold 120μl		
1	40 μl Allyl amine	40μl Hexane	40μl Allyl alcohol
2	60μl Allyl amine	60μl Allyl alcohol	
3	120 μl Allyl amine		
4	120 μl Allyl alcohol		
5	120 μl Hexane		
6	120 μl Unmodified Control		

Table 2.1: Diagram showing quantities and layer format of modified spheres incorporated into scaffold

The individual modifications were packed into the modified syringes to the specified volumes, and then the scaffolds were seeded with $1x10^6$ MSCs in 100 μl of serum free media (both Lonza, UK) for 60 minutes at 37^oC. The scaffolds were then ejected from the syringes into a 6 well plate, filled with MSC media with 5% serum (Lonza, UK). The samples were cultured on a rocker plate for 7, 14 and 28 days, with 2 mL media added every 3 days. The samples were then fixed with glutaraldehyde and processed using the histological processing technique described above.

2.2. Methods for preparation and analysis of silane modified borsilicate glass

2.2.1. Preparation and modification of borsilicate glass.

Glass was used as a substrate for the modifications in the initial investigation of the response of MSCs and and primary human osteoblast-like cells cultured with silanes.

Glass was cleaned using a 0.5M solution of sodium hydroxide (Sigma, UK) for 30 minutes in a ultrasonic bath, the samples were then washed in 3 changes of distilled water, and placed in 1M nitric acid for 30 minutes in an ultrasonic bath. Samples were then washed with 3 changes of distilled water and dried in a 50^{o}C oven. Clean coverslips were then modified using the silanes in table 2.2 in 0.1M solutions for 30 minutes. Samples were then washed with isopropyl alcohol for 5 minutes and then washed with distilled water.

2.2.2. Atomic Force Microscopy(AFM)

The modified coverslips (both Glass and PLGA-coated) were attached to glass microscope slides using double sided adhesive tape. The samples were examined using an AFM microscope (operated by Mark Murphey at Liverpool John Moores University). 3 samples of each modification were examined and 4 areas on each of the samples were scanned in tapping mode on 500nm scan area. The maximum feature height was measured, and averaged (using Argile light software). The results were analysed using ANOVA.

2.2.4. Ninhydrin on films and glass

The concentration of the $–NH_2$ groups on the silane modified surfaces were measured using a ninhydrin assay. 0.35g of ninhydrin (Fluka, UK) was dissolved in 100mL of ethanol.

1mL of this solution was placed on each of the samples and incubated for 5 minutes at 90^{o}C. The solution was removed from the coverslips and diluted 1:3 with ethanol. Light absorbance were measured spectroscopically at 600nm. A standard curve of each of the above listed silanes concentrations was measured and plotted and the resulting equation from each curve was used to apply to the unknown concentrations (see appendix for standard curves/equations). The coverslips were photographed showing a colour change on the surface of the substrate, to qualitatively asses the distribution of the NH_2 groups across the surface.

2.2.5 Water contact angle (WCA) measurements

Double sided materials were used for this technique, as the WCA were measured using a Camtel DCA machine (Camtel LTD, UK) which takes the reading from both sides of the material inserted into the water. These measurements were repeated 6 times for each modification. The results were analysed using ANOVA to see if there was any significant difference between the surfaces.

2.2.6. Material modification and PBS interaction

Silane modified glass discs were placed into a 24 well plate, in addition to an untreated glass control. The sample tests were conducted as follows:

Concentration of minerals in PBS solution	CL3	CL4	CL6	CL7	CL11	Untreated control
H_20	x	x	x	x	x	x
34.25mM sodium chloride, 0.675mM potassium chloride, 2.5mM phosphate	x	x	x	x	x	x
68.5mM sodium chloride, 1.35mM potassium chloride, 5mM phosphate	x	x	x	x	x	x
137mM sodium chloride, 2.7mM potassium chloride,	x	x	x	x	x	x

10mM phosphate						

Table 2.2. Matrix of experiments conducted using varying concentrations of PBS

One PBS tablet (Sigma, UK) was dissolved in 200mLs of distilled water. The following dilutions of PBS were made using distilled water; 0%, 25% 50% and 100%.

The plate was incubated at 37^{o}C for 7 days. The samples were removed from the and left to dry at room temperature for 24 hours. The samples were then examined using X-ray analysis and stained by Von Kossa stain for mineralisation.

2.2.7. Von Kossa stain as 2.1.18

2.2.8. X-ray analysis of glass and films

Elemental analysis of the surfaces was undertaken to determine if the coverslips taken from PBS solutions had mineralised. Baseline data of the dry film was also measured to ensure that there was no background mineralisation occurring and that the minerals present were as a direct result of chemical interaction when the surfaces were exposed to PBS.

The coverslips that were exposed to PBS and water were removed from the PBS solution and allowed to air dry for 24 hours.

Dry modified films and glass coverslips were coated with carbon using a carbon coater (EMTECH, UK). X-ray microanalysis was performed using a Leo 1550 SEM (Zeiss, UK) with an INCA system (Oxford Instruments). Points of analysis were imaged at 5 locations on the film. From each of these fields 10 spectra were generated at random. The resulting data were analyzed using ANOVA, to determine any statistically significant difference between the elements on the surfaces.

2.2.9. Culture of Mesenchymal stem cells (MSC) as in 2.1.8

2.2.10. Application of Mesenchymal stem cell to modified Glass

Passage 5 MSCs were allowed to reach confluence, trypsined as described in section 2.1.8 and pelleted. The individual pellets from each flask were re-suspended in 1mL of media each and pooled into one centrifuge tube. These cells were then pelleted again, and re-suspended in 5mL of mesenchymal stem cell media (Lonza, UK) media. 200µl of the cell suspension were removed and the cell number was counted using a haemocytometer (AGAR, UK) on an inverted light microscope (Zeiss Ltd, Germany). Cells found in 5 areas were counted and averaged, this number corresponding with the cell number $x10^4$ per mL of cell suspension. A total cell number (in the 5mL cell suspension) was determined, and the cells were re-suspended to make the seeding density $5x10^5$ cells in 100µl media.

The pre-prepared materials were sterilised using 10 sec exposure to ultra violet (UV) light with ozone on both sides, and placed into a sterile 24 well tissue culture plate (SLS, UK). A 100µl aliquot of the cell suspension was then pipetted onto each material, and incubated at 37^oC for 30 minutes. Two mL of media was then added to each well. Samples were then cultured for 7, 14 and 28 days at 37^oC and 5% CO_2.

2.2.11. Von Kossa staining of Coverslips

Media was removed from wells and coverslips were washed using a 10% Dulbecco's PBS solution. PBS was removed and the cells on the coverslips were fixed using a 2% formaldehyde 4% sucrose solution (Sigma UK) for 15 minutes. Fixative was then removed

and samples were washed with PBS. After 3 submersions in distilled water the protocol outlined in section 2.1.18 was followed.

2.2.12. SEM

The modified glass coverslips with primary human Mesenchymal stem cells were removed from culture, washed with PBS and fixed using 2.5% glutaraldehyde solution, for 15 minutes. The samples were then washed with PBS, and submerged in 70% ethanol for 15 minutes, then 90% ethanol for 15 minutes followed by two changes of 100% ethanol for 15 minutes. The samples were then dried using a critical point dryer (Prion, UK). Dry samples were then affixed to aluminium SEM stubs (Agar Scientific, UK) using double sided carbon sticky tabs (Agar Scientific, UK). The samples were then coated with 20nm of chromium using a sputter coater (EMTECH, UK). The coated samples were observed under a Leo 1550 FESEM (Zeiss, UK).

2.2.13. Preparation of RNA using Trizol (Sigma, UK)

Scaffolds or coverslips were removed from media at the appropriate time points, and placed into clean 24 well tissue culture plates (SLS Ltd, UK). Samples were washed using sterile Dulbecco's PBS (Sigma, UK) to remove any non-adherent cells. Scaffolds were crushed manually and 500µl of Trizol (Sigma, UK) added to each well and incubated at room temperature for 5 minutes. Trizol reagent (Sigma, UK) then removed from the scaffolds and placed into DNA/RNA-free micro-centrifuge tube (SLS, UK) and frozen until required at -80 ^{o}C, at which point they were defrosted at room temperature.

100µl of chloroform (BDH, UK) was added to defrosted samples and vortexed. Samples were spun at 18,000g for 5 minutes. The upper layer of each preparation was then removed and placed into a new tube. 300µl of isopropanol (Sigma, UK) was then added, and

centrifuged at 18,000g for 15 minutes. The supernatant was removed, without disturbing the RNA pellet. 500µl of 100% ethanol was added, and sample spun for 5 minutes at 18,000g. The supernatant was removed and replaced with 200µl of 70% ethanol and spun for 2 minutes at 18,000g. The supernatant was removed and pellet was re-suspended 10µl of DNA/RNA-free ultra pure water. (Sigma, UK) Generic DNA contamination was eliminated using commercially available DNAse kits (Invitrogen UK).

8µl of RNA sample was inserted into a DNA/RNA free micro-centrifuge tube (SLS, UK). 1µl of 10X DNase reaction buffer and 1 µl DNase I Amp grade was added (Invitrogen, UK). Tubes were incubated at room temperature for 15 minutes and the DNase I was inactivated by the addition of 1µl of 25mM EDTA solution (Invitrogen, UK) before heating to 65^{o}C for 10 minutes.

First strand cDNA was synthesised using kit (Invitrogen, UK) 10µl of DNase treated RNA was added to a DNA/RNA micro-centrifuge tube. 1µl of oligo(dT), 1µl of 10mM dNTP mix and 1µl of sterile distilled water was added per reaction. Samples were heated to 65^{o}C for 5 minutes, then incubated on ice for 1 minute. 4µl of 5X first strand buffer, 1µl of 0.1M DTT, 1µl of RNaseOUT, and 1µl SuperScript III RT was added to each tube, mixed and incubated at 50^{o}C for 1 hour. The reaction was inactived by heating to 70^{o}C for 15 minutes. The resulting cDNA was used as a template for rt-PCR.

2.2.14 rt-PCR

qrt-PCR was conducted using primers for osteopontin, osteocalcin, osteonectin, collagen I, collagen II, and CBFA-1, with all results normalised against the housekeeping gene B-Actin. 20µl of forward and 20µl of reverse primers were mixed with 160µl of DNA/RNA-free water. The following reagents were added in triplicate to the wells of a rt-

PCR 96 well plate (BIO-RAD, UK): 2µl cDNA template, 7.5µl SyBR green (BIO-RAD, UK), 4.5µl DNA/RNA-free water, and 1µl diluted primer (as above). rt-PCR was conducted using i-cycler (BIO-RAD,UK), using optimum temperatures for each primer (table 2.4).

Target	Accession number	Primer bases	Temp in ^{o}C
B-Actin	NM001101	GGACCTGACTGACTACCTCGCC ATCTCTTGCTCGAAG	53.9
Collagen I	NM000088	GCCACTCCAGGTCCTCAGCCAC AGCACCAGCAACAC	54.5
Osteocalcin	NM000711	AGCGAGGTAGTGAAGAGACGAA AGCCGATGTGGTCAG	55.2
Osteopontin	NM000582	GCGAGGAGTTGAATGGTGCTTG TGGCTGTGGGTTTC	53.9
Osteonectin	BC008011	GCTGGATGATGAGAACAACACA AGAAGTGGCAGGAAGAG	53.4
Collagen II	NM001844	GAGCAGCAAGAGCAAGGAGAA GTGGACAGCAGGCGTAGGAAG	54.3
CBFA I	AH005498	GGCAGTTCCCAAGCATTTCGCA GGTAGGTGTGGTGTG	54.5
Sclerostin		CTGGTTAAGAAAGTTGGATAAG AAGGTTACACAGCAAGTTAG	53.8

Table 2.4. Primer bases for the corresponding gene of interest, and temperature at which reaction takes place.

All samples were run for 40 cycles using pre-programmed settings on i-cycler. The threshold cycle (Ct) (the cycle at which the instrument detects the amplification generated fluorescence above the background fluorescence) was measured in triplicate in each case and averaged. The experiment was repeated 6 times. The results were shown as the $\Delta\Delta ct$,[1] and were normalised to the housekeeping gene, B-actin.

2.2.15. Immunostaining for Confocal Microscopy

Cells on the silane-modified glass and PLGA were fixed using a 2% formaldehyde (Sigma, UK) and 4% sucrose (Sigma, UK) fixative. The samples were washed in PBS. The

samples were blocked/permabolised using a solution of 1% BSA PBS with 0.1% triton X100 (Sigma, UK) with 10% normal horse serum (Vector, UK) added, for 45 minutes at 37^{o}C. The samples were then washed using 1% BSA PBS.

The samples were stained using antibodies for osteocalcin (BD biosciences, UK), CBFA1(BD biosciences, UK), collagen I and II(Abcam, UK) and stro-1(Abcam, UK). The antibodies were diluted as below:

Antibody	Dilution in 1% BSA PBS
Osteocalcin	1/500
CBFA 1	1/500
Stro-1	1/500
Collagen I	1/1000
Collagen II	1/500

Table 2.5. List of primary antibodies and the dilutions at which they were used for the antibody staining

100µl of primary antibody were added to the samples, and incubated at 4^{o}C for 16 hours. Collagen I and II antibodies were added to the same sample to create a dual stain, the remaining antibodies were used as single stains. The samples were washed using 1% BSA PBS. The secondary antibodies (all from Life Technologies, UK) were added as below.

Primary antibody	**Secondary antibody**
Osteocalcin	Rhodamine
CBFA-1	Texas red goat anti rat
Stro-1	Alexa fluor 633 goat anti mouse
Collagen I	594 HTC Chicken anti rabbit
Collagen II	488 HTC anti mouse IgG 2a

Table 2.6. Table of primary antibodies with the corresponding secondary antibody.

100µl of each the secondary antibodies were added to the samples and incubated at 37^{o}C in the dark for 1 hour. Samples were then washed using PBS, and the osteocalcin, CBFA1 and Stro-1 samples stained using Oregon green (Life technologies, UK) to detect

actin cytoskeleton. The samples were then washed with PBS and examined using a confocal microscope (Zeiss, UK) after being mounted using Vecta shield with Dapi (Vector UK).

2.2.16. Isolation of primary human osteoblast-like cells

The extent to which the surfaces can could induce MSC along an osteogenic differentiation pathway was investigated at key temporal points. MSCs are a good model for the initial cell response to surfaces, and the primary human osteoblast-like cells are a good model for later stage events in the osteogenic pathway.

Human bone fragments taken from osteo-arthritis surgery were washed with a solution of PBS with streptomycin and penicillin (Sigma, UK). The bone was then cut into 1-2mm diameter pieces, and 6-8 of the bone pieces were placed in a 9cm diameter disposable Petri dish with 10mL of DMEM culture media enriched with foetal bovine serum (Sigma, UK). 5mL of media was removed and replaced every 2 weeks. Cultures were left until cells migrated from the bone and populated the culture dish and reached confluence which was 6-8 weeks.

2.2.17. Primary human osteoblast like cells on silane modified glass

The silane modified glass coverslips were inserted into a 24 well tissue culture plastic plate. Primary human osteoblasts-like cells were washed with PBS then covered with 2 mL of Trypsin EDTA (Sigma, UK). The cells were incubated at 37^{o}C, and observed microscopically to check the progression of the trypsin digestion, when the cells started to lift off the plastic Petri dish 2mL of media was added to stop the reaction. $5x10^{-4}$ primary human osteoblasts were suspended in 100µl of DMEM media (Sigma, UK) and seeded onto the glass surfaces and incubated at 37^{o}C for 1 hour. After the hour incubation 2mL of

DMEM media (Sigma, UK) was added to each well. These samples were cultured for 7, 14 and 28 days.

2.2.18. Primary human osteoblasts-like cells on silane modified PLGA films

The silane modified PLGA films were inserted into a 24 well tissue culture plastic plate. Then treated as protocol 2.2.17.

2.2.19. Von Kossa staining of human osteoblast samples

As in section 2.1.18

2.2.20. SEM of primary human osteoblast samples.

As in 2.2.12

2.2.21. Nodule count and measurement

Nodule size was measured using the SEM. All nodules on each sample were measured across their widest diameter, using the micometer application on the annotation bar of the SEM. Every nodule was measured and the mean was noted, to provide the mean nodule size for each sample.

The numbers of nodules on each sample was counted using a light microscope (Zeiss, Germany) at low magnification so whole sample could be enumerated.

2.2.22. rt-PCR of osteoblast like cells

As in section 2.2.13

2.3. Preparation and silane modification of PLGA films and spheres

2.3.2. PLGA (85:15mw) film production and modification

PLGA films were produced as an initial investigation into the viability of PLGA as a substrate for silane modification.

Clean 12mm glass cover-slips were coated with chromium using an Emtech 575x sputter coater (Emtech, UK), to provide a surface for the PLGA film to form hydrogen bonds with. 100 µl of 10 % 85:15 PLGA (Sigma, UK) in chloroform was spin-coated onto the chromium coated cover slips using a WS-400B-6NPP/LITE spin coater (Laurell Technologies Corporation, UK). Oxygen plasma was used to functionalize the polymer using a plasma coater (Emtech, UK), at the previously optimised settings of 30kW for 2 minutes (see appendix).

The PLGA films were then modified with the following silanes:

Modification abbreviation	Silane used for modification
CL3	(3-Aminopropyl)triethoxysilane (Sigma)
CL4	4-(triethoxyslyl)butan-1-amine (fluorochem)
CL6	3-(2-Aminoethylamino) propyldimethoxymethylsilane (Sigma)
CL7	N-(6-Aminohexyl)amnomethyltriethoxysilane (fluorochem)
CL11	11-Aminoundecyltriethoxysilane (fluorochem)

Table 2.8 Index of silanes used for modifications

The silanes were diluted to 0.1M solutions with isopropyl alcohol. The PLGA films were then covered with these solutions for 30 minutes at room temperature. The solutions were then washed using isopropyl alcohol, and distilled water. Samples were left to dry at room temperature for 24 hours, followed by vacuum oven at room temperature for 24 hours.

2.3.3. AFM microscopy

The modified coverslips (both Glass and PLGA coated) were stuck to a glass microscope slide using double sided adhesive tape. The samples were examined using an AFM microscope (operated by Dr. Mark Murphey at Liverpool John Moores University). 3 samples of each modification were examined and 4 areas on each of the samples were scanned in tapping mode on 500nm scan area. The maximum feature height was measured, and their mean noted (using Argile light software). The results were analysed using ANOVA.

2.3.4. Ninhydrin on films and glass

The assay was conducted as in section 2.2.4

2.3.5. Preparation of Double Sided Materials for WCA

Double sided materials were required for this technique as the water contact angle is measured when the material is dipped into water. If the different sides were composed of different materials (ie, glass and polymer) the results would be unreliable.

Materials were prepared by coating glass coverslips with 20nm of chromium using an EMTECH 575X sputter coater (EMTECH, UK). This was repeated on both sides of coverslip. 1g of 85:15 PLGA was dissolved in 10 mL of Chloroform (Sigma, UK). The PLGA solution was spin coated onto the chromium coated glass using a WS-400B-6NPP/LITE spin coater (Laurell Technologies Corporation, UK), and dried overnight at room temperature before being inserted into a vacuum oven for 48 hour. The process was then

repeated for the other side of the coverslip. The materials were then modified with the silanes mentioned above in table 2.8, on both sides.

2.3.6. WCA measurements

Conducted as in section 2.25

2.3.7. SEM of modified films

Conducted as in section 2.1.6

2.3.8. Application of Mesenchymal stem cell to modified PLGA films.

Conducted as in section 2.2.10.

2.3.9. Von Kossa staining of Coverslips

Conducted as in section 2.18

2.3.10. Sphere Manufacture for Silane Modifications

85:15 PLGA (Sigma, UK) spheres were constructed using polyvinylalcohol (PVA) solution. 1g of PLGA was dissolved in 10 mL of tetrachloromethane added to a solution of 30 mL PVA (Sigma, UK) in a drop by drop method and stirred continuously for 72 hours until all solvent has evaporated. Spheres were then filtered and sieved so that only the particles

measuring 100-300μm were used. The spheres were then dried at room temperature for 48 hours.

2.3.11. Silane modification of spheres

PLGA spheres were oxygen plasma treated for 2 minutes at 30Kw, then submerged in 10 mLs of 0.1M silane in isopropyl alcohol on a rocker plate for 20 minutes (see appendix for optimisation data). The resultant solution was then filtered using a polypropylene funnel and flask (SLS, UK) to avoid silane retention by surface attachment to the glass flask. The beads were washed with 10mLs of isopropyl alcohol. The solution collected was then analysed using the ninhydrin technique to determine the amount of amine groups transferred to the spheres in this process (2.3.12). The spheres were then dried in a vacuum oven for 24 hours, and stored under vacuum until used.

2.3.12. Ninhydrin assay of modified spheres

The concentration of the $–NH_2$ groups on the silane modified spheres were measured using the ninhydrin assay. As it was difficult to measure accurately the concentration of $–NH_2$ tethered to the spheres directly, an indirect method was used. The concentration of the silane coating solution was known (1M) and the concentration of the coating solution was measured after the coating of the spheres took place, to determine the concentration of silane that remained on the spheres. A standard curve of each of the silanes concentrations was measured and plotted and the resulting equation from each curve was used to apply to the unknown concentrations (see appendix for standard curves/equations). Assay was then conducted as in section 2.2.4.

2.3.13. SEM of PLGA spheres

The modified spheres were mounted onto aluminium SEM stubs (Agar, UK) using double sided carbon stickers (Agar UK). The spheres were then coated with 40nm of chromium to illuminate charge, and observed under the SEM (Zeiss, UK) to determine if there were any macro-topographical differences between the modifications.

2.3.14. MSC on PLGA system

Silane modified Spheres were incorporated into the 3D injectable system described in section 2.1.

2.3.15. Histology

The histological investigation of the 3D scaffolds was undertaken to examine the penetration of cells into the scaffold, and to ascertain the degree of cell differentiation.

2.3.16. Fixation

Samples were removed from culture at 7, 14 and 28 day time points. They were fixed with a 2.5% solution of glutaraldehyde (Sigma, UK) for 48 hours, and dehydrated by successive 2 hour submersions in 70, 90 and 100% ethanol solutions respectively.

2.3.17. Embedding of Samples in Glycomethacrylate Resin

Samples were embedded using Technovit 8100 (TAAB, UK). 100mL of base glycomethacrylate solution were mixed with 1 sachet of hardener 1. To 90mL of this solution 3mL of hardener 2 was added. Samples were then placed into moulds and covered with the embedding solution and placed in a vacuum on ice for 20 minutes. Samples were then removed from the vacuum oven, mineral oil was placed on top of the embedding solution, and then they were then placed at -55^{o}C for 4 days and 4^{o}C for 6 hours prior to ejection from the moulds.

2.3.18. Sectioning

As in section 2.1.15

2.3.19. H and E stain

As in section 2.1.16

2.3.20. Van Geison stain

As in section 2.2.17

2.3.21. Von Kossa stain

As in section 2.1.18

2.3.22. Alcian Blue stain

As in section 2.1.19

2.3.24. Alizarin Red stain

As in section 2.1.20

2.3.25. Sample preparation for LDH Assay

As in section 2.1.10

2.3.26. LDH Assay

As in section 2.1.11

1. Benedetto, A., Abete, M.C., Squadrone, S. Towards a quantitative application of real-time PCR technique for fish DNA detection in feedstuffs Food Chemistry **126** 1436–1442(2011)

Chapter 3: Results: Plasma Polymer Deposition Modifications to Injectable PLGA System

3.1 Introduction

The injectable PLGA system was modified with four different surface modifications. These modifications include allylamine, allylalcohol, hexane and acrylic acid. The active terminal groups that are deposited on the surfaces treated with these plasmas are listed in the table below:

Chemical modification	Terminal group deposited
Allyl amine	$-NH_2$
Allyl Alcohol	-OH
Hexane	$-CH_3$
Acrylic Acid	-COOH

Table 3.1, **Chemical modification.** Themost abundant chemical group deposited from specific chemical modification.

All of the above chemical modifications have been selected because they are terminal groups found in the extracellular matrix, and are thought to play a role in the osteogenic and chondrogenic differentiation pathways[1]. The chemical groups have been shown to be the active regions on many osteogenic peptides, which have been used extensively in the past as an attempt to mimic the ECM, and have shown positive results[2,3]. There are several reasons why the use of peptides to mimic ECM are limited, the most striking reason being the prohibitive expense of producing peptides on a large scale[4], so applications for medical devices are limited. The use of stable chemistries as an instigator of MSC differentiation could improve the efficiency of the injectable system by applying and refining the knowledge

gained from all of the studies involving peptides[5,6,] and larger proteins intended to mimic some aspects of the ECM.

Applying these surface chemistries to an injectable system is novel, and this chapter of results aims to screen the four surface chemistries and asses their ability to cause the differentiation of MSCs in this *in vitro* model, which uses cured pieces of the injectable system, comprising of two components as demonstrated in figure 3.1.

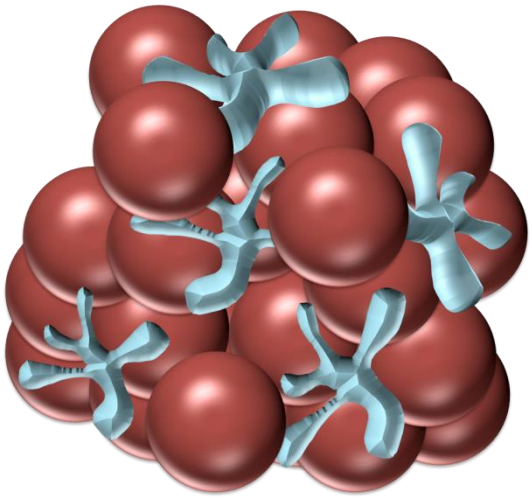

Figure 3.1, **The two phase injectable scaffold**. Red spheres carry the chemical modification and the amorphous shapes represent the adhesive component.

The red spheres are the components that carry the surface modifications and the blue amorphous shapes are the PEG-treated PLGA adhesive component, which cures at 37^{o}C. The two components are mixed together in a modified syringe and the powders are seeded with MSCs whilst compacted into the syringe. The system cures as the MSCs are adhering prior to the scaffold being ejected from the modified syringe mould. The scaffolds are cultured in 6 well plates on a rocker plate to allow the flow of nutrients throughout the porous scaffold.

The materials were characterised using water contact angle, SEM and XPS prior to the incorporation of the material into the in vitro model. This *in vitro* system was analysed

using electron microscopy and LDH assay to determine cell number, histological staining techniques and analysis to determine the expression of differentiation markers throughout the scaffolds.

3.2 Water contact angle of modified materials.

The water contact angle of the polymers changed after modification of the polymer. The allyl amine modified PLGA showed a statistically significant difference in water contact angle, (using ANOVA and Tukey statistical tests) when compared to an untreated control ($p=<0.05$) (figure 3.2). The allyl amine modification introduced a more hydrophilic surface than the control. The hexane showed some statistical significance and introduces a significantly more hydrophobic surface. The acrylic acid showed a significantly more hydrophilic surface, than the untreated control and the other modifications. The allyl alcohol modification also demonstrated a significant difference, showing the modification to be more hydrophilic than the control. All these data are advancing angles only, and demonstrate that different surface energy and charge has been created on these surfaces. The advancing angle is more significant than the retreating angle because it is this initial contact that is relevant to cellular contact with the biomaterial.

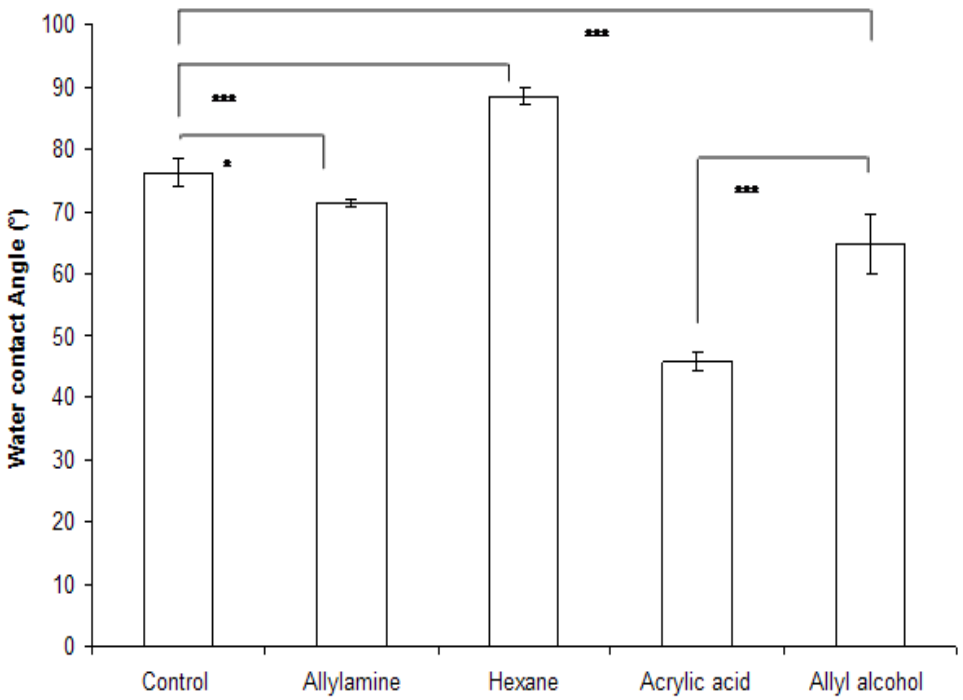

Figure 3.2 Water contact angle of modified PLGA to measure changes in surface energy.

Modified spheres were compacted into cakes (n=10). Starred bars indicate level of significance as determined by ANOVA and Tukey statistical tests * represent the level of significance (* p=<0.05, ***p=<0.01)

3.3 SEM of modified spheres

The SEM images of the treated spheres show no macro-topographical changes after the surface modifications have been applied when compared to the untreated spheres. The spheres all appeared to be smooth and largely undamaged following modification. The diameter of the spheres ranged from 30μm up to 300μm.

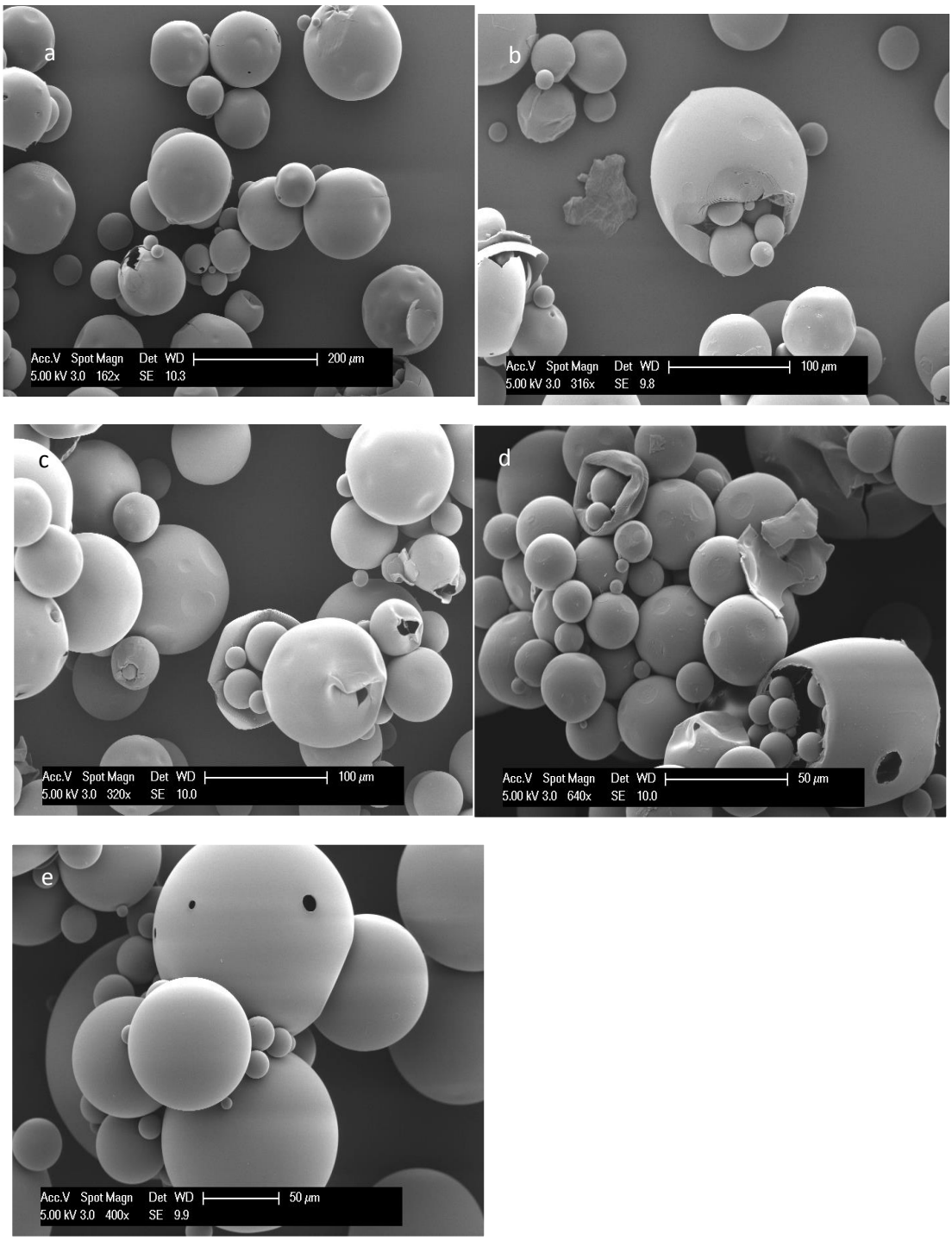

Figure 3.3. **SEM images of the plasma treated spheres**. Spheres were treated with the plasma polymer deposition system and images were taken of the spheres using a secondary electron detector 5kV accelerating voltage. The labelled images refer to the following modifications (a) Allyl amine, (b) Allyl alcohol, (c) Hexane, (d) Acrylic acid, and (e) untreated PLGA.

3.4 X-ray Photoelectron spectroscopy (XPS)

Six separate batches of modified spheres were analyzed using X-ray photoelectron spectroscopy (XPS) to determine the elemental composition of the modified surfaces (n=6). The summary table highlights the average and standard deviations of the repeats (table 3.2). These XPS data demonstrated the increased concentration of carbon on the hexane modified surfaces (84.2% weight ±1.0). As it is hypothesized that the hexane modified surface would be enriched with methyl groups, this confirms the success of the modification. The XPS spectra for the allyl amine modification showed the presence of nitrogen on the surface(10.1% weight ±1.0). This was indicative of the presence of amine groups, again demonstrating the successful transfer of surface chemistries to the substrate. The increase in the surface oxygen seen on the acrylic acid modification (21.3% weight ±1.2) is indicative of the transfer of carboxyl groups. The allyl alcohol modification did not show any major changes detectable by XPS from the control, but this is likely to be explained by the limitations of the XPS technique as hydrogen is undetectable by XPS, and it is likely that it would be hydroxyl groups deposited on the allyl alcohol surface.

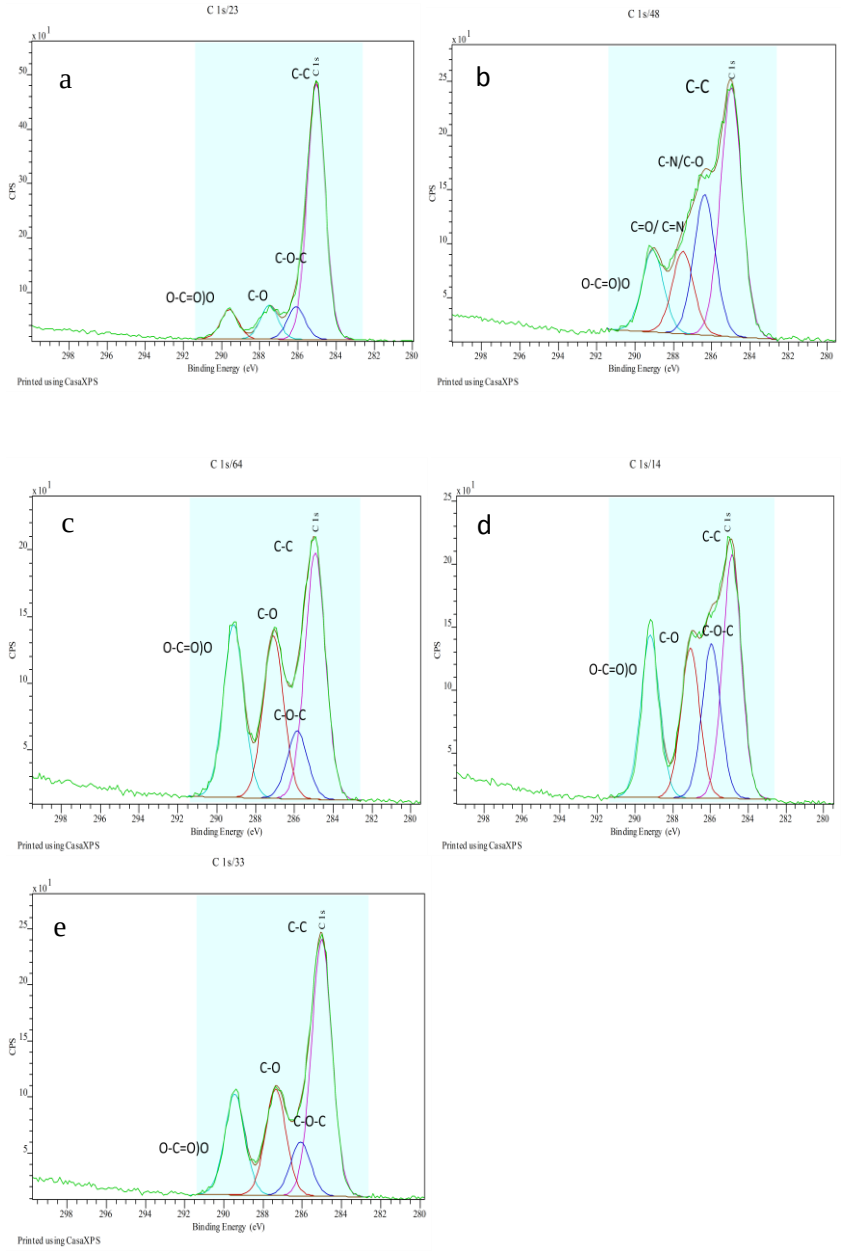

Figure 3.4. **X-ray photoelectron spectroscopy (XPS)** Spheres were treated with the plasma polymer deposition system and spectra of the modified spheres and an untreated control were taken (n=6). The labelled spectra are typical examples of the spectra taken and refer to the following modifications (a)Hexane, (b) allyl amine, (c) allyl alcohol, (d) acrylic acid, and (e) Unmodified spheres and show the presence of chemistry specific bonds (outlined on spectra).

Modifications	Carbon	Nitrogen	Oxygen
Untreated	78.9 ±1.9		21.1±1.9
Allylamine	62.7±4.2	10.1±1.0	23.5±4.0
Hexane	84.2±1.0		15.8±1.0
Acrylic acid	55.7±1.5		43.0±0.6
Allylalcohol	77.4±1.2		21.3±1.2

3.5 Cryo SEM of MSCs on plasma treated 3D scaffolds

The cryo SEM images (Figure 3.5) show the morphology of the MSCs when cultured on the surfaces for 14 days. The allylamine-modified scaffold lead to the cells presenting a flattened morphology, showing good infiltration into the scaffold and the presence of ECM. The allyl alcohol-modified scaffold had cells presenting a very rounded morphology. The untreated and hexane-treated scaffold had cells presenting classical stem cell morphologies.

This investigation demonstrated that the morphology of the cells on the different modified scaffolds was not the same, and that there was a significant quantity of ECM found on the allyl amine-modified scaffold.

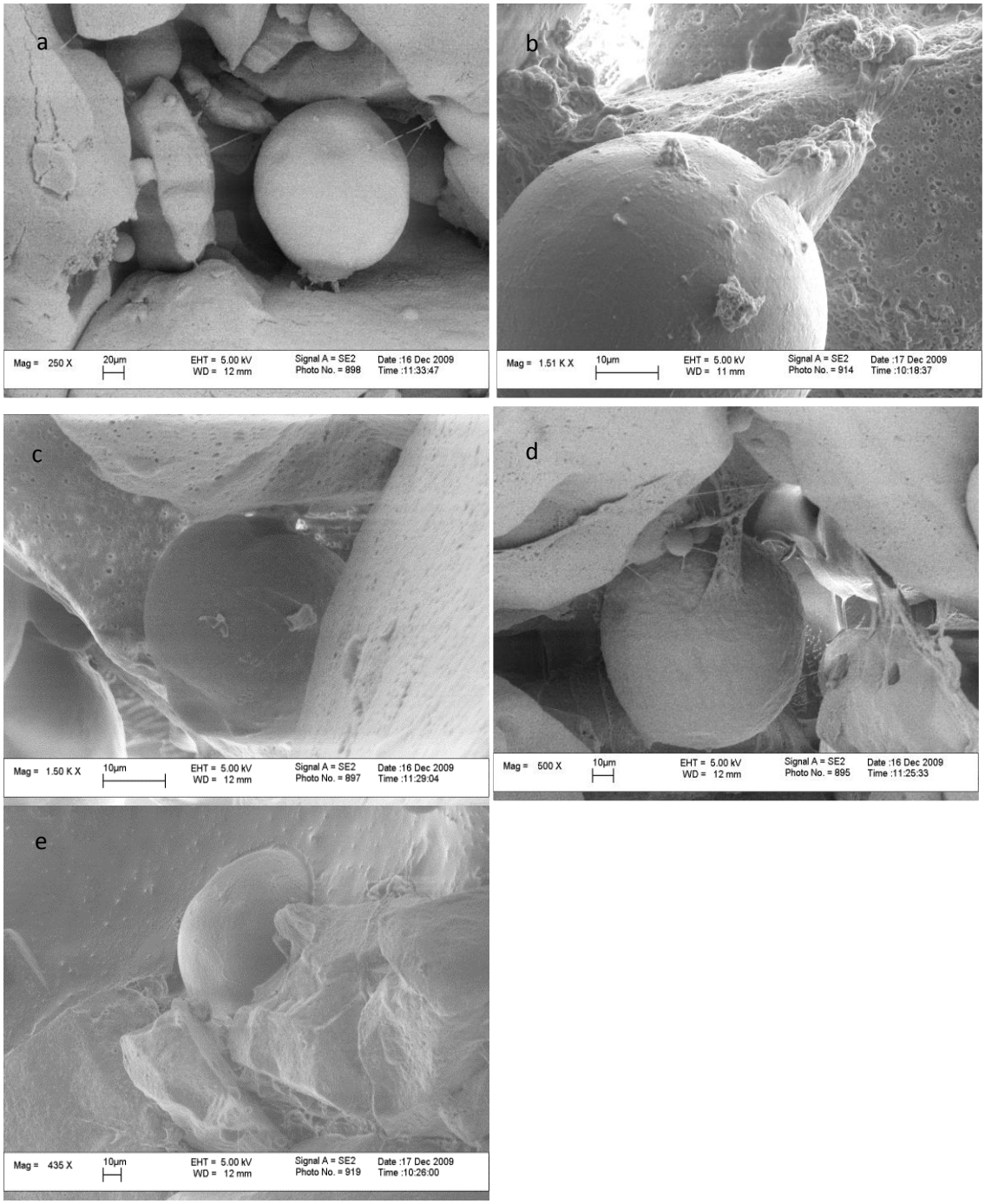

Figure 3.5:Cryo SEM images of Mesenchymal stem cell seeded onto the modified injectable system. (a) Hexane, (b) Allyl alcohol, (c) Acrylic acid,(d)Allyl amine, and(e) Untreated scaffold.

3.6 LDH assay to detect cell number on 3D scaffold

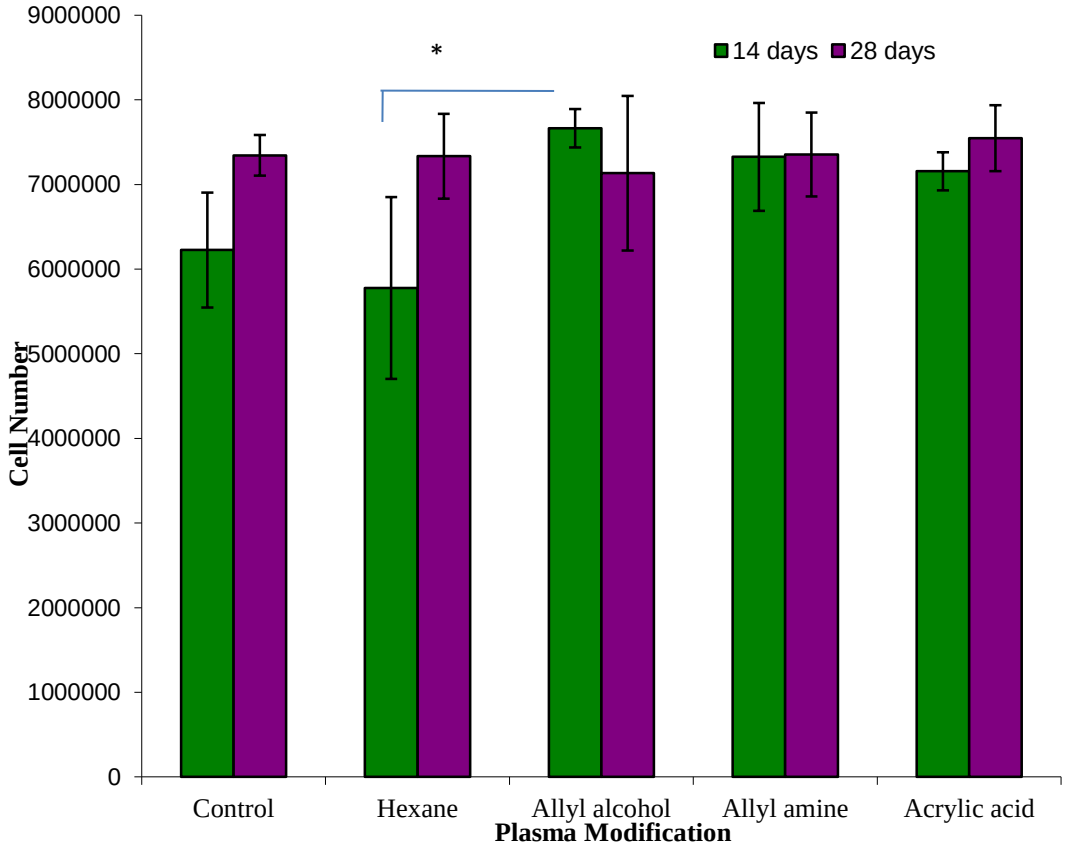

Figure 3.6, **LDH assay analysis of cell number on modified scaffolds.** Scaffolds were seeded with MSC for 14 and 28 days, and an LDH assay was conducted on the modified and untreated scaffolds after maceration at these timepoints. (N=4) * Indicates a statistically significant difference of p=<0.05

The LDH assay was conducted to determine cell number. The data shown were the mean and standard deviation of 4 repeats. They demonstrated an initial increase in cell number over a 14 day period (initial seeding density was 0.5 $x10^6$), then proliferation between 14 and 28 days in the control, hexane and acrylic acid scaffolds but a plateau between 14 and 28 days for the allyl alcohol and allyl amine scaffolds. There was a

statistically significant difference between the cells at 14 days on the hexane and the allyl alcohol scaffolds ($p=0.05$).

These results support the Cryo SEM (figure 3.5) examination because the plateau of the cell number could be indicative of stem cell differentiation. As this plateau was observed only on the allyl alcohol and allyl amine scaffolds, it is likely that stem cell differentiation was limited to these two scaffolds.

3.7 Histological analysis of Plasma treated scaffolds

	Hexane			Allyl alcohol			Allyl amine			Acrylic acid			Untreated PLGA		
	200µm	400µm	600µm	200µm	400µm	600µm	200µm	400µm	600µm	200µm	400µm	600µm	200µm	400µm	600µm
Van Geison	+	+	+	+	+	+	+	+	+	+	+	+	+	+	+
Alcian Blue	-	-	-	-	-	-	-	-	-	-	-	-	-	-	-
Alizian Red	-	-	-	-	-	-	-	-	-	-	-	-	-	-	-
Von Kossa	-	-	-	-	-	-	-	-	-	-	-	-	-	-	-

Table 3.3,Summary of Histological staining at 7 days MSC were cultured on scaffolds for 7 days and then processed and analysed using the histological stains mentioned above. Microns refer to location of section when taken from scaffold.+ = positive staining, -= negative staining

	Hexane			Allyl alcohol			Allyl amine			Acrylic acid			Untreated PLGA		
	200µm	400µm	600µm	200µm	400µm	600µm	200µm	400µm	600µm	200µm	400µm	600µm	200µm	400µm	600µm
Van Geison	+	+	+	+	+	+	+	+	+	+	+	+	+	+	+
Alcian Blue	-	-	-	+	+	+	-	-	-	-	-	-	-	-	-
Alizian Red	-	-	-	-	-	-	-	-	-	-	-	-	-	-	-
Von Kossa	-	-	-	-	-	-	-	-	-	-	-	-	-	-	-

Table 3.4. ,Summary of Histological staining at 14 days MSC were cultured on scaffolds for 7 days and then processed and analysed using the histological stains mentioned above. Microns refer to location of section when taken from scaffold.+ = positive staining, -= negative staining

	Hexane			Allyl alcohol			Allyl amine			Acrylic acid			Untreated PLGA		
	200µm	400µm	600µm	200µm	400µm	600µm	200µm	400µm	600µm	200µm	400µm	600µm	200µm	400µm	600µm
Van Geison	+	+	+	+	+	+	+	+	+	+	+	+	+	+	+
Alcian Blue	-	-	-	+	+	+	-	-	-	-	-	-	-	-	-
Alizian Red	-	-	-	-	-	-	+	+	+	-	-	-	-	-	-
Von Kossa	-	-	-	-	-	-	+	+	+	-	-	-	-	-	-

Table 3.5 ,Summary of Histological staining at 28 days MSC were cultured on scaffolds for 7 days and then processed and analysed using the histological stains mentioned above. Microns refer to location of section when taken from scaffold.+ = positive staining, -= negative staining

The histological examination of the scaffolds was repeated 3 times. The samples containing MSCs were sectioned at 7μm and sections were stained at 200 μm intervals throughout the scaffold to determine if there was a homogeneous response throughout the scaffold. The images presented are of the 28 day samples (experimental details 2.1.12-20).

The histological examination of the scaffolds (figures 3.7-3.11) reveal strong infiltration of cells throughout most of the scaffolds (as demonstrated by the H and E staining in figures 3.7d, 3.8d, 3.9d, 3.10d) and less observable infiltration in acrylic acid (figure 3.7e). The cells acted consistently throughout the scaffolds, with the notable production of GAG on the allyl alcohol scaffold at every measured physical point (ascertained by the positive alcian blue staining throughout, figure 3.10e) from 14 days onwards. The allyl alcohol scaffold also showed positive Van Giesons stain (figure 3.10c) for collagen from day 7, but no positive staining for alizian red or Von Kossa which would denote calcification or a more generalized mineralization.

Conversely, the allyl amine-treated scaffold showed positive alizian red (figure 3.7b) and Von Kossa(figure 3.7a) at 28 days but not before, and no alcian blue staining. There was however positive Van Gieson (figure 3.7c) staining at all time points.

The hexane and acrylic acid treated scaffolds both showed positive staining for the Van Gieson staining (figure 3.9c), but no positive staining for GAG (figure 3.9e) or mineralization(figure 3.9 a and b). The untreated control also showed a positive Van Geisons stain but no other positive staining for the other differentiation markers (figure 3.11 a-e).

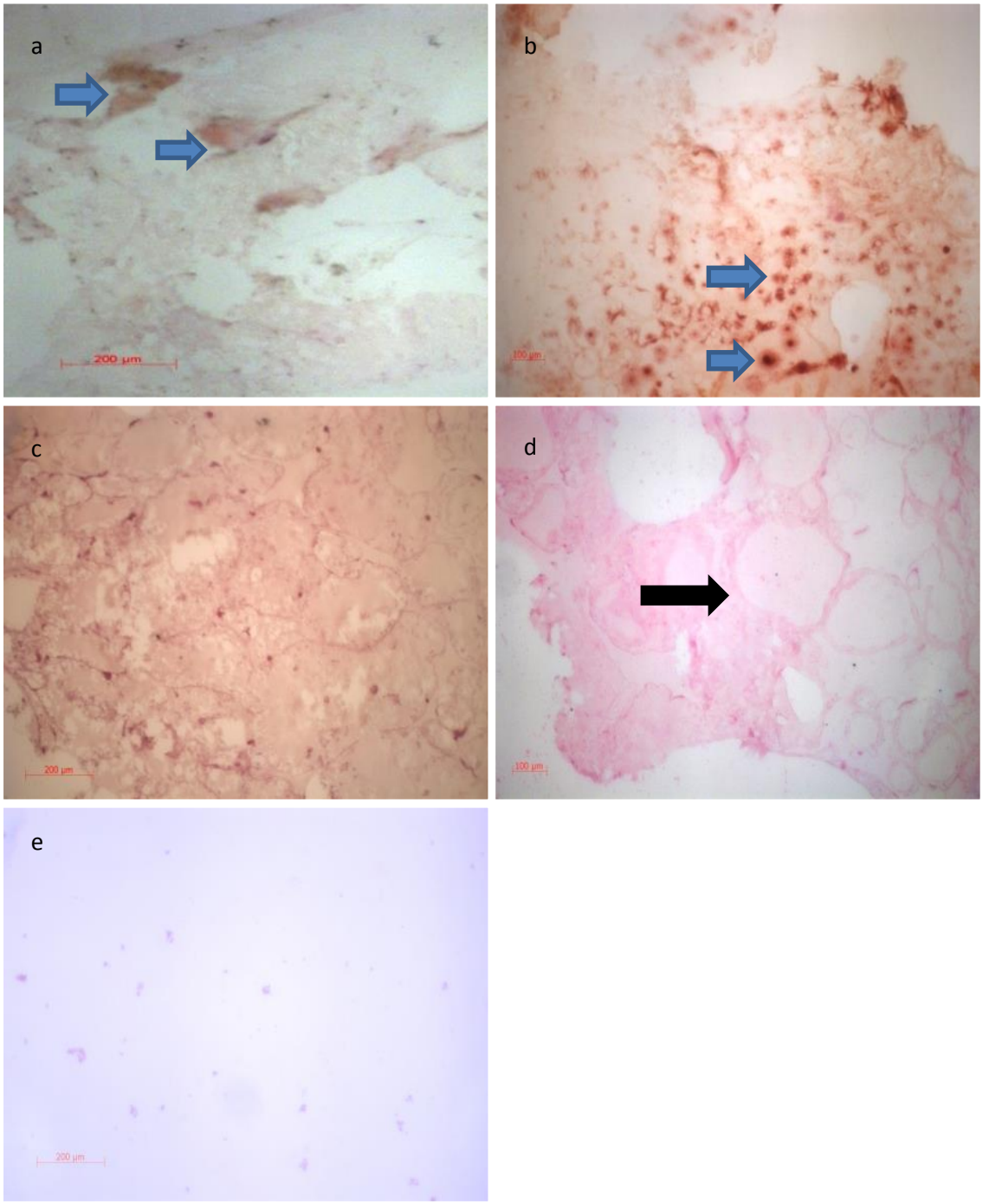

Figure 3.7:**Histological analysis of allyl amine-treated scaffolds**. Scaffolds were cultured with MSCs for 28 days, histologically processed and stained with (a) Von Kossa for mineralization, (b) Alizarin red for mineralization, (c) Van Geison for collagen, (d)H and E for cellular morphology and density and (e)Alcian blue for gylosaminoglycan.Blue arrows indicate areas of mineralisation and black arrow indicates area of dense cell population

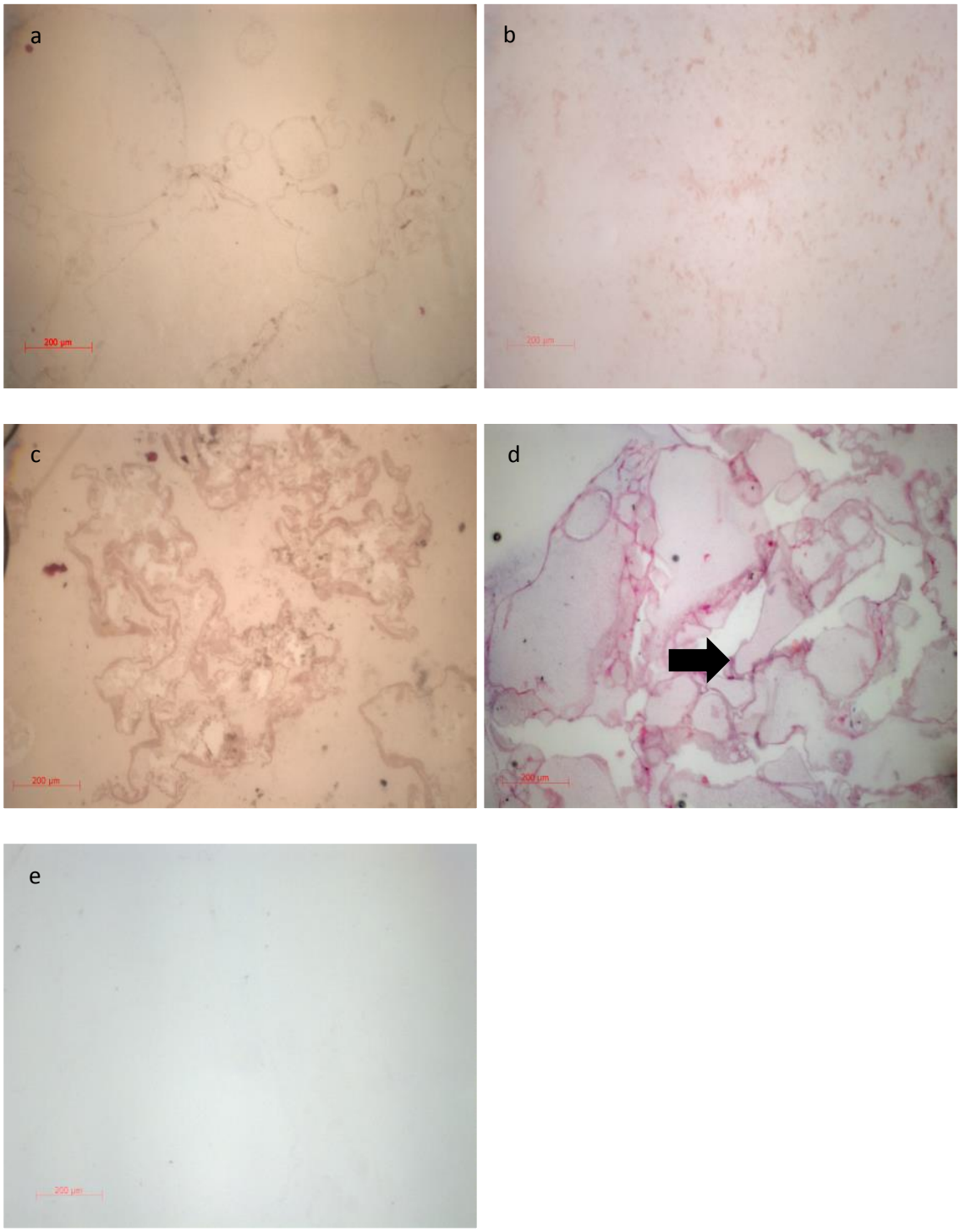

Figure 3.8: **Histological analysis of hexane-treated scaffolds**. Scaffolds were cultured with MSCs for 28 days, histologically processed and stained with (a) Von Kossa for mineralization, (b) Alizarin red for mineralization, (c) Van Geison for collagen, (d)H and E for cellular morphology and density and (e)Alcian blue for gylosaminoglycan.Black arrow indicated dense population of cells but no other staining present to show any differentiation

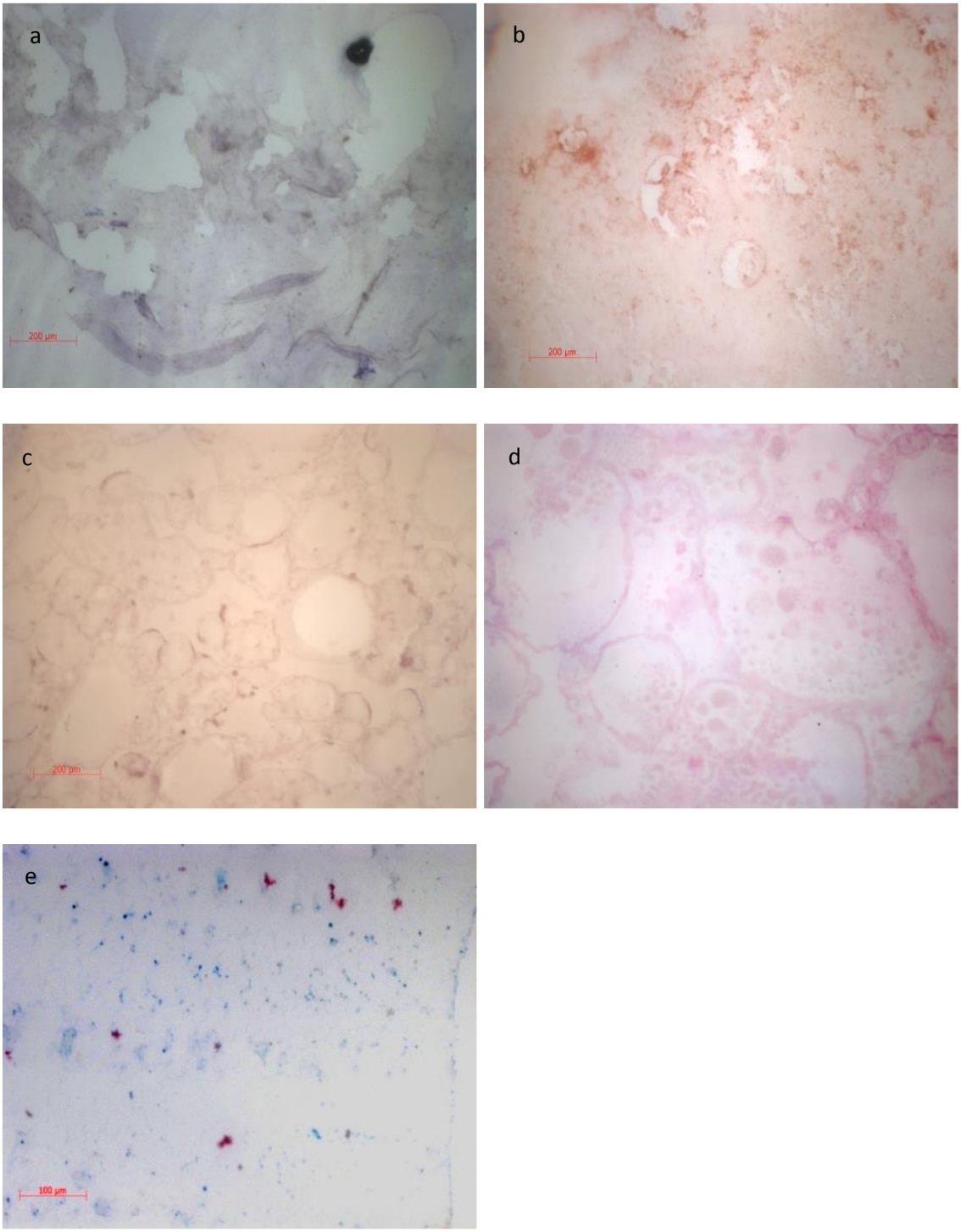

Figure 3.9: **Histological analysis of acrylic acid-treated scaffolds**. Scaffolds were cultured with MSCs for 28 days, histologically processed and stained with (a) Von Kossa for mineralization, (b) Alizarin red for mineralization, (c) Van Geison for collagen, (d)H and E for cellular morphology and density and (e)Alcian blue for gylosaminoglycan.

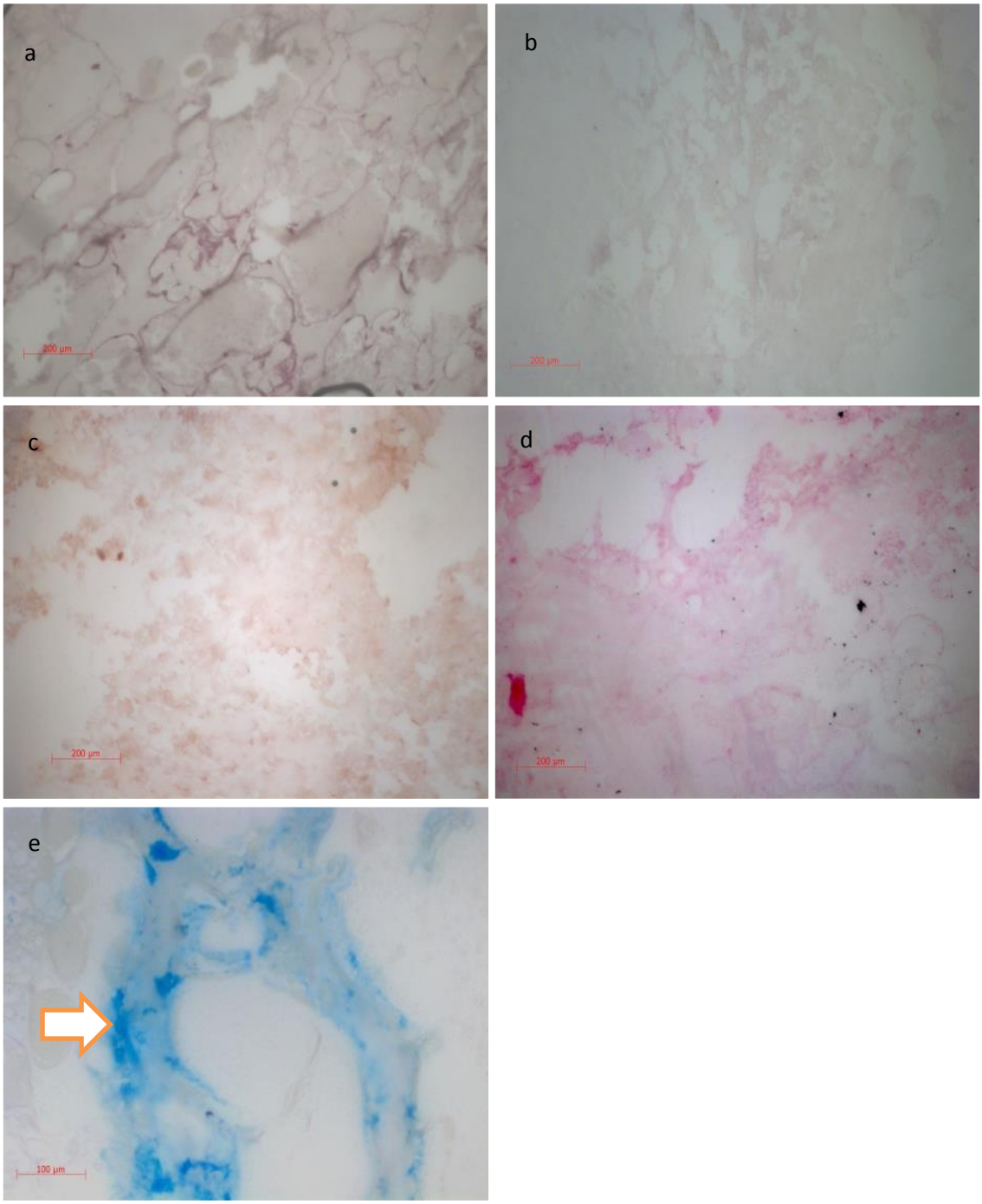

Figure 3.10: **Histological analysis of allyl alcohol-treated scaffolds**. Scaffolds were cultured with MSCs for 28 days, histologically processed and stained with (a) Von Kossa for mineralization, (b) Alizarin red for mineralization, (c) Van Geison for collagen, (d)H and E for cellular morphology and density and (e)Alcian blue for gylosaminoglycan (GAG). White arrow indicated positive GAG staining

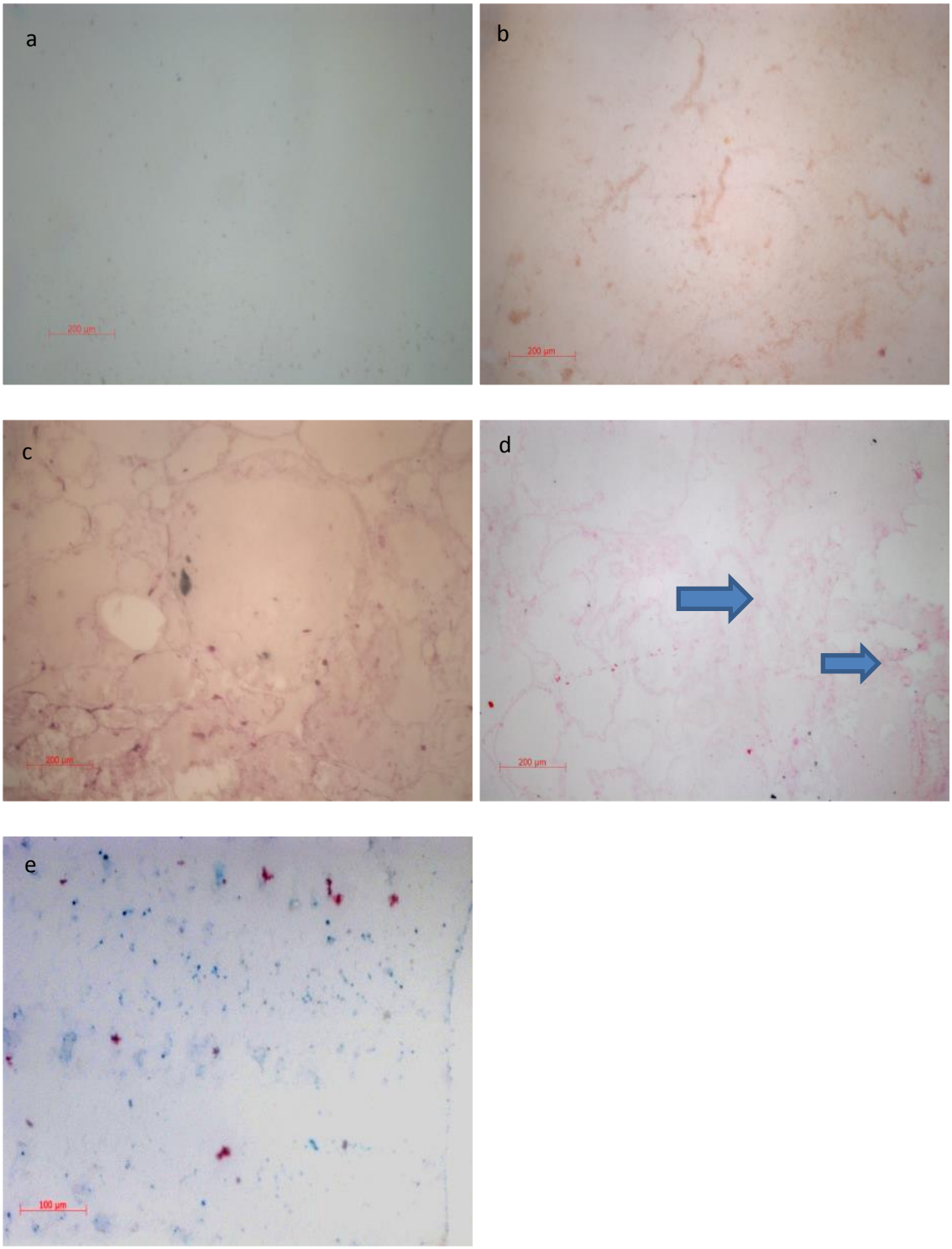

Figure 3.11 **Histological analysis of untreated scaffolds**. Scaffolds were cultured with MSCs for 28 days, histologically processed and stained with (a) Von Kossa for mineralization, (b) Alizarin red for mineralization, (c) Van Geison for collagen, (d)H and E for cellular morphology and density and (e)Alcian blue for gylosaminoglycan.Blue arrows indicate areas of cells stained with eosin.

3.8 Histological analysis of Dual and triple modifications.

	Triple Modification	Dual Modification	Hexane	Allyl Amine	Allyl Alcohol	Untreated Control
Alizian red	Banded + area	Mixed response	-	+	-	-
Alcian Blue	Banded + area	Mixed response	-	-	+	-

Table 3.6: **Histological analysis of dual and triple modifications.** Allyl amine and allyl alcohol modified spheres were compacted in two layers of the same scaffold (dual modification) and allyl amine, hexane and allyl alcohol were compacted into three layers of the same scaffold (triple modification). The scaffolds were processed and stained using alizian red and alcian blue. + indicates positive staining found, -indicates no staining.

The scaffold carrying three modifications showed positive staining for Alcian blue, in an isolated area at one end of the scaffold while simultaneously showing positive Alizian red staining at the opposite end of the scaffold. The central portion of the scaffold showed positive mineralization staining but in a fine honeycomb type presentation, with the 3 distinct areas in defined bands. The dual modification did not show banded separation like the triple modification, and there was a mixed cellular response. The single modifications showed positive Alcian blue staining on the allyl alcohol scaffold, positive Alizian red and Von Kossa staining on the allyl amine scaffold, and positive van Gieson staining on all of the scaffolds.

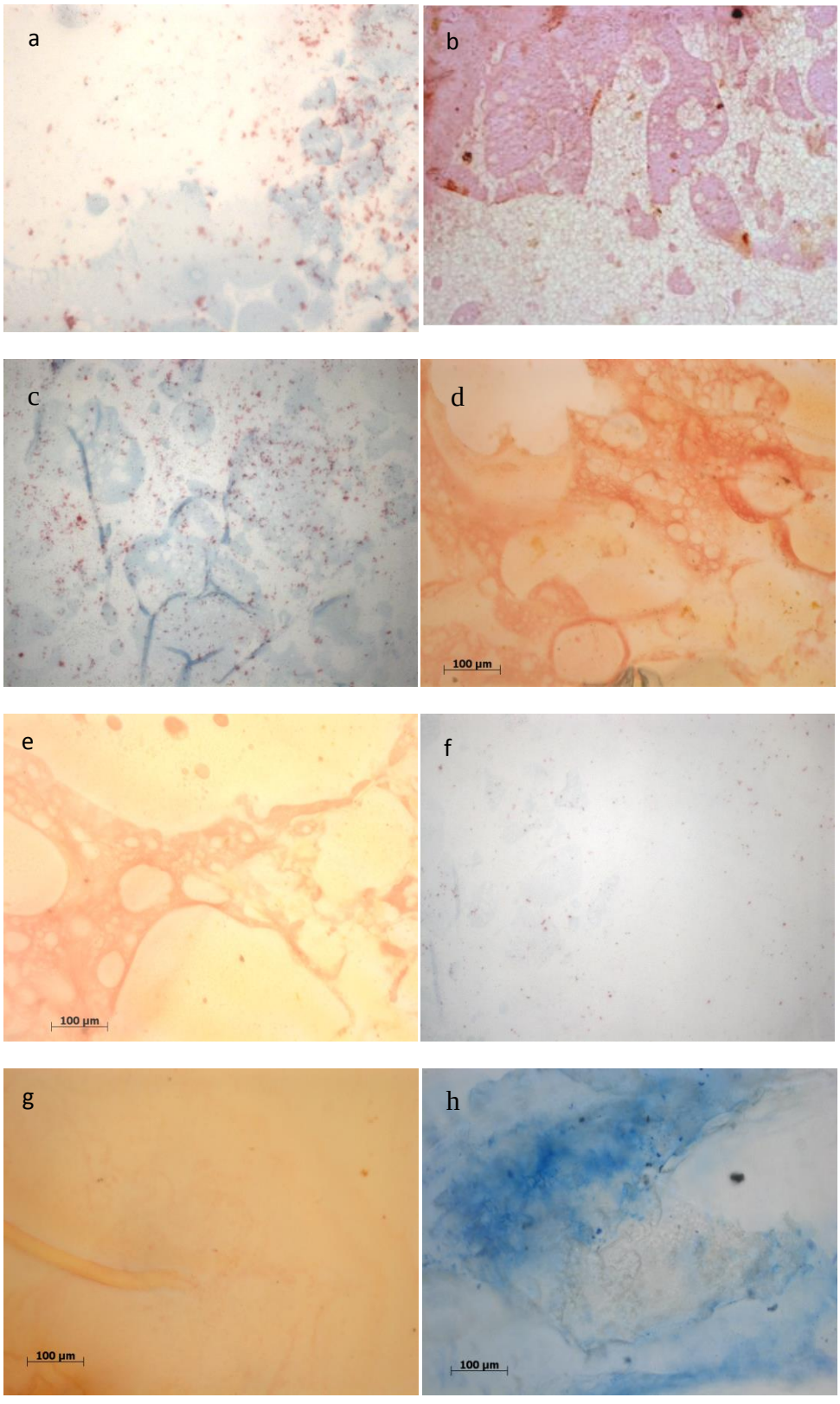

Figure 3.12 **Images from dual and triple scaffold modifications**. Allyl amine and allyl alcohol modified spheres were compacted in two layers of the same scaffold (dual modification) and allyl amine, hexane and allyl alcohol were compacted into three layers of the same scaffold (triple modification). The scaffolds were processed and stained using alizian red and alcian blue. (a)Alcian blue stain of triple modification scaffold, (b) Alizian red of triple modification scaffold, (c) Alcian blue of dual modification, (d) Alizarin red of dual modification, (e) Alizarin red stain of single allyl amine modified scaffold, (f) Alcian blue stain of single allyl amine modified scaffold, (g) Alizarin red of single allyl alcohol modified scaffold, and (h) Alcian blue single modification allyl alcohol scaffold

3.9 Discussion of Plasma modifications

The material characterization data demonstrated that the transfer of the chemistries to the surfaces was successful, as a change in surface energy was clearly demonstrated by the water contact angle measurements (figure 3.2). This alone testifies that the surfaces have changed, but the XPS data (figure 3.4 and table 3.2) confirms the change in the surfaces chemical composition. Together, with the SEM images which show no macro-topographical changes to the surfaces (figure 3.3), the evidence supports the hypothesis that the chemistries have been introduced in such a manner that they have been responsible for the phenotypical changes in the human MSCs.

The true evidence of differentiation is in the direct staining of the products of the cells and this is supported by the histological analysis conducted (tables 3.3-3.5, and figures 3.7-3.11). The presence of a collagen matrix was confirmed by consistent Van Gieson staining through the scaffold (figures 3.7-3.11). Van Gieson stains collagen but does not differentiate between the different types of collagen. Further histological examination of the scaffolds revealed an osteogenic response throughout the amine treated scaffold (figure 3.7), where positive Von Kossa staining was concentrated in nodules and seen in every sample point throughout the scaffold. The Von Kossa stain targets calcified ECM using silver nitrate to react to the phosphate which accompanies calcium in mineralized matrix in an acidic environment[7], and as mineralization of the ECM is one of the key markers of osteogenic differentiation it is often seen as a definitive test. It does not however indicate that there is bone formation, and caution should be taken before making this statement, as the staining does not indicate the calcium to phosphate ratio, which is crucial when determining the mineral formation of bone.[7] The alizarin red stain, which also stains mineralized matrix, was consistent with the Von Kossa stain (figure 3.7), showing patches of mineralized matrix in nodules thoughout the amine-modified scaffold.

The LDH assay (figure 3.6)demonstrated that all the modifications support cell expansion, but there is a plateau of cell numbers on the amine modification between 14 and 28 days. There are a few possible explanations for this result, there is evidence as explained above that the cells are starting to differentiate by 28 days, and this could indicate that the cells present in the scaffold are starting to enter a differentiation phase, and are in a non-proliferating state.

Another possible explanation is the transfer of nutrients within the scaffold becomes slower as the pores become blocked with cells and ECM, causing either some cell death or that the cells have become non-proliferative. There is the possibility that both of these processes are occurring to some extent. There is evidence in the histology at day 28 that the amine modification induces an osteogenic response from the cells, but there is also evidence that some of the pores are starting to fill with cellular material, a phenomena that is demonstrated further by the H and E staining (figure 3.7). It may be that the flattened morphology of the cells on this scaffold (demonstrated by the cryo SEM) (figure 3.5) leads to a reduction in the nutrient flow through the scaffold. This suggests that a bioreactor may be necessary; to increase cell number at 28 days and also increased osteogenic differentiation.

The histological examination of the scaffolds showed that the hydroxyl modification was the only modification to support chondrogenic differentiation, as there were patches of positive Alcian blue staining within the serial sections. Alcian blue stains GAGs which are markers of chondrogenesis (figure 3.10). The positive Alcian blue staining was supported by the cryo SEM visualization of cellular morphology (figure 3.5). The cells on the scaffold appeared to be a rounded which is entirely consistent with chondrocytic behavior *in vitro*.[8] The Van Gieson stain was consistent throughout the scaffold, highlighting the collagen, which was present throughout the scaffold. Combined with the Alcian blue stain, and the absence of any Von Kossa or Alizian red staining, the data indicates material-induced chondrogenic differentiation associated with the hydroxyl modification.

There was no evidence of differentiation on the hexane modification (figure 3.8), consistent with published data, showing that this surface chemistry is a useful tool in the maintenance of stem cell phenotype, as the LDH assay demonstrated that the MSCs do proliferate on this modification, the cell number increasing between 14 and 28 days.[1, 9] There is a statistically significant difference between the hexane-modified scaffolds and the allyl alcohol-modified scaffolds at 14 days. This shows that the cells do not proliferate as quickly on the $-CH_3$ surfaces as on the allyl-alcohol surfaces. The hexane surface, as stated previously, seems to maintain stem cell phenotype, and it may be that the reduced cell number means that the cells are unable to create enough signaling growth factors to permit differentiation in these circumstances, at the correct time point. Conversely, the allyl alcohol-modified surface is conducive to enough cells binding in the initial period to create sufficient growth factors to differentiate when enough time has elapsed. This phenomenon may be investigated further by analyzing the intergrin binding molecule concentrations.

The evidence discussed above directly supports the hypothesis that the surface chemistry influences the lineage of MSCs when deposited on a 3D substrate (in this case an injectable PLGA bone regeneration system).

3.10 Dual and triple modifications

The data obtained from the modifications in single cultures was an invaluable insight into what could be possible from these modifications. The possibility of osteochondral defect treatment is something that would have wide reaching impact in regenerative medicine.The data suggest that controlling the surface chemistry of a scaffold can influence the fate of the cells migrating onto it, and fitting that into a wider context,potentially this could give rise to an injectable system consistent with the goals set out in the introduction. It could theoretically be used on many different types of material, and may not just be limited to the single effects seen. There are several specific areas in the

muscleroskeletal system which could benefit from a material which could increase the rate and quality of the repair, but are not homogeneous in their origin. The junctions between tissues, where they meet are often areas that do not heal well, but are multilayered so that a "one size fits all" approach would be wholly inappropriate.

The example of the osteochondral junction is an area that has had much investigation and little success in terms of repair, and could be greatly advanced by a smart material approach. Differing modifications spanning in bands across the same scaffold may well be a way to influence cells to form different populations, localizing the cell signaling and restricting it to certain areas within a scaffold. This could have wide reaching applications as an approach, and merited further investigation within this thesis.

The results from the single modification study, reported earlier, showed that the allyl amine modified scaffold lead to an osteogenic effect. The hydroxyl groups provided by the allyl alcohol modification were highlighted as a chemical modification that could achieve a chondrogenic effect, and during this dual and triple modification study, the modifications were put together in one scaffold to ascertain if it was possible to achieve the differentiation of MSCs into two different populations within opposite ends the same scaffold. To carry this idea further the hexane modification was utilized as a buffer in the central portion of the scaffold, as this modification deposited methyl groups which had previously been thought to retain MSC phenotype.[10]

As the identification of the phenotypic changes in these samples were localized, it was inappropriate to do any techniques that would homogenize the sample (such as rtPCR) so the option for identification purposes on these samples was restricted to the histological examination of scaffolds, which proved to be an ideal technique to examine the markers of differentiation within the scaffolds. The results showed that the dual scaffold with allyl amine and allyl alcohol modifications with no hexane layer showed no separation in the layers, and a mixed response from the MSCs (figure 3.12). There were no defined layers of staining when the Alcian blue and alizarin red stains were used. However, when the scaffold contained a layer of methyl rich hexane modification, there were

clearly defined bands of positive Alcian blue and alizarin red staining (figure 3.12). The area in-between the allyl alcohol and the allyl amine groups showed a positive alizarin red staining, which showed a honeycomb type structure, which could have been indicative of the early stages of mineralization within the methyl-rich layer. When comparing the scaffold to the natural osteochondral junction, the calcified cartilage layer is the layer that occurs between the bone and cartilage. The migration of calcification through the methyl-rich layer in the scaffold could be occurring because the signals between the two separate populations on stem cells have produced a gradient conducive to the production of a calcified cartilage layer.

While this is a very interesting result in terms of what is possible from a scaffold, and the parameters of localized surface chemistries, the plasma modifications are limited in their application, as it is difficult to achieve information about the concentration of the chemistries, and so difficult to characterize the surface enough to apply these modifications in a clinical setting. To actually transfer these findings to a clinically applicable model, the chemistry of the surfaces would have to be considerably more defined, and for this reason the pursuit of a chemical modification that can be easily measured and applied is still a priority. Wet chemical techniques are easier to monitor for consistency than using plasma, as the volume and concentration of the coating solution can be monitored accurately, where plasma is very difficult to monitor with any degree of accuracy.

1. Curran, J.M., Chen, R. & Hunt, J. A Controlling the phenotype and function of mesenchymal stem cells in vitro by adhesion to silane-modified clean glass surfaces. *Biomaterials* **26**, 7057-67 (2005).

2. Phillips, J.E., Petrie, T. A, Creighton, F.P. & García, A.J. Human mesenchymal stem cell differentiation on self-assembled monolayers presenting different surface chemistries. *Acta biomaterialia* **6**, 12-20 (2010).

3. Uematsu, K. Hattori,K., Ishimoto,Y. & Yamauchi,Y. Cartilage regeneration using mesenchymal stem cells and a three-dimensional poly-lactic-glycolic acid (PLGA) scaffold. *Biomaterials* **26**, 4273-9 (2005).

4. Chu, P.K. Enhancement of surface properties of biomaterials using plasma-based technologies.*Surface and Coatings Technology* **201**, 8076-8082 (2007).

5. Puppi, D., Chiellini, F., Piras, A.M. & Chiellini, E. Progress in Polymer Science Polymeric materials for bone and cartilage repair. *Progress in Polymer Science* **35**, 403-440 (2010).

6. Kroeze, R.J., Helder, M.N., Govaert, L.E. & Smit, T.H. Biodegradable Polymers in Bone *Tissue Engineering*. *Materials* **2**, 833-856 (2009).

7. Bonewald, L.F. Harris,S.E., Rosser,J.&Dallas,M.R. Von Kossa staining alone is not sufficient to confirm that mineralization in vitro represents bone formation. *Calcified tissue international* **72**, 537-47 (2003).

8. Chen, G., Sato, T., Tanaka, J. & Tateishi, T. Preparation of a biphasic scaffold for osteochondral tissue engineering. *Materials Science and Engineering:* C**26**, 118-123 (2006).

9. Goddard, J.M. & Hotchkiss, J.H. Polymer surface modification for the attachment of bioactive compounds. *Progress in Polymer Science* **32**, 698-725 (2007).

10. Curran, J.M., Pu, F., Chen, R. & Hunt, J. A. The use of dynamic surface chemistries to control msc isolation and function. *Biomaterials* **32**, 4753-60 (2011).

Chapter 4: Silane Modifications on Glass Substrate

Introduction

The aim of this chapter and chapter five is to use different application techniques to modify the surface chemistry of PLGA, and translate the baseline 2D effects into a 3D system, to enhance the differentiation of MSCs within a 3D platform.

The ultimate aim of the following result chapters is to enhance the efficiency of an injectable osteogenic regeneration system. For this reason the focus has been on molecules that have been seen in previous work to instigate an osteogenic response from MSCs. The literature, while supporting the osteogenic nature of the molecules used, does show that there is some conflict in the results reported by different studies[1,2]. It is therefore necessary to determine and optimise the material variables that induce osteogenesis.

By highlighting a core set of chemical groups (CH_3, COOH, NH_2 and OH) which were applied to a 3D system by a plasma polymer deposition technique, then focusing on one group (NH_2), which showed the most successful results for the purposes of osteogenic differentiation, we are refining the variables that will ultimately allow the application of the surface chemistries. Using the $–NH_2$ terminal group with a different application technique that allows greater control of the presentation of the terminal group allows us to explore variation in chain length. The potential of presenting the amine terminal group in a different way, will lead on from the initial plasma treated data and will attempt to elucidate the mechanism of the response seen, thereby enhancing the consistency of the response.

Initially, the starting point of this work studied a polymer plasma deposition system that was able to deposit chemical groups onto a surface in a random fashion. It was possible

with this technique to confirm the presence of different surface chemistries, but very difficult to determine the concentration of those terminal groups on the surface other than varying times of exposure, and power levels which were really dictated by what the underlying substrate could withstand before damage was incurred. The main positive feature about this technique was the application of this plasma could be performed on a 3D substrate, but it was impossible to define the exact concentration of the amine groups on the surface. Because of this, it would be very difficult to apply these chemistries to a bone regenerating material with the level of consistency required for the production of medical devices. For this purpose they need to be applied in a quantifiable and defined way, which can be measured *in situ* as the surface is being modified.

Silanes have been shown to be very versatile in this area[3], and because the preparation technique is by wet chemistry rather than an ionized gas technique, there is more potential for developing an assay to measure the deposition of chemical groups onto the surface during the manufacturing process. The technique that has been developed in this thesis is novel, using ninhydrin. The use of ninhydrin to detect free amine is well established.[4],[5]. Ninhydrin solution binds to available amine sites and instigates a colour change, from yellow to dark purple, which is measurable spectroscopically. The novelty in this application is to provide both qualitative and quantitative information from the same sample. It was possible, at the endpoint of the manufacturing process, to react all the amine in the defined coating solution with ninhydrin to determine what concentration of the coating solution had been deposited onto the surface. The amine on the surface was also stained purple (the qualitative confirmation of the deposition of the surface chemistries), but the concentration of the amines deposited was calculated by a simple deduction method:

$$SC=OC-PCC$$

Where the surface concentration (SC) is equal to the original concentration of the coating solution (OC) minus the post coating concentration of the coating solution (PCC). All these concentrations were determined by creating a standard curve of the specific amine linked silanes reacted with a ninhydrin solution and measured spectroscopically at 590nM. See appendix for details of standard curves, the derived equation and r^2 values which support the validity of the assay.

The ability to obtain an absolute concentration on these samples, on 2D films or 3D spheres is a clear step forward in the characterization of the materials, which is not possible with the plasma polymer deposition technique. This is one clear reason why this technique, providing all other things are equal, would be a superior technique to the plasma modification. Another reason why this technique could be considered to be superior to plasma is the simplicity of the equipment required to coat the samples. As this is a wet chemical technique, it is a simple technique to perform requiring less specialized equipment to conduct. This would be a consideration if this technique was ever to be scaled up, and as a wet chemical technique, would have the potential to coat a whole porous scaffold (depending on the interconnectivity of the pores).

While the plasma modifications can provide a good screening method for applying chemistries to a surface and very good proof of principle techniques, a technique that is more defined, simpler to manufacture, reproduce and monitor would be required if this was to go any further, and the silane modifications could meet the parameters required for that to occur.

In this chapter a range of different silanes with the same terminal groups were used to modify a glass substrate. This initial investigation was conducted to determine if there was any discernable difference between the modifications on a flat easily defined environment (i.e. glass), prior to the modification of a more complex degradable polymer which would

bring more variables into the experimentation. The following investigation determines by what degree the length of the hydrocarbon chain presenting the terminal group affects the efficiency by which the silane coats the surface, surface topography and osteogenicity. MSCs and primary osteoblast-like cells were used to determine the osteogenicity of the surfaces.

4.1 Surface characterization of silane modified glassusing AFM microscopy:

AFM Microscopy of the silane modified glass revealed differences in the maximum feature height of the surfaces. The features of CL3 and CL4 (fig 4.1.2 and 4.1.3) were similar and showed a significant difference to untreated glass, they displayed a rough microstructure, which was quite uniform. CL6 and CL7(fig 4.1.4 and 4.1.5) displayed a roughness with defined clumping of features, less uniform surface with less of the micro-structure roughness seen in CL3 and CL4. CL11 (fig 4.1.6) showed a macro-topographical landscape with similar micro-structural topographical roughness to CL3 and CL4.

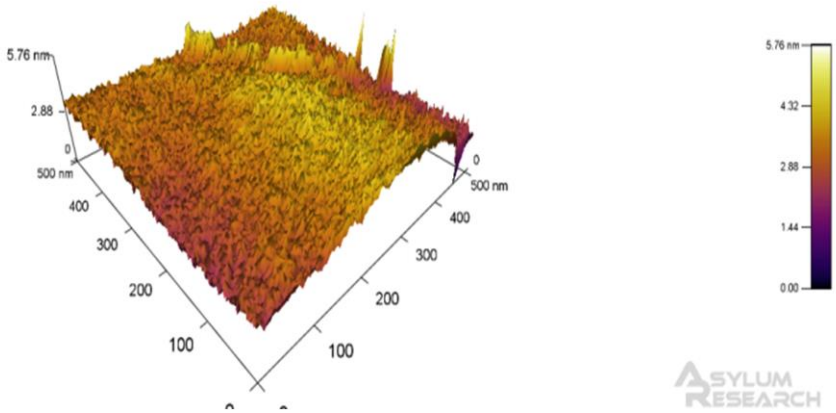

Figure 4.1.1 **AFM micrograph of untreated borosilicate glass.** 12mm diameter glass coverslips were cleaned as stated in protocol. AFM images taken from 5 areas per sample, representative image shown

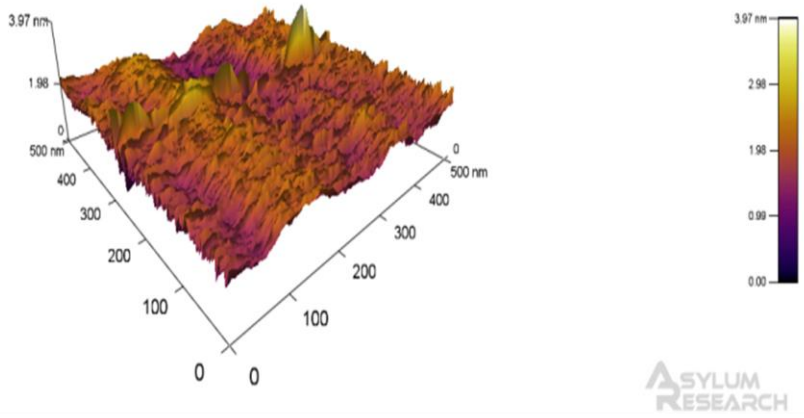

Figure 4.1.2 **AFM image of borosilicate glass treated with CL3.** 12mm diameter glass coverslips were cleaned as stated in protocol, and modified using oxygen plasma, then the CL3 silane. AFM images taken from 5 areas per sample, representative image shown

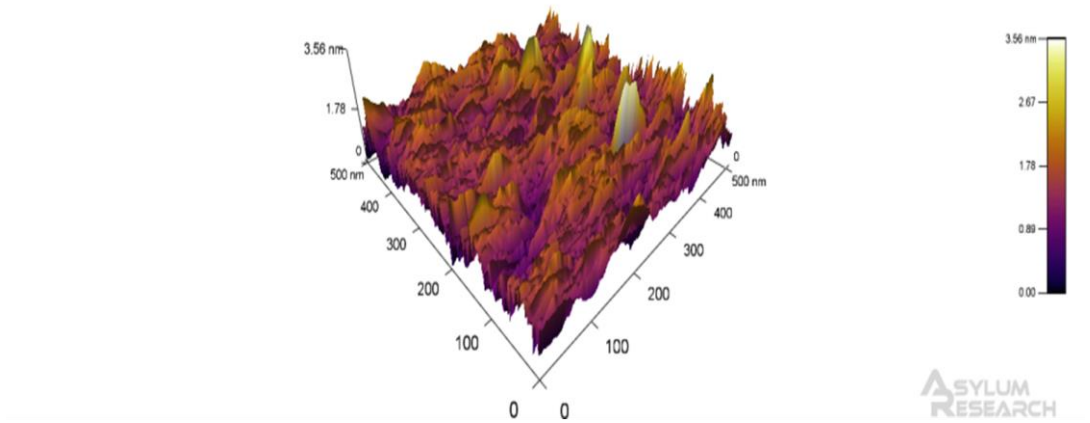

Figure 4.1.3 **AFM micrograph or borosilicate glass treated with CL4**. 12mm diameter glass coverslips were cleaned as stated in protocol, and modified using oxygen plasma, then the CL4 silane. AFM images taken from 5 areas per sample, representative image shown

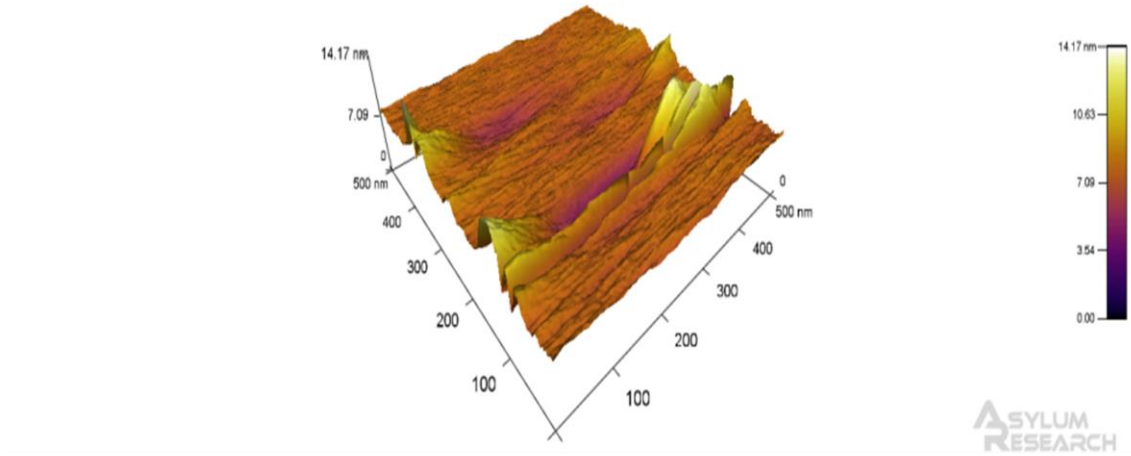

Figure 4.1.4 AFM micrograph of borosilicate glass treated with CL6. 12mm diameter glass coverslips were cleaned as stated in protocol, and modified using oxygen plasma, then the CL6 silane. AFM images taken from 5 areas per sample, representative image shown

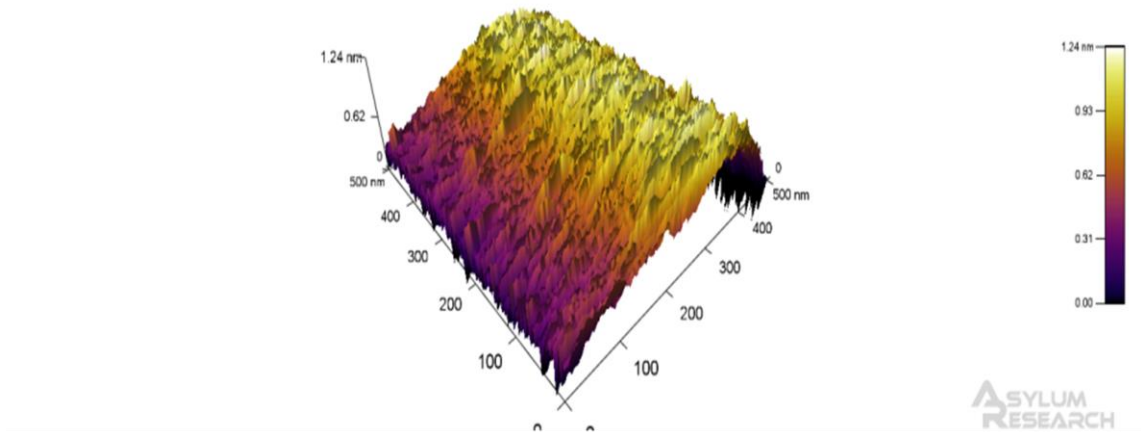

Figure 4.1.5 borosilicate glass treated with CL7. 12mm diameter glass coverslips were cleaned as stated in protocol, and modified using oxygen plasma, then the CL7 silane. AFM images taken from 5 areas per sample, representative image shown

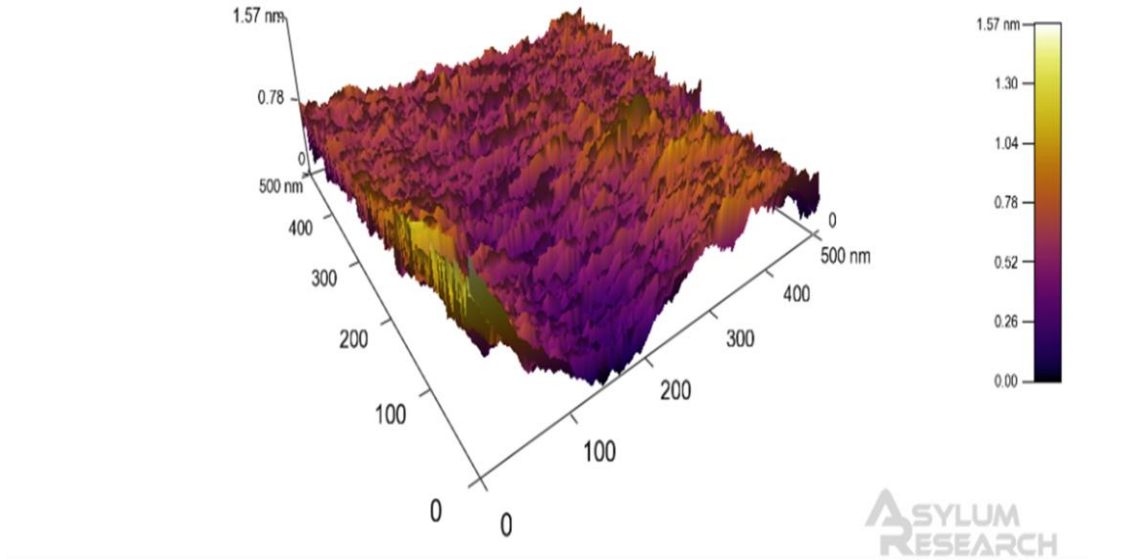

Figure 4.1.6 borosilicate glass treated with CL11. 12mm diameter glass coverslips were cleaned as stated in protocol, and modified using oxygen plasma, then the CL7 silane. AFM images taken from 5 areas per sample, representative image shown

4.2 Ninhydrin assay of silane modified borosilicate glass:

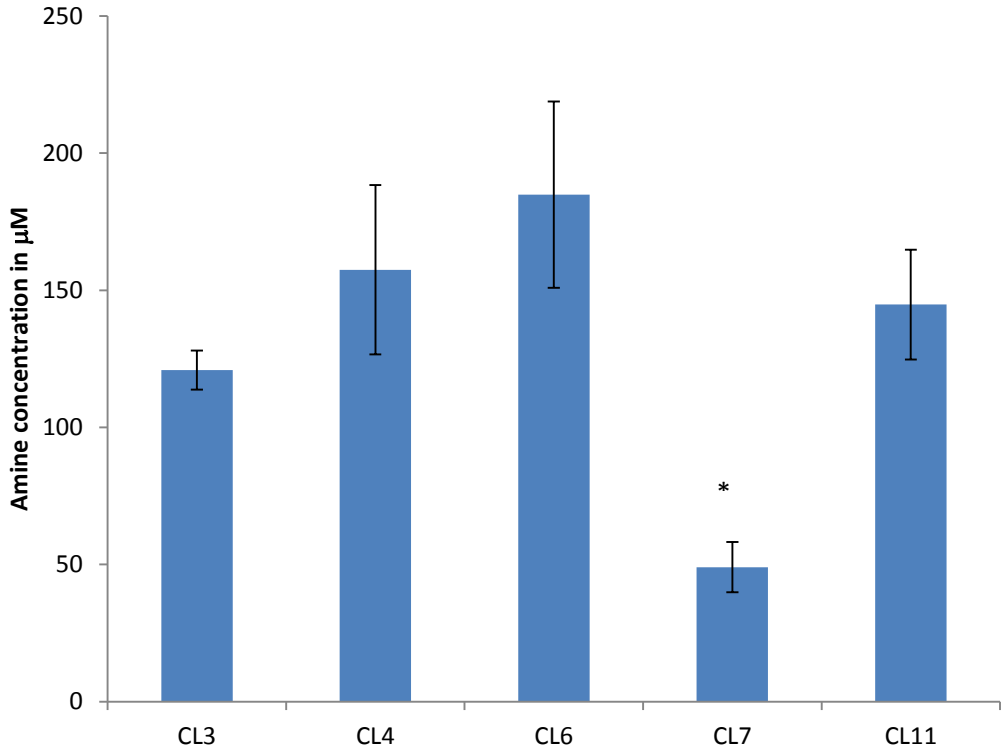

Figure 4.2 **Amine concentration determined by ninhydrin assay**.Ninhydrin assay conducted to determine the concentration of amine groups on the surfaces. Stars indicate statistically significant difference from other modifications ($p<0.05$)

Ninhydrin assay demonstrated that there was no statistical difference between the concentration of the amine groups on CL3, CL4, CL6 or CL11, but there was a significant difference between these modifications and CL7 which was significantly lower than the other modifications. (As defined by ANOVA to a 95% confidence interval)

4.3 Dynamic water contact angle of silane modified borosilicate glass (advancing angle):

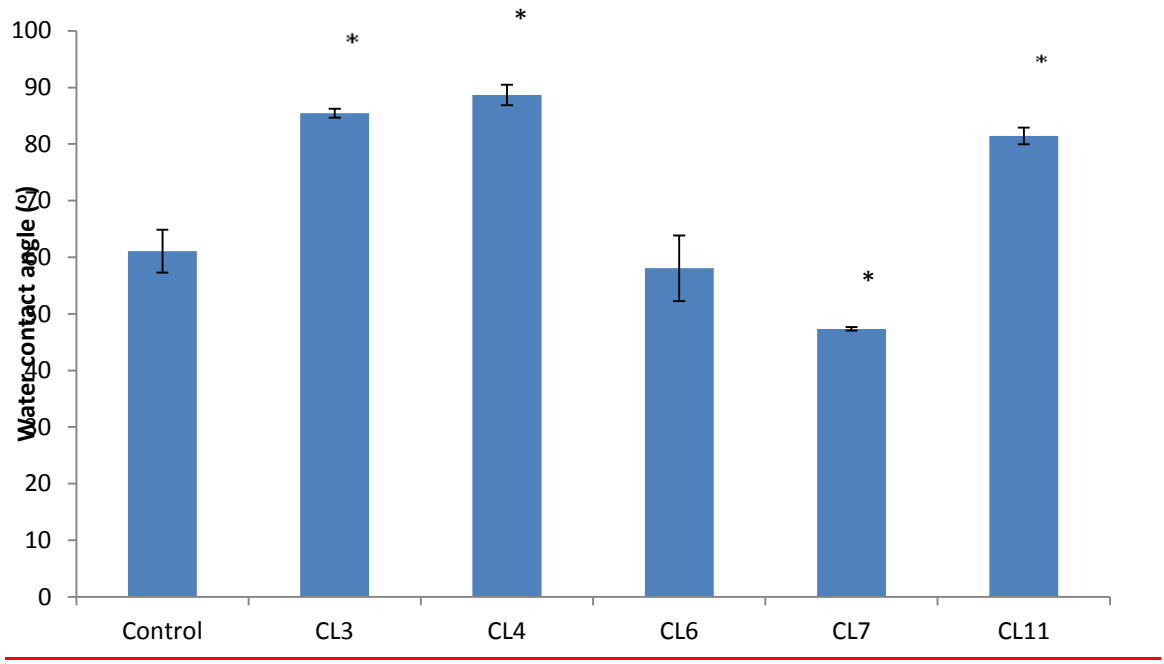

Figure 4.3: **Advancing water contact angle of modified glass surfaces**. Water contact angle was measured to determine changes in surface energy between the modifications *p<0.05,

Water contact angle of the modified glass showed that there was a statistical difference between the control and the CL3, 4, 7 and 11, but there was no statistically significant difference between the control and CL6. There was no statistically significant difference between CL3, 4 and 11, but there was a difference between these modifications and CL6 and 7. (As defined by ANOVA to a 95% confidence interval)

4.4 Interaction of silane modified surfaces with phosphate buffered saline solutions.

The biomimetic characteristics of the silane modified surfaces were investigated, due to some reported interactions between calcium carbonate and phosphate solutions and certain self-assembled monolayer interactions. [6] The results indicated there was some biomimetic properties demonstrated by the surface treated with CL11 when it was left in contact with a phosphate buffered saline solution for 7 days. Von Kossa stain was performed as an initial qualitative test to determine if there was any mineralisation on the surface. This was evident so further more detailed investigation was warranted. X-ray microanalysis of the surfaces was conducted.

Time point	**7 day**				**14 day**				**28 day**			
Concentration of PBS (%)	0	25	50	100	0	25	50	100	0	25	50	100
CL3	-	-	-	-	-	-	-	-	-	-	-	-
CL4	-	-	-	-	-	-	-	-	-	-	-	-
CL6	-	-	-	-	-	-	-	-	-	-	-	-
CL7	-	-	-	-	-	-	-	-	-	-	-	-
CL11	-	+	+	+	-	+	+	+	-	+	+	+
Untreated	-	-	-	-	-	-	-	-	-	-	-	-

Table 4.1: PBS interactions with modified glass. + indicated positive Von Kossa staining for mineralisation

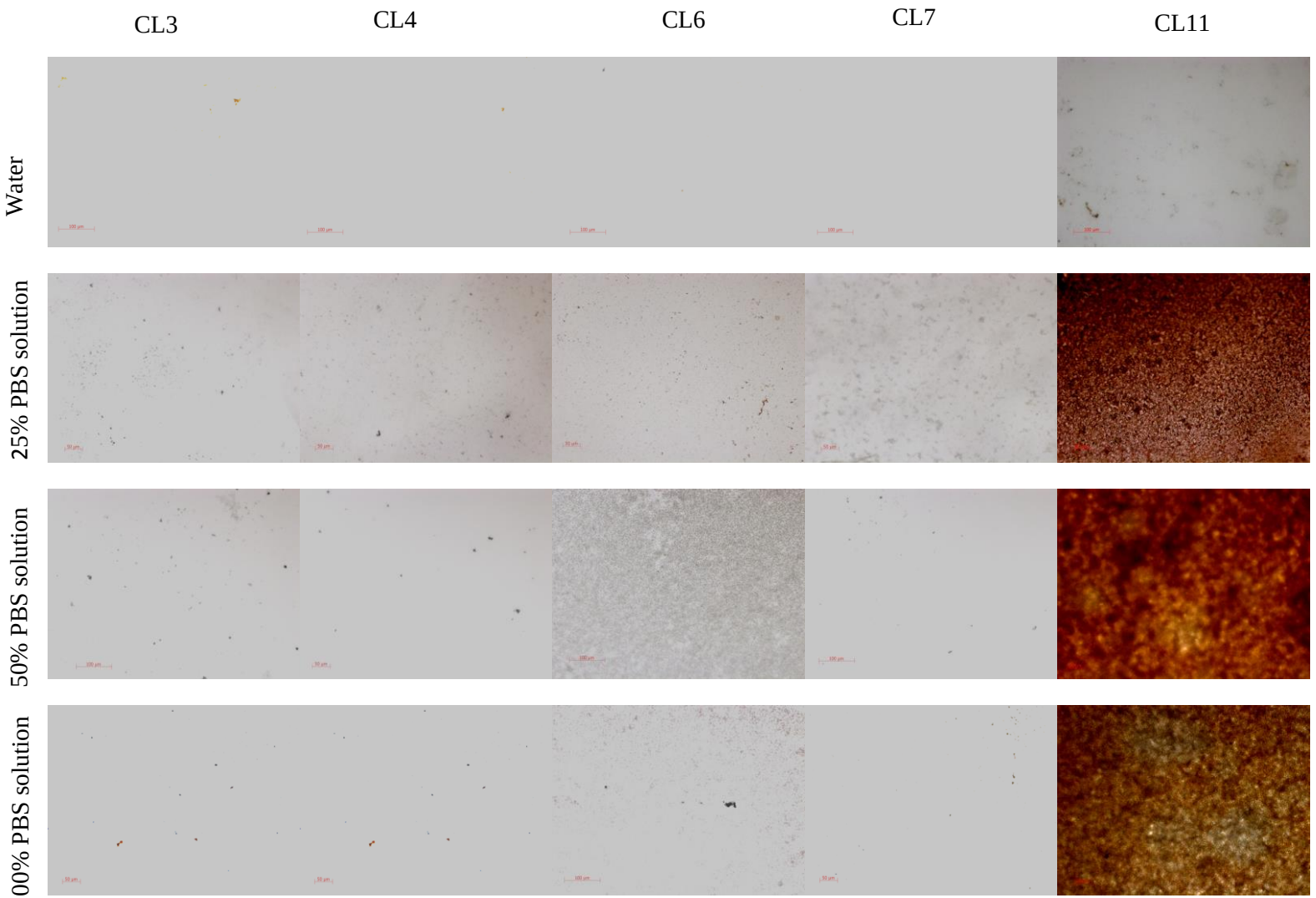

Figure 4.4 **Mineral deposition study**, Images show surfaces exposed to differing concentrations of PBS for 7 days, then stained using von Kossa's stain for mineralisation, positive staining (brown) shown on CL11.

X-ray microanalysis of surfaces after PBS exposure for 7 days.

The mineral deposition study demonstrated that the CL11 surface is capable of attracting deposits of phosphorous from PBS solutions, where as the other surfaces do not. The concentration of the PBS in the solution is not relevant at the concentrations tested as the phosphorous deposited did not vary significantly. There was a significant difference between the untreated control and all three PBS concentrations at 7 days on the CL11 surface.

There is also a significantly increased concentration of carbon on the CL11 treated surface when compared to the other treated surfaces. This is likely to be theincreased hydrocarbon chain length of CL11. The differences between the other carbon levels are not detectable with this technique.

The probability of finding phosphorous on the CL11 modification when exposed to any concentration of PBS is very high. This was calculated using the total number of spectra taken, divided by the number of positive spectra found on the samples(table 4.2). 50 spectra from each sample were used, taken from randomly selected areas, and 3 repeats were conducted. This way of interpreting the data shows the incidence of the presence of the phosphorous which is more meaningful than just using the averages of the spectra, when only a few spectra are positive for the element on the CL6 and CL7 modifications.

When both analysis techniques are taken into account the presence of phosphorus on CL11 is shown to be significantly more concentrated than the other modifications, but also, and perhaps more meaningful, its presence is significantly more frequent.

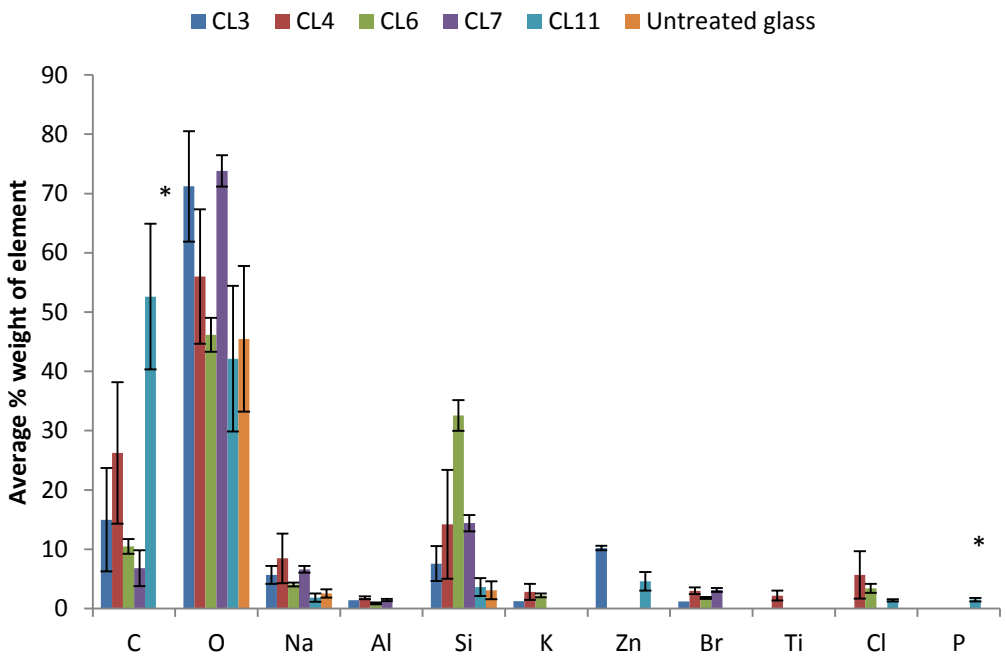

Figure 4.5**: X-ray analysis of elemental composition of Silane treated glass in 25%** PBS. Silane modified glasses were exposed to PBS for 7 days and then analysed using Xray analysis.. *p<0.05.

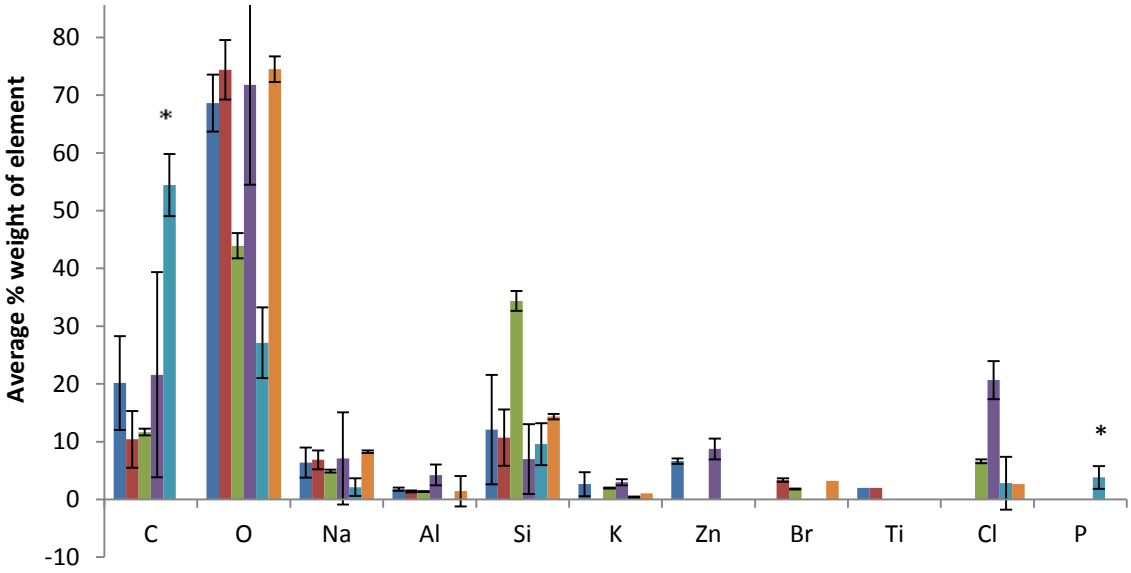

Figure 4.6: **X-ray analysis of elemental composition of Silane treated glass in 50% PBS.** Silane modified glasses were exposed to PBS for 7 days and then analysed using Xray analysis.. *p<0.05.

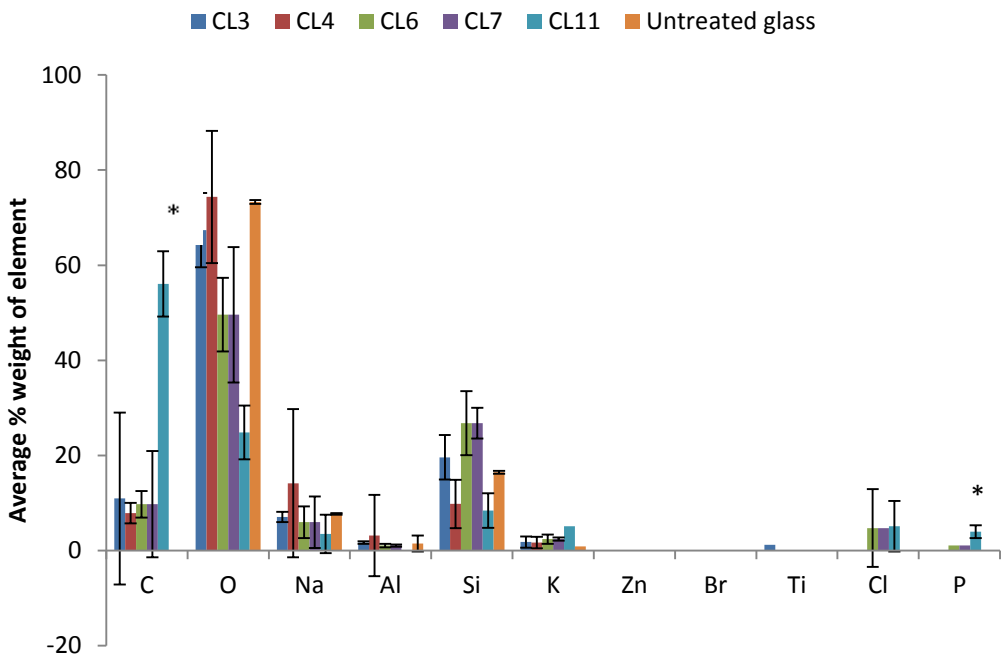

Figure 4.7: **X-ray analysis of elemental composition of Silane treated glass in 100% PBS**. Silane modified glasses were exposed to PBS for 7 days and then analysed using Xray analysis**.** *p<0.05.

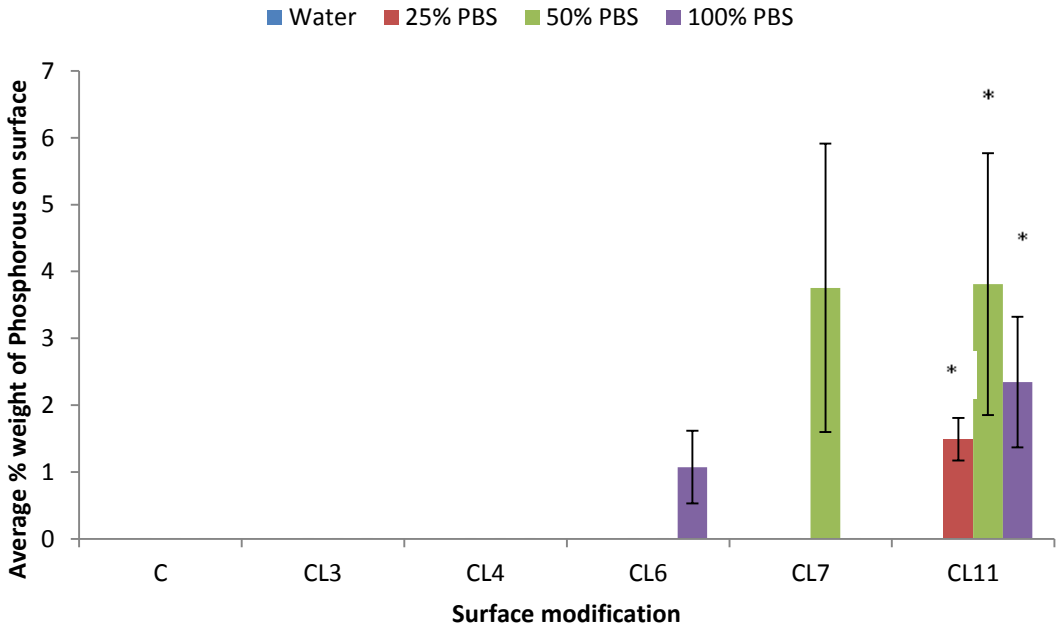

Figure 4.8**: Concentration of phosphorous on silane modified surfaces.** Surfaces were exposed to varying concentrations of PBS for 7 days. *=p<0.05. C is an untreated glass control.

Insidence of Phosphorous on surfaces:

	C	CL3	CL4	CL6	CL7	CL11
Water	0	0	0	0	0	0
25% PBS	0	0	0	0	0	0.43
50% PBS	0	0	0	0	0.05	1
100% PBS	0	0	0	0.45	0	0.9

Table 4.2: **Probability of phosphorous occurring on the surfaces**.
Probability of phosphorous occurring on the glass surfaces after 7 days exposure to PBS was calculated 0 = no probability and 1= high probability.

4.6 Human mesenchymal stem cell interactions with silane modified glass after 7, 14 and 28 days incubation, stained with Von Kossa's stain for mineralisation.

The Von Kossa staining of the control untreated glass cultured with MSCs showed no positive staining at 7, 14 or 28 days. The CL3, 4, 6, 7 all showed a small amount of mineralisation, but the CL11 showed an extensive degree of mineralisation at 7 days which was sustained through to 28 days..

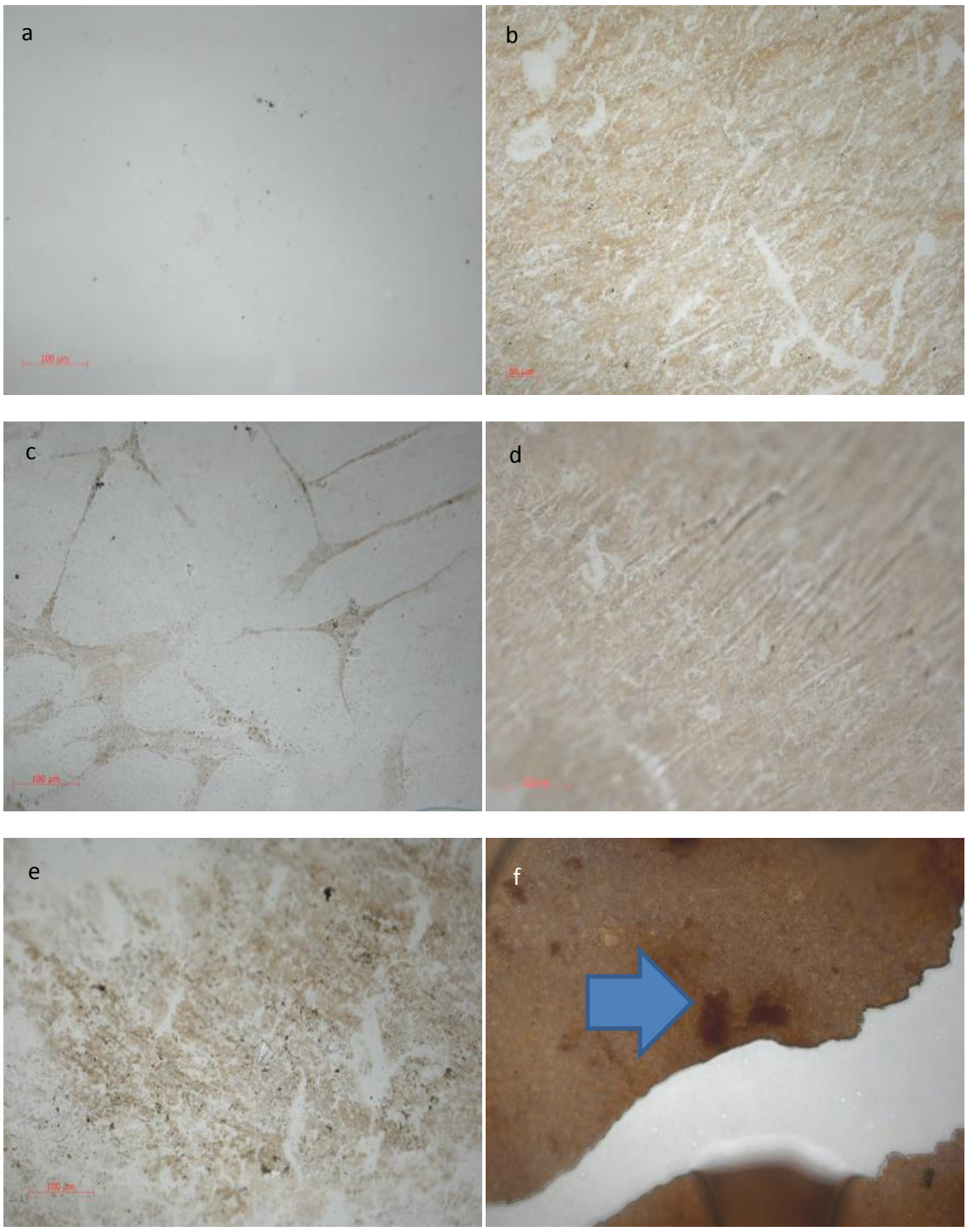

Figure 4.9: **MSC on modified glass after 7 days incubation** MSCs on modified glass after 7 days incubation and stained with Von Kossas stain for mineralisation, (a) unmodified glass, (b) CL3, (c) CL4, (d) CL6. (e) CL7 and (f) CL11. Blue arrow indicates strong mineralisation of surface

4.7: SEM investigation of Human mesenchymal stem cell interactions with silane modified glass after 7, 14 and 28 days incubation.

The SEM examination of the hMSCs on the silane modified glass revealed that CL3 and 4 demonstrated very flat cellular morphology, that formed a monolayer from 7 days that was maintained until 28 days.

CL6 had many rounded cells, that appeared to reducein number by 28 days. CL7 showed a monolayer formation by 7 days that was maintained throughout the 28 days period.

CL11 showed a monolayer formation at 7 days that was starting to produce a dense matrix by 14 days. By 28 days the cells were completely covered by this dense matrix that appeared to have a pitted texture when examined at high magnification.

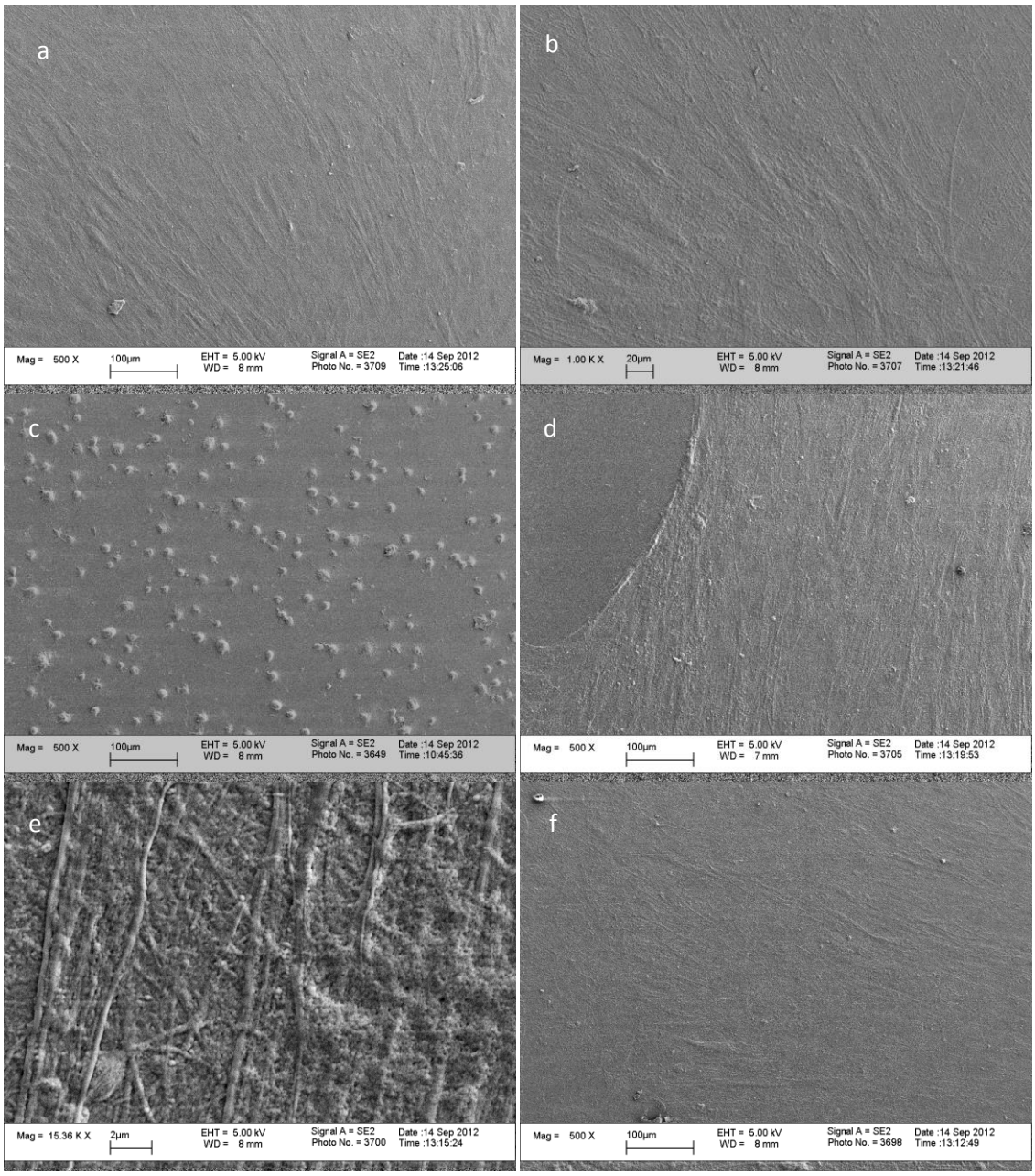

Figure 4.10: **SEM images of human MSCs cultured on modified glass for 7 days**. MSC were cultured on the modified glasses for 7 days, fixed with glutaraldehyde, critical point dried, and coated with chromium. Representative images were then taken using a field emission scanning electron microscope. (a) CL3, (b) CL4, (c) CL6, (d) CL7, (e) CL11* and (f) untreated control*Shown at higher magnification to highlight ECM detail.

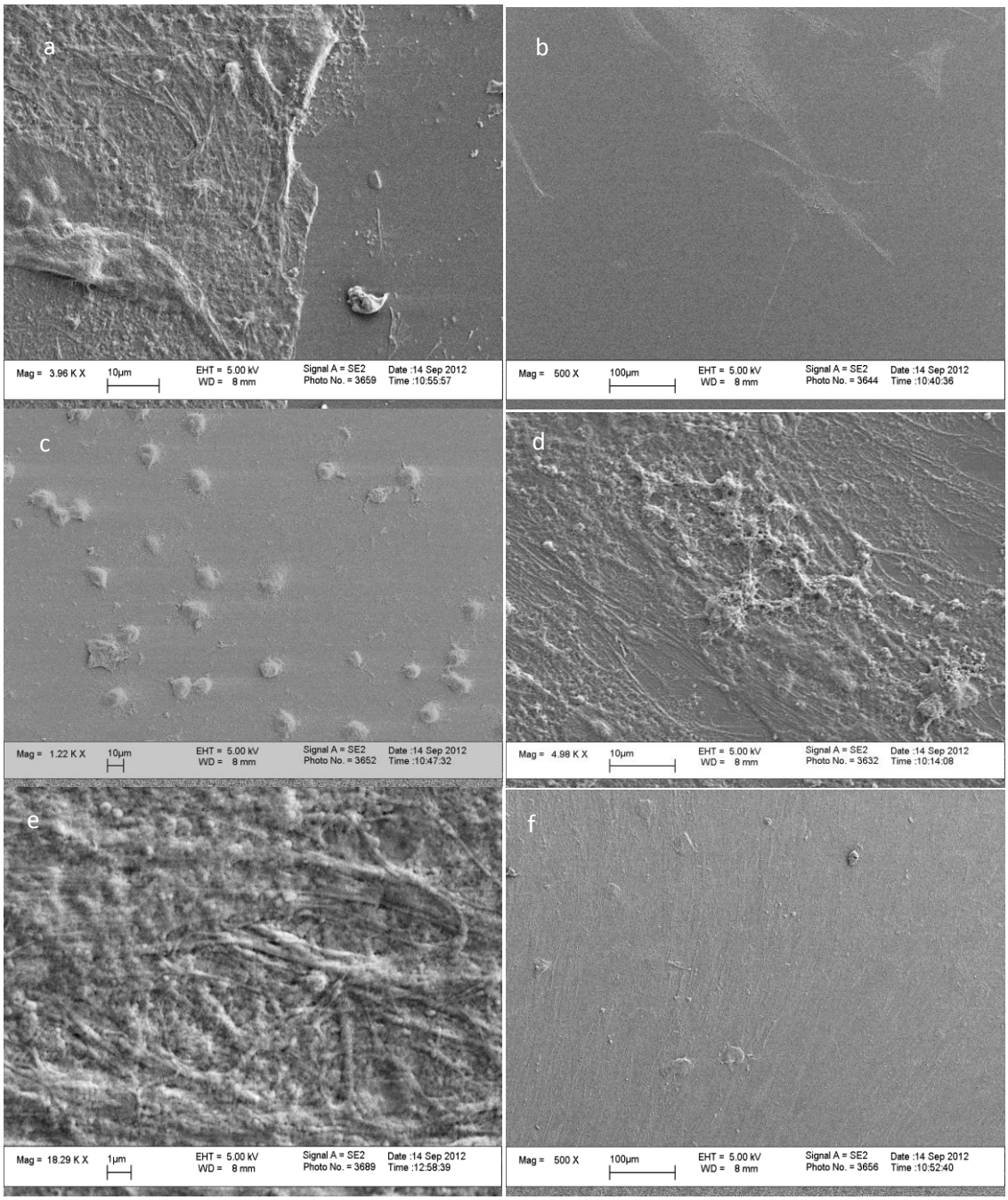

Figure 4.11: **SEM images of human MSCs cultured on modified glass for 14 days**. MSC were cultured on the modified glasses for 14 days, fixed with glutaraldehyde, critical point dried, and coated with chromium. Representative images were then taken using a field emission scanning electron microscope. (a) CL3, (b) CL4, (c) CL6, (d) CL7, (e) CL11 and (f) untreated control. All images shown at varying magnifications to highlight details.

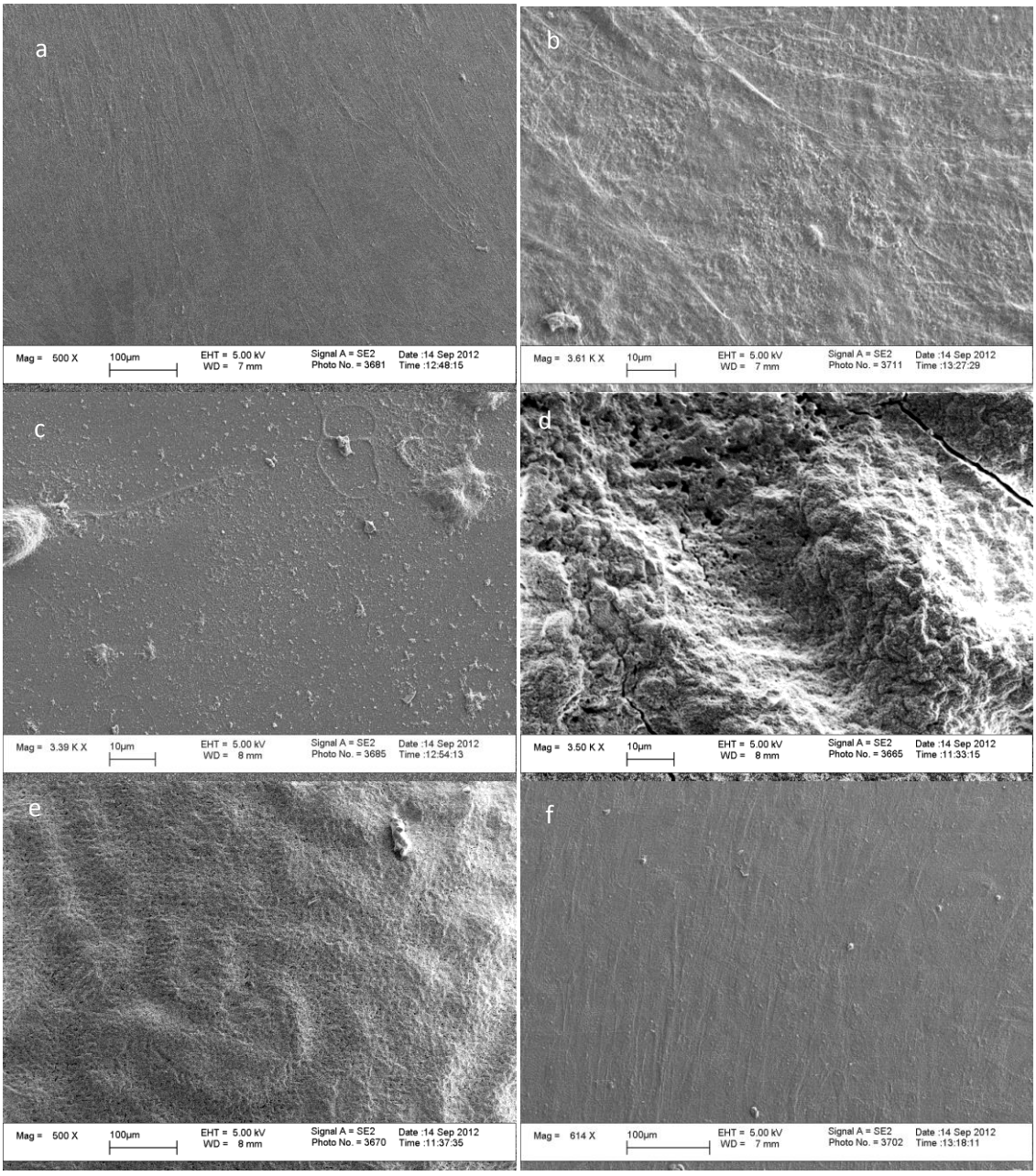

Figure 4.12: SEM images of human MSCs cultured on the modified glass for 28 days. MSC were cultured on the modified glasses for 28 days, fixed with glutaraldehyde, critical point dried, and coated with chromium. Representative images were then taken using a field emission scanning electron microscope. (a) CL3, (b) CL4, (c) CL6, (d) CL7, (e) CL11 and (f) untreated control

4.8: Real time Polymerase Chain Reaction (rt PCR) investigation into human mesenchymal stem cell interactions with silane modified glass after 7, 14 and 28 days incubation.

MSC scultured on CL3 modified glass demonstrated a minor upregulation of ostepontin at 7 days but no other significant upregulations.

MSCs cultured on CL4 showed upregulation of osteopontin at 7, 14 and 28 days along with an up-regulation of osteonectin at 7 days and expression of CBFA 1 at 14 and 28 days.

CL7 showed an upregulation of osteopontin, collagen 1, osteonectin at 7 days and sclerostin at 14 days. The MSCs exposed toCL11 showed upregulation of osteopontin, collagen I, Osteonectin and osteocalcin at 7 days and sclerostin and osteocalcin at 14 days, with osteocalcin being upregulated to a lesser degree at 28 days.

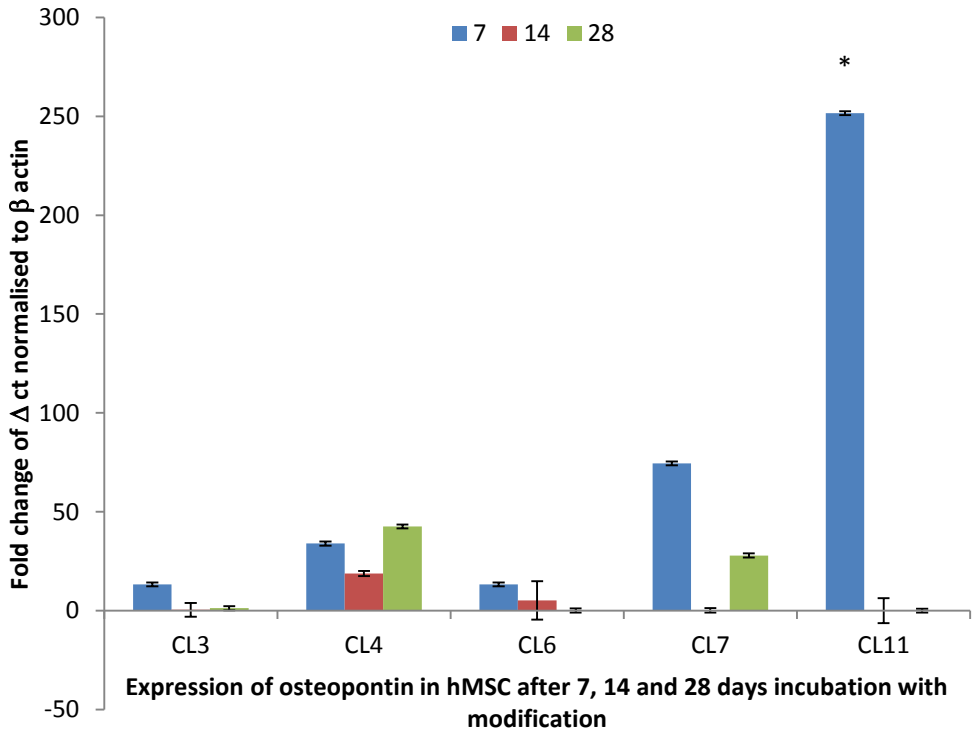

Figure 4.14: **Expression of osteopontin by human MSCs on modified glass at 7, 14 and 28 days.** Scaffolds were processed for rt-PCR, and N=6 and data normalised to β-actin housekeeping gene. Data was analysed using the ΔΔct method of analysis

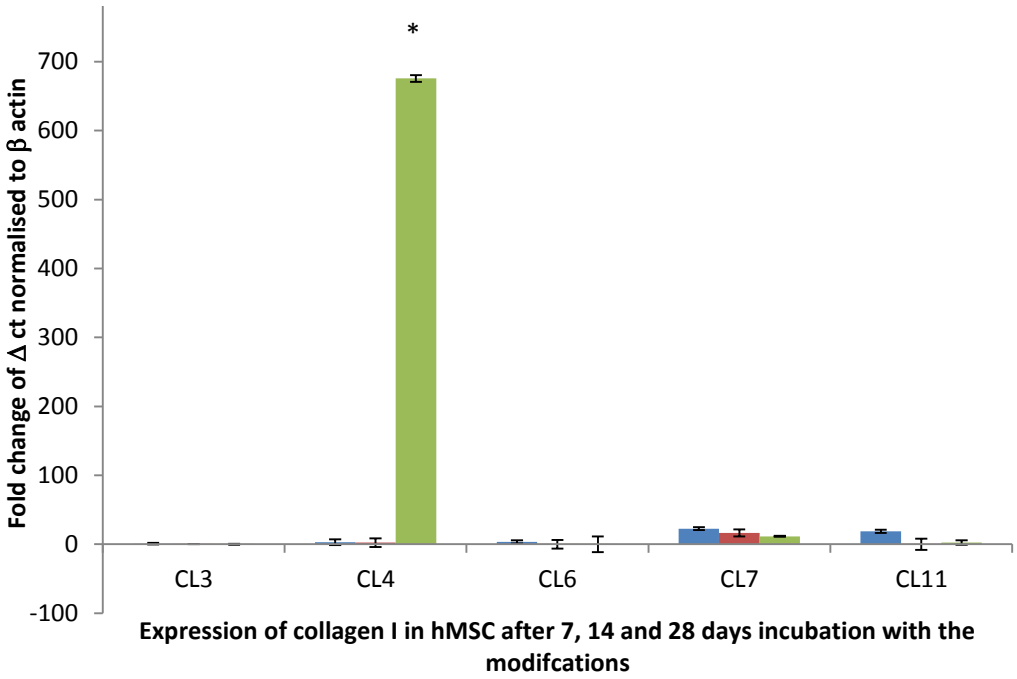

Figure 4.15: **Expression of collagen I by human MSCs on modified glass at 7, 14 and 28 days.** Scaffolds were processed for rt-PCR, and N=6 and data normalised to β-actin housekeeping gene. Data was analysed using the ΔΔct method of analysis

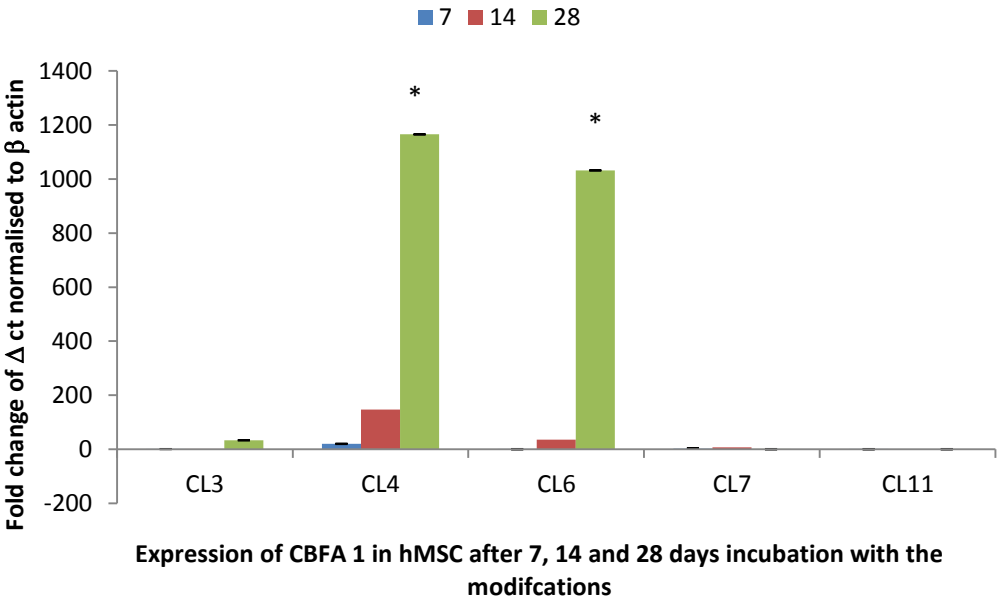

Figure 4.16**Expression of CBFA 1 by human MSCs on modified glass at 7, 14 and 28 days.** Scaffolds were processed for rt-PCR, and N=6 and data normalised to β-actin housekeeping gene. Data was analysed using the ΔΔct method of analysis

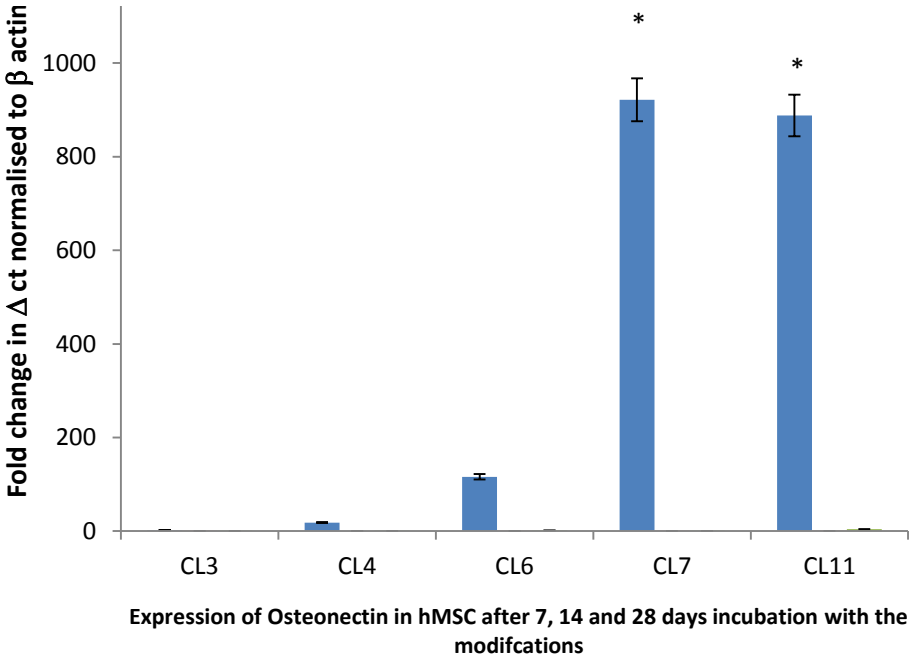

Figure 4.17: **Expression of osteonectin by human MSCs on modified glass at 7, 14 and 28 days.** Scaffolds were processed for rt-PCR, and N=6 and data normalised to β-actin housekeeping gene. Data was analysed using the ΔΔct method of analysis

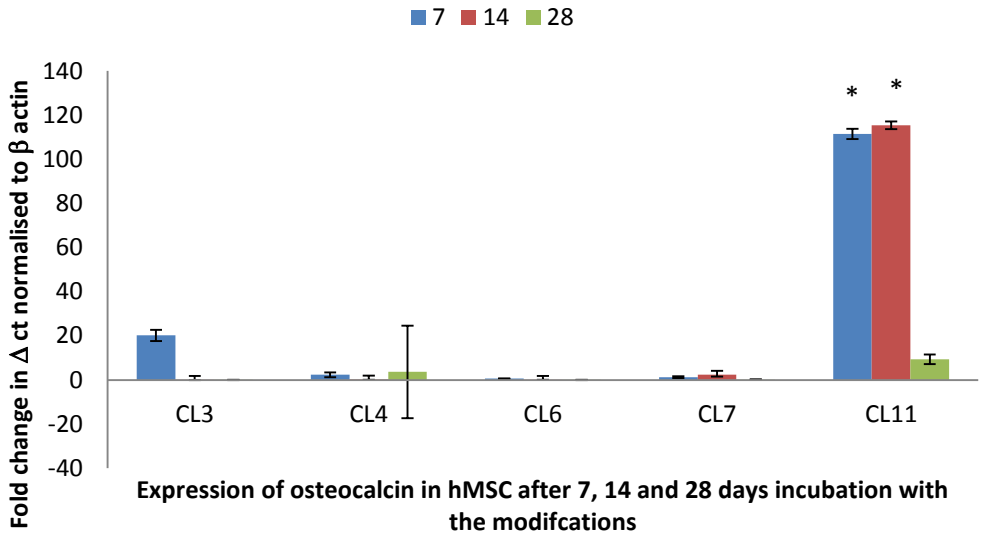

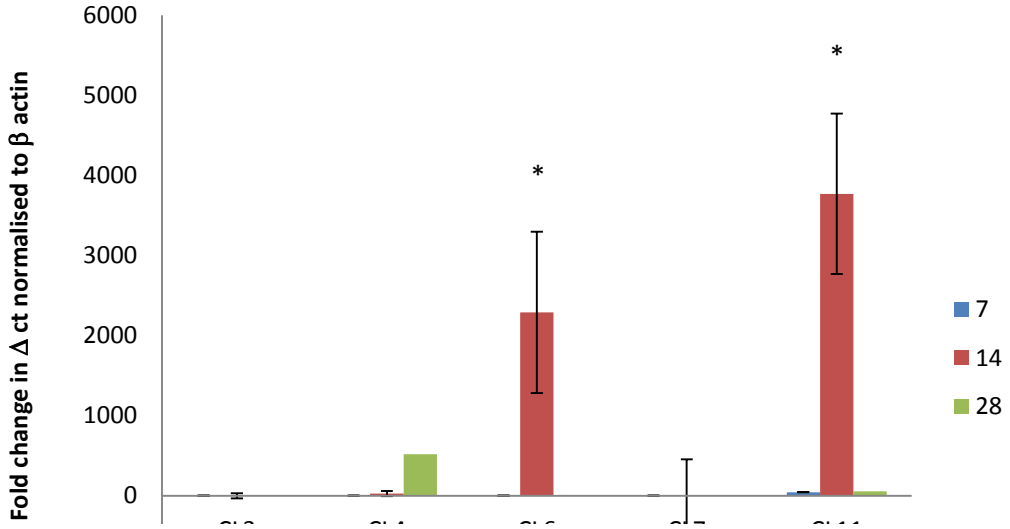

Figure 4.18: **Expression of osteocalcin by human MSCs on modified glass at 7, 14 and 28 days.** Scaffolds were processed for rt-PCR, and N=6 and data normalised to β-actin housekeeping gene. Data was analysed using the ΔΔct method of analysis

14 and 28 days. Scaffolds were processed for rt-PCR, and N=6 and data normalised to β-actin housekeeping gene. Data was analysed using the ΔΔct method of analysis

4.9: Confocal microscopy investigation into human mesenchymal stem cell interactions with silane modified glass after 7, 14 and 28 days incubation.

The MSC marker Stro-1 showed that the mesenchymal stem cells on the control untreated sample were still demonstrating a MSC phenotype after 28 days. This combined with no expression of CBFA 1 and Osteocalcin confirms that the MSCs have not spontaneously differentiated.

CL3 demonstratedpositive collagen I and Stro-1 staining at 7 days, combined with negative CBFA1 and Osteocalcin. By 14 days the CBFA 1 and Osteocalcin were mildly positive.

CL4 showed positive Collagen I staining at 7 days, no Stro-1 staining, and no CBFA 1 or osteocalcin staining until 28 days.

CL6 only showed positive collagen staining throughout the 28 day period.

CL7 started to show positive CBFA 1 and Osteocalcin by 28 days but nothing at the earlier time points.

CL11 demonstrated a thick matrix that stained for osteocalcin and collagen I by 7 days, showing an extensive and thick pitted matrix by 14 days with was maintained through to 28 days.

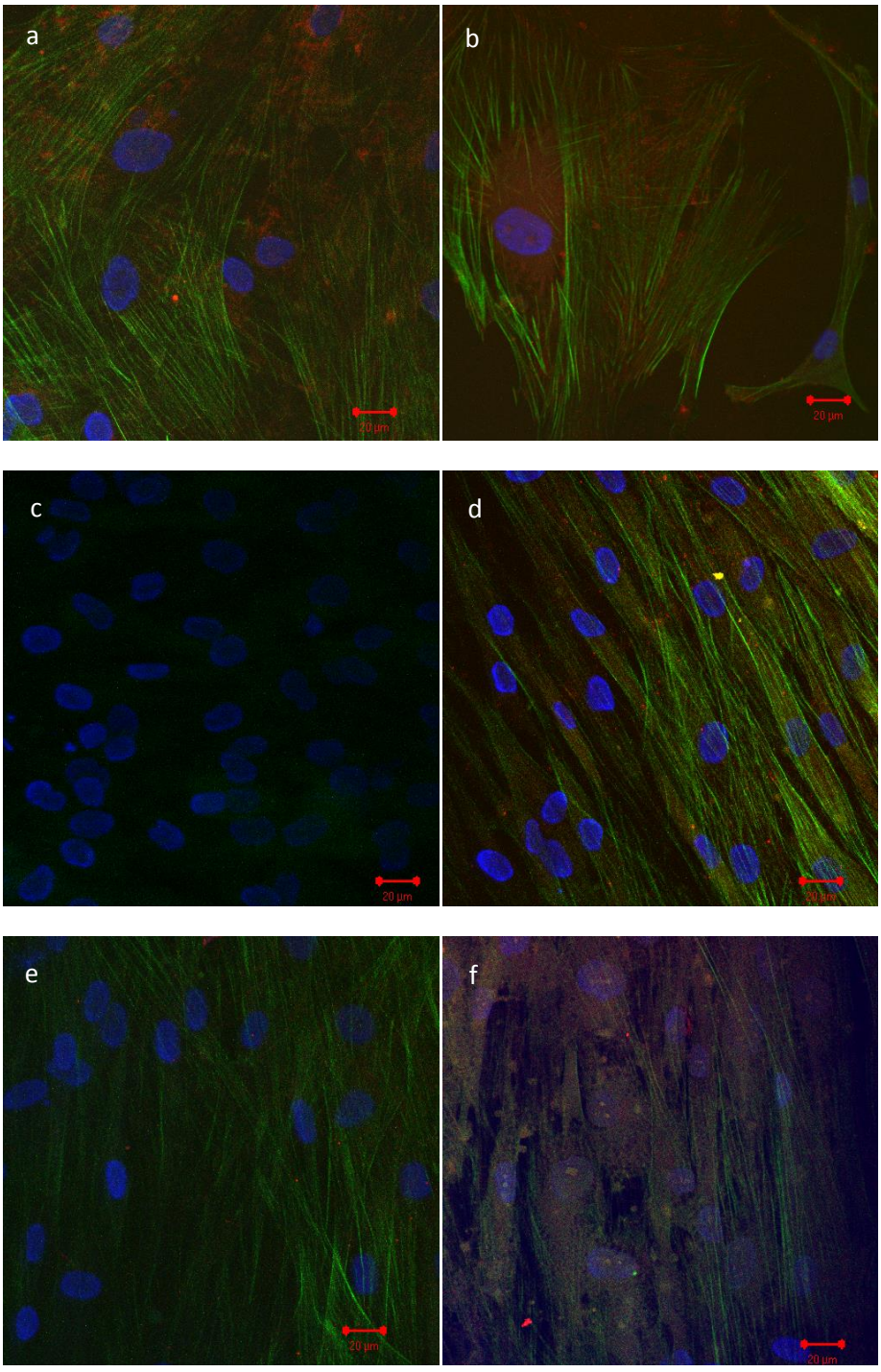

Figure 4.20: **Immunostaining of MSCs cultured on modified glass at 7 days.** MSC were cultured on silane modified glass for 7 days and stained with Stro-1, DAPI and Oregeon green. Blue staining shows nuclei, green staining shows actin filaments and red staining shows presence of stro-1 (a)untreated control, (b) CL3 (c) CL4, (d) CL6, (e) CL7 and (f) CL11

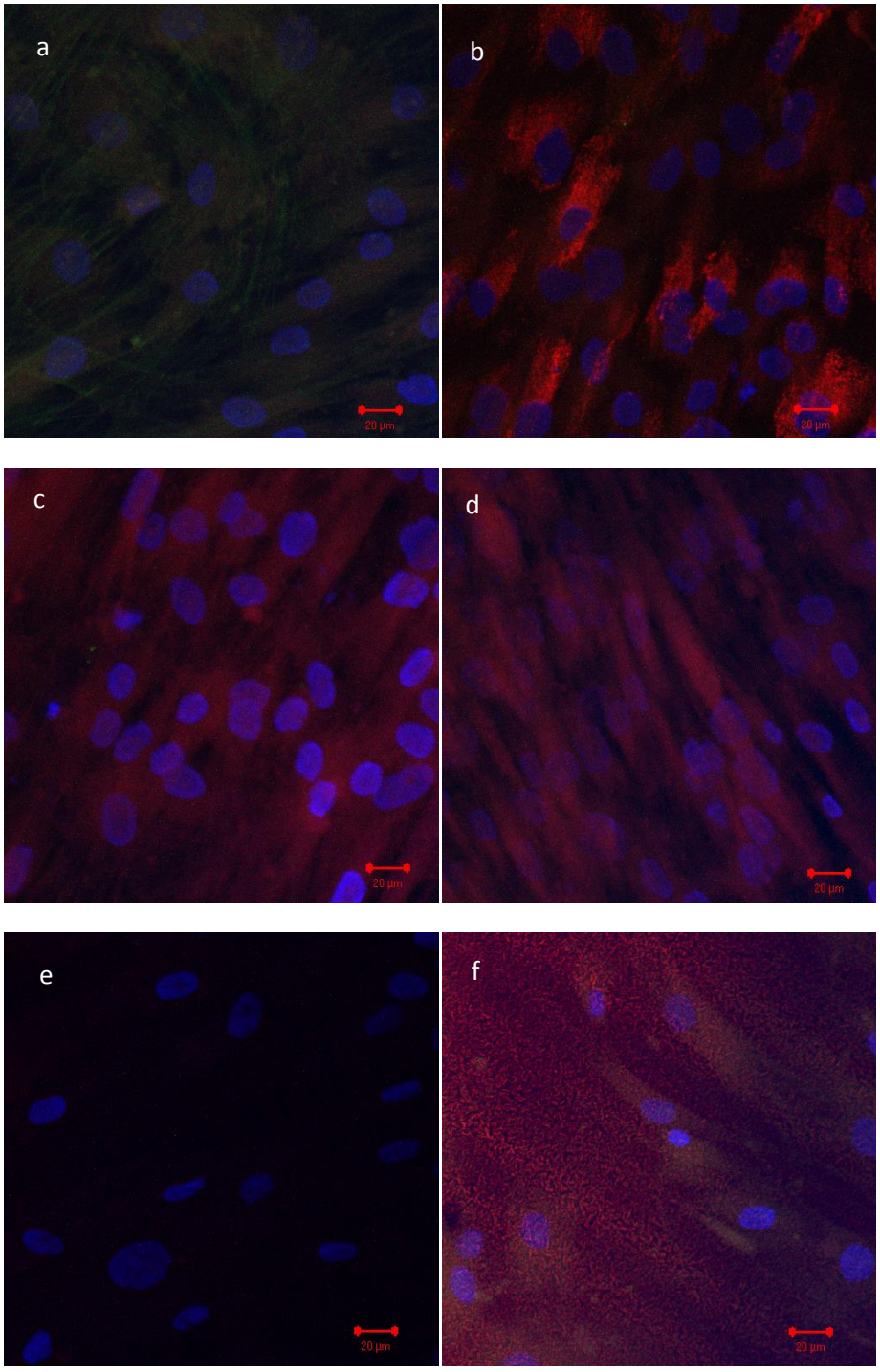

Figure 4.21: **Immunostaining of MSCs cultured on modified glass at 7 days.** MSC were cultured on silane modified glass for 7 days and stained with collagen I, DAPI and Oregeon green. Blue staining shows nuclei, green staining shows actin filaments and red staining shows presence of collagen I (a)untreated control, (b) CL3 (c) CL4, (d) CL6, (e) CL7 and (f) CL11I

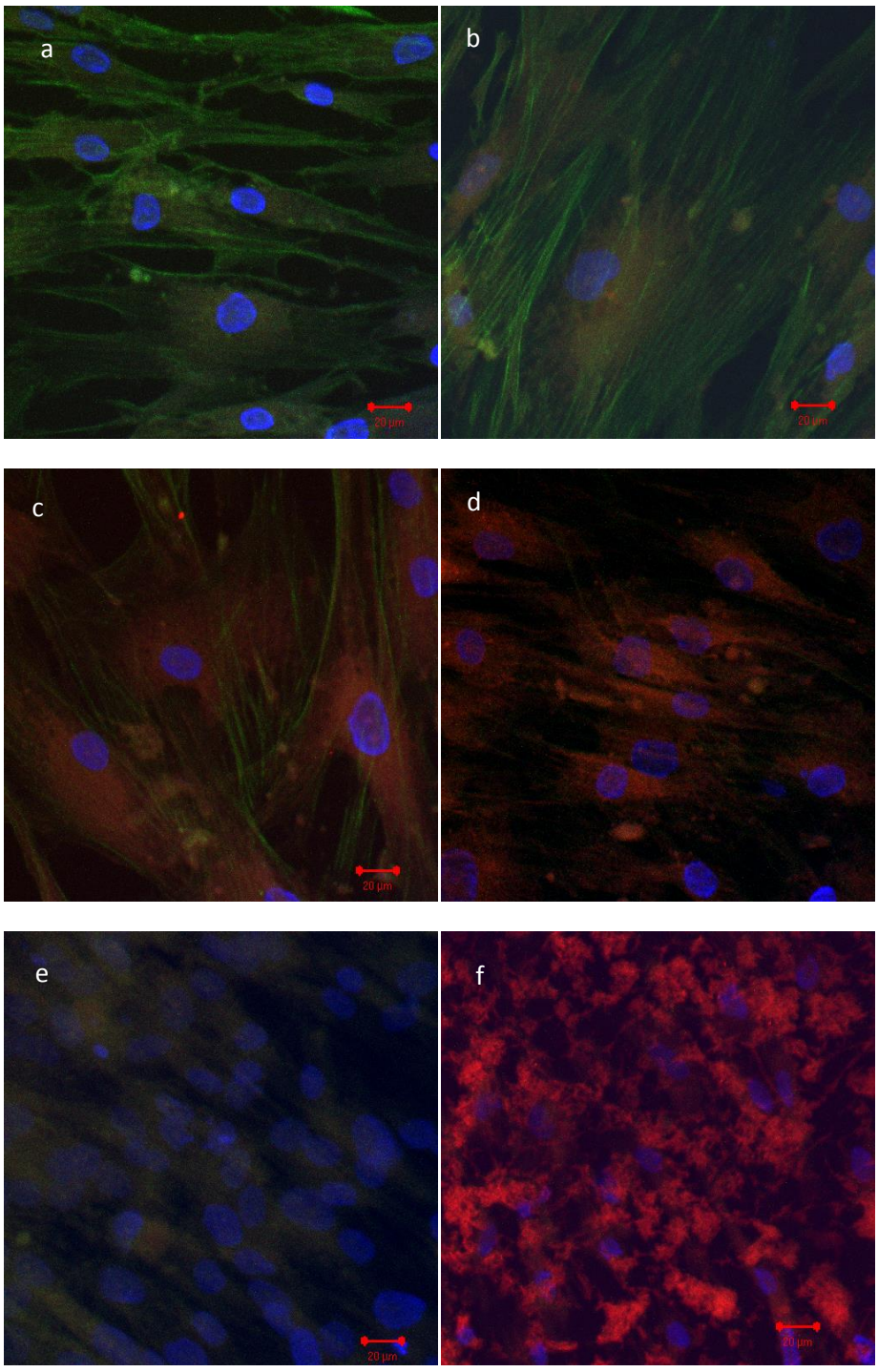

Figure 4.22: **Immunostaining of MSCs cultured on modified glass at 7 days.** MSC were cultured on silane modified glass for 7 days and stained with osteocalcin, DAPI and Oregeon green. Blue staining shows nuclei, green staining shows actin filaments and red staining shows presence of osteocalcin (a)untreated control, (b) CL3 (c) CL4, (d) CL6, (e) CL7 and (f) CL11

4.10: The interaction of primary human osteoblast-like cells with silane modified glass for 7, 14 and 28 days, stained with Von Kossa's stain for

The Von Kossa stain on the osteoblasts cultured on the silane modified surfaces revealed several effects of note. There was a response seen on the CL3 and CL4 treated surfaces which lead to the formation of mineralised nodules by 7 days. This response was maintained throughout the culture period of 28 days and restricted to the CL3 and CL4 modifications. A statistically insignificant number of nodules was seen on the other modifications which supported cell expansion throughout the culture period but with no observed change in phenotype during this time.

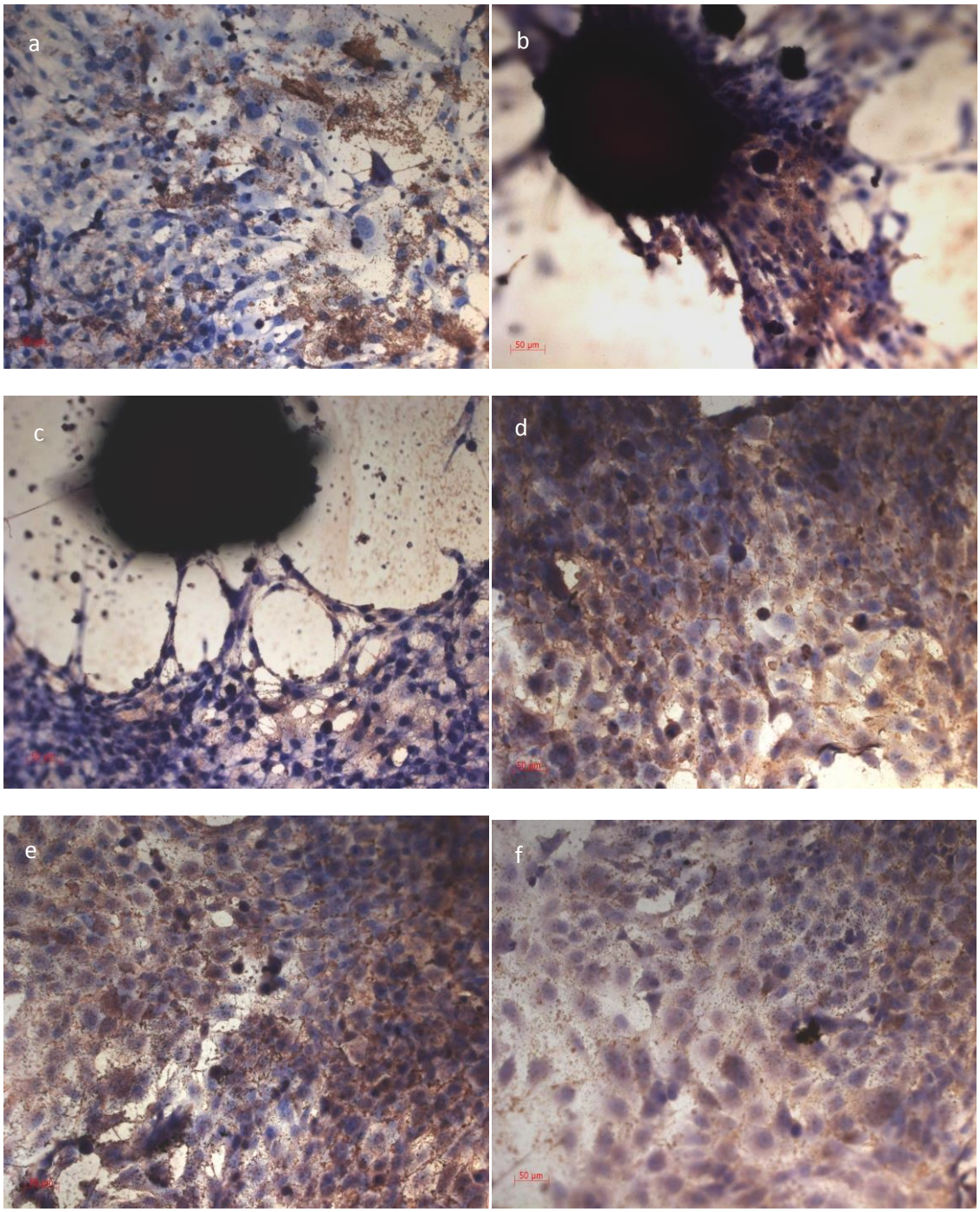

Figure 4.23 **Osteoblast-like cells cultured on silane modified glass for 7 days.** Osteoblast like cells were cultured on the silane modified glass (and an untreated control) for 7 days, then stained with Von Kossa's stain for mineralisation (a) untreated glass control, (b) CL3, (c) CL4, (d) CL6, (e) CL7 and (f) CL11.

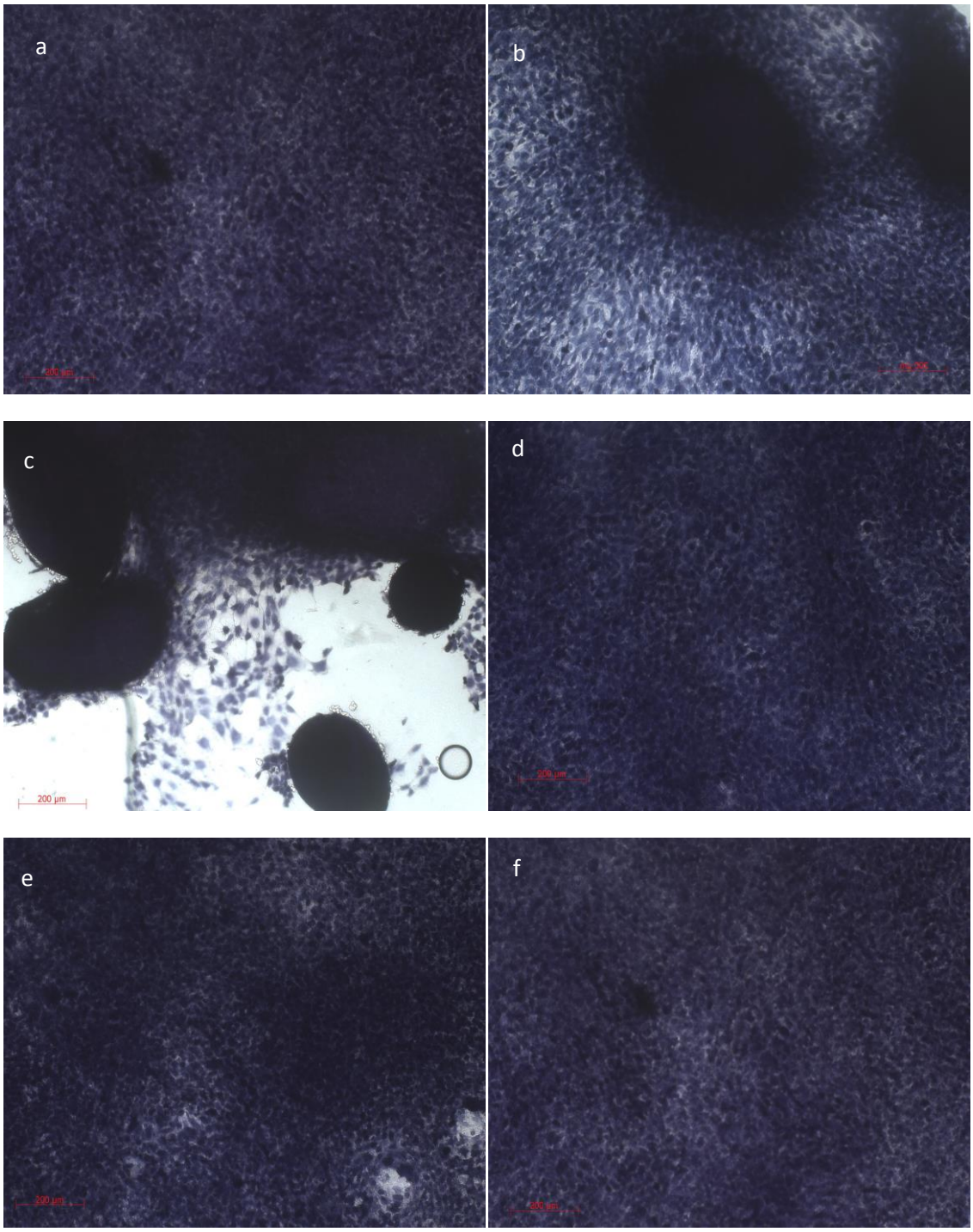

Figure 4.24, **Osteoblast-like cells cultured on silane modified glass for 14 days.** Osteoblast like cells were cultured on the silane modified glass (and an untreated control) for 14 days, then stained with Von Kossa's stain for mineralisation (a) untreated glass control, (b) CL3, (c) CL4, (d) CL6, (e) CL7 and (f) CL11..

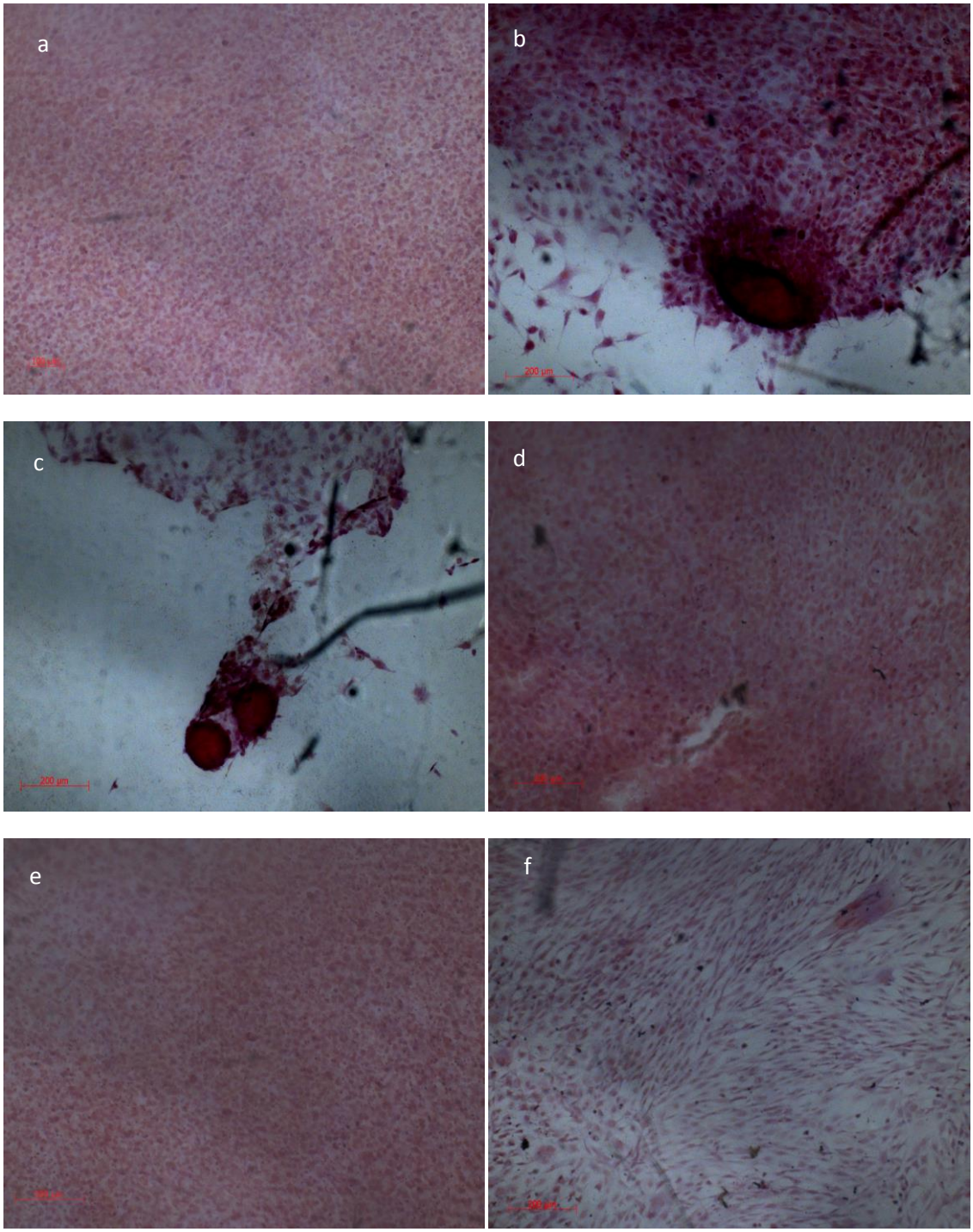

Figure 4.25 **Osteoblast-like cells cultured on silane modified glass for 28 days.** Osteoblast like cells were cultured on the silane modified glass (and an untreated control) for 28 days, then stained with Von Kossa's stain for mineralisation (a) untreated glass control, (b) CL3, (c) CL4, (d) CL6, (e) CL7 and (f) CL11.

4.11: Investigation of the number of nodules formed by primary human osteoblast like cells after 7, 14 and 28 days incubation with silane modified glass

The number of nodules were counted visually, and the resulting data displayed in figure4.26. The nodule number is significantly reduced at 28 days on both CL3 and CL4, when compared to 14 day figures for the same modification analysed by Ttest, the results showed significant differences to the 95% confidence interval. There is a significant increase between CL4 at 7 days and CL4 at 14 days (to a 95% confidence interval), whereas there is a plateau between 7 and 14 days on CL3.

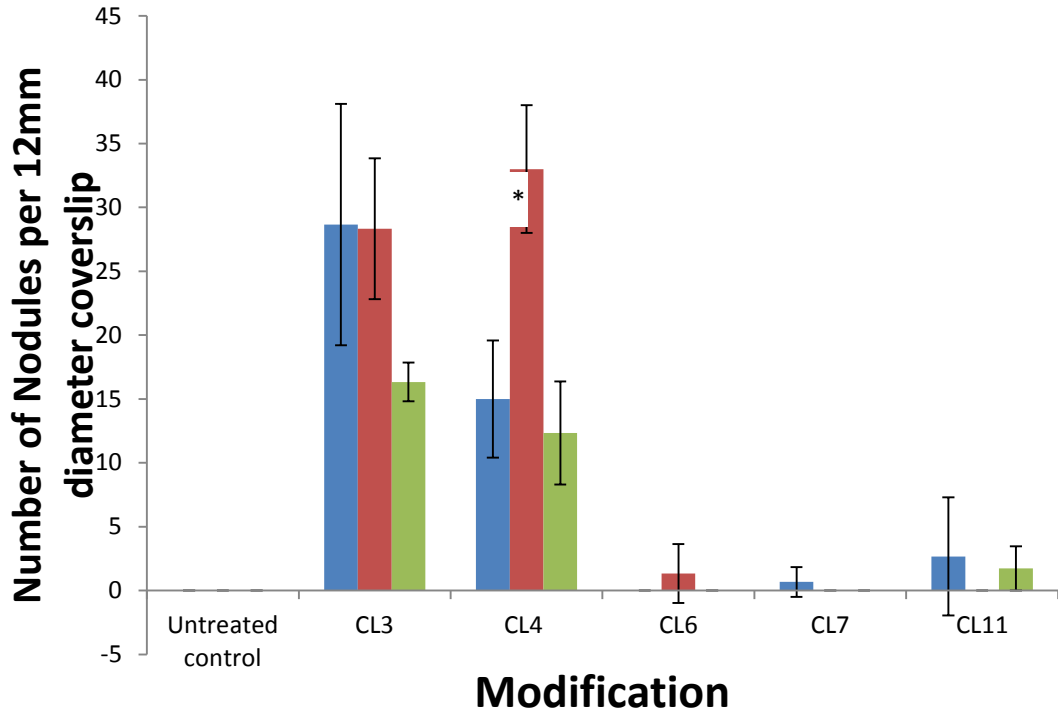

Figure 4.26: **Quantity of nodules formed on the modified surfaces.** The nodules were counted using a light microscope. (N=16) Seris 1,2 and 3 correspond to 7, 14 and 28 days, results show avage and error bars show standards deviation from the mean

4.12: Investigation of the size of nodules formed by primary human osteoblast-like cells after 7, 14 and 28 days incubation with silane modified glass.

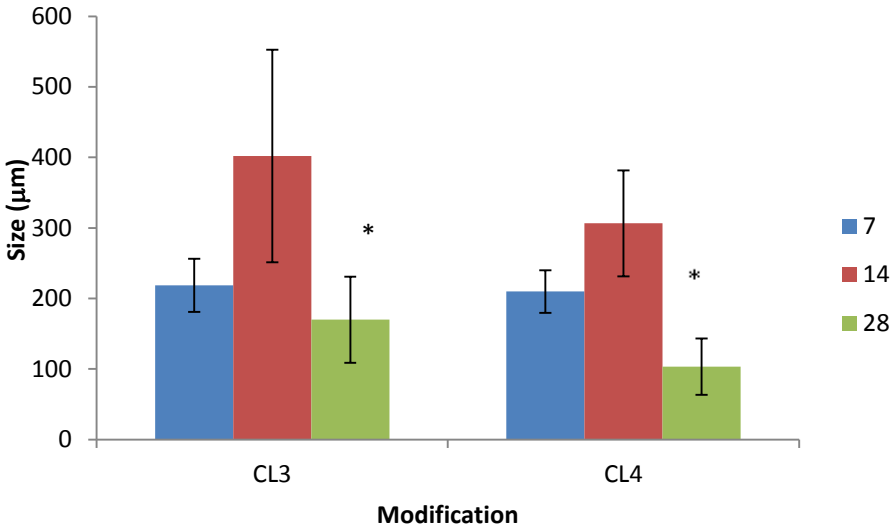

Figure 4.27: **Size of nodules on the modified surfaces** Nodules on surfaces treated with CL3 and CL4 were measured after after 7,14 and 28 days results show avage and error bars show standards deviation from the mean.

The size of the nodules also changed significantly (to a 95% confidence interval as determined by T test) between 14 and 28 days (figure 4.27). These results could indicate that the size of the nodule could reach a critical mass before being released by the surface, and that this occurs between 14 and 28 days.

4.13: SEM investigation of primary human osteoblast like cells after 7, 14 and 28 days incubation with silane modified glass

The SEM images above clearly demonstrate the nodule formation. The nodules on CL3 and CL4 appear to be covered in extracellular matrix, which appears to mature as the incubation time progresses. The higher magnification image (figure 4.31) shows a more detailed image of the extracellular matrix produced with what appears to be smoother mineralised areas. This mineralisation is also demonstrated by the positive von Kossa staining from early in the culture period. (figure 4.23)

The extracellular matrix is also produced in abundance on the CL11 surface, but in the absence of nodule formation to any significant degree (figure 4.32).

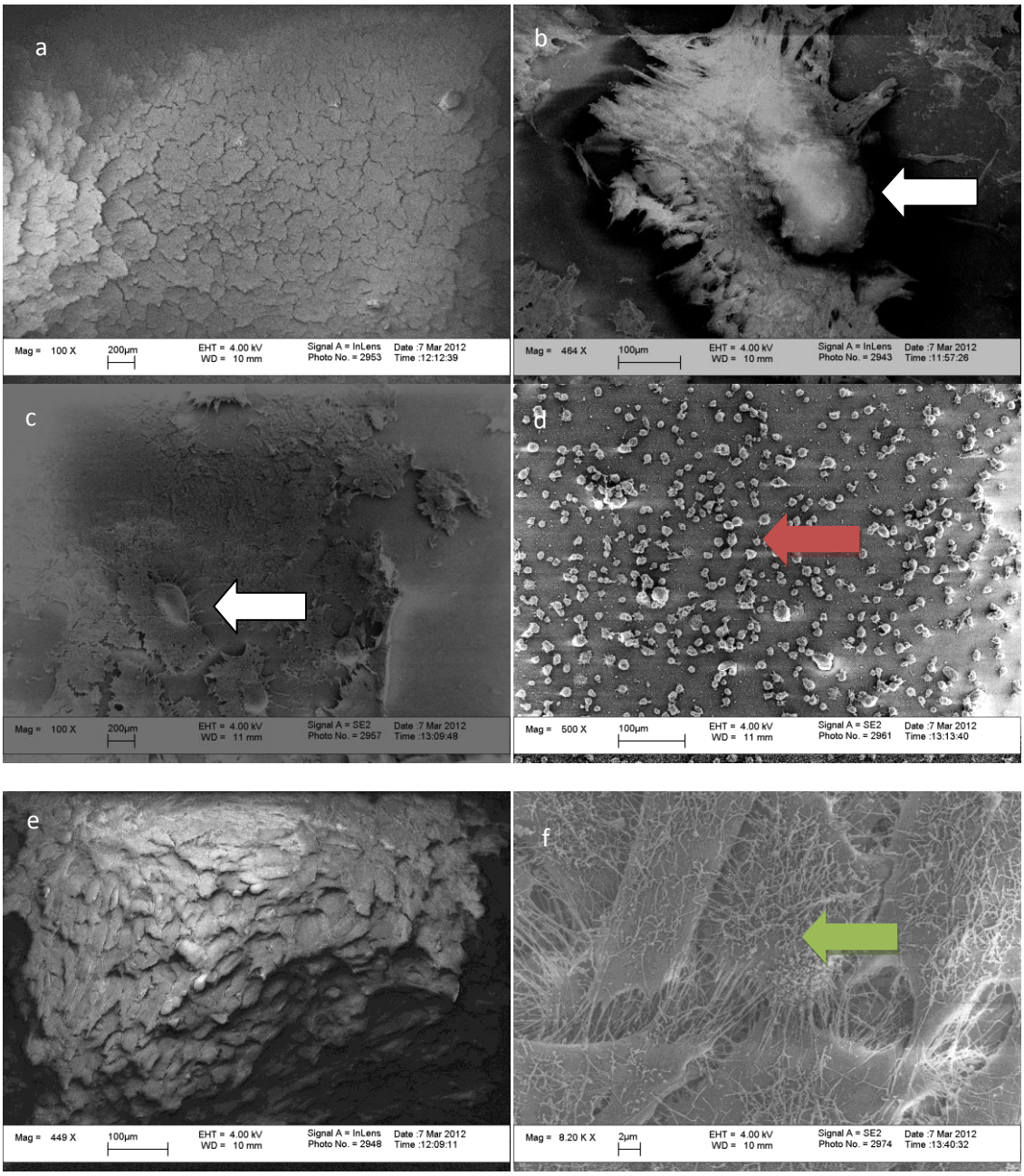

Figure 4.28, **SEM micrographs of Osteoblast-like cells cultured on silane modified glass after 7 days incubation**. Osteoblast –like cells were isolated from human trabecular bone and seeded onto the silane modified surfaces. (a) untreated glass, (b) CL3, (c) CL4, (d) CL6 , (e) CL7 and (f) CL11. White arrows indicate nodules, green arrow indicates production of ECM on CL11 and red arrow shows very rounded cells on CL6 modification

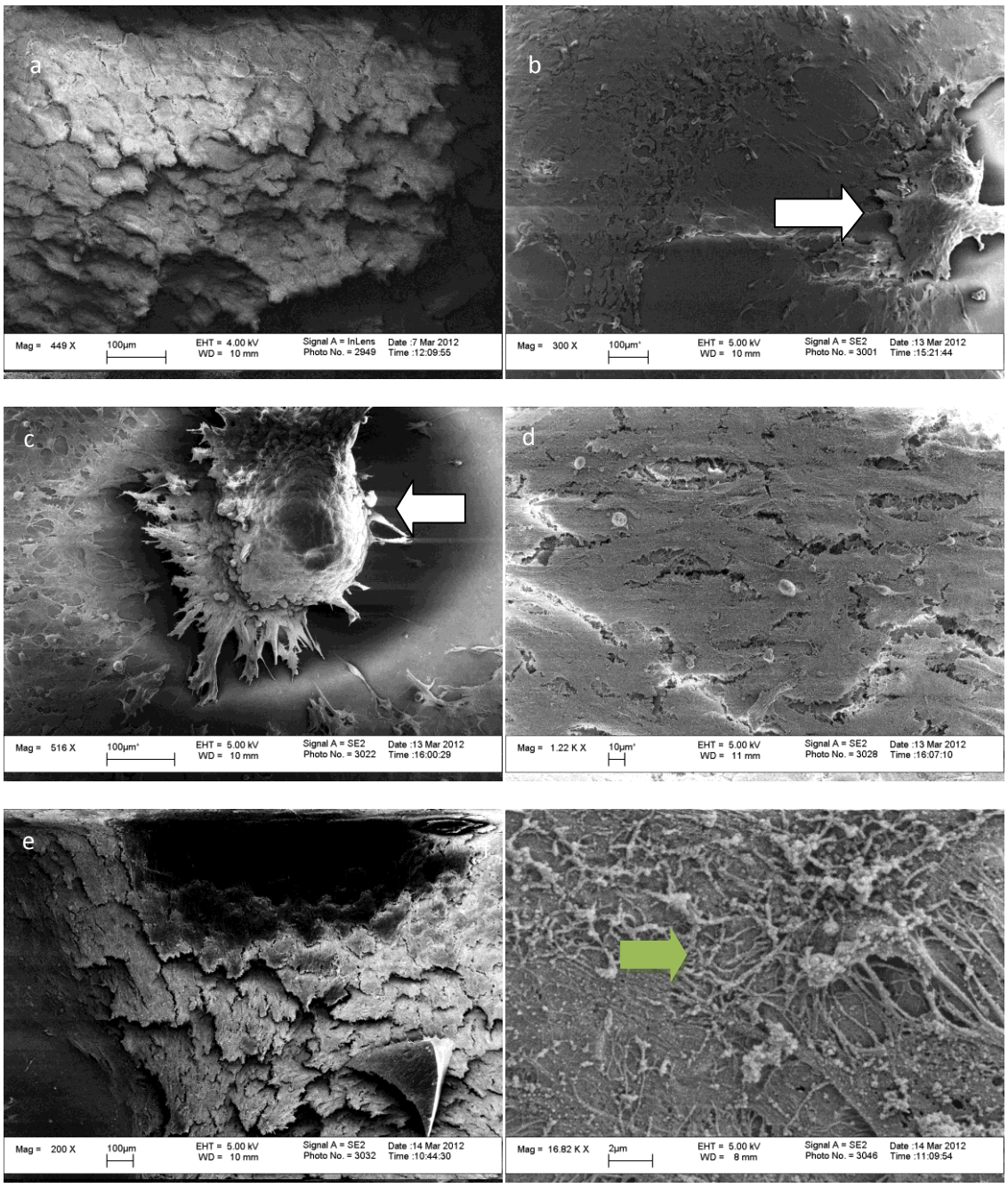

Figure 4.29, **SEM micrographs of Osteoblast-like cells cultured on silane modified glass after 14 days incubation**. Osteoblast –like cells were isolated from human trabecular bone and seeded onto the silane modified surfaces. (a) untreated glass, (b) CL3, (c) CL4, (d) CL6 , (e) CL7 and (f) CL11. White arrows indicate nodules, green arrow indicates production of ECM

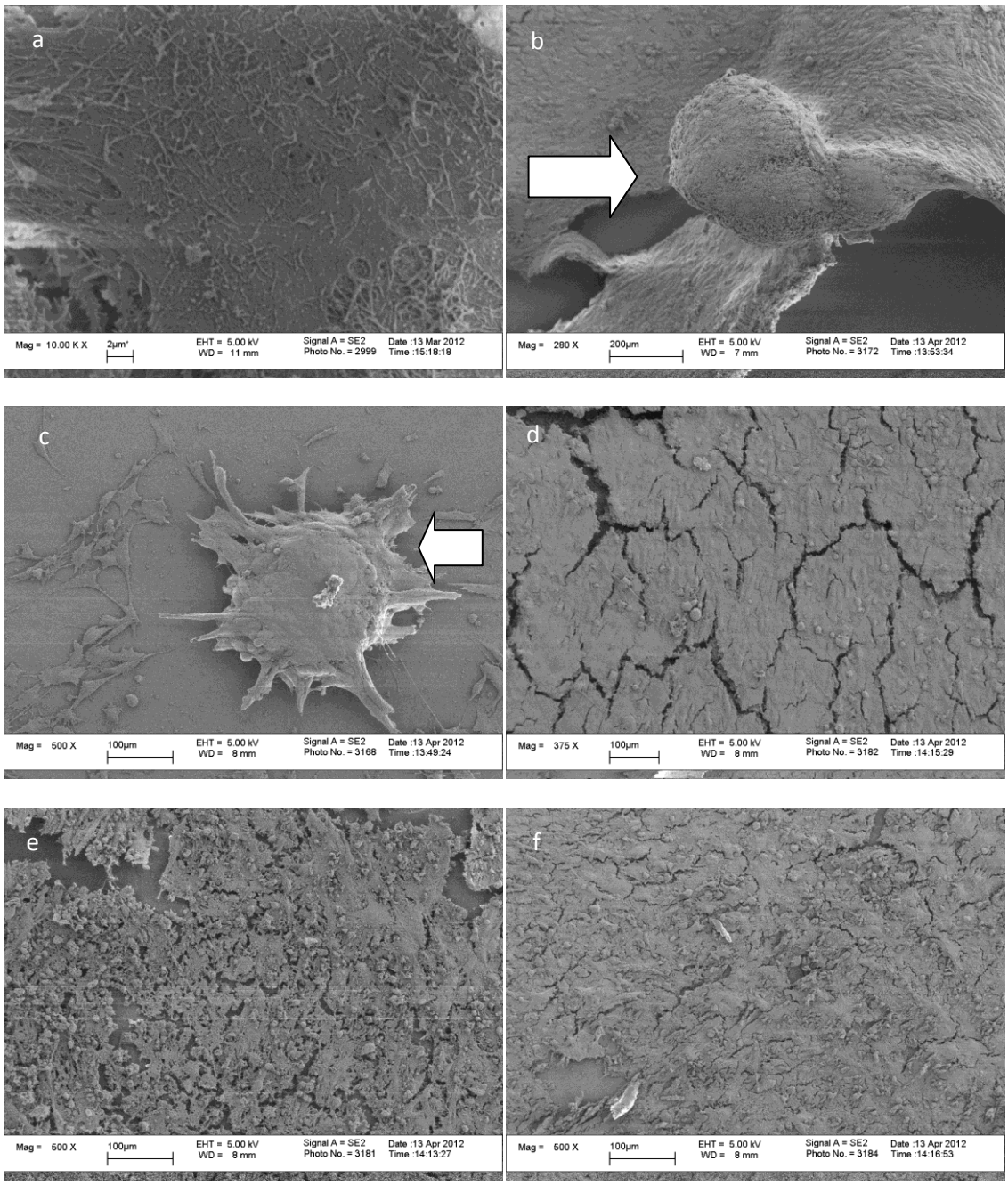

Figure 4.30 **SEM micrographs of Osteoblast-like cells cultured on silane modified glass after 28 days incubation**. Osteoblast –like cells were isolated from human trabecular bone and seeded onto the silane modified surfaces. (a) untreated glass, (b) CL3, (c) CL4, (d) CL6 , (e) CL7 and (f) CL11. White arrows indicate nodules,

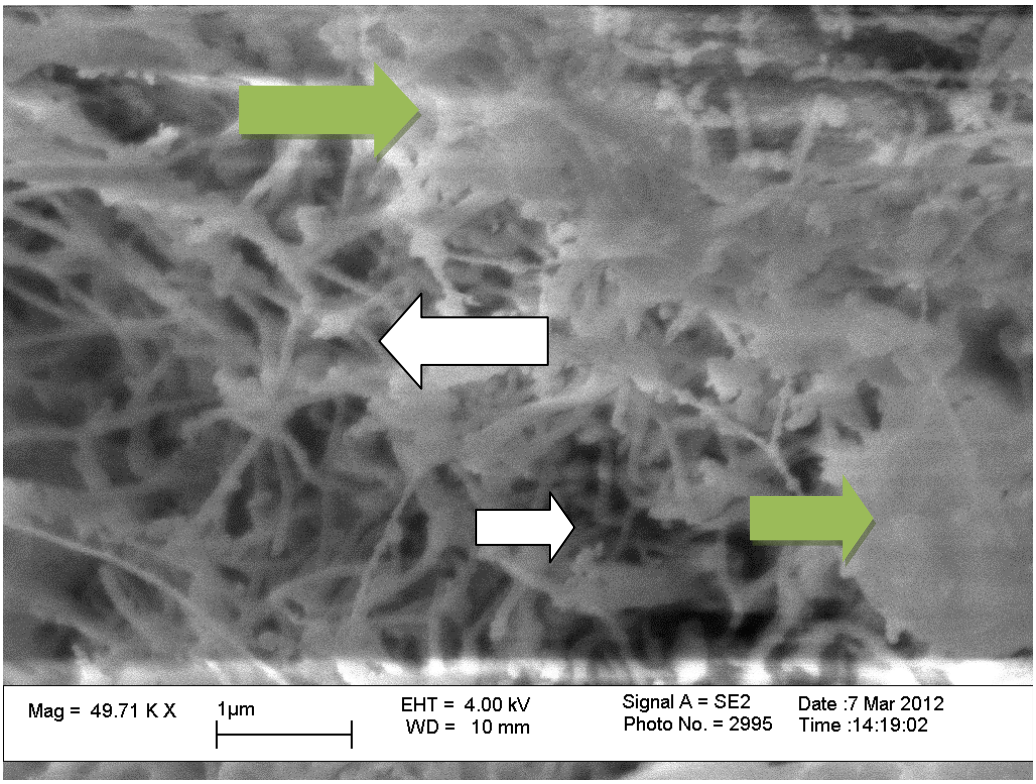

Figure 4.31: **SEM micrographs of Osteoblast-like cells cultured on silane modified glass after 7 days incubation**. Osteoblast –like cells were isolated from human trabecular bone and seeded onto the silane modified surfaces Image taken from surface of nodule formed at 7 days incubation on CL3. White arrows highlight the fiberous nature of the matrix, and green arrows show areas of smooth mineralisation

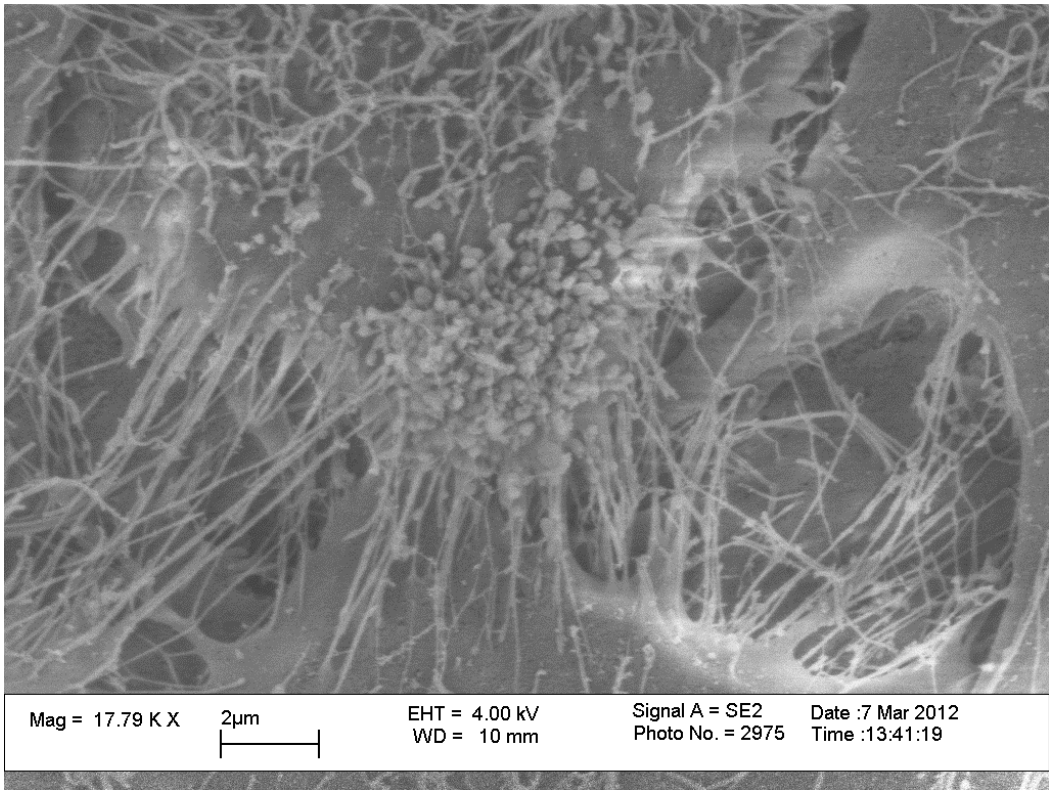

Figure 4.32: **SEM micrographs of Osteoblast-like cells cultured on silane modified glass after 7 days incubation**. Osteoblast –like cells were isolated from human trabecular bone and seeded onto the silane modified surfaces. High magnification image of cells after 7 days incubation on CL11. Highlighting the output of matrix by the cells, while cells remain in monolayer.

4.14: Real time Polymerase Chain Reaction (rtPCR) investigation of primary human osteoblast like cells after 7, 14 and 28 days incubation with silane modified glass.

There is a significant upregulation of sclerositin in the osteoblasts exposed to the CL3 and CL4 modifications after 14 and 28 days. The expression is less after 28 days and peaks at 14 day. Osteopontin is expressed in cells exposed to CL7 at 14 days but not after. Osteocalcin was expressed in early time points forcells exposed to CL3, CL4 , CL6 and CL7 and was expressed later at 28 days for CL11.There was no significant expression of Collagen I by these cells, and there was no significant expression of CBFA1, but this may be expected as it is an early differentiation marker and a transcription factor with is usually only expressed during early in a cells differentiation. Sclerostin, a maker of the osteocytic pathway is switched on in the cells exposed to CL3 and CL4-modified glass, which correlates with the samples having significant nodule formation.

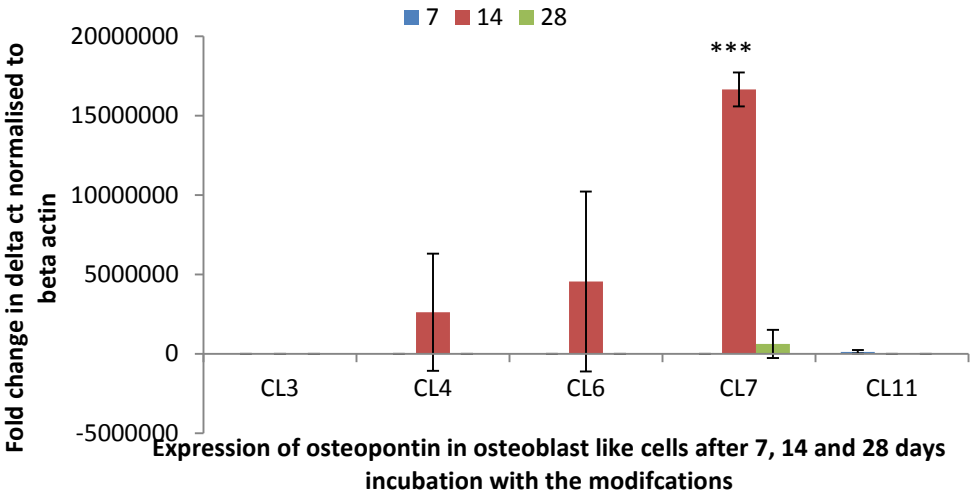

Figure 4.33, **Expression of osteopontin in human osteoblast like cells after 7, 14 and 28 day incubation with silane modified glass**. Osteoblast like cells were isolated from human trabecular bone and processed for rtPCR. Expression of osteopontin was measured and normalised to expression of B-Actin and unmodified scaffold. Data shown is average expression and standard deviation from mean. *=p<0.10, **=p<0.05, ***=p=<0.01

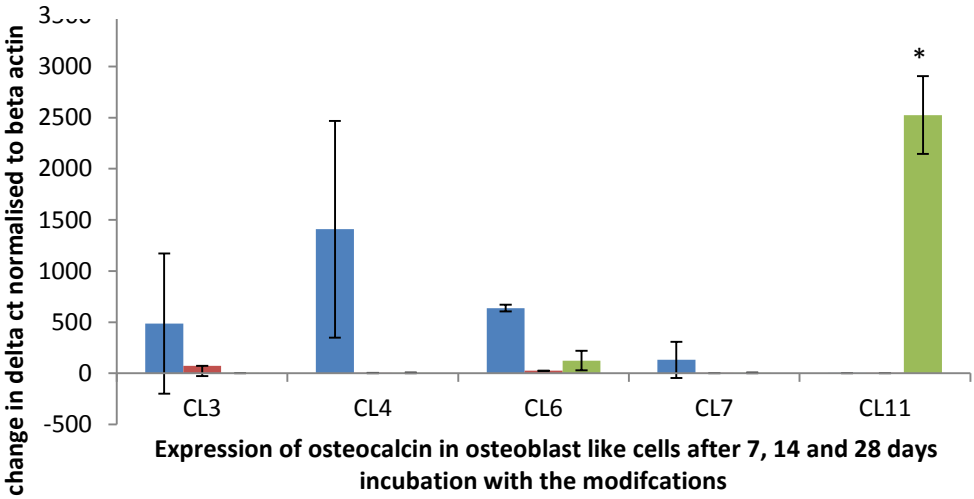

Figure 4.34, **Expression of osteocalcin in human osteoblast like cells after 7, 14 and 28 day incubation with silane modified glass**. Osteoblast like cells were isolated from human trabecular bone and processed for rtPCR. Expression of osteopontin was measured and normalised to expression of B-Actin and unmodified scaffold. Data shown is average expression and standard deviation from mean. *=p<0.10, **=p<0.05, ***=p=<0.01

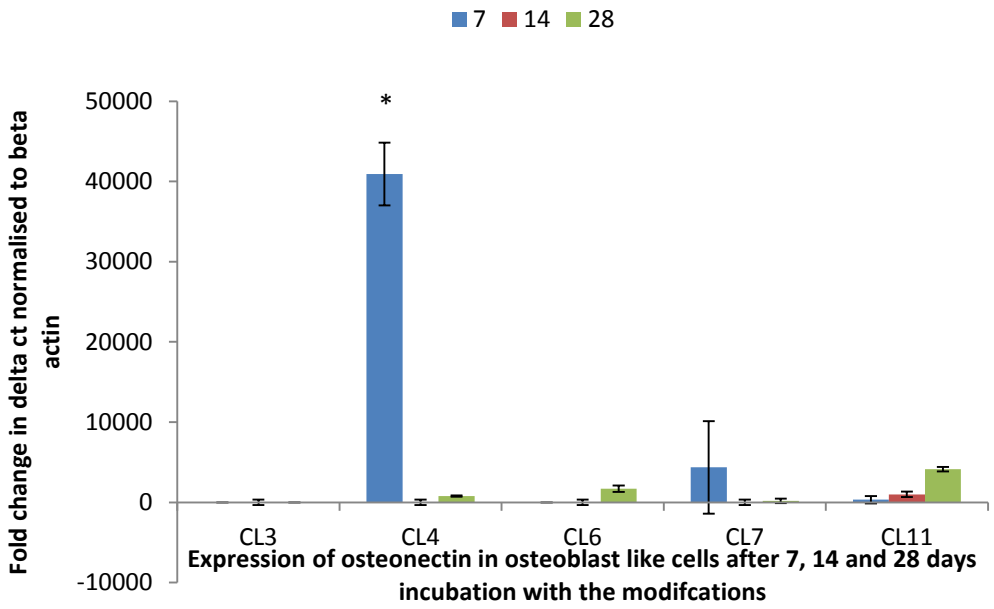

Figure 4.35, **Expression of osteonectin in human osteoblast like cells after 7, 14 and 28 day incubation with silane modified glass**. Osteoblast like cells were isolated from human trabecular bone and processed for rtPCR. Expression of osteopontin was measured and normalised to expression of B-Actin and unmodified scaffold. Data shown is average expression and standard deviation from mean.

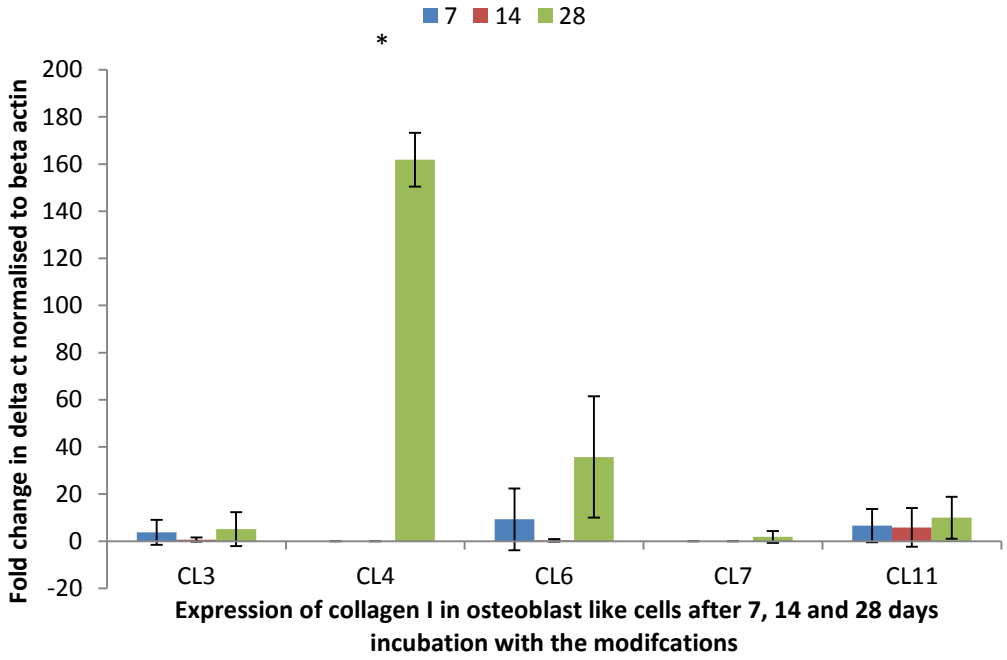

Figure 4.36, **Expression of collagen I in human osteoblast like cells after 7, 14 and 28 day incubation with silane modified glass**. Osteoblast like cells were isolated from human trabecular bone and processed for rtPCR. Expression of osteopontin was measured and normalised to expression of B-Actin and unmodified scaffold. Data shown is average expression and standard deviation from mean. *=p<0.10, **=p<0.05, ***=p=<0.01

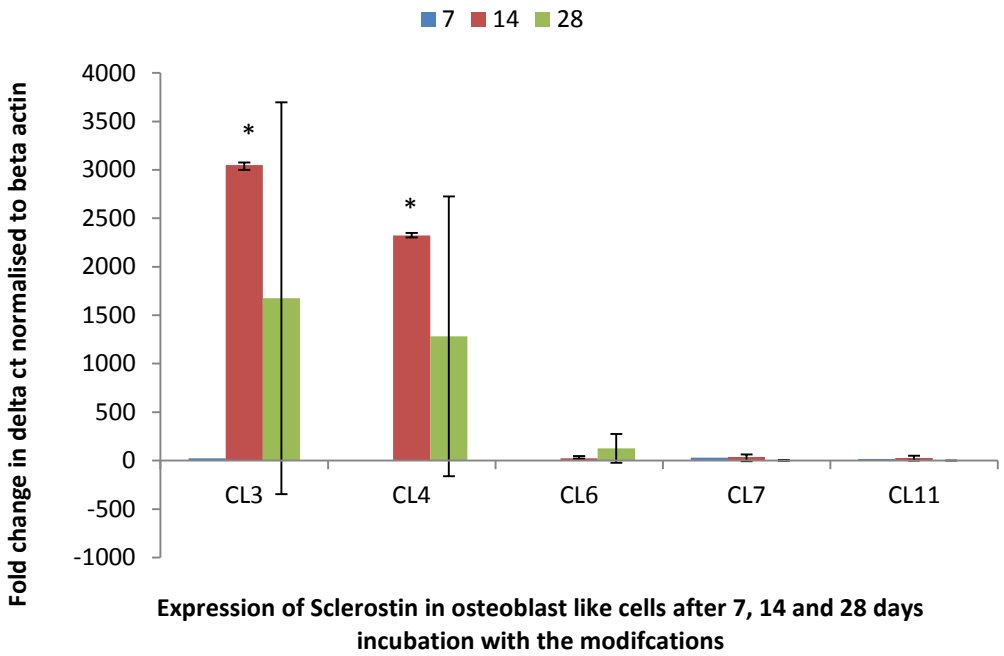

Figure 4.38, , **Expression of sclerostin in human osteoblast like cells after 7, 14 and 28 day incubation with silane modified glass**. Osteoblast like cells were isolated from human trabecular bone and processed for rtPCR. Expression of osteopontin was measured and normalised to expression of B-Actin and unmodified scaffold. Data shown is average expression and standard deviation from mean. *=p<0.10, **=p<0.05, ***=p=<0.01

4.15:Discussion of silane modifications on glass.

To determine if the hypothesis that presentation of a key terminal group was an important factor in influencing osteogenicity, baseline data was produced on a model substrate, in this case glass. To examine the potential of chemical modifications the response was measured using both human MSCs and primary human osteoblast-like cells. These cells make a suitable model to examine the initial phase of osteogenic differentiation as discussed in the literature review and described in detail in several studies[3, 1, 7,8,9, 10.] The osteoblast model represents a more mature environment, further along the differentiation pathway[11],[12].[13].

The various chemistries influence the surface properties of glass when applied. The material properties of the surfaces were changed significantly when the silanes were applied. When the

variance of mean was examined using ANOVA ($p=\geq 0.05$) CL3, CL4 and CL11 showed a significantly different water contact angle when compared to the control, and to CL6 and CL7. CL6 and CL7 did not differ significantly from the control (figure 4.3).

The ninhydrin assay for amine concentration (figure 4.2) demonstrated that its concentration on CL7 was significantly less than any of the other modifications when analysed using ANOVA ($p=\geq 0.05$). This indicates that it may be the concentration of amine that is responsible for the change seen in the water contact angle.

The difference seen on CL7 could be due to the amine chains clumping and not forming a complete self-assembled monolayer(SAM), which is less stable, and less likely to withstand the vigorous washing procedure.[14]

The AFM images of the CL7 modification (figure 4.1.1-4.1.6)show the formation of clumps of matter which formrelatively (from a nanotopography standpoint) large ridges. This pattern was also seen on the CL6 surface, but the concentration of the amine on CL6 was significantly higher than CL7. The inconsistency of the results would be explained by a multiple layer clumping effect, where the silanes do not form full SAMs, and where some of the clumps are washed away by the vigorous washing procedure but some remain in situ, the clumps that remain *in situ* on CL6, would easily explain the raised concentration on the CL6, as equally the removal of the clumps via washing could explain the reduced concentration seen on CL7. The SEM images on the modified glass showed no differences on the modified glass, which highlights that this topographical phenomenon is seen only at the nanoscale.

The AFM highlights the differences in nanotopography, and maximum feature height of the surfaces (figure 4.1.7). There is a statistically significant difference in the maximum feature height between the modified surfaces. This could give some indication of the thickness of the silane coatings. While the scale of the AFM images are unlikely to indicate directly that there is a difference between the silanes on an atomic scale, the marked difference in the maximum feature height of the

silanes does indicate that the longer chain silanes produce a thicker coating than the shorter chain lengths.

Taken together the three characterization techniques (AFM, Ninhydrin and WCA) demonstrates clearly that the range of silanes used in this study successfully altered the glass substrate. They created different surface topographies when examined on the nanoscale, in addition to the change in surface chemistry. There was an increased concentration of amine groups after modification. Amine groups have been demonstrated in previous studies to show osteogenic capacity.[6,15] There has been a large amount of research focused around the influence of surface nanotopography on stem cells and it has been demonstrated that there is an optimum surface topography for osteogenic differentiation.[16] The key points from the studies that were successful in creating an osteogenic topography were that they created a surface that had an optimal surface roughness, but only when it was not ordered. The experiment that highlighted this particularly well used a titanium surface with mechanically punched pits. The pits were osteogenic when punched in an irregular grid formation, but showed no osteogenic potential when they were in a regular grid formation If this topography could be achieved successfully, and consistently using a silane coating, it would be a step forward in the area of bone regeneration.

Mineral deposition on silane treated glass

The mineralization process is one of the key progressions of the bone regeneration process. The development of biomimetic surfaces attempts to fulfill this important step in the regeneration process by chemical interactions where a material can self-mineralize. The ability of some SAMs to cause the nucleation of minerals on surfaces offers a route to accelerate the osteogenic process, and cause early mineralisation[6]. This phenomenon was described by Towoefe *et al* where the SAM in question, while not produced from the same chemical used in this study, demonstrated an extended carbohydrate chain similar in length to the long chain amines used in this work. To demonstrate the ability of the surfaces produced for this study to self-mineralize, the surfaces were exposed to different concentrations of PBS for 7 days. The resulting surfaces were then examined using a Von

Kossa stain for mineralization (figure 4.4), and X-ray microanalysis (figures 4.5-4.8) to show the elemental composition of the surfaces. After 7 days the CL11 modification showed positive mineralization of the surfaces, demonstrated by positive Von Kossa staining at 7 days, and the abundant presence of phosphate detected with X ray analysis (figures 4.5-4.8). The presence of phosphate in hydrogel has previously been shown to induce an osteogenic response[17] so the ability of the surface of CL11 to attract and bind phosphorous could be indicative of this type of event. The probability of the surface modification on CL11 being the cause of the phosphate detected using X-ray microanalysis was calculated in table 4.2, which suggested that the collelation was statistically significant($p \geq 0.95$) None of the other chain lengths showed this effect.

Mesenchymal stem cell response to silane modified glass

The cellular response to the silane-modified glass was examined using rtPCR to determine the expression of genes at defined time points (figures 4.14-4.19). The cells were examined for the expression of several markers of stem cell differentiation that are key to the osteogenic pathway. CBFA1 was the first gene to be examined, as it is considered to be the corner pin of the osteogenic differentiation process[18,19]. It is only present in the early phases of differentiation and for a relatively short period of time[19]. There was no positive expression of CBFA1 on CL3, CL7 or CL11 at any of the time points tested, but there was up regulation on CL4 and 6 at 28 days. There was an expression of osteonectin which is a key protein in the osteogenesis process [,20, 21,22] at 7 days by the cells on CL4, CL6 CL7 and CL11, the most prominent response seen with CL7 and CL11 which were statistically significant when analysed by ANOVA ($p \leq 0.05$). There was a statistically significant difference in the expression of osteopontin, which also plays a role in osteogenesis [20], on CL7 and CL11 at 7 days, and osteocalcin (a vital mineralization protein)[23,24,]was expressed at 7 and 14 days on CL11, which was greatly reduced at 28 days. Sclerostin, a marker of embedded osteocytes and so a clear indicator of osteogenic maturity[,25,26,27] was expressed by CL11 at 14 days. Taken together, these results suggest that osteogenic markers are present consistently on the CL11 sample. The absence of CBFA1 on CL11 may be due to the initial time point (7 days) being too late to pick up an initial burst of expression following initial contact. It is a gene that may only be expressed for a short period of time.

The expression of osteonectin, osteopontin and osteocalcin all indicate that the cells are capable of producing these proteins, which are heavily linked to osteoblastic activity. The results show that the expression of these genes drops out after 7-14 days, and there is then a positive expression of the osteocyte marker sclerostin on CL11 at 14 days. This shows that the cells on CL11 have the capacity to differentiate into osteocytes, which is the next phase of osteogenic differentiation after the cells have passed through the osteoblast phase. For the cells to achieve this status, they must become embedded in a thick ECM, composed of osteocalcin, and collagen amongst other proteins.[25,26]

Examining the cells using SEM to determine their morphology and matrix production was performed to provide more evidence of differentiation.(Figures 4.10-4.13). The 7 day time point revealed that CL3, CL4 and CL7 all had very flat adhered cells. Cells were very rounded in morphology on CL6 but flat and adhered and producing many proteinacious extrusions on CL11. By 14 days the cell numbers on CL6 were reduced, CL3 and CL4 and CL7 were all demonstrating a very flat monolayer of cells, and CL11 was showing a dense formation of matrix over a monolayer of very flat adhered cells. By 28 days, there were even fewer cells on CL6, but CL3, CL4 and CL7 were demonstrating flat cells with some protein production. The CL11 sample was covered in a dense matrix that seemed to be becoming pitted in its appearance, with the cells that were completely obscured by ECM. This is verified by the PCR data, showing the upregulation of matrix genes on CL11, and then the expression of sclerostin which could only be produced if the cells were embedded in a thick ECM, which completely encased the cells.

The presence of the ECM was confirmed by the SEM images of the samples. Identification of the presence of osteogenic markers by confocal microscopy confirms the composition of the ECM which was produced by the cells. One of the many advantages of confocal microscopy is that cells and proteins can be stained fluorescently when in multiple layers. 3D matrix can be scanned in layers and an image of the whole sample can be produced, rather than the SEM which is restricted to just the top.

Confocal microscopy was also used to detect a marker of MSC plasticity, Stro-1 (figures 4.20-4.22). This marker is a way of identifying undifferentiated cells, and its absence in these samples only occurs if the cells have already begun differentiation[28],[29]. If Stro-1 is absent and other positive markers of osteogenic differentiation such as CBFA1 and Osteocalcin are present, then it is likely that the cells are committed to an osteogenic fate.

The MSCs on the untreated control expressed Stro-1 at 7, 14 and 28 days. This, in conjunction with the absence of any of the osteogenic markers, confirms that the MSCs have not spontaneously differentiated. The confocal staining of the modified glass showed that Stro 1 was expressed at 7 days, but not at 14 days and there was positive staining for Osteocalcin and CBFA1. CL4 modified samples showed positive collagen 1 staining at 7 days but not Stro-1, although no differentiation markers were expressed until 28 days. CL6 showed positive Collagen I staining throughout the 28 day period, but was not positive for any of the osteogenic markers. CL7 showed some positive CBFA1 staining at 28 days, but nothing before that time point, so this could not be described as a truly osteogenic response. The most interesting result, however, came from the CL11 surface. The CL11 sample showed matrix by 7 days which was positive for osteocalcin and collagen, and by 14 days was showing a thick, pitted morphology. This response was maintained through to the 28 day time point, and is a good osteogenic response from the cells.

The Von Kossa stain for mineralization was used to determine the extent of mineralization in the samples. This process is well established and has been used in many studies to determine the extent of mineralisation[11],[22]. It should however not be used as a definitive test for the production of bone, and if possible there should be other confirmatory tests if there is a positive result.[30] The samples showed some positive staining on all of the modifications, however it was more marked on the CL11 sample. The control untreated glass showed no positive staining.

The results all support the hypothesis that CL11-modified surfaces modification is a powerful stimulant to MSCs, and is able to induce an osteogenic response from them in the absence of any exogenous growth factors. There are a few different possibilities that could explain the root cause of

that osteogenic differentiation. This surface has several osteogenic properties, including topography which possesses the parameters that induce an osteogenic response, as confirmed by AFM microscopy including the correct size of feature, which appears to have a very powerful effect on stem cells.[31,16,32,33]

The abundant availability of CL11 amine groups, which as discussed in the introduction is inductive of osteogenesis[3]. The ability of the CL11 surface to harness phosphorous[6], in a biomimetic way may well be contributing to the availability of minerals to the cells. It could be that in their productive osteoblastic state the cells require greater quantities of the minerals that are available more readily on the CL11 surfaces.

It may be that the ability of CL11 surfaces to procure minerals and make them available accelerates the process of osteogenic differentiation and eventually allows the it to progress to the next phase, osteocytic differentiation. This is demonstrated quite clearly by the expression of sclerostin at 14 days, with thick matrix production, and it could be that the pits formed in this matrix is the start of rudimentary re-modeling. For future work, it would be very interesting to study the MMPs as markers of re-modeling and to extend the study further in time, to 2 months.

Primary human osteoblastlike-cells on silane modified glass

The primary human osteoblast-like cell model used represents an advanced stage in the osteogenic pathway. Examining how these cells interact with the modified surfaces are an attempt to demonste how mature cells will react to the surface modifications, giving an impression of what the longer term effects may be. There was an interesting response observed at the first time point, Von Kossa staining (figures 4.23-4.25) showed mineralized nodules formation on the CL3 and CL4 surfaces. This reaction was not seen on the other surfaces, where the cells remained in monolayer throughout the 28 day period. The nodule formation on CL3 and CL4 could be explained by the progression of the osteogenic differentiation of the cells. Primary human osteoblasts have been shown to form nodules[12] when in 3D culture on bioactive glass, but only in the presence of exogenous growth factors. This stimulus in this incidence could have come purely from the material.

The formation of nodules on the CL3 and CL4 surfaces was confirmed by SEM, and Von Kossa stain. As the cells used in this model were already capable of producing ECM, all of the samples including the untreated glass control stained positive for mineralization (Von Kossa) at 7 days, however the cells on the untreated control were less densely mineralized by 28 days than the silane treated samples. The cells on CL6, CL7 and CL11 all retained the ability to produce matrix which became mineralized.

The SEM of surfaces with osteoblasts revealed that there was an extensive production of ECM on the CL3 and CL4 samples when the cells were clumped together in the nodule (figure 4.28-4.32). The ECM appears to mature throughout the 28 day period and goes from an obvious fibrous formation of proteins at 7 days to a more dense, mineral-covered matrix at 14 days and by 28 days the cells appeared to be embedded in this matrix.

The size of the nodules (figure 4.27) was shown to increase over a 14 day period and then significantly decrease. This occurrence when combined with the statistically significant drop in total number of nodules (figure 4.26) at 28 days could be indicative of the nodules reaching a critical size and then detaching from the surface. This would warrant further investigation as a material that could product and then release these boney nodules might have interesting applications for filling bone defects.

The PCR figures (4.33-4.38) of these samples revealed an interesting response. All data were normalized to the untreated glass control so the expression shown was above the baseline of normal osteoblast activity on glass. The osteogenic markers are only above the baseline activity at 7 days and not statistically significant after this time point. Interestingly on CL3 and CL4 the expression of sclerostin was notable at 14 and 28 days. As this is a marker specifically for osteocytic activity, this along with the reduction of normal osteoblastic markers after 7 days is indicative of the further differentiation of the cells along the osteogenic pathway. All the results are consistent with this hypothesis.

Interestingly CL11 does not seem to have the same powerfully osteogenic effect on the osteoblasts as it does on human MSCs. CL11 does however, seem to maintain the osteoblasts and allows them to form a mineralized matrix; the cells were shown by SEM to produce large quantities of ECM. The Von Kossa staining shows that mineralization is occurring, on this sample, but there are no nodules present. It has been documented earlier that the CL11-modified glass surfaces have the ability to attract phosphorous (see PBS interaction figure 4.4, and hMSC data figures 4.5-4.8). In this experiment, because the cells are mature osteoblasts, they are covered in minerals such as phosphorous and calcium. It could be that the cells are "captured" by the surface, and that the minerals on the surface of the cells are used to adhere the cell to the surface in an irreversible way. This would explain why the CL11 samples are not forming nodules, as the cells are unable to migrate. CL6 and CL7 have not shown any significant osteogenic potential in any of the tests, and were not shown to produce any significant matrix. The cells on CL6 were very rounded until between 7 and 14 days at which point they started to form a monolayer. This delayed adhesion could be responsible for the lack of osteogenic markers seen from this modification.

The differences observed between the chain lengths and their osteogenic effects could be attributed to several things. The procurement of minerals by CL11, the topography that is induced at the nanoscale and the mimicry of the ECM by the chemical modification could be key factors in these results.

The results indicate that CL11 could be a powerful inducer of osteogenic differentiation, and would accelerate the differentiation of MSCs, in the absence of exogenous growth factors. In osteoblasts, while CL11 maintains the production of matrix, it does not allow the already mature cells to continue down the osteogenic pathway to the osteocytic phenotype, but if the initial interaction with the surface is at the MSC stage, differentiation can be induced right along the osteoblastic lineage to osteocytic fate. This could be explained by the hypothesis mentioned earlier where the mineralized surfaces of the cells can be chemically bound to the CL11 surface. To define this with a time line of events, it appears that mineralization of the surface happens initially and quite rapidly [6], before the cells adhere to the mineralized surface. If the cells have minerals on the surface (as in the

osteoblast-like cell model) this time line initially is disrupted and the cells captured in the initial mineralization phase, hindering migration (and their ability to form nodules). To extend this study further, this hypothesis could be tested by looking at the movement of the cells across the surface. Time lapse imagery of the cells over a 7 day period may answer this question, but ideally an intergrin binding profile could be examined in more detail to determine the factors in play at the initial adherence.

In the instance of the CL3 and CL4 nodule formation, it is likely that it is the amine rich surfaces and the topography that instigates the formation of nodules. The surfaces do not have the same self-mineralizing properties and so the phenomenon can't be related directly to mineral deposition on the surfaces. It is either the topography or chemistry which instigates this process, not the presence of phosphorous alone.

1. Phillips, J.E., Petrie, T. A, Creighton, F.P. & García, A.J. Human mesenchymal stem cell differentiation on self-assembled monolayers presenting different surface chemistries. *Acta biomaterialia* **6**, 12-20 (2010).

2. Curran, J.M., Pu, F., Chen, R. & Hunt, J. A. The use of dynamic surface chemistries to control msc isolation and function. *Biomaterials* **32**, 4753-60 (2011).

3. Curran, J.M., Chen, R. & Hunt, J. A. Controlling the phenotype and function of mesenchymal stem cells in vitro by adhesion to silane-modified clean glass surfaces. *Biomaterials* **26**, 7057-67 (2005).

4. Rahman, N. & Kashif, M. Application of ninhydrin to spectrophotometric determination of famotidine in drug formulations. *Il Farmaco* **58**, 1045-1050 (2003).

5. Rahman, N. & Azmi, S.N. Spectrophotometric method for the determination of amlodipine besylate with ninhydrin in drug formulations. *Farmaco* **56**, 731-5 (2001).

6. Toworfe, G.K., Bhattacharyya, S., Composto, R.J., Adams, C.S. & Shapiro, I.M. Effect of functional end groups of silane self-assembled monolayer surfaces on apatite formation , fibronectin adsorption and osteoblast cell function. 26-36 (2009) 7.
Guo, L. Kawazoe,N.,& Hoshiba,T. Osteogenic differentiation of human mesenchymal stem cells on chargeable polymer-modified surfaces. *Journal of biomedical materials research. Part A* **87**, 903-12 (2008).

8. Hoshiba, T., Kawazoe, N., Tateishi, T. & Chen, G. Development of stepwise osteogenesis-mimicking matrices for the regulation of mesenchymal stem cell functions. *The Journal of biological chemistry* **284**, 31164-73 (2009).

9. Kundu, B. & Kundu, S.C. Osteogenesis of human stem cells in silk biomaterial for regenerative therapy. *Progress in Polymer Science* **35**, 1116-1127 (2010).

10. Chen, Y., Shao, J.-Z., Xiang, L.-X., Dong, X.-J. & Zhang, G.-R. Mesenchymal stem cells: a promising candidate in regenerative medicine. *The international journal of biochemistry & cell biology* **40**, 815-20 (2008).

11. Ferrera, D. Poggi, S ., Biassoni, C., & Dickson, G.R. Three-dimensional Cultures of Normal Human Osteoblasts: Proliferation and Differentiation Potential In Vitro and Upon Ectopic Implantation in Nude Mice. **30**, 718-725 (2002).

12. Gough, J.E., Jones, J.R. & Hench, L.L. Nodule formation and mineralisation of human primary osteoblasts cultured on a porous bioactive glass scaffold. *Biomaterials* **25**, 2039-2046 (2004).

13. Gough, J.E., Notingher, I. & Hench, L.L. Osteoblast attachment and mineralized nodule formation on rough and smooth 45S5 bioactive glass monoliths. *Journal of biomedical materials research. Part A* **68**, 640-50 (2004).

14. Schwartz, D.K. Mechanisms and kinetics of self-assembled monolayer formation. *Annual review of physical chemistry* **52**, 107-137 (2001).

15. Curran, J.M., Chen, R. & Hunt, J. A The guidance of human mesenchymal stem cell differentiation in vitro by controlled modifications to the cell substrate. *Biomaterials* **27**, 4783-93 (2006).

16. McNamara, L.E. RJ McMurray, MJP Biggs,& Dalby.M. Nanotopographical control of stem cell differentiation. *Journal of tissue engineering* **2010**, 120623 (2010).

17. Dadsetan, M. Giuliani,M.,& Wanivenhaus,F. Incorporation of phosphate group modulates bone cell attachment and differentiation on oligo(polyethylene glycol) fumarate hydrogel. *Acta biomaterialia* **8**, 1430-9 (2012).

18. Makita, N. Suzuki,M., Asami,S., Takahata,R.,& Kohzaki,D.. Two of four alternatively spliced isoforms of RUNX2 control osteocalcin gene expression in human osteoblast cells. *Gene* **413**, 8-17 (2008).

19. Huang, L., Teng, X.Y., Cheng, Y.Y., Lee, K.M. & Kumta, S.M. Expression of preosteoblast markers and Cbfa-1 and Osterix gene transcripts in stromal tumour cells of giant cell tumour of bone. *Bone* **34**, 393-401 (2004).

20. Nakase, T., Takaoka,K., Hirakawa, K.,& Hirota, S. Alterations in the expression of osteonectin, osteopontin and osteocalcin mRNAs during the development of skeletal tissues in vivo. *Bone and mineral* **26**, 109-22 (1994).

21. Koblinski, J.E., Wu, M., Demeler, B., Jacob, K. & Kleinman, H.K. Matrix cell adhesion activation by non-adhesion proteins. *Journal of cell science* **118**, 2965-74 (2005).

22. Mathews, S., Bhonde, R., Kumar, P. & Totey, S. Extracellular matrix protein mediated regulation of the osteoblast differentiation of bone marrow derived human mesenchymal stem cells. *Differentiation* 1-8 (2012).

23. Theyse, L.F.H., Mol, J. A, Voorhout, G., Terlou, M. & Hazewinkel, H. A W. The efficacy of the bone markers osteocalcin and the carboxyterminal cross-linked telopeptide of type-I collagen in evaluating osteogenesis in a canine crural lengthening model. *Veterinary journal* **171**, 525-31 (2006).

24. Harwood, P.J. (ii) An update on fracture healing and non-union. *Orthopaedics and Trauma* **24**, 9-23 (2010).

25. Bragdon, B. Moseychuk,O. Saldanha,S.,& King,D.. Bone morphogenetic proteins: a critical review. *Cellular signalling* **23**, 609-20 (2011).

26. Bohner, M., Galea, L. & Doebelin, N. Calcium phosphate bone graft substitutes: Failures and hopes *Journal of the European Ceramic Society*. **32**, 2663-2671 (2012).

27. Loots, G.G. Kneissel,M., Keller,H., Baptist,& M. Sclerostin in Van Buchem disease Genomic deletion of a long-range bone enhancer misregulates sclerostin in Van Buchem disease. *Genome* **15**: 928-935 (2005).

28. Kassem, M. Mesenchymal Stem Cells: Biological Characteristics and Potential Clinical Applications. *Cloning and Stem Cells* **6**, 369-374 (2004).

29. Dominici, M. Le Blanc,K. Mueller,I.,& Slaper-Cortenbach,I .Minimal criteria for defining multipotent mesenchymal stromal cells. The International Society for Cellular Therapy position statement. *Cytotherapy* **8**, 315-7 (2006).

30. Bonewald, L.F. Harris, S.E., Rosser, J.,& Dallas, M.R. von Kossa staining alone is not sufficient to confirm that mineralization in vitro represents bone formation. *Calcified tissue international* **72**, 537-47 (2003).

31. Wilkinson, A. Meek R.M.D. Biomimetic microtopography to enhance osteogenesis in vitro. *Acta biomaterialia***7**, 2919-25 (2011).

32. Sjöström,T., Dalby, M.J. Hart,A., Tare,R., Oreffo,R.O.C.,& Su.B. Fabrication of pillar-like titania nanostructures on titanium and their interactions with human skeletal stem cells. *Acta biomaterialia* **5**, 1433-41 (2009).

33. Dalby, M.J., McCloy, D., Robertson, M., Wilkinson, C.D.W. & Oreffo, R.O.C. Osteoprogenitor response to defined topographies with nanoscale depths. *Biomaterials* **27**, 1306-15 (2006).

Chapter 5: Mesenchymal Stem Cell Response to Silane Modification of PLGA Films and Injectable 3D System

Transferring the silane-coating technology from a flat glass surface onto a 2D polymer surface is an important step for the successful translation of surface modifications to a clinical setting. Ultimately, the goal is to achieve the same the optimised behaviour established on the glass surfaces on a PLGA sphere, and thin in the 3D system described in the plasma modification chapter. While this is our objective, it is by no means a certain proposition, as the surface energy of PLGA is very different to that of glass and this step requires more investigation before it can be taken to the 3D platform. Therefore initial tests will be conducted on flat PLGA films. There is a precedent applying the chemistries in a 2D system before attempting any 3D modifications, and most successful studies take this route of investigation.[1]

This chapter will detail the translation of modifications onto PLGA films, steps taken to optimise the deposition of chemical groups and the associated cell responses. This will be done using an *in vitro* MSC model. Once the parameters are defined and explored, the surface modifications will be applied to PLGA spheres and incorporated into the 3D system.

PLGA has different material properties to glass and is technically challenging to process, so for this reason some techniques used on the glass surfaces in chapter 4, are unsuitable for the samples generated in this chapter. It is not possible, for example to use SEM on the cells on the PLGA film, as the film becomes too disrupted in the process required to process the cells, therefore different techniques are sometimes deployed. The base line data seen in the silane-modified glass chapter, demonstrated significantly modified

cell responses when. The challenge now is to see if the modifications are applicable to the very different PLGA surfaces.

5.1: AFM microscopy of flat PLGA films

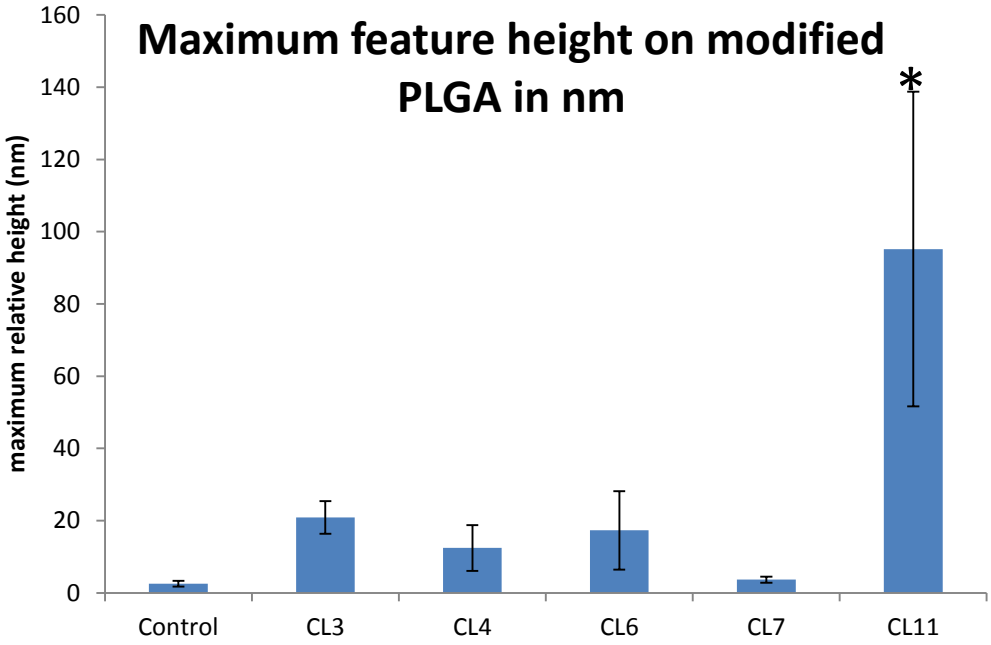

Figure 5.1: **Maximum feature height of silane modified surfaces.** Measured using AFM. 5 areas were measured on each sample (n=3) Error bars indicate the standard deviation and * indicates statistical significance ($p<0.05$)

The maximum feature height was calculated using the maximum peak on 50 nm area at 5 separate areas on a sample. This was repeated 3 times. The data was analysed using ANOVA to determine significant differences in the variance of mean ($p=<0.95$). CL11 had a significantly greater maximum peak height than all the other modifications, indicating that the coverage of the silanes was significantly increased on CL11, and implying that the topography of CL11 is significantly different.

The examination of the PLGA films with AFM showed a topographical difference between the different modifications. CL3 and CL4 had a similar morphology of surface features to each other, being a similar height, and pattern. There was a well dispersed and relatively

uniform nanotopography that appeared to stay uniform in its coverage across the entirety of the samples. CL6 and CL7 demonstrated a more clumped macrotopography, where the coverage was less uniform and more nodular in its presentation. CL11 was interesting because it combined the two morphologies, showing a macrotopography that was covered in a nanotopography similar to that of seen in the CL3 and CL4 modifications.

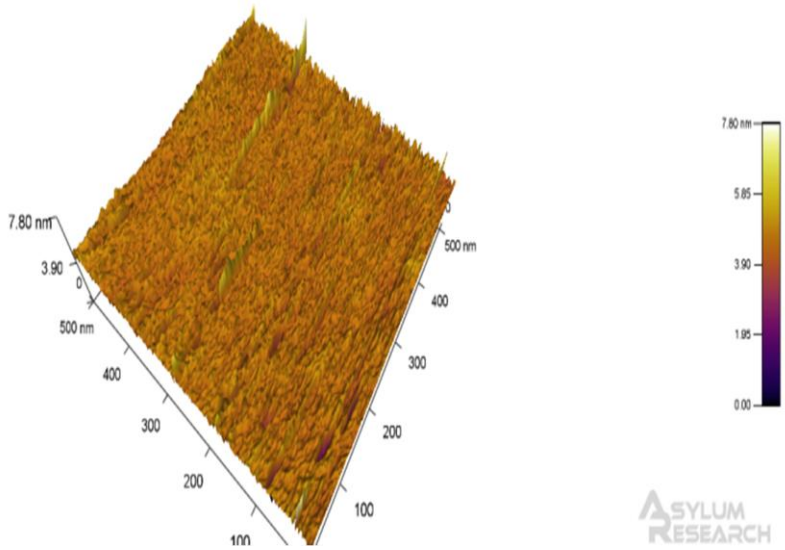

Figure 5.2: **AFM micrograph of untreated PLGA film.** 12mm diameter glass coverslips were cleaned as stated in protocol and spin coated with PLGA. AFM images taken from 5 areas per sample, representative image shown

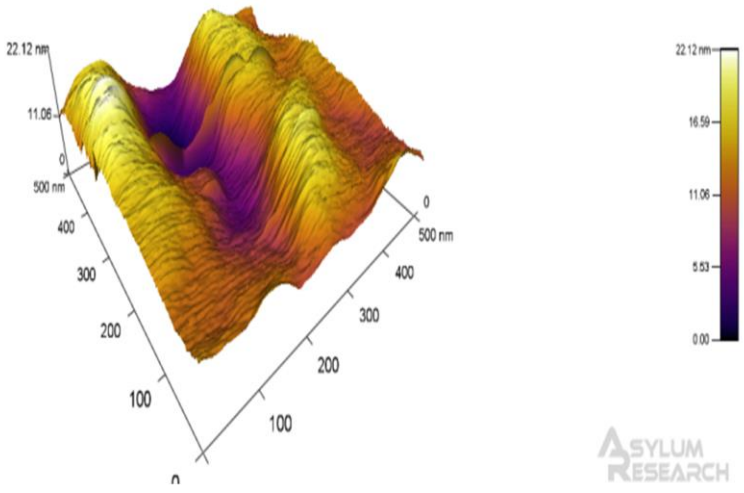

Figure 5.3: **AFM micrograph of CL3 treated PLGA film.** 12mm diameter glass coverslips were cleaned as stated in protocol and spin coated with PLGA, then modified with CL3. AFM images taken from 5 areas per sample, representative image shown.

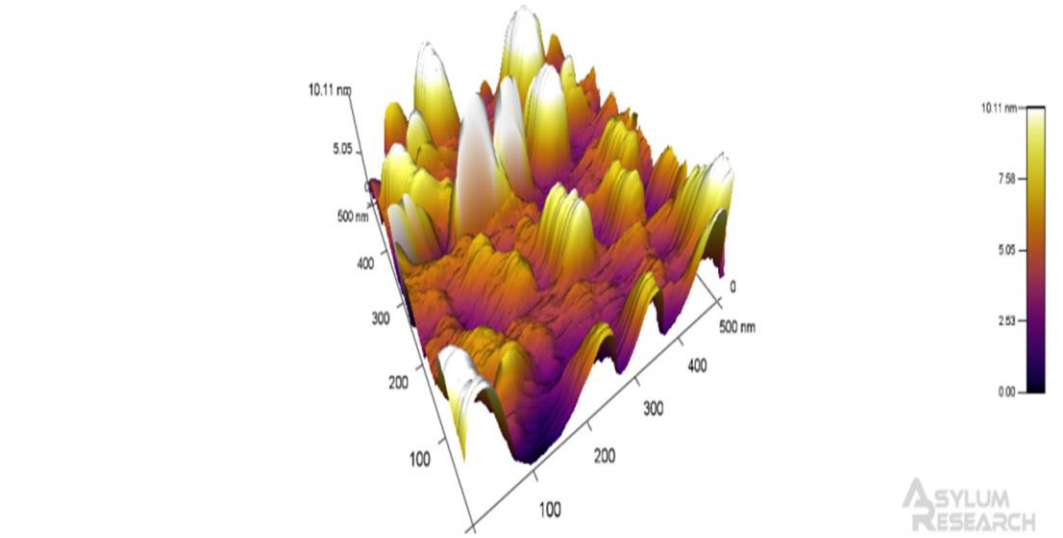

Figure 5.4: **AFM micrograph of CL4 treated PLGA film.** 12mm diameter glass coverslips were cleaned as stated in protocol and spin coated with PLGA, then modified with CL4. AFM images taken from 5 areas per sample, representative image shown.

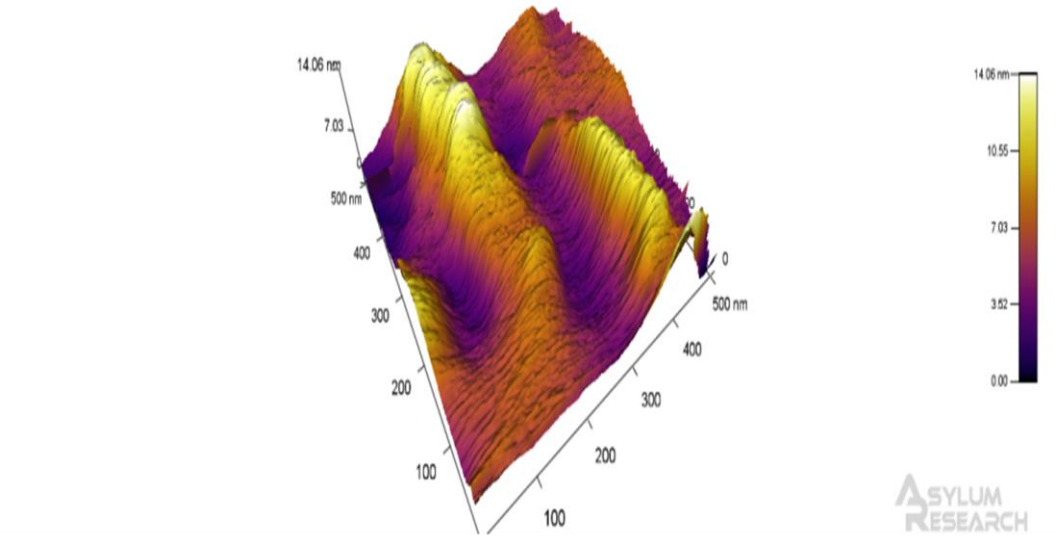

Figure 5.5: **AFM micrograph of CL6 treated PLGA film.** 12mm diameter glass coverslips were cleaned as stated in protocol and spin coated with PLGA, then modified with CL6. AFM images taken from 5 areas per sample, representative image shown.

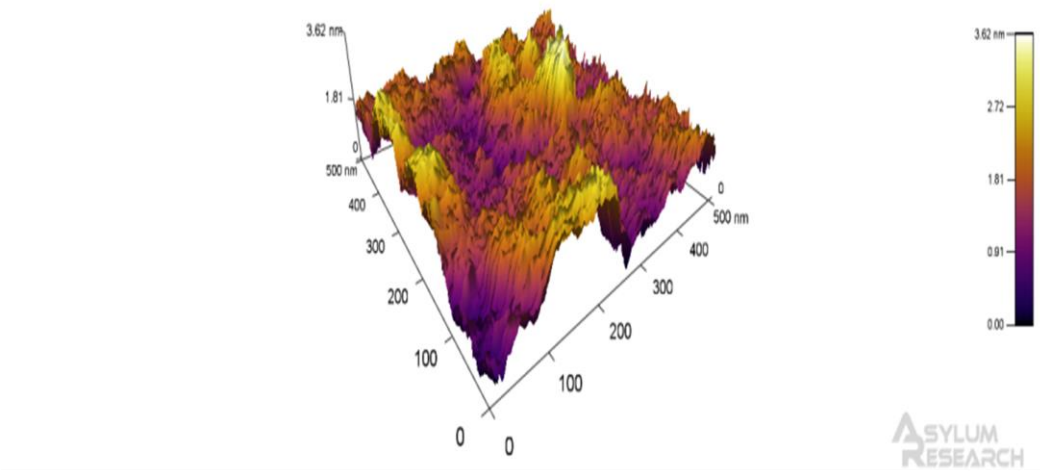

Figure 5.6: **AFM micrograph of CL7 treated PLGA film.** 12mm diameter glass coverslips were cleaned as stated in protocol and spin coated with PLGA, then modified with CL7. AFM images taken from 5 areas per sample, representative image shown.

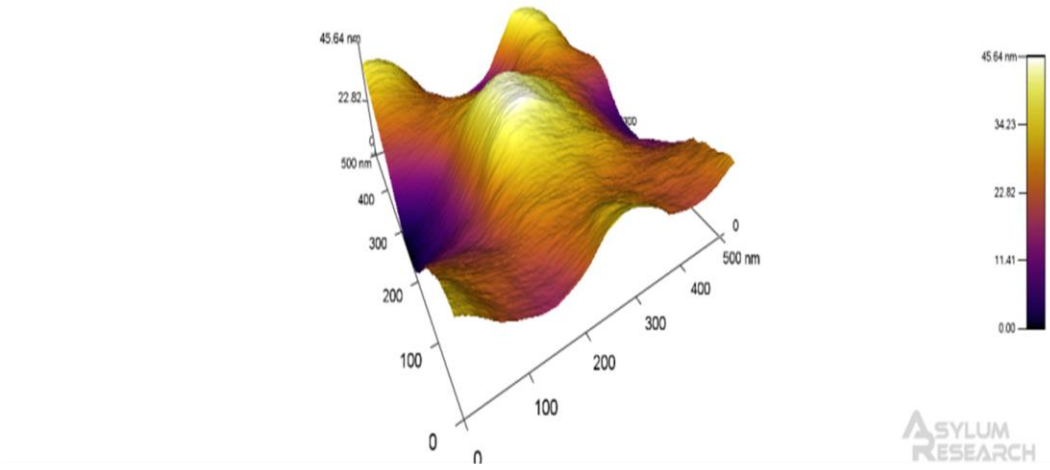

Figure 5.7: **AFM micrograph of CL11 treated PLGA film.** 12mm diameter glass coverslips were cleaned as stated in protocol and spin coated with PLGA, then modified with CL11. AFM images taken from 5 areas per sample, representative image shown.

5.2: Ninhydrin Assay of flat PLGA films

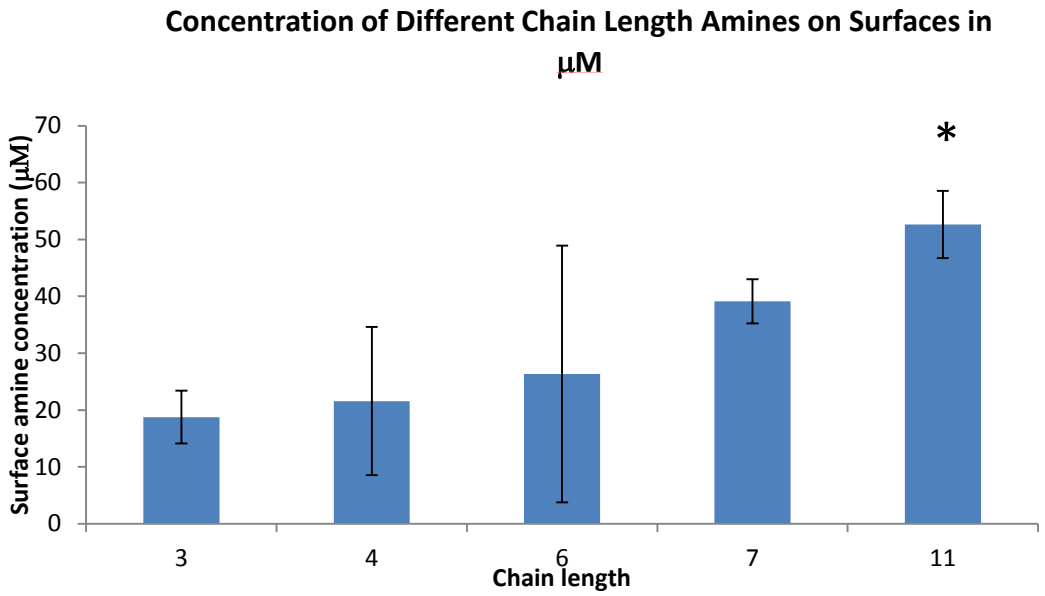

Figure 5.8. **Ninhydrin assay of amine concentration on the modified PLGA surfaces**. Concentration of amine on surfaces was measured by ninhydrin assay. Results show averages and error bars show standard deviation from mean *=p<0.05

The concentration of amine on the surfaces was measured using the ninhydrin assay. CL11 demonstrated a significantly higher concentration of amines when compared to the other modifications (p=>0.05). CL3, CL4, C6 and CL7 showed no statistically significant differences in the variance of their means.

5.3: Dynamic Water Contact Angle of flat PLGA films

The advancing angle of the dynamic water contact angle was used as a representation of the actual surface energy that cells are exposed to when they are seeded on a surface. This is more relevant to the experiment than the receding angle, which is not shown in this chart.

The statistical analysis showed that there were significant differences between all of the modifications and the control (the stars indicate degree of difference) and significant differences between CL3 and CL6, and CL6 and CL11 ($p=>0.05$).

There is an inverse linear correlation between the chain length/number of carbon atoms in the chain of the silane molecule and the advancing water contact angle ($r^2=0.9645$) which is above the 95% confidence interval and so statistically significant.

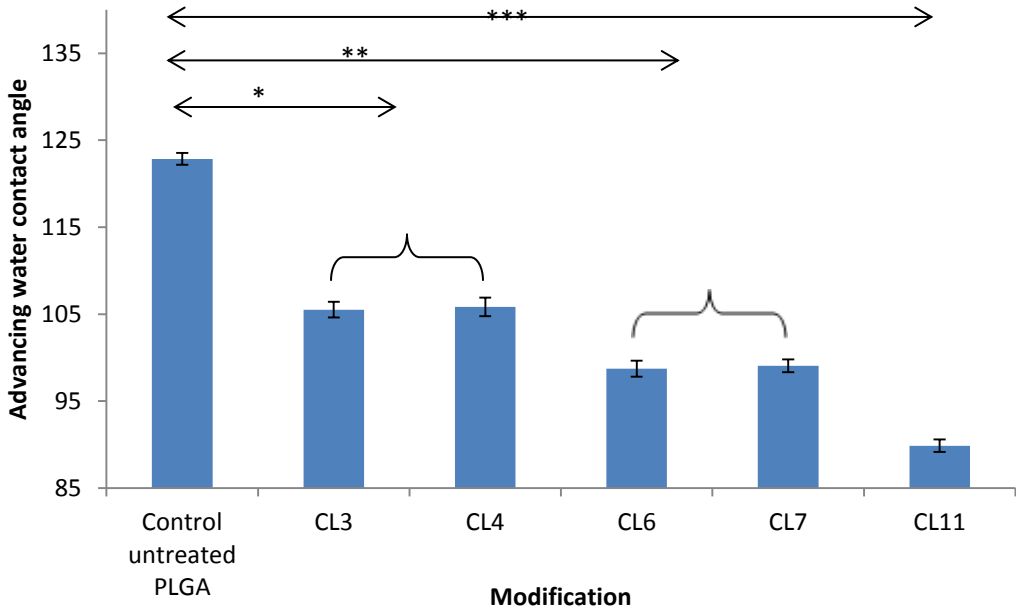

Figure 5.9: **Dynamic water contact angle** The average advancing angle across the mid point of the surface was measured (n=6) Stars indicate degree of difference between untreated control and CL3 and 4 and CL6 and 7 and CL11. Error bars indicate standard deviation. *=p<0.10, **=p<0.05, ***=p=<0.01

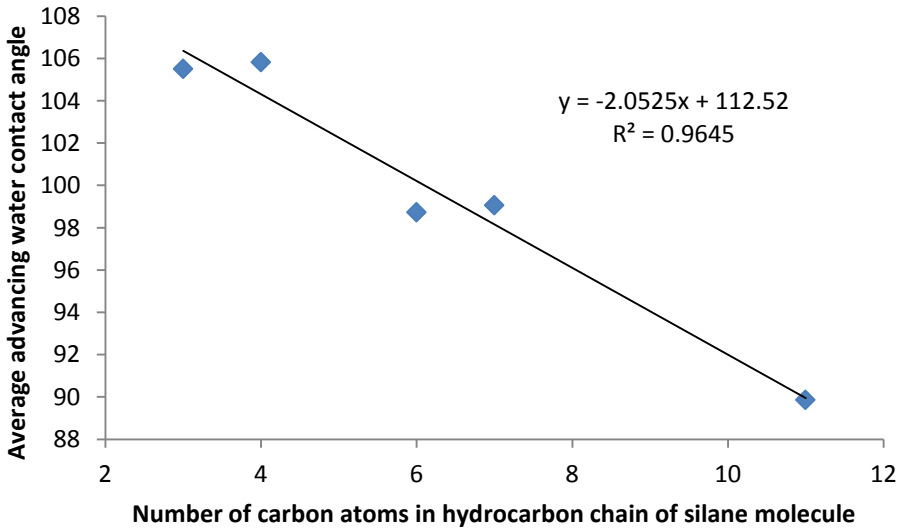

Figure 5.10: **Correlation between dynamic water contact angle and number of carbon atoms in hydrocarbon chain of silane molecule.** Results were plotted as a correlation and R^2 value showed a significant correlation.

5.4: SEM microscopy of flat PLGA films

The SEM images of the PLGA films show a lack of features on the macroscale, apart from on the CL11 sample, which shows a disordered cracked structure on part of the sample.

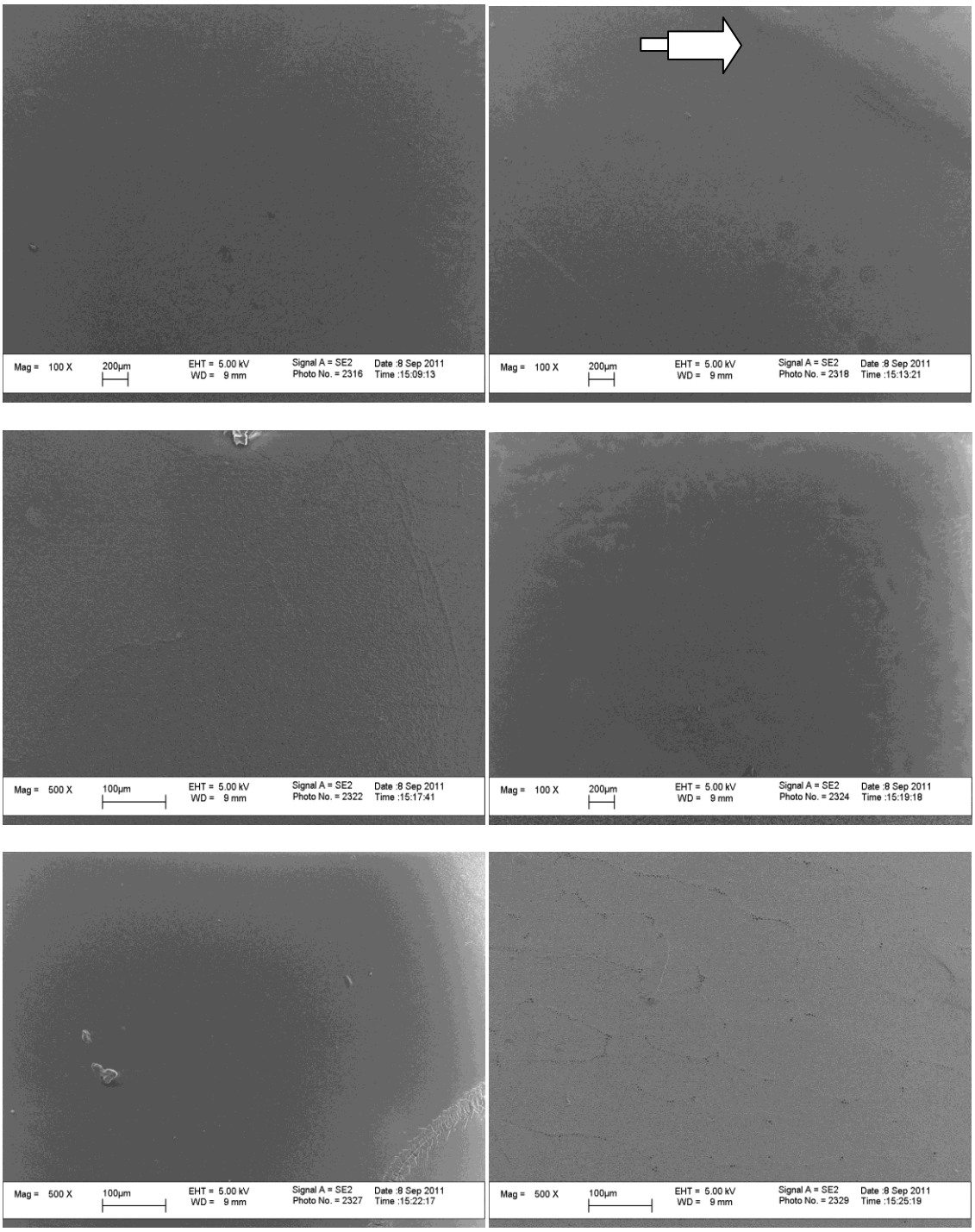

Figure 5.11: **SEM of modified PLGA films.** Films were modified with (a) Untreated PLGA(b),CL3 (c),CL4 (d),CL6 (e) CL7and (f) CL11. White arrows indicate macroscopic topographical structures on CL11

5.5: Light microscopy of flat PLGA films seeded with Mesenchymal stem cells and stained with Von Kossa's stain for mineralisation.

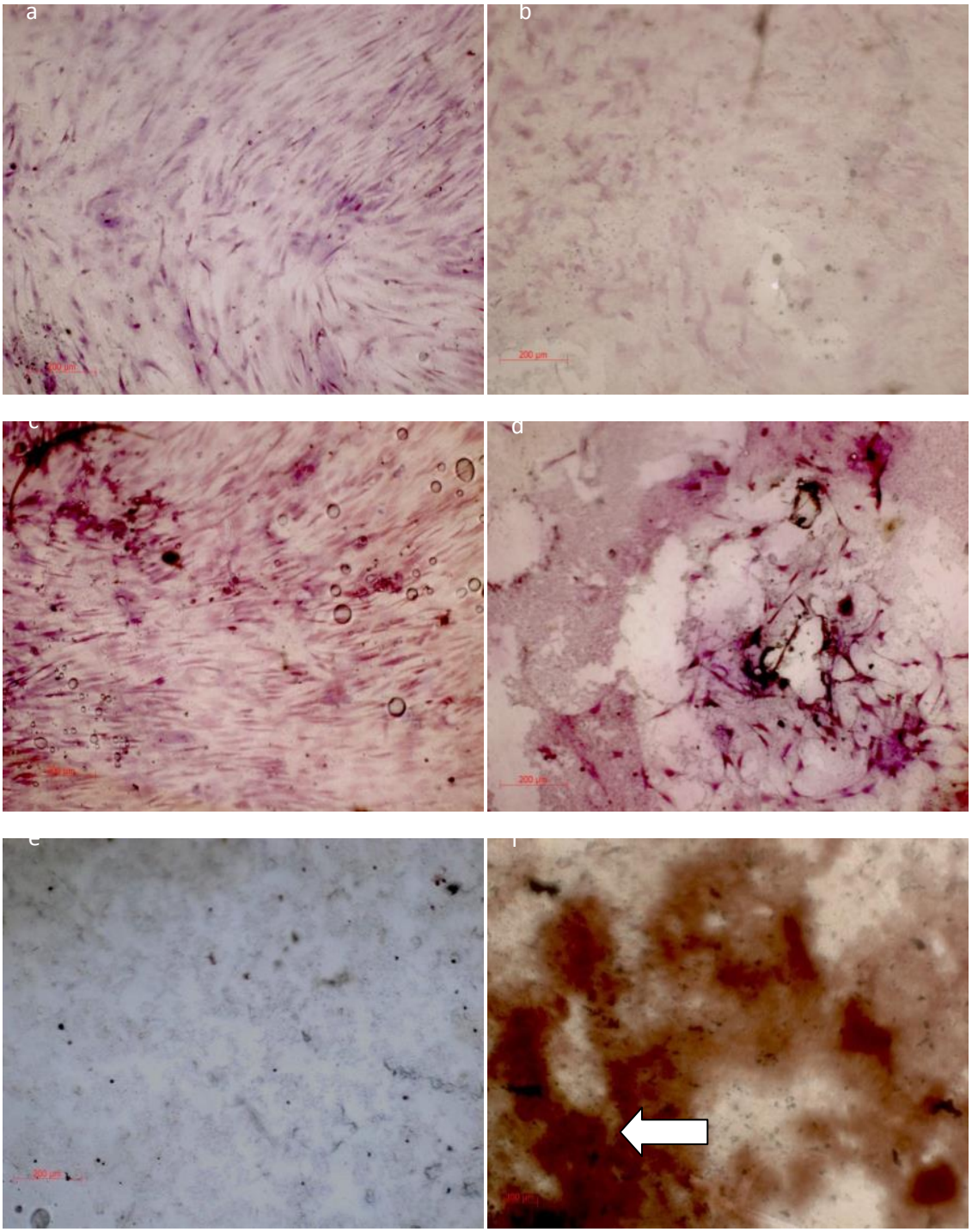

Figure 5.12: **hMSC on modified PLGA films**. Films were modified with the following modifiections;(a)untreated PLGA (b) CL3 (c) CL4, (d) CL6, (e) CL7, and (f) CL11. After 7 days incubation with hMSC they were fixed and stained with Von Kossa stain for mineralization. (f) White arrows show positive mineralization staining on CL11 modification.

The modified PLGA films were seeded with MSC and cultured for 7, 14 and 28 days. They were then stained using Von Kossa's stain for mineralisation. Positive staining occurred after 7 days on the CL11 treated surface. The images in fig. 5.12 depict the widespread mineralisation by brown staining. Dark blue/purple staining shows the cell nuclei present. The cells were shown to be in monolayer formation by 7 days on CL3, CL4 and the untreated sample, but were more disrupted on the CL6 and CL7 treated surface. CL11 showed that there were a good coverage of cells (which appeared to have formed a good monolayer) under a mineralised topography. In areas where there was no mineralisation staining there was still a full coverage of cells.

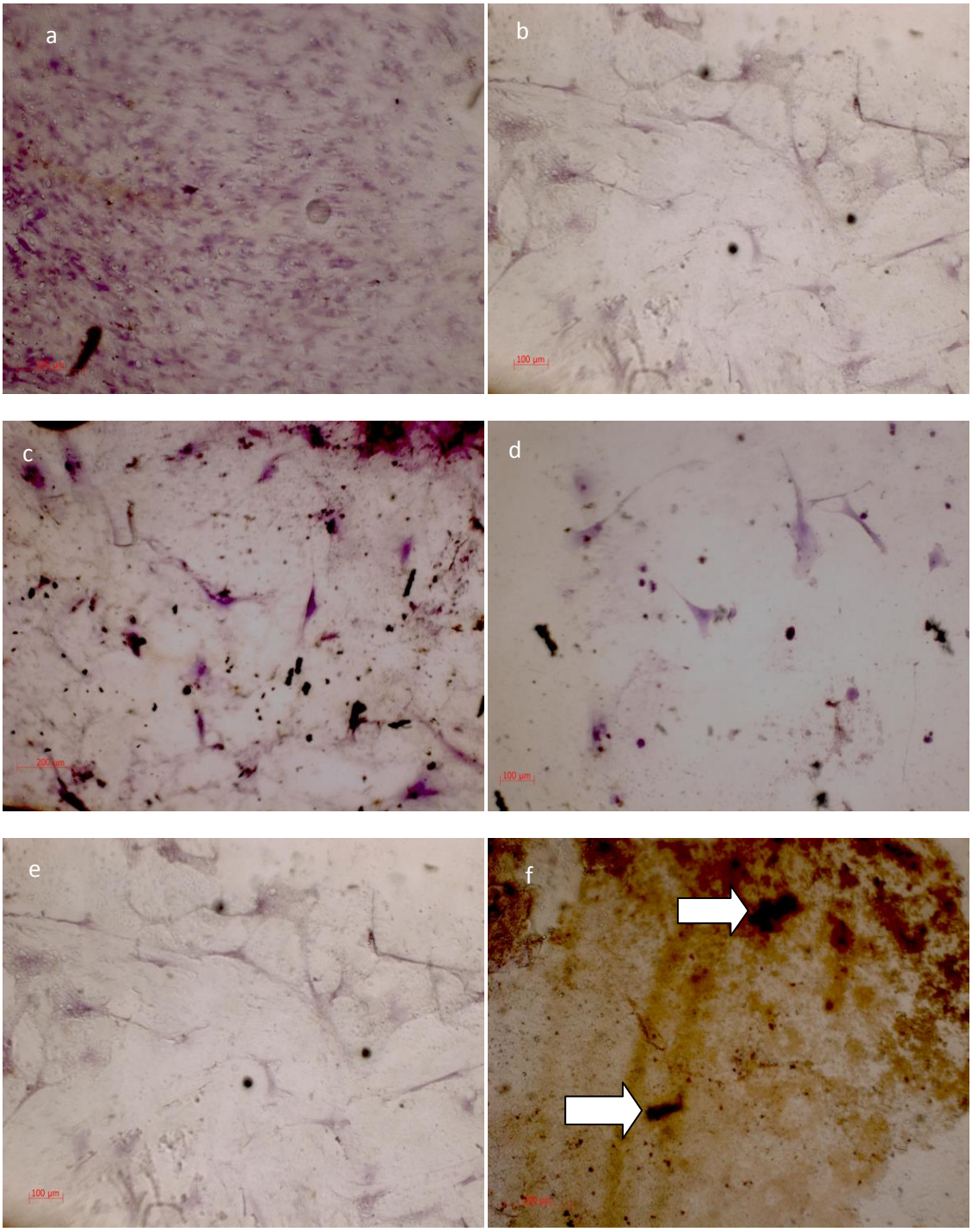

Figure 5.13 **hMSC on modified PLGA films**. Films were modified with the following modifiections;(a)untreated PLGA (b) CL3 (c) CL4, (d) CL6, (e) CL7, and (f) CL11. After 14 days incubation with hMSC they were fixed and stained with Von Kossa stain for mineralization. (f) Shows positive mineralization staining on CL11 modification.

The 14 day incubation time point revealed that there was a reduced number of cells on CL3, CL4, CL6 , CL7, and CL11 but there was still a mineralised response from CL11, and a good coverage of cells on this surface. The untreated control had a full monolayer at 14 days incubation.

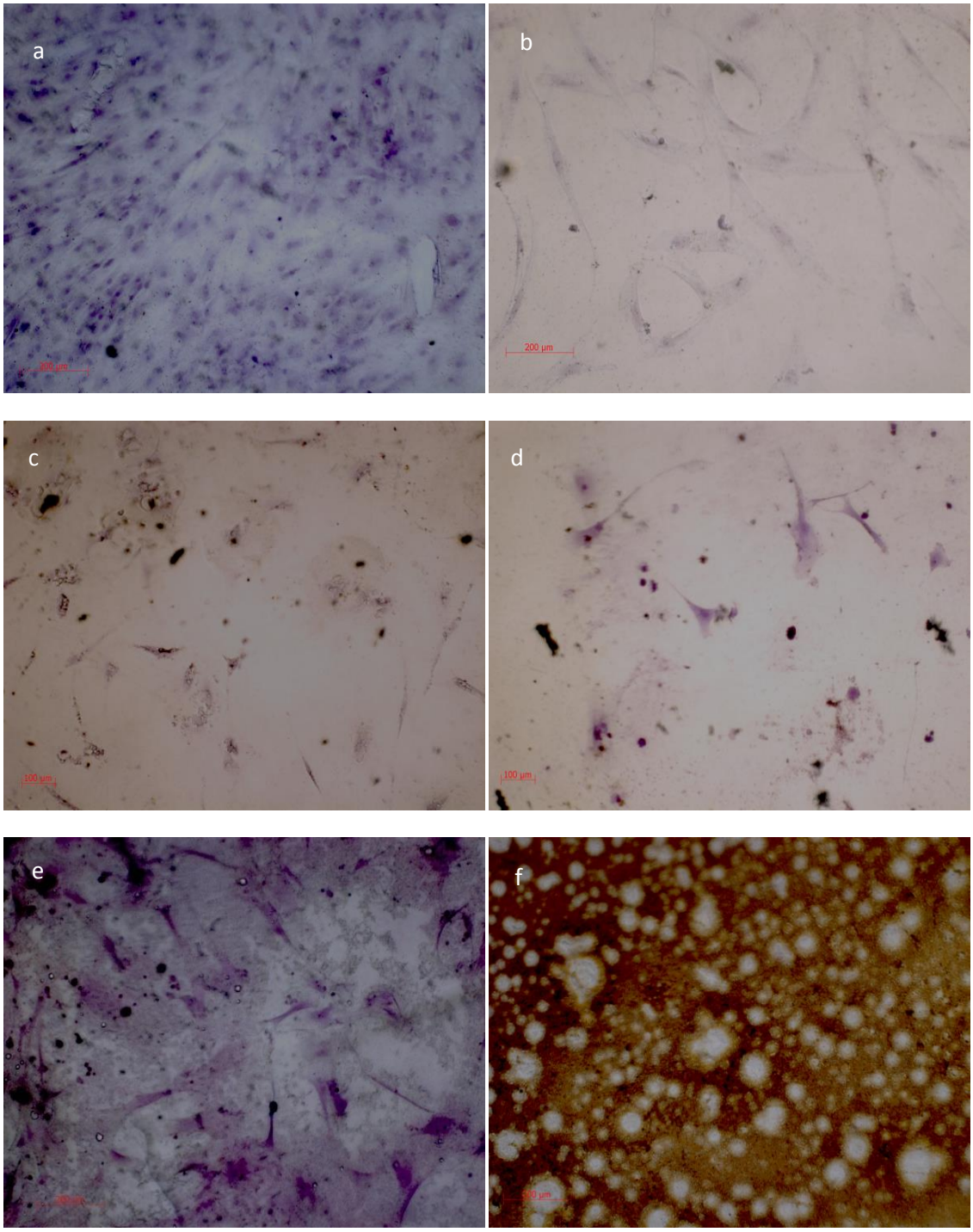

Figure 5.14: **hMSC on modified PLGA films**. Films were modified with the following modifiections;(a)untreated PLGA (b) CL3 (c) CL4, (d) CL6, (e) CL7, and (f) CL11. After 28 days incubation with hMSC they were fixed and stained with Von Kossa stain for mineralization. (f) Shows positive mineralization staining on CL11 modification.

After 28 days, there were cells still present on all the surfaces, and they appeared to have remained at the same percentage coverage as 14 days, with no further decrease in cell number. The most notable change was on CL11, which demonstrated a dense coverage of mineralisation, which stained dark brown with Von Kossa's stain for mineralisation.. The layer appeared to have formed pits, which could be the beginning of the remodelling process.

5.6: Ninhydrin assay to determine the concentration of amine groups deposited onto spheres during silanisation.

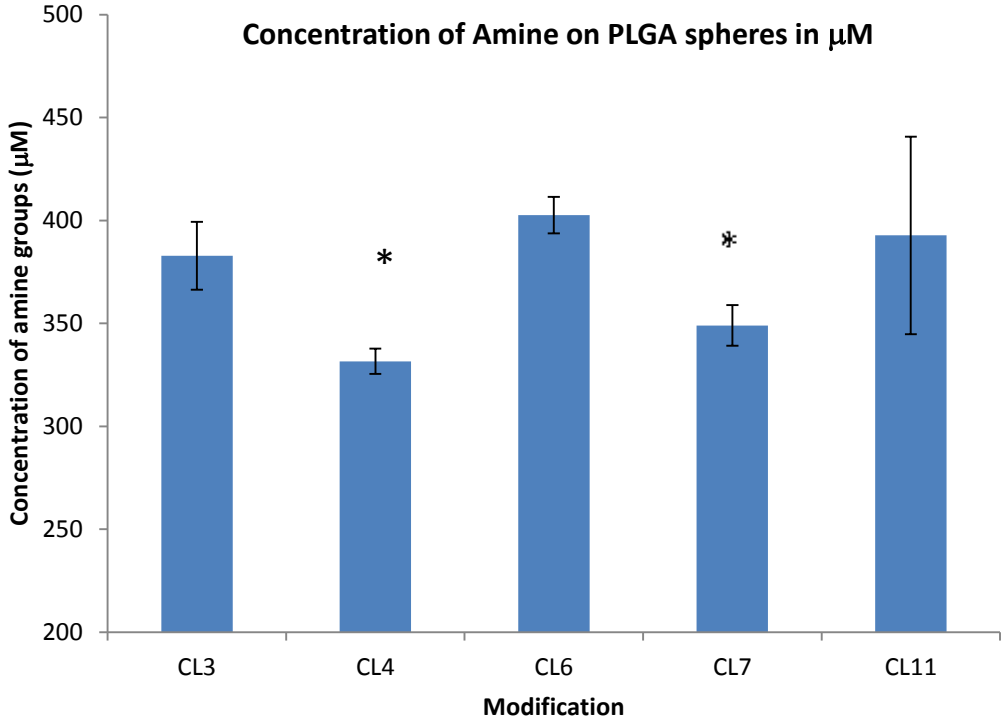

Figure 5.15: **Mean concentration of amine groups on treated PLGA spheres**. The concentration of amine groups was measured by nynhydrin assay. Error bars show standard deviation from the mean (n=4). Star indicates statistically significant reduction in coverage when compared to CL3, CL6 and CL11 (p=<0.05).

The concentration of amine groups on the surfaces of the spheres was measured using the ninhydrin assay developed in this thesis. Four separate repeats were tested at the point of application of the silanes to the surfaces. The concentrations of the amines were variable, and considerably higher than on the flat PLGA surface (p=<0.05).

5.7: Histological examination of silane-treated spheres incorporated into the PLGA system.

	CL3			CL4			CL6			CL7			CL11			Untreated PLGA		
	200µm	400µm	600µm	200µm	400µm	200µm	400µm	600µm	600µm	200µm	400µm	600µm	200µm	400µm	600µm	200µm	400µm	600µm
H & E	+	+	+	+	+	+	+	+	+	+	+	+	+	+	+	+	+	+
Van Geison	-	-	-	-	-	-	-	-	-	-	-	-	-	-	-	-	-	-
Alcian Blue	-	-	-	-	-	-	-	-	-	-	-	-	-	-	-	-	-	-
Alizian Red	-	-	-	-	-	-	-	-	-	-	-	-	-	-	-	-	-	-
Von Kossa	-	-	-	-	-	-	-	-	-	-	-	-	-	-	-	-	-	-

Table 5.1: **Summary of histological staining** 3D scaffolds were cultured with MSCs and incubated for 7, 14 and 28 days. Scaffolds were then processed for histological analysis and sectioned. + = presence of positive staining, - = no staining.

The histological analysis of the scaffolds revealed the presence of cells throughout the scaffolds at 7, 14 and 28 days, but the cells had not proliferated greatly and there was no positive staining from any of the differentiation marker stains (Von Kossa, Alizarin red, Van Gieson, and Alcian blue). There was no evidence of collagen production (Van Gieson), and no evidence of any mineralization (Von Kossa, Alizarin red). Very few cells were evident on the control untreated scaffold after 28 days and these results correlate with the LDH assay results showing a lack of cells after 28 days on this scaffold.

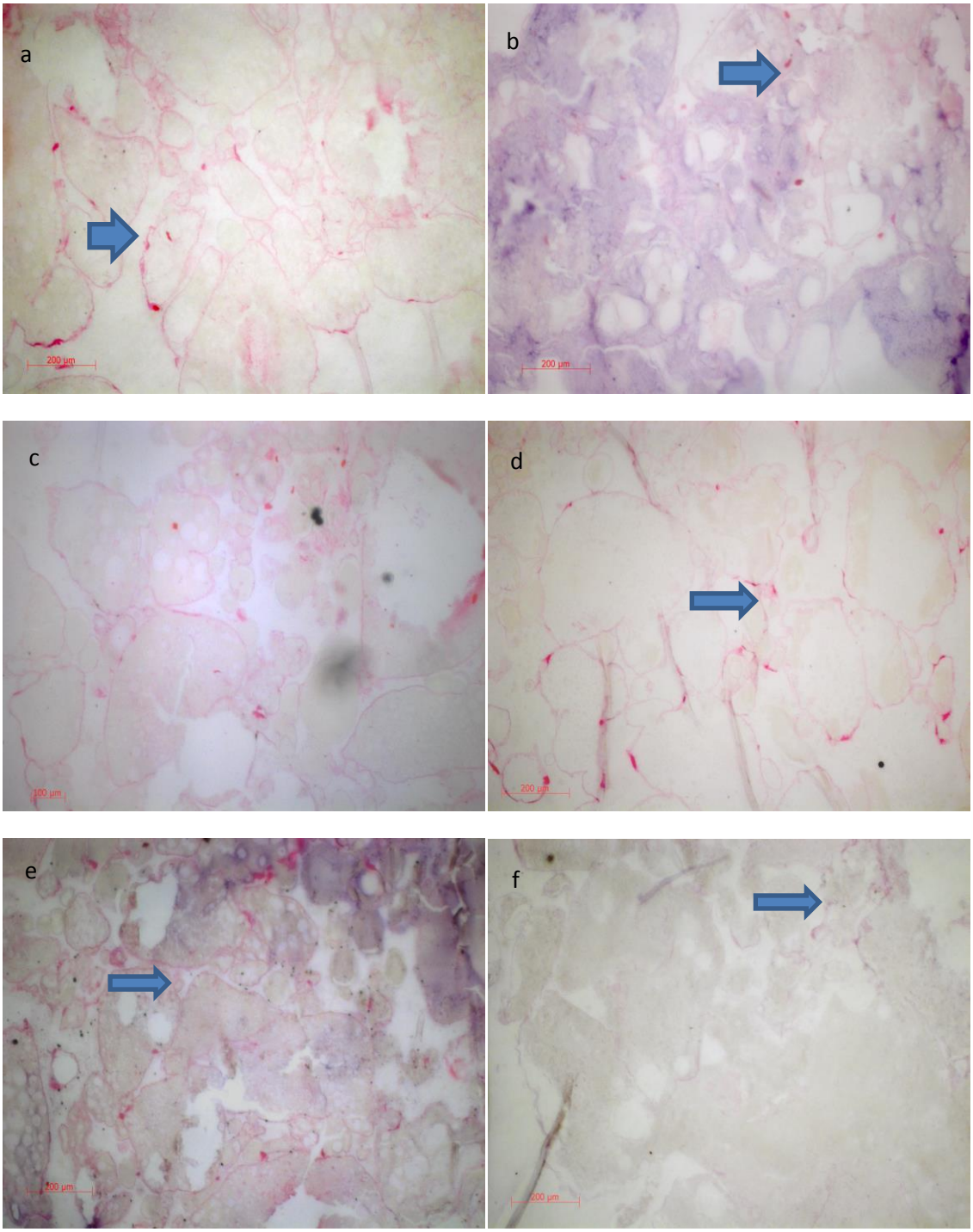

Figure 5.16: **hMSC on modified PLGA scaffolds. Scaffolds were** modified with with (a) CL3 (b) CL4, (c) CL6, (d) CL7, (e) CL11 and (f) untreated PLGA and cultured for 28 days. After incubation the samples were processed, sectioned and stained with H and E. Blue arrows show presence of cells stained by eosin

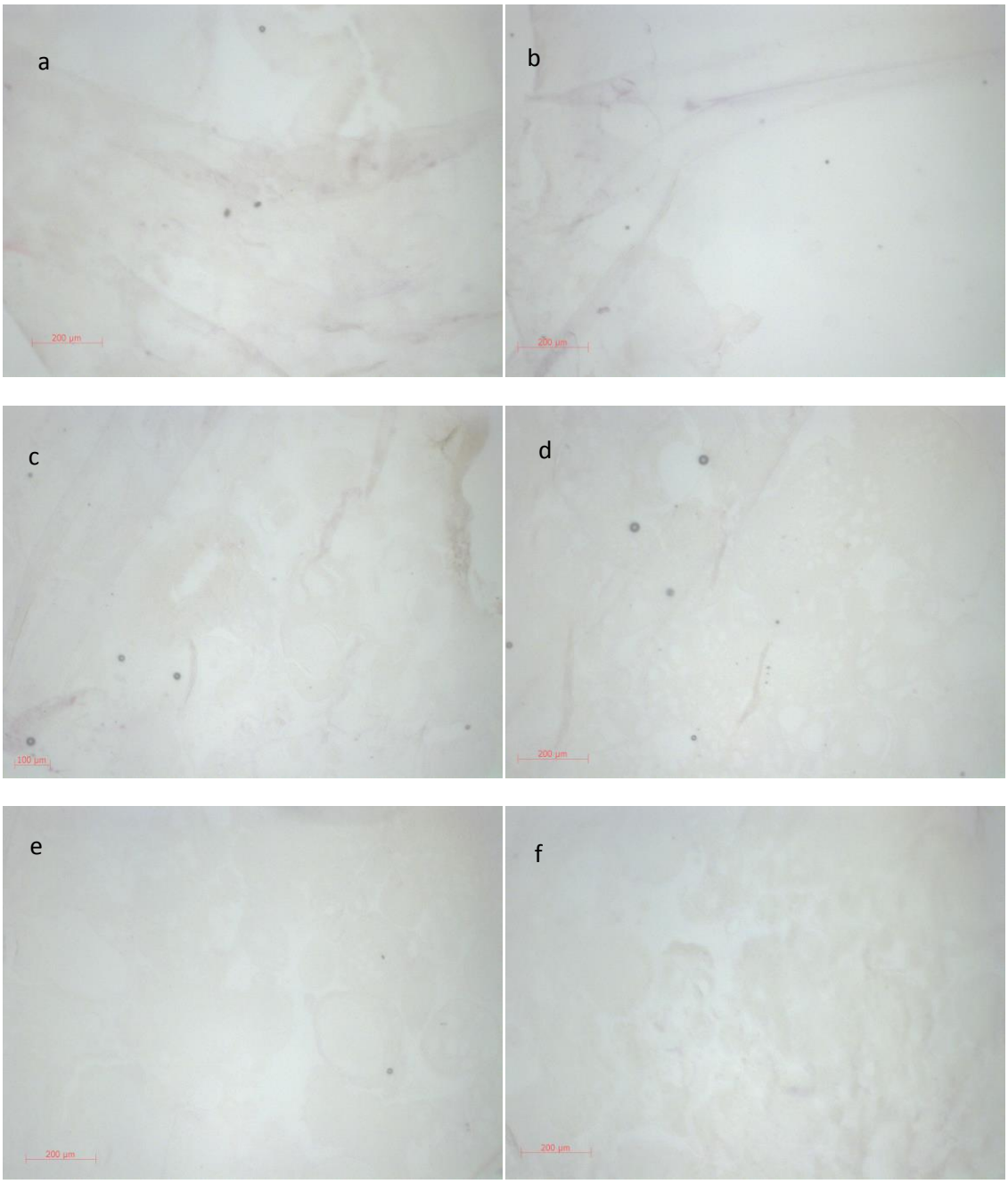

Figure 5.17 **hMSC on modified PLGA scaffolds. Scaffolds were** modified with with (a) CL3 (b) CL4, (c) CL6, (d) CL7, (e) CL11 and (f) untreated PLGA and cultured for 28 days. After incubation the samples were processed, sectioned and stained with Von Kossa's stain for mineralisation.No positive staining found.

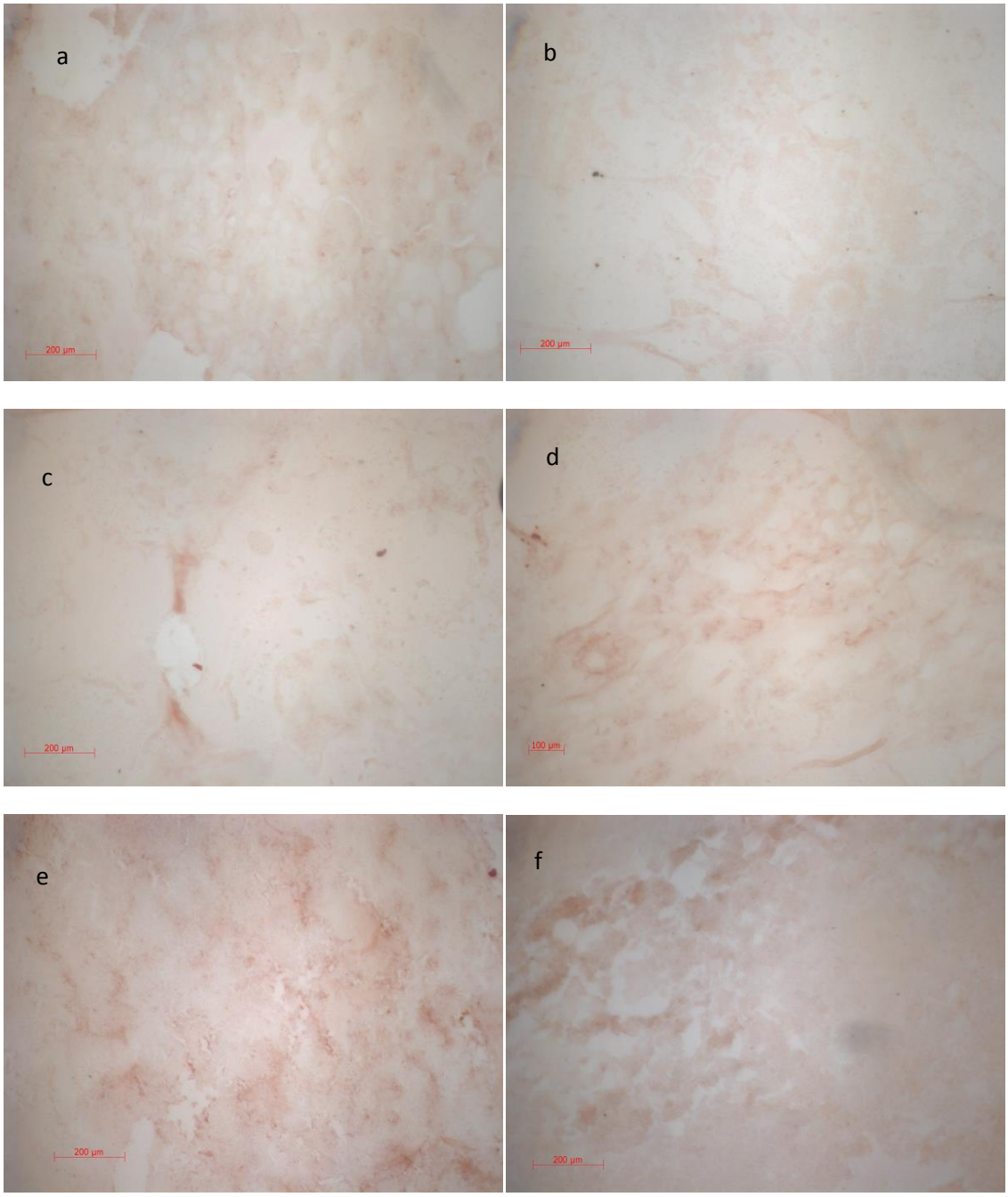

Figure 5.18 **hMSC on modified PLGA scaffolds. Scaffolds were** modified with with (a) CL3 (b) CL4, (c) CL6, (d) CL7, (e) CL11 and (f) untreated PLGA and cultured for 28 days. After incubation the samples were processed, sectioned and stained with Alizarin red for mineralisation. No positive staining found.

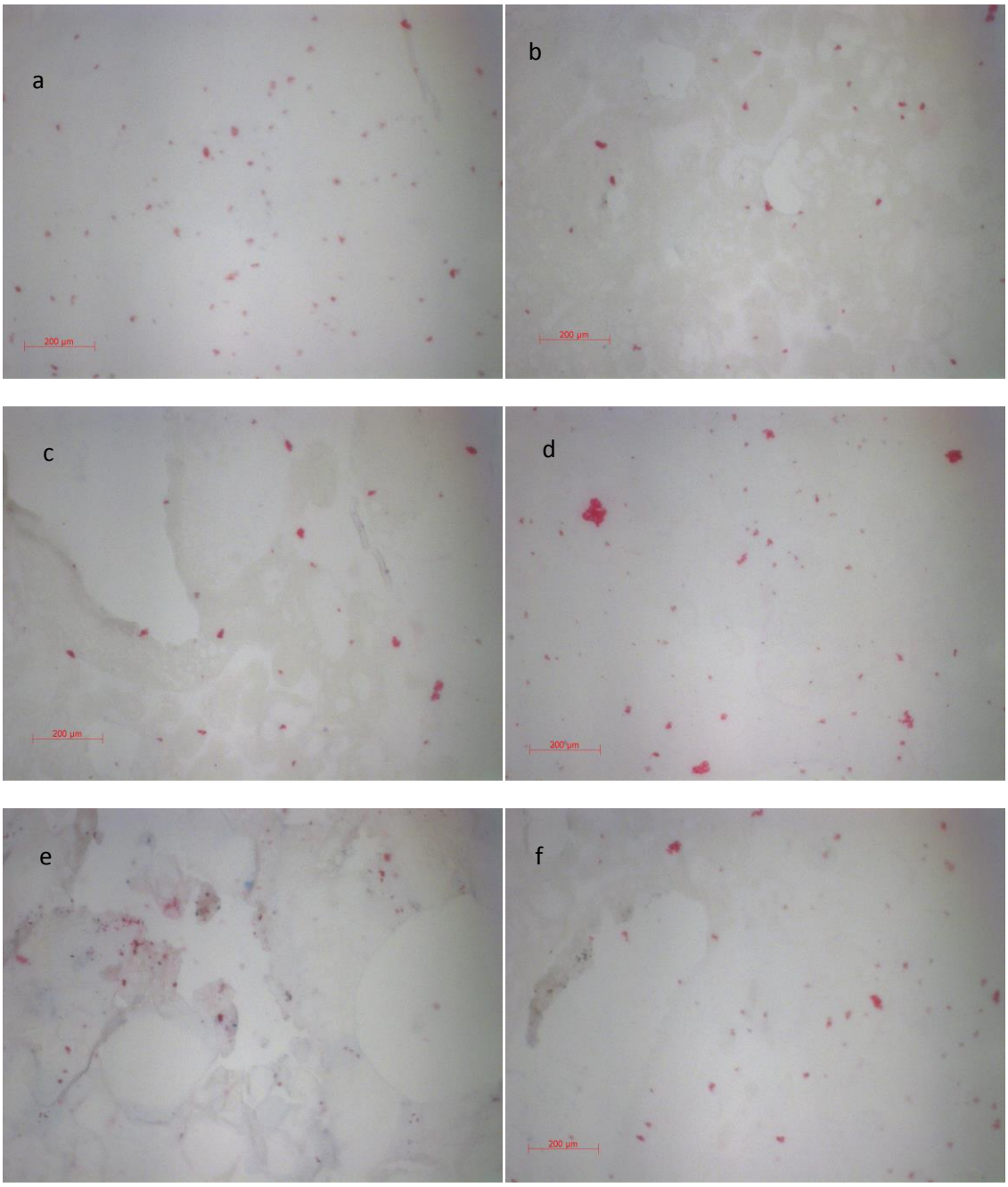

Figure 5.19 **hMSC on modified PLGA scaffolds. Scaffolds were** modified with with (a) CL3 (b) CL4, (c) CL6, (d) CL7, (e) CL11 and (f) untreated PLGA and cultured for 28 days. After incubation the samples were processed, sectioned and stained with Alcian blue stain for Glycosaminoglycan (GAG), no positive staining found.

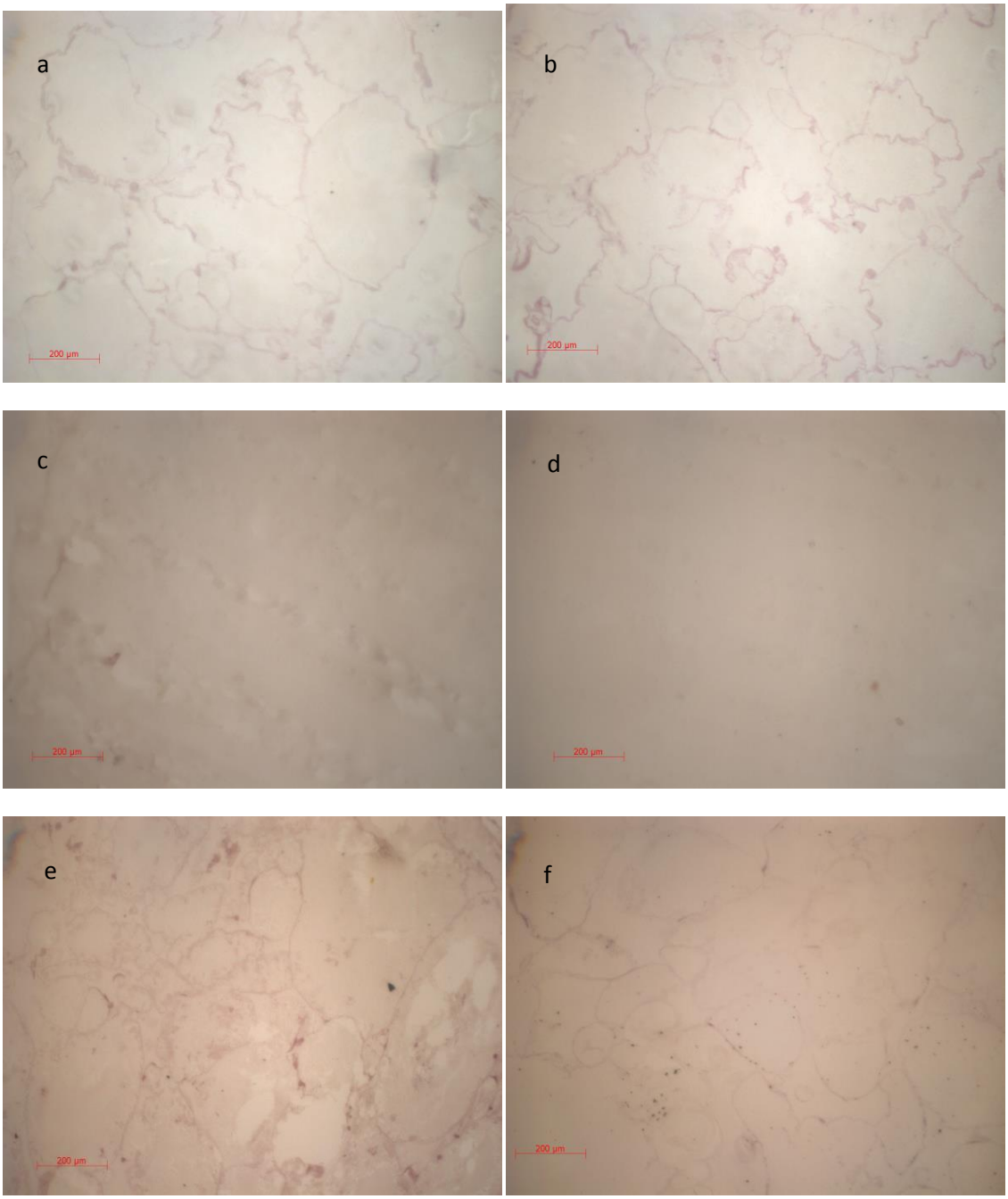

Figure 5.20 **hMSC on modified PLGA scaffolds. Scaffolds were** modified with with (a) CL3 (b) CL4, (c) CL6, (d) CL7, (e) CL11 and (f) untreated PLGA and cultured for 28 days. After incubation the samples were processed, sectioned and stained with. Van Giesons stain for collagen. No significant positive staining found

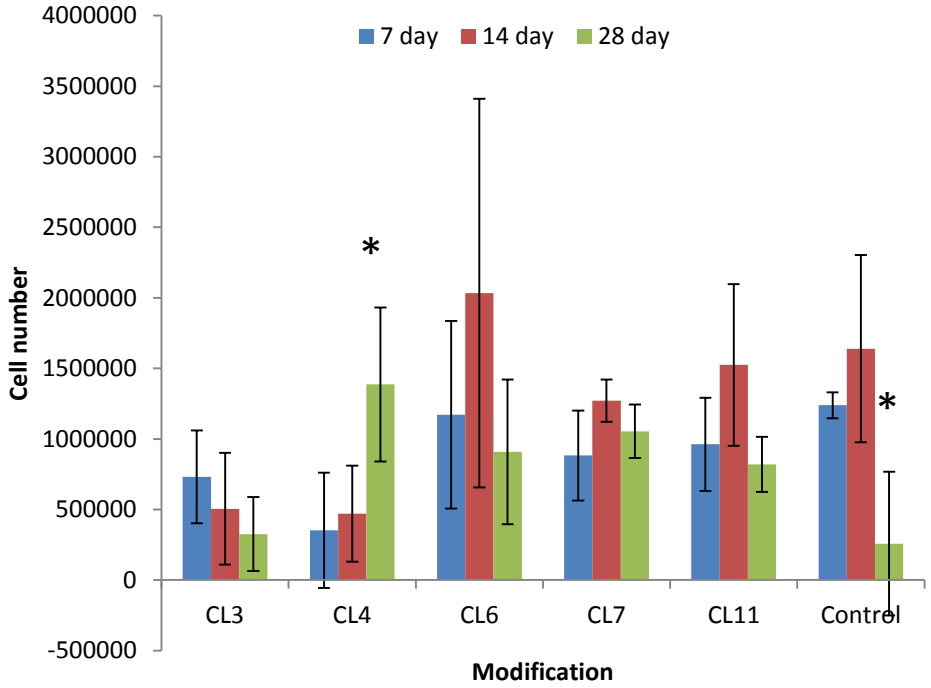

Figure 5.21 **LDH assay for cell number**. hMSC were seeded into silane modified scaffolds and cultured for 7, 14 and 28 days. Error bars indicate standard deviation from mean. *shows a statically significant difference ($p<0.05$), than the same modification at 7 days.

There was evidence of cells on the scaffolds, confirmed by the H and E staining and the LDH assay, but no differentiation was detected by the other histological staining procedures. As the cells were seeded with 1 million cells initially, there is no evidence of proliferation beyond this point on the scaffolds, when you take into account the standard deviations. There is no statistically significant increase in cell number over time with the exception of CL4 which showed a statistically significant difference in cell number after 28 days than the initial 7 day count ($p=<0.05$). There was evidence of cells after 28 days, but there was no evidence of stem cell differentiation within any of the scaffolds, as demonstrated by the histological staining undertaken previously. The control untreated

scaffold showed a statistically significant drop in cell number between 14 and 28 days. This was not seen on any of the treated samples.

5.9: Discussion of the transfer of silane modifications onto PLGA films and spheres and the subsequent cellular responses.

The transfer of the surface chemistries to flat PLGA films was successful, and instigated an interesting response in terms of the dynamic water contact angle. The water contact angle had an inverse relationship to the chain length of the modification (figure 5.9). This is an unusual result, because when the molecule is considered the longer chain molecule will introduce more CH_2 groups to the surface, which in turn should theoretically increase surface hydrophobicity. This was not observed. This could be because the substrate, PLGA, is already very hydrophobic, the addition of silane groups with hydrophilic end groups ($-NH_2$) leading to an increase in hydrophillicity despite the hydrophobic chain molecules. The hydrophobic chains only act as a spacer physically keeping the hydrophilic NH_2 groups away from the very hydrophobic substrate, creating a layer which would be in contact with cells, that is hydrophilic, and conducive to cell growth.

The Atomic force microscopy (AFM) investigation (Figure 5.2-5.7) of the surfaces was quite revealing, the images showing quite variable coverage from the different modifications on the PLGA films. The maximum peak height exemplifies the hypothesis that the CL11 modification is considerably different from the other modifications. The CL11 modification appears to have two layers of microstructure, that being the macro-topography and also the nano-topography. It is likely that it is the unique combination of the two, combined with the surface energy demonstrated by the advancing dynamic water contact angle that seems to create the active surface demonstrated in this thesis.

The application of the silanes to 3D polymer system was unsuccessful in this instance from the standpoint of cell response. There was no evidence of differentiation on any of the modifications when examined using histological techniques. There was evidence of cells on the system but they

were not producing matrix. The stains used would have identified the key proteins necessary for differentiation throughout the scaffold and they were all negative.

One possible reason for this is that the concentration of the silanes on the surface of the spheres was not the same as the concentration on the films which were successful (in the instance of CL11). It is likely that it would be possible to optimize the techniques further by taking a close look at the coating methods in more detail. The coating technique involves a flow of silane to stop the spheres from clumping, and the wash steps can't be as vigorous as that on a film or glass surface. This leads to the concentration of silanes being significantly higher (10 fold) on the spheres than films. It is likely that the coating technique and washing procedures would need to be heavily modified to allow the sufficient coating and washing of the spheres while avoiding the clumping that is detrimental to the materials effectiveness. Further work would involve the examination and identification of a suitable solvent that could wash the system appropriately without causing damage to the PLGA, or leave any cytotoxic residues, as demonstrated in pharmaceutical release studies that the role of the solvent used to make the spheres, and also modify them, may play more of a role than merely dissolving the polymers and then evaporating[2]. Further optimization of this may be a crucial next step in this work.

Another possible reason why the application of the surface chemistries onto a 3D system did not cause stem cell differentiation could be that the modification protocol caused the chemical groups to be too closely packed together, creating steric hindrance, and not allowing the surface chemistry to be accessible by large protein molecules involved in stem cell differentiation [3,4]. Obtaining a similar concentration of the surface groups will be key to the success of further work in this area, that combined with the development of suitable techniques to investigate the surface chemistry and topography on spherical samples, to allow better optimization of the technique.

Full exploration and optimization of the reactions involved in the coating of PLGA spheres and the investigation of the subsequent effects on cell interactions would be an ideal progression for this work, and is likely to lead to the creation of the biomimetic 3D system which would be applicable

for the purposes of bone regeneration and would be a good step forward in the clinical treatment on non-union bone fracture, and may lead to further applications in osteochondral repair. To obtain this goal, much more work on the transfer of the chemistries to the 3D system will have to be conducted.

1. Koegler, W.S. Griffith, L.G. Osteoblast response to PLGA tissue engineering scaffolds with PEO modified surface chemistries and demonstration of patterned cell response. *Biomaterials* **25**, 2819-30 (2004).

2. Ito, F. Fujimori, H. Honnami, H. Kawakami, H. Study of types and mixture ratio of organic solvent used to dissolve polymers for preparation of drug-containing PLGA microspheres. *European Polymer Journal* **45**, 658-667 (2009).

3. Cavalcanti-Adam, E. A., Micoulet,A., Blümmel, J.. Lateral spacing of integrin ligands influences cell spreading and focal adhesion assembly. *European journal of cell biology* **85**, 219-24 (2006).

4. Selhuber-Unkel, C. Erdmann,T., Lopez-Garcia, M. Cell adhesion strength is controlled by intermolecular spacing of adhesion receptors. *Biophysical journal* **98**, 543-51 (2010).

Chapter 6: Discussion of Results and Further Work

There is significant evidence in the review of current work (chapter 1) to show a clear, unequivocal need for bone regeneration system that could be applied in non-union fracture that occurs in circumstances such as trauma and bone cancer surgery. Autologous bone transplantation is the first line treatment for non-union bone fracture and has success, depending on the type of bone harvested, with cancellous bone containing numerous osteogenic factors but without much mechanical strength, and cortical bone having good mechanical strength but fewer easily available factors[1,2]. The use of autologous bone as a treatment has many obstacles. Only limited donor sites are suitable for an autologous bone graft and this is a limitation that increases with the age of the patient.[2] Donor site morbidity is also a very serious problem, with pain lasting in some cases for longer than the repair takes to heal[3]. Minor complications from this procedure included superficial infections and hematomas. More serious complications included herniation through large bone graft donor sites, vascular injuries, serious infections, neurological injuries, and further fractures.[4]

The other current treatments for non-union fractures include several specialised surgical techniques, such as compression plating and supracondylar femoral nailing[5], and many surgeons use techniques like this to treat non-unions. There are problems associated with invasive surgeries such as soft tissue stripping and damage, localised infection and nerve damage. Compression plating has a 1 in 10 incidence of nerve damage when used in non-union humeral shaft fractures[5] and for this reason the supracondylar nailing can be seen as a better option, this is often true, but also has its drawbacks, and its success is dependent on the stability of the fit between the nail and the internal cavity, as instability will cause further complications.[5] These surgical techniques are only suitable for certain non-union fractures, and not when large pieces of bone are required.

Allografts, another relatively common treatment, are usually human cadaver bones, that are processed to remove any of the osteogenic cells, and leave an osteoconductive scaffold for the patient own cells to infiltrate and colonise. The problems associated with using this type of material is the risk of infection and immunogenicity/patient rejection. Generally the donor bone is cleaned and stripped of any of the cellular/osteogenic components, and is screened for infectious diseases such as HIV, but there is always a small risk with this sort of tissue. The cleaning of the allograft denatures not only any potential hazardous viruses, but also the factors that would be useful to the in-growth of native cells, so in these cases it is likely that exogenous growth factor would be necessary.

Alternative material solutions are available, and currently used. Ceramic scaffolds containing BMPs are used to treat non union fractures and there has been success with these materials, is one study the use of BMP-7 was shown to cause healing in non-union fractures after 4 months, where previous surgical techniques including grafts had failed, with a success rate of 92% (of 28 patients).[6] While this is very impressive, the cases may not reflect the general population of non-union fractures.

Non-union bone fracture has a very serious impact on the patient, and with up to 10% of all fractures becoming non-union[4] (this figure depends upon the location of the fracture, but will rise to 50% of all open tibia fractures) it is also a considerable economic problem. In the US it is estimated that the treatment of non-union fractures was around 14.6 billion US dollars per annum[4]**.** There is a very great need for a more cost effective solution than autologous transplant or the use of BMP treated material grafts. Both of these treatments cost in the region of £15,000 per patient, if the non-union fracture is in the long bones[7]. This is prohibitively expensive and would not be an option in developing countries. Cheaper treatments would be a real possibility if a biomaterial with an osteo-inductive surface

chemistry was developed, particularly if the active surface was composed of a synthetic chemical rather than a peptide or growth factor.

If this treatment had the advantage of being injectable, like the one outlined in this thesis, it would not only be cheaper to produce than peptide treated materials and other alternatives, but it would also be less invasive for the patient, and ultimately require less hours of surgery (which is the major cost associated with a non-union fracture, with the more complicated non-unions requiring several separate surgical procedures).

There are many benefits to a regenerative technique using PLGA that possesses an osteogenic surface, which include the controllable degradation rate[8], and the conducive osteogenic environment it provides to stem cell and osteoblast-like cells. This technique would bypass the majority of the negative, problematic side effects observed in the autologous bone graft. It would, as an advanced active material method, be capable of containing a powerful biological stimulus, that instigates the migration of the patients own stem cells, providing an *in situ* tissue engineering solution.

A scaffold that creates an environment which causes recruitment of native bone marrow-derived MSCs and which could also stimulate them following their infiltration *in vivo*, may be an achievable goal. The work conducted in this thesis demonstrated potential in this field. The individual results have been discussed in isolation in previous chapters but their significance will now be discussed when considering the context of the complete study.

The initial experimentation was undertaken using a range of surface chemistries on a 3D PLGA system (chapter 3). It was important to characterise these surfaces sufficiently to ascertain that they had been deposited on the surfaces. While there were limitations to the characterisation of the surfaces, the techniques employed assessed a full spectrum of the surfaces properties. XPS (figure 3.4) identified the presence of chemical elements and

energies associated with the species deposited, and SEM identified the surfaces were undamaged by the plasma chemical deposition process (figure 3.3). It was important at this stage to identify that the different surface chemistries were not inducing topographical changes that were vastly different from each other. This was to determine that it was in fact the chemistry that was responsible for the response seen. The water contact angle was measured to show any changes in surface energy. At this point the nanotopography was not taken into consideration as the measurement of the surfaces nanotopography is technically very challenging when the substrate is polymer spheres.

This analysis all confirmed that the surfaces had been modified in such a way that the surface chemistry had altered, while the macrotopography had remained similar to that of the untreated control.

Markers of differentiation were highlighted in the direct staining of the cells and their ECM via the histological analysis (tables 3.3-3.5, and figures 3.7-3.11). Consistent Van Gieson staining through the scaffold (figures 3.7-3.11) stained collagen, but does not differentiate between the different types of collagen. Further histological examination of the scaffolds revealed an osteogenic response throughout the amine treated scaffold (figure 3.7), where Von Kossa staining was concentrated in nodules and seen in every sample point throughout the scaffold. The Von Kossa reagent stains calcified ECM using silver nitrate to react to the phosphate which accompanies calcium in mineralized matrix in an acidic environment[9], and as mineralization of the ECM is one of the key markers of osteogenic differentiation it is often seen as a definitive test. It does not however indicate that there is bone formation, and caution should be taken before making this statement, as the staining does not indicate the calcium to phosphate ratio, which is crucial when determining the mineral formation of bone.[9] The alizarin red stain, which also stains mineralized matrix, was

consistent with the Von Kossa stain (figure 3.7), showing areas of mineralized matrix in nodules throughout the amine-modified scaffold.

The LDH assay (figure 3.6) demonstrated that all the modifications support cell expansion, but there is a plateau of cell numbers on the amine modification between 14 and 28 days. There are a number of possible explanations for this result: there is evidence as explained above that the cells are starting to differentiate by 28 days, and this could indicate that the cells present in the scaffold are starting to enter a differentiation phase, and are in a non-proliferating state.

Alternatively, another explanation is that the transfer of nutrients within the scaffold slows as the pores become blocked with cells and ECM, causing either some cell death or that the cells have become non-proliferative. Both of these processes could be occurring. There is evidence in the histology at day 28 that the amine modification induces an osteogenic response from the cells, but there is also evidence that some of the pores are starting to fill with cellular material, a phenomenon that is demonstrated further by the H and E staining (figure 3.7). It may be that the flattened morphology of the cells on this scaffold (demonstrated by the cryo SEM) (figure 3.5) leads to a reduction in the nutrient flow through the scaffold. This suggests that a bioreactor may be necessary, to increase cell number at 28 days and also increased osteogenic differentiation.

The histological examination of the scaffolds showed that the hydroxyl modification was the only modification to support chondrogenic differentiation, as there were patches of positive Alcian blue staining within the serial sections. Alcian blue stains GAGs which are markers of chondrogenesis (figure 3.10). The positive Alcian blue staining was supported by the cryo SEM visualization of cellular morphology (figure 3.5). The cells on the scaffold appeared to be a rounded which is entirely consistent with chondrocytic behavior *in vitro.*[10]

The Van Gieson stain was consistent throughout the scaffold, highlighting the collagen, which was present throughout the scaffold. Combined with the Alcian blue stain, and the absence of any Von Kossa or Alizian red staining, the data indicates material-induced chondrogenic differentiation associated with the hydroxyl modification.

There was no evidence of differentiation on the hexane modification (figure 3.8), consistent with published data, showing that this surface chemistry is a useful tool in the maintenance of stem cell phenotype, as the LDH assay demonstrated that the MSCs do proliferate on this modification, the cell number increasing between 14 and 28 days.[11, 10] There is a statistically significant difference between the hexane-modified scaffolds and the allyl alcohol-modified scaffolds at 14 days. This shows that the cells do not proliferate as quickly on the $–CH_3$ surfaces as on the allyl-alcohol surfaces. The hexane surface, as stated previously, seems to maintain stem cell phenotype, and it may be that the reduced cell number means that the cells are unable to create enough signaling growth factors to permit differentiation in these circumstances, at the correct time point. Conversely, the allyl alcohol-modified surface is conducive to enough cells binding in the initial period to create sufficient growth factors to differentiate when enough time has elapsed. This phenomenon may be investigated further by analyzing the intergrin binding molecule concentrations.

To summarise: when the MSCs were introduced to the 3D system, there was several positive effects seen, including a positive osteogenic response in the allyl amine treated scaffold and a positive chondrocytic effect seen in the allyl alcohol treated scaffolds. These results fuelled the further investigation of the surface chemistries and lead to the initial osteochondral investigation, using a single scaffold to differentiate two separate populations of stem cells within one scaffold. These initial positive results had further potential that will be discussed later in this chapter, and as stand-alone results they were very promising, but the

investigation of this work took the positive effect seen in the osteogenic amine modification and pursued it in a more definable way.

The osteogenic effect seen using amine was reported in other studies that showed both amine promoting an osteogenic effect and the opposite, where the amine groups did not support osteogenesis[11],[12]. This lead to the assumption that more factors were involved other than just the presence of an amine terminal group, and that the presentation of this terminal group could be an important factor. The area merited a closer look, and due to the inflexible nature of the plasma coating with regards to the presentation of the moiety, a logical progression was to investigate a modification that could be altered subtly to change presentation, and so suitable amine terminated silanes were investigated, which had varying chain length.

To determine if the presentation of a key terminal group was an important factor in influencing osteogenicity, baseline data was produced on a model substrate (in this case glass). To examine the potential of chemical modifications the response was measured using both human MSCs and primary human osteoblast-like cells. These cells make a suitable model to examine the initial phase of osteogenic differentiation as discussed in the literature review and described in detail in several studies[11,12, 13,14,15, 16.] The osteoblast model represents a more mature environment, further along the differentiation pathway[17],[18].[19].

The chemistries influence the surface properties of glass when applied. The material properties of the surfaces were changed significantly when the silanes were applied. When the variance of mean was examined using ANOVA ($p=\geq 0.05$) CL3, CL4 and CL11 showed a significantly different water contact angle when compared to the control, and to CL6 and CL7. CL6 and CL7 did not differ significantly from the control (figure 4.3).

The ninhydrin assay for amine concentration (figure 4.2) demonstrated that its concentration on CL7 was significantly less than any of the other modifications when analysed using ANOVA ($p=\geq 0.05$). This indicates that it may be the concentration of amine that is responsible for the change seen in the water contact angle.

The difference seen on CL7 could be due to the amine chains clumping and not forming a complete self-assembled monolayer (SAM), which is less stable, and less likely to withstand the vigorous washing procedure.[20]

The AFM images of the CL7 modification (figure 4.1.1-4.1.6) demonstrate the formation of clumps of matter which form relatively (from a nanotopographical standpoint) large ridges. This pattern was also seen on the CL6 surface, but the concentration of the amine on CL6 was significantly higher than CL7. The inconsistency of the results would be explained by a multiple layer clumping effect, where the silanes do not form full SAMs, and where some of the clumps are washed away by the vigorous washing procedure but some remain in situ, the clumps that remain *in situ* on CL6, would easily explain the raised concentration on the CL6, as equally the removal of the clumps via washing could explain the reduced concentration seen on CL7. The SEM images on the modified glass showed no differences on the modified glass, which highlights that this topographical phenomenon is seen only at the nanoscale.

The AFM highlights the differences in nanotopography, and maximum feature height of the surfaces (figure 4.1.7). There is a statistically significant difference in the maximum feature height between the modified surfaces. This could give some indication of the thickness of the silane coatings. The marked difference in the maximum feature height of the silanes does indicate that the longer chain silanes produce a thicker coating than the shorter chain lengths.

Taken together the three characterization techniques (AFM, Ninhydrin and WCA) demonstrate that the range of silanes used in this study successfully altered the glass substrate. They created different surface topographies when examined on the nanoscale, in addition to the change in surface chemistry. There was an increased concentration of amine groups after modification. Amine groups have been demonstrated in previous studies to show osteogenic capacity.[21,22] Surface nanotopography on stem cells has been extensively researched and it has been demonstrated that there is an optimum surface topography for osteogenic differentiation.[23] The key points from the studies that were successful in creating an osteogenic topography were that they created a surface that had an optimal surface roughness, but only when it was not ordered. The experiment that highlighted this particularly well used a titanium surface with mechanically punched pits. The pits were osteogenic when punched in an irregular grid formation, but showed no osteogenic potential when they were in a regular grid formation[24]. If this topography could be achieved successfully, and consistently using a silane coating, it would be a step forward in the area of bone regeneration.

The material coating in this study showed another potentially osteoinductive property that was investigated using an experiment to observe the mineralization potential of the surfaces in the absence of any osteogenic cells.

Mineralization is a key progression of the bone regeneration process. The development of biomimetic surfaces attempts to fulfill this important step in the regeneration process by chemical interactions where a material can self-mineralize. The ability of some SAMs to cause the nucleation of minerals on surfaces offers a route to accelerate the osteogenic process, and cause early mineralisation[21]. This phenomenon was described by Towoefe *et al* where the SAM in question, while not produced from the same chemical used in this study, demonstrated an extended carbohydrate chain similar in length to the long chain

amines used in this work. To demonstrate the ability of the surfaces produced for this study to self-mineralize, the surfaces were exposed to different concentrations of PBS for 7 days. The resulting surfaces were then examined using a Von Kossa stain for mineralization (figure 4.4), and X-ray microanalysis (figures 4.5-4.8) to show the elemental composition of the surfaces. After 7 days the CL11 modification showed positive mineralization of the surfaces, demonstrated by positive Von Kossa staining at 7 days, and the abundant presence of phosphate detected with X ray analysis (figures 4.5-4.8). The presence of phosphate in hydrogel has previously been shown to induce an osteogenic response[25] so the ability of the surface of CL11 to attract and bind phosphorous could be indicative of this type of event. The probability of the surface modification on CL11 being the cause of the phosphate detected using X-ray microanalysis was calculated in table 4.2, which suggested that the correlation was statistically significant($p \geq 0.95$) None of the other chain lengths showed this effect.

The next phase of the investigation was to use an MSC model to investigate how these cells interact with the silanes, on a model surface, in this instance, glass.

The cellular response to the silane-modified glass was examined using rtPCR to determine the expression of genes at defined time points (figures 4.14-4.19). The cells were examined for the expression of several markers of stem cell differentiation that are key to the osteogenic pathway. CBFA1 was the first gene to be examined, as it is considered to be the corner pin of the osteogenic differentiation process[26,27,]. It is only present in the early phases of differentiation and for a relatively short period of time.[27] There was no positive expression of CBFA1 on CL3, CL7 or CL11 at any of the time points tested, but there was up regulation on CL4 and 6 at 28 days. There was an expression of osteonectin which is a key protein in the osteogenesis process [,28, 29,30]at 7 days by the cells on CL4, CL6 CL7 and CL11, the most prominent response seen with CL7 and CL11 which were statistically significant when

analysed by ANOVA ($p \leq 0.05$). There was a statistically significant difference in the expression of osteopontin, which also plays a role in osteogenesis[28], on CL7 and CL11 at 7 days, and osteocalcin (a vital mineralization protein)[31,32,]was expressed at 7 and 14 days on CL11, which was greatly reduced at 28 days. Sclerostin, a marker of embedded osteocytes and so a clear indicator of osteogenic maturity[33,34,35] was expressed by CL11 at 14 days. Taken together, these results suggest that osteogenic markers are present consistently on the CL11 sample. The absence of CBFA1 on CL11 may be due to the initial time point (7 days) being too late to pick up an initial burst of expression following initial contact.[36] It is a gene that may only be expressed for a short period of time. The expression of osteonectin, osteopontin and osteocalcin all indicate that the cells are capable of producing these proteins, which are heavily linked to osteoblastic activity. The results show that the expression of these genes drops out after 7-14 days, and there is then a positive expression of the osteocyte marker sclerostin on CL11 at 14 days. This shows that the cells on CL11 have the capacity to differentiate into osteocytes, which is the next phase of osteogenic differentiation after the cells have passed through the osteoblast phase. For the cells to achieve this status, they must become embedded in a thick ECM, composed of osteocalcin, and collagen amongst other proteins.[33,34]

Examining the cells using SEM to determine their morphology and matrix production was performed to provide more evidence of differentiation(Figures 4.10-4.13). The 7 day time point revealed that CL3, CL4 and CL7 all had very flat adhered cells. Cells were very rounded in morphology on CL6 but flat and adhered and producing many proteinacious extrusions on CL11. By 14 days the cell numbers on CL6 were reduced, CL3 and CL4 and CL7 were all demonstrating a very flat monolayer of cells, and CL11 was showing a dense formation of matrix over a monolayer of very flat adhered cells. By 28 days, there were even fewer cells on CL6, but CL3, CL4 and CL7 were demonstrating flat cells with some protein

production. The CL11 sample was covered in a dense matrix that seemed to be becoming pitted in its appearance, with the cells that were completely obscured by ECM. This is verified by the PCR data, showing the up-regulation of matrix genes on CL11, and then the expression of sclerostin which could only be produced if the cells were embedded in a thick ECM, which completely encased the cells.[35]

The presence of the ECM was confirmed by the SEM images of the samples. Identification of the presence of osteogenic markers by confocal microscopy confirms the composition of the ECM which was produced by the cells. One of the many advantages of confocal microscopy is that cells and proteins can be stained fluorescently when in multiple layers. 3D matrix can be scanned in layers and an image of the whole sample can be produced, rather than the SEM which is restricted to just the top.

Confocal microscopy was also used to detect a marker of MSC plasticity, Stro-1(figures 4.20-4.22). This marker is a way of identifying undifferentiated cells, and its absence in these samples only occurs if the cells have already begun differentiation[37],[38]. If Stro-1 is absent and other positive markers of osteogenic differentiation such as CBFA1 and Osteocalcin are present, then it is likely that the cells are committed to an osteogenic fate.

The MSCs on the untreated control expressed Stro-1 at 7, 14 and 28 days. This, in conjunction with the absence of any of the osteogenic markers, confirms that the MSCs have not spontaneously differentiated. The confocal staining of the modified glass showed that Stro 1 was expressed at 7 days, but not at 14 days and there was positive staining for Osteocalcin and CBFA1. CL4 modified samples showed positive collagen 1 staining at 7 days but not Stro-1, although no differentiation markers were expressed until 28 days. CL6 showed positive Collagen I staining throughout the 28 day period, but was not positive for any of the osteogenic markers. CL7 showed some positive CBFA1 staining at 28 days, but

nothing before that time point, so this could not be described as a truly osteogenic response. The most interesting result, however, came from the CL11 surface. The CL11 sample showed matrix by 7 days which was positive for osteocalcin and collagen, and by 14 days was showing a thick, pitted morphology. This response was maintained through to the 28 day time point, and is a good osteogenic response from the cells.

The Von Kossa stain for mineralization was used to determine the extent of mineralization in the samples. This process is well established and has been used in many studies to determine the extent of mineralisation[17],[30]. It should however not be used as a definitive test for the production of bone, and if possible there should be other confirmatory tests if there is a positive result.[9] The samples showed some positive staining on all of the modifications, however is was more marked on the CL11 sample. The control untreated glass showed no positive staining.

The results all support the hypothesis that CL11-modified surfaces modification is a powerful stimulant to MSCs, and is able to induce an osteogenic response from them in the absence of any exogenous growth factors. There are a few different possibilities that could explain the root cause of that osteogenic differentiation. This surface has several osteogenic properties, including topography which possesses the parameters that induce an osteogenic response, as confirmed by AFM microscopy including the correct size of feature, which appears to have a very powerful effect on stem cells.[39,23,40,41]

The abundant availability of CL11 amine groups, which as discussed in the introduction is inductive of osteogenesis[11]. The ability of the CL11 surface to harness phosphorous[21], in a biomimetic way may well be contributing to the availability of minerals to the cells. It could be that in their productive osteoblastic state the cells require greater quantities of the minerals that are available more readily on the CL11 surfaces.

It may be that the ability of CL11 surfaces to procure minerals and make them available accelerates the process of osteogenic differentiation and eventually allows the it to progress to the next phase, osteocytic differentiation. This is demonstrated quite clearly by the expression of sclerostin at 14 days, with thick matrix production, and it could be that the pits formed in this matrix is the start of rudimentary re-modeling. For future work, it would be very interesting to study the MMPs as markers of re-modeling and to extend the study further in time, to 2 months.

After the investigation using MSC, another model was used with shows a response from a more mature cell, and gives an insight into the later phases of the osteogenic pathway. A primary human osteoblast-like cell model was used. Examining how these cells interact with the modified surfaces are an attempt to demonste how mature cells will react to the surface modifications, giving an impression of what the longer term effects may be. There was an interesting response observed at the first time point, Von Kossa staining (figures 4.23-4.25) showed mineralized nodules formation on the CL3 and CL4 surfaces. This reaction was not seen on the other surfaces, where the cells remained in monolayer throughout the 28 day period. The nodule formation on CL3 and CL4 could be explained by the progression of the osteogenic differentiation of the cells. Primary human osteoblasts have been shown to form nodules[18] when in 3D culture on bioactive glass, but only in the presence of exogenous growth factors. This stimulus in this incidence could have come purely from the material.

The formation of nodules on the CL3 and CL4 surfaces was confirmed by SEM, and Von Kossa stain. As the cells used in this model were already capable of producing ECM, all of the samples including the untreated glass control stained positive for mineralization (Von Kossa) at 7 days, however the cells on the untreated control were less densely mineralized by 28 days than the silane treated samples. The cells on CL6, CL7 and CL11 all retained the ability to produce matrix which became mineralized.

The SEM of surfaces with osteoblasts revealed that there was an extensive production ofECM on the CL3 and CL4 samples when the cells were clumped together in the nodule (figure 4.28-4.32). The ECM appears to mature throughout the 28 day period and goes from an obvious fibrous formation of proteins at 7 days to a dense mineral-covered matrix at 14 days and by 28 days the cells appeared to be embedded in this matrix.

The size of the nodules (figure 4.27) was shown to increase over a 14 day period and then significantly decrease. This occurrence when combined with the statistically significant drop in total number of nodules (figure 4.26) at 28 days could be indicative of the nodules reaching a critical size and then detaching from the surface. This would warrant further investigation as a material that could product and then release these boney nodules might have interesting applications for filling bone defects.

The PCR figures (4.33-4.38) of these samples revealed an interesting response. All data were normalized to the untreated glass control so the expression shown was above the baseline of normal osteoblast activity on glass. The osteogenic markers are only above the baseline activity at 7 days and not statistically significant after this time point. Interestingly on CL3 and CL4 the expression of sclerostin was notable at 14 and 28 days. As this is a marker specifically for osteocytic activity, this along with the reduction of normal osteoblastic markers after 7 days is indicative of the further differentiation of the cells along the osteogenic pathway. All the results are consistent with this hypothesis.

CL11 does not have the same powerfully osteogenic effect on the osteoblasts as it does on human MSCs. CL11 does however, seem to maintain the osteoblasts and allows them to form a mineralized matrix; the cells were shown by SEM to produce large quantities of ECM. The Von Kossa staining shows that mineralization is occurring, on this sample, but there are no nodules present. It has been documented earlier that the CL11-modified glass

surfaces have the ability to attract phosphorous (see PBS interaction figure 4.4, and hMSC data figures 4.5-4.8). In this experiment, because the cells are closer down the differentiation pathway to mature osteoblasts, they are covered in minerals such as phosphorous and calcium. It could be that the cells are "captured" by the surface, and that the minerals on the surface of the cells are used to adhere the cell to the surface in an irreversible way. This would explain why the CL11 samples are not forming nodules, as the cells are unable to migrate. CL6 and CL7 have not shown any significant osteogenic potential in any of the tests, and were not shown to produce any significant matrix. The cells on CL6 were very rounded until between 7 and 14 days at which point they started to form a monolayer. This delayed adhesion could be responsible for the lack of osteogenic markers seen from this modification.

The differences observed between the chain lengths and their osteogenic effects could be attributed to several things. The procurement of minerals by CL11, the topography that is induced at the nanoscale and the mimicry of the ECM by the chemical modification could be key factors in these results.

The results indicate that CL11 could be a powerful inducer of osteogenic differentiation, and would accelerate the differentiation of MSCs, in the absence of exogenous growth factors. In osteoblasts, while CL11 maintains the production of matrix, it does not allow the already mature cells to continue down the osteogenic pathway to the osteocytic phenotype, but if the initial interaction with the surface is at the MSC stage, differentiation can be induced right along the osteoblastic lineage to osteocytic fate. This could be explained by the hypothesis mentioned earlier where the mineralized surfaces of the cells can be chemically bound to the CL11 surface. To define this with a time line of events, it appears that mineralization of the surface happens initially and quite rapidly [21], before the cells adhere to the mineralized surface. If the cells have minerals on the surface (as in the

osteoblast-like cell model) this time line initially is disrupted and the cells captured in the initial mineralization phase, hindering migration (and their ability to form nodules). To extend this study further, this hypothesis could be tested by looking at the movement of the cells across the surface. Time lapse imagery of the cells over a 7 day period may answer this question, but ideally an intergrin binding profile could be examined in more detail to determine the factors in play at the initial adherence.

In the instance of the CL3 and CL4 nodule formation, it is likely that it is the amine rich surfaces and the topography that instigates the formation of nodules. The surfaces do not have the same self-mineralizing properties and so the phenomenon can not be related directly to mineral deposition on the surfaces. It is either the topography or chemistry which instigates this process, not the presence of phosphorous alone.

To summarise, because it was necessary to characterise these surfaces in a more accurate way, it was likely that the silanes examined would show only very small differences, the work was undertaken using a model substrate (in this case glass in chapter 4). The base line data was discussed in detail in chapter 4, but the over-reaching hypothesis of this work was that the presentation of the chemistry was of similar importance to the terminal group. It was demonstrated that the presentation of the amine terminal groups influenced nanotopography, this was demonstrated very clearly with the use of a AFM (figures 4.1.1-4.1.6). The data collected by the AFM brought the possibility that the surfaces nanotopography was a very important factor in the induction of osteogenicity from mesenchymal stem cells, and that while the chemistry does have an effect (as demonstrated by the plasma modifications) the topography can indeed have a very strong effect.[40]

Other work done around the silane and SAM methods of surface modification pointed towards another factor that was becoming apparent. The self-mineralising properties of the

silane with the longest chain length was evident in the more in depth surface analysis, and the experimental work involving exposing the surfaces to a Phosphate buffered saline (PBS) solution[21]. This self-mineralising effect could be responsible for some of the phenotypical changes in the cells exposed to these surfaces, and could be responsible for the nucleation of minerals that stimulate osteogenic events.

The wet chemical technique for the application of silanes had advantages over the plasma modification. Whilst the main reason for choosing the chemistries was the alterable nature of the way they present their terminal group, the concentration of amine could also be measured more accurately using a ninhydrin solution which was a technique developed in this thesis. Ninhydrin is a long established detector of free amine groups, but the use of it to detect tethered amine groups is a novel application of it.

The main focus of this thesis was the PLGA bone regeneration system, and for all the baseline data to progress the surface chemistries had to be conducted on PLGA before it was to be useful in the bone regeneration system. The decision was made to make incremental steps when doing this. The first step was the modification of flat films.

The transfer of the surface chemistries to flat PLGA films was successful, and instigated an interesting response in terms of the dynamic water contact angle. The water contact angle had an inverse relationship to the chain length of the modification (figure 5.9). This is an unusual result, because when the molecule is considered the longer chain molecule will introduce more CH_2 groups to the surface, which in turn should theoretically increase surface hydrophobicity. This was not observed. This could be because the substrate, PLGA, is already very hydrophobic, the addition of silane groups with hydrophilic end groups (-NH_2) leading to an increase in hydrophillicity despite the hydrophobic chain molecules. The hydrophobic chains only act as a spacer physically keeping the hydrophilic NH_2 groups away

from the very hydrophobic substrate, creating a layer which would be in contact with cells, that is hydrophilic, and conducive to cell growth.

The AFM investigation (Figure 5.2-5.7) of the surfaces showed variable coverage from the different modifications on the PLGA films. The maximum peak height exemplifies the hypothesis that the CL11 modification is considerably different from the other modifications. The CL11 modification appears to have two layers of microstructure, that being the macrotopography and also the nanotopography. It is likely that it is the unique combination of the two, combined with the surface energy demonstrated by the advancing dynamic water contact angle that seems to create the active surface demonstrated in this thesis.

The application of the silanes to 3D polymer system was unsuccessful in this instance from the standpoint of cell response. There was no evidence of differentiation on any of the modifications when examined using histological techniques. There was evidence of cells on the system but they were not producing matrix. The stains used would have identified the key proteins necessary for differentiation throughout the scaffold and they were all negative.

One possible reason for this is that the concentration of the silanes on the surface of the spheres was not the same as the concentration on the films which were successful (in the instance of CL11). It is likely that it would be possible to optimize the techniques further by taking a close look at the coating methods in more detail. The coating technique involves a flow of silane to stop the spheres from clumping, and the wash steps can not be as vigorous as that on a film or glass surface. This leads to the concentration of silanes being significantly higher (10 fold) on the spheres than films. It is likely that the coating technique and washing procedures would need to be heavily modified to allow the sufficient coating

and washing of the spheres while avoiding the clumping that is detrimental to the materials effectiveness.

Another possible reason why the application of the surface chemistries onto a 3D system did not cause stem cell differentiation could be that the modification protocol caused the chemical groups to be too closely packed together, creating steric hindrance, and not allowing the surface chemistry to be accessible by large protein molecules involved in stem cell differentiation [42],[43]. Obtaining a similar concentration of the surface groups will be key to the success of further work in this area that, combined with the development of suitable techniques, investigate the surface chemistry and topography on spherical samples to allow better optimization of the technique.

The transfer of these chemistries into a 3D sphere will require further optimisation to determine if it is possible to obtain the concentration that is conducive to osteogenesis onto the surface of a sphere, and if the geometry of the surface of the spheres within this size range is conducive to the SAM formation. If the concentration is too high there is a possibility of steric hindrance, and if it is too low, there may be an imperfect siloxane layer which would make the sample less stable.There are studies to suggest that the surface roughness effects the formation of the SAM layer, and that the thickness of the layer is proportionate to the roughness of a surface, so the surface roughness of the underlying sphere could be investigated, to determine if the spheres roughness could be a factor in causing an elevation in the concentration of amines[44]. If this were to be the situation, steps could be taken to try to reduce the surface roughness of the polymer. Other studies have demonstrated that for 3D coating of porous scaffolds, a dynamic coating environment it likely to be required, whereas on a 2D surface the static coating environment was sufficient[45]. Further work would also involve the examination and identification of a suitable solvent that could wash the system

appropriately without causing damage to the PLGA, or leave any cytotoxic residues, as demonstrated in pharmaceutical release studies that the role of the solvent used to make the spheres, and also modify them, may play more of a role than merely dissolving the polymers and then evaporating[46]. Further optimization of this may be a crucial next step in this work.

The potential of these surface chemistries is however highlighted in chapter 4, when we were able to obtain a very powerful response from both MSC, and primary osteoblast-like cells. The surfaces can push cells down an osteogenic lineage and promote the rapid mineralisation at early time points. This is a significant advance when considering this is the use of a synthetic chemical, and not a growth factor or a peptide. The steps we have taken give a good foundation for further work, and while more optimisation is necessary to take this technology further, the first steps have been made.

This injectable system could also be used as a carrier for the patient's own MSCs. It is the product of long debate as to if using the patient's MSCs is a genuine practical option when treating non-union bone fracture as it is a problematic area in itself, many culture methods would have to be refined before this became a viable option[47,48], and it may be that the source of cells and the number of cells required for a sizable repair would be too many to cultivate in a timely manner for a patient treatment. This would also be very expensive, and would not offer the benefits like cost effectiveness, long term stability of an off the shelf product that could be used universally.

The plasma results (Chapter 3) gave an insight into the further potential of surface chemistry on 3D systems, and the next steps that could be taken. There are two potential pathways this work may take in the future, if it were to be revisited. One would be to channel energies into defining the characterisation of the surfaces and finding new more accurate techniques to do so, and the other would be to experiment with the potential of putting

various other modifications onto the surfaces with plasma, to see if there would be more extensive wider reaching applications in other areas of regenerative medicine, focusing on soft tissues more.

In its present state the more accurate characterisation of the surfaces involved would need to be investigated before the applications of chemistries using plasma would be a clinically relevant technique. The unpredictable nature of plasma modification is where the technique falls down, and until the surface chemistry concentration is definable with this technique it will be a theoretical exercise. There are some spectroscopy techniques that may clear this picture up in the future.In particular, destructive techniques such as time of flight mass spectroscopy may be able to define the surface concentrations to the level that would be required.

To assess fully the potential of the materials osteogenic capability, it will be necessary to conduct some animal model work. There are several relevant animal experiments that could be conducted. Initially a subcutaneous rodent model [49],[50] could be conducted to investigate the ability of stem cells delivered with the material to differentiate. This would require a full histological analysis using markers mentioned earlier in this thesis to determine the level of differentiation. This would be a good first line in vivo experiment, and could be used to investigate some of the biocompatibility (ie, the inflammatory response) and the cellular migration throughout the scaffold. If the correct techniques are deployed it will be possible to differentiate between host cells migrating into the scaffold and the implanted cells. The use of fluorescent trackers [51],[52] or chromosomal differences are used increasingly more commonly to do this type of work.

The next logical step would be the investigation of critical bone defect models[53], but as the amine rich allyl amine modification was the only result to show sufficient osteogenic potential, it is likely that only this modification should be pursued for this application.

The potential of using several well defined chemical modifications together in a scaffold to direct cells down different lineages would have impact in the wider field of regenerative medicine, and would potentially be useful for any of the junctions in tissue where one tissue becomes another, the most striking potential being within the osteochondral junction, on which some preliminary work was done in chapter 3. There have been several studies conducted that used biomaterials to tackle this problem, [54], [55],[56], but most of this work used biphasic materials, with different degradation rates. The benefit of using this injectable system is it is only the surface chemistry which is different across the body of the biomaterial, the underlying scaffold is the same material, and so would degrade at the same rate. There is far more work to conduct on this, and taking the dual and triple modifications from an in vitro model to an in vivo model would be a good step forward with this. There is a massive potential for this work to take place, and a knee model could show some of the potential that the in vitro work pointed towards. If a delivery system could be designed that would allow the application of a multi-layered scaffold delivery, initially in the absence of cells but perhaps later moving towards a stem cell delivery model, a great deal of information could be gained from the application of this scaffold into an osteochondral defect.

Initially it would be important to gain a response from the materials in the absence of any additional cells, to see what sort of native migration is demonstrated. The material should be injected into an osteochondral defect that penetrates the medual cavity, so that the infiltration of stem cells and osteoblast like cells into the scaffold can be measured. The subsequent dissection and histological examination of the knee would be likely to reveal the extent of regeneration from the native cells and demonstrate the osteoconductive nature of the

material. Ideally this would be sufficient and make the treatment meet the requirements outlined earlier.

The next experiment would see the incorporation of pre-cultured cells into the material prior to the injection into the aforementioned cavity. This would be a more complicated procedure that would require timing and precision in the growth of enough cells to transplant. This set of experiments would go some way to show how the materials would behave in vivo and give some insights into how this material might behave and degrade over time, depending on how long the experiment is conducted.

The potential of the silane modifications has not been reached within this work (chapter 5), as further optimisation is required to successfully apply the silanes to a 3D system. The successful application and characterisation of these surface chemistries to glass and a flat film (Chapter 4 and 5) was an insight into the possibilities that will be accessible with this technology in the future. The chain length (and therefore the presentation of the terminal group) has proved to be very important on the expression of markers from mesenchymal stem cells and mature primary bone cells (Chapter 4). The preference of the cells to the different chain lengths, with mesenchymal stem cells taking stimulus from the longer CL11 chain length and the mature osteoblasts gaining stimulus to differentiate from osteoblasts to osteocytes on the shorter chain lengths warrants further investigation.

This delicate and subtle dynamic demonstrated numerous times throughout the thesis is changed significantly when applied to a 3D sphere (Chapter 5). There are many areas where this application needs to be optimised. The physical environment in which the self-assembled monolayer of the silane forms needs to be optimised, to achieve a full layer on a spherical substrate. It is likely that this will need to occur in a dynamic environment, which

adds a further level of complication. The flat surface is coated in a static application, which has proven to be much simpler[57].

To transfer the chemistry successfully, the precise environment will need to be optimised. Work on this was started, and first attempts were shown to be unsuccessful in terms of differentiation stem cells (chapter 5), but the characterisation techniques are now in place, and further work into optimising the dose of amine groups transferred to the PLGA spheres would be possible now, as the ninhydrin test would be suitable to measure the quantity of amines bound to the surface of the spheres accurately and the next step towards optimisation would be to try to obtain the same concentration of amine groups using similar chain lengths on the 3D system that is successful of the flat films (Chapter 4 and 5).

The first step in this process would be to optimise the amount of oxygen groups that are successfully transferred to the PLGA spheres. After that the concentration of silanes and the precise flow/dynamic incubation required to achieve controllable coverage would be optimised. Clear characterisation of the surfaces would be essential at this point, and then the spheres could go into the complex dynamic culture with cells.

Further work could also be done on the potential of the surfaces to harness osteogenic minerals, some of which are found on the surfaces of osteogenic cells. CL11 showed a potential for phosphate deposition, which creates a biomimetic surface, and could potentially be used to increase mineralisation in the absence of cells[21]. This could have applications in regenerative medicine where mineralisation is necessary, even in the absence of a cellular component. If the material can start the mineralisation process before the infiltration of cells, this is likely to accelerate the healing process by way of giving the cellular component less work to do, or giving the native cells a more powerful osteogenic signal, to which they can respond.

The mineralisation capacity of these materials could be explored for the applications of other mineralised tissues, calcified cartilage, and dental treatments are just a few of the further reaching applications that become apparent. Coatings of dental fillings or where there has been loss of mineralisation due to tooth decay could be an interesting application, and a more detailed investigation into this application could take place.

There may also be applications of this work for cell selection, if indeed the minerals are present on the cell surfaces of differentiated cells, it may be a way to separate the cells with osteogenic potential from a fraction of bone marrow, or speed of which the osteoblast like cells can migrate from a bone chip into a coated petri dish. Currently osteoblast like cells are isolated using standard plastic petri dishes, and the isolation process takes several weeks of culture to isolate a few million cells. It would be an advantage to speed up the isolation process as this would also be an indication of the potential osteoconductive nature of these modifications.

The work with the primary human osteoblast like cells showed several areas for potential further research (Chapter 4). The CL3 and CL4 modifications showed an ability to stimulate the cells into forming nodules, which appeared, after staining and SEM investigation, to be mineralised. When they reached a critical size the nodules appeared to detach from the material, and further investigation into the viability of these nodules should be investigated. I would suggest a full histological investigation into the nodules, that are released from the surfaces to check the viability of the centre of the nodules and if any mineralisation occurs sub surface.

While this was an unexpected result from this work, it certainly has some potential for growth. A surface that could produce nodules of bone, that are viable, would certainly have applications in transplantation, perhaps not as part of the injectable system but delivered on

their own without a carrier. It could be hypothesised that mineralised nodules of bone would have a greater chance of remaining in the area they are required to be in than previous attempts to transplant either mature osteogenic cells or stem cells.

However, if the nodules could be seeded across the area of non-union fracture they may increase the capacity to heal, and would be osteoinductive and osteogenic, and there would be a potential for the application of the nodules as part of aosteoconductive scaffold, with a mineralising silane coating (like CL11 has demonstrated). This combination of pre-treated osteoblast and/osteocyte like cells along with a mineralising silane environment may harmonise quite well. If the cells are already being pushed in to an osteocytic state and the silane induces a mineralisation process then cells may start to go down a regulatory pathway and help maintain the osteogenic response long term. This is an area for further development and looking at applying the silanes to an osteoconductive porous scaffold such as a classical ceramic or metallic material would be an interesting avenue of investigation.

This thesis has identified a few potential pathways of research, and shows that the coatings/modifications developed need not be limited to the constraints of an injectable bone regeneration system. The wider potential of chemical modifications has also become apparent[11]. The potential seen in some of the surface modifications to repress the differentiation of mesenchymal stem cells or osteoblasts (chapter 4) is also interesting and should be pursued, as the spontaneous differentiation of mesenchymal stem cells in tissue culture is one of the potential pitfalls in stem cell cultures, which is an area that needs far more research before cellular medicine is a true reality[37]. If a simple synthetic chemical modification, (that controls surface energy and deposits its own topography), can achieve the maintenance of the stem cell phenotype for longer periods of time (particularly for adult stem cells that do lose some of the ability to differentiate after multiple passages in culture), the

vast cell numbers that are necessary for even the smallest transplant will become a more realistic goal.

If materials have the potential to stimulate differentiation in a reproducible and relatively inexpensive way, there will be no need for the expensive and potentially compromising xenological components of tissue culture media, such as growth factors. If the growth factors are produced by the cultured cells themselves, there will be less risk of interspecies incompatibility and it will be a step towards the widespread clinical use of stem cells.

There would also potentially be a way to produce growth factors that does not require animals or animal products, so it could potentially have a commercial benefit, if it were possible to isolate the growth factors from the culture media where they are released. This is just a possibility, but highlights the potential of these surfaces to the greater scientific community, and not just for the applications of regenerative medicine or stem cell biology. To carry this out however would require significant investment and a thorough and expensive investigation into the metablomic potential of the cells on these surfaces.

As stated above there are numerous opportunities for further research that have been opened up from this initial investigation, and they are certainly not restricted to the field of injectable systems, bone regeneration, stem cell research or even regenerative medicine, but could have a more wider reaching cell culture and dental applications, give us an insight into cell cycles and material chemistry, that has not been demonstrated previously.

In conclusion, this work has developed into a novel study that could develop further into wider reaching research that has clinical applications for osteochondral tissue repair and bone regeneration. The advancement in osteochondral repair could impact the treatment of osteochondral disease, such as osteoarthritis. The bone regeneration however was the main

focus of this thesis, and it is the osteogenicity of amine-rich modifications that has become apparent. By exploring the presentation of the amine groups, it has become apparent that the small differences in chain length influence surface nanotopography, and that this in itself can be a driving factor of osteogenicity. Some of the conflicting reports about surface chemistry could be due to changes made on the nanoscale that perhaps were not highlighted by the surface characterisation conducted[12],[11]. The terminal group is an important factor that influences the osteogenic potential of a surface, however the presentation of the terminal group, and the nanotopography that brings about, may also be key factors.

1. Dinopoulos, H., Dimitriou, R. & Giannoudis, P.V. The Surgeon , Journal of the Royal Colleges of Surgeons of Edinburgh and Ireland Bone graft substitutes: What are the options? *The Surgeon* 1-10 (2012).

2. Zimmermann, G. & Moghaddam, A. Allograft bone matrix versus synthetic bone graft substitutes. *Injury* **42**, S16-S21 (2011).

3. Nassr, A. Khan, MH Ali, M.H., Espiritu,M.T.,Hanks, S.E.. Donor-site complications of autogenous nonvascularized fibula strut graft harvest for anterior cervical corpectomy and fusion surgery: experience with 163 consecutive cases. *The Spine Journal* **9**, 893-898 (2009).

4. Ronga, M., Fagetti, A.,Canton, G. Paiusco, E.,Surace,M.F, Cherubino, P. Clinical applications of growth factors in bone injuries: experience with BMPs. *Injury* **44 Suppl 1**, S34-9 (2013).

5. Bajaj, S.K., Mohan, N.R. & Kumar, C.S. Supracondylar Femoral Nail in the management of non-union of humeral shaft fractures. *Injury* **35**, 523-7 (2004).

6. Zimmermann, G., Wagner, C., Schmeckenbecher, K., Wentzensen, a & Moghaddam, a Treatment of tibial shaft non-unions: bone morphogenetic proteins versus autologous bone graft. *Injury* **40 Suppl 3**, S50-3 (2009).

7. Crowley, D.J., Kanakaris, N.K. & Giannoudis, P.V. *Injury*. (2007).

8. Félix Lanao, R.P., Leeuwenburgh, S.C.G., Wolke, J.G.C. & Jansen, J. a Bone response to fast-degrading, injectable calcium phosphate cements containing PLGA microparticles. *Biomaterials* **32**, 8839-47 (2011).

9. Bonewald, L.F., Harris, S.E., Rosser, J. Dallas, S.L.Boskey,A.. von Kossa staining alone is not sufficient to confirm that mineralization in vitro represents bone formation. *Calcified tissue international* **72**, 537-47 (2003).

10. Goddard, J.M. & Hotchkiss, J.H. Polymer surface modification for the attachment of bioactive compounds. *Progress in Polymer Science* **32**, 698-725 (2007).

11. Curran, J.M., Chen, R. & Hunt, J. A. Controlling the phenotype and function of mesenchymal stem cells in vitro by adhesion to silane-modified clean glass surfaces. *Biomaterials* **26**, 7057-67 (2005).

12. Phillips, J.E., Petrie, T. A, Creighton, F.P. & García, A.J. Human mesenchymal stem cell differentiation on self-assembled monolayers presenting different surface chemistries. *Acta biomaterialia* **6**, 12-20 (2010).

13. Guo, L.Kawasoe, N.,Hoshiba, T. Osteogenic differentiation of human mesenchymal stem cells on chargeable polymer-modified surfaces. *Journal of biomedical materials research. Part A* **87**, 903-12 (2008).

14. Hoshiba, T., Kawazoe, N., Tateishi, T. & Chen, G. Development of stepwise osteogenesis-mimicking matrices for the regulation of mesenchymal stem cell functions. *The Journal of biological chemistry* **284**, 31164-73 (2009).

15. Kundu, B. & Kundu, S.C. Osteogenesis of human stem cells in silk biomaterial for regenerative therapy. *Progress in Polymer Science* **35**, 1116-1127 (2010).

16. Chen, Y., Shao, J.-Z., Xiang, L.-X., Dong, X.-J. & Zhang, G.-R. Mesenchymal stem cells: a promising candidate in regenerative medicine. *The international journal of biochemistry & cell biology* **40**, 815-20 (2008).

17. Ferrera, D.,Proggi, S., Biassoni, C. Three-dimensional Cultures of Normal Human Osteoblasts: Proliferation and Differentiation Potential In Vitro and Upon Ectopic Implantation in Nude Mice. **30**, 718-725 (2002).

18. Gough, J.E., Jones, J.R. & Hench, L.L. Nodule formation and mineralisation of human primary osteoblasts cultured on a porous bioactive glass scaffold. *Biomaterials* **25**, 2039-2046 (2004).

19. Gough, J.E., Notingher, I. & Hench, L.L. Osteoblast attachment and mineralized nodule formation on rough and smooth 45S5 bioactive glass monoliths. *Journal of biomedical materials research. Part A* **68**, 640-50 (2004).

20. Schwartz, D.K. Mechanisms and kinetics of self-assembled monolayer formation. *Annual review of physical chemistry* **52**, 107-137 (2001).

21. Toworfe, G.K., Bhattacharyya, S. Composto, R.J., Adams, C.S. & Shapiro, I.M. Effect of functional end groups of silane self-assembled monolayer surfaces on apatite formation , fibronectin adsorption and osteoblast cell function. 26-36 (2009). 22. Curran, J.M., Chen, R. & Hunt, J. A The guidance of human mesenchymal stem cell

differentiation in vitro by controlled modifications to the cell substrate. *Biomaterials* **27**, 4783-93 (2006).

23. McNamara, L.E., Strongom, T.Burgess, K. Kim, J. Lui,E. Gordenov, S.Moghe,P., Meek,D. Oreffo, R. Su, B. Dalby,M.J. Nanotopographical control of stem cell differentiation. *Journal of tissue engineering* **2010**, 120623 (2010).

24. McMurray, R.J., Gadegaard, N., Tsimbouri, P M, Burgess,K. V. McNamara, L.E., Tare, R. Murawski, K., Kingham, E., Oreffo, R., Dalby, M.J.. The control of human mesenchymal cell differentiation using nanoscale symmetry and disorder. *Nature materials* **6**, 997-1003 (2007).

25. Dadsetan, M., Giuliani, M.,Wanivenhaus, F.,Brett Runge, M.Charlesworth, J.E.,Yaszemski, Michael J. Incorporation of phosphate group modulates bone cell attachment and differentiation on oligo(polyethylene glycol) fumarate hydrogel. *Acta biomaterialia* **8**, 1430-9 (2012).

26. Makita, N. Suzuki, M., Asami, S., Takahata, R., Kohzaki, D., Kobayashi, S.,Hakamazuka, T. Hozumi, N. Two of four alternatively spliced isoforms of RUNX2 control osteocalcin gene expression in human osteoblast cells. *Gene* **413**, 8-17 (2008).

27. Huang, L., Teng, X.Y., Cheng, Y.Y., Lee, K.M. & Kumta, S.M. Expression of preosteoblast markers and Cbfa-1 and Osterix gene transcripts in stromal tumour cells of giant cell tumour of bone. *Bone* **34**, 393-401 (2004).

28. Nakase, T.,Takaoka, K., Hirakawa, K., Hirota, S., Takemura, T., Onoue, H., Takebayashi, K., Kitamura, Y., Nomura, S. Alterations in the expression of osteonectin, osteopontin and osteocalcin mRNAs during the development of skeletal tissues in vivo. *Bone and mineral* **26**, 109-22 (1994).

29. Koblinski, J.E., Wu, M., Demeler, B., Jacob, K. & Kleinman, H.K. Matrix cell adhesion activation by non-adhesion proteins. *Journal of cell science* **118**, 2965-74 (2005).

30. Mathews, S., Bhonde, R., Kumar, P. & Totey, S. Extracellular matrix protein mediated regulation of the osteoblast differentiation of bone marrow derived human mesenchymal stem cells. *Differentiation* 1-8 (2012).doi:10.1016/j.diff.2012.05.001

31. Theyse, L.F.H., Mol, J. A, Voorhout, G., Terlou, M. & Hazewinkel, H. a W. The efficacy of the bone markers osteocalcin and the carboxyterminal cross-linked telopeptide of type-I collagen in evaluating osteogenesis in a canine crural lengthening model. *Veterinary journal (London, England : 1997)* **171**, 525-31 (2006).

32. Harwood, P.J. (ii) An update on fracture healing and non-union. *Orthopaedics and Trauma* **24**, 9-23 (2010).

33. Bragdon, B. *et al.* Bone morphogenetic proteins: a critical review. *Cellular signalling* **23**, 609-20 (2011).

34. Bohner, M., Galea, L. & Doebelin, N. Calcium phosphate bone graft substitutes: Failures and hopes. **32**, 2663-2671 (2012).

35. Loots, G.G. Nakase, T., Takaoka, K., Hirakawa, K., Hirota, S., Takemura, T., Onoue, H., Takebayashi, K., Kitamura, Y., Nomura, S. sclerostin in Van Buchem disease Genomic deletion of a long-range bone enhancer misregulates sclerostin in Van Buchem disease. (2005).

36. Blonder, J., Xiao, Z. & Veenstra, T.D. Proteomic profiling of differentiating osteoblasts. *Expert review of proteomics* **3**, 483-96 (2006).

37. Kassem, M. Mesenchymal Stem Cells: Biological Characteristics and. **6**, 369-374 (2004).

38. Dominici, M.,Le Blanc, K.,Mueller, I., Slaper-Cortenbach, I., Marini, F., Krause, D., Deans, R., Keating, A., Prockop, D. Horwitz, Em. Minimal criteria for defining multipotent mesenchymal stromal cells. The International Society for Cellular Therapy position statement. *Cytotherapy* **8**, 315-7 (2006).

39. Wilkinson, A., Hewitt, R N., McNamara, L.E., McCloy, Meek, R M.Dalby, M. J., Biomimetic microtopography to enhance osteogenesis in vitro. *Acta biomaterialia* **7**, 2919-25 (2011).

40. Sjöström, T., Dalby, M.J., Hart, A., Tare, R., Oreffo, R O C., Su, B. Fabrication of pillar-like titania nanostructures on titanium and their interactions with human skeletal stem cells. *Acta biomaterialia* **5**, 1433-41 (2009).

41. Dalby, M.J., McCloy, D., Robertson, M., Wilkinson, C.D.W. & Oreffo, R.O.C. Osteoprogenitor response to defined topographies with nanoscale depths. *Biomaterials* **27**, 1306-15 (2006).

42. Cavalcanti-Adam, E. Micoulet, A.,Blümmel, J.,Auernheimer, J.,Kessler, H.,Spatz, J. P ., Lateral spacing of integrin ligands influences cell spreading and focal adhesion assembly. *European journal of cell biology* **85**, 219-24 (2006).

43. Selhuber-Unkel, C.,Erdmann, T.,López-García, M.,Kessler, H.,Schwarz, U., Spatz, J P. Cell adhesion strength is controlled by intermolecular spacing of adhesion receptors. *Biophysical journal* **98**, 543-51 (2010).

44. Koltsov, A., Cornu, M.-J. & Loison, D. Characterization by different analytical techniques of SiO2 and silane thin films deposited on rough hot-dip galvanized steel surfaces. *Surface and Coatings Technology* **206**, 2759-2768 (2012).

45. Santos, J.L., Oliveira, H.,Pandita, D.,Rodrigues, J.,Pêgo, A.,Granja, P.,Tomás, H. Functionalization of poly(amidoamine) dendrimers with hydrophobic chains for improved gene delivery in mesenchymal stem cells. *Journal of controlled release: official journal of the Controlled Release Society* **144**, 55-64 (2010).

46. Ito, F. Ito, F.,Fujimori, H., Honnami, H.,Kawakami, H., Kanamura, K., Makino, K. Study of types and mixture ratio of organic solvent used to dissolve polymers for

preparation of drug-containing PLGA microspheres. *European Polymer Journal* **45**, 658-667 (2009).

47. Hwang, N.S., Varghese, S. & Elisseeff, J. Controlled differentiation of stem cells. *Advanced drug delivery reviews* **60**, 199-214 (2008).

48. Zhukareva, V., Obrocka, M., Houle, J.D., Fischer, I. & Neuhuber, B. Secretion profile of human bone marrow stromal cells: donor variability and response to inflammatory stimuli. *Cytokine* **50**, 317-21 (2010).

49. Okamoto, Y.,Sonoyama, W.,Ono, M.,Akiyama, K.,Fujisawa, T.,Oshima, M.,Tsuchimoto, Y.,Matsuka, Y.,Yasuda, T.,Shi, S., Kuboki, T. Simvastatin induces the odontogenic differentiation of human dental pulp stem cells in vitro and in vivo. *Journal of endodontics* **35**, 367-72 (2009).

50. Huang, J.,Yang, P., Leng, Y.X., Wang, J., Sun, H., Chen, J.Y.,Wan, G.J. In vivo differentiation of adipose-derived stem cells in an injectable poloxamer-octapeptide hybrid hydrogel. *Tissue & cell* **43**, 344-9 (2011).

51. Weir, C. Morel-Kopp, M., Gill, A.,Tinworth, K.,Ladd, L.,Hunyor, S.,Ward, C. Mesenchymal stem cells: isolation, characterisation and in vivo fluorescent dye tracking. *Heart, lung & circulation* **17**, 395-403 (2008).

52. Idris, N.M. Li, Z. Ye, L. Sim, E., Wei., Mahendran, R.,Ho, P., Chi-Lui. Z.Tracking transplanted cells in live animal using upconversion fluorescent nanoparticles. *Biomaterials* **30**, 5104-13 (2009).

53. Rimondini, L. Nicoli-Aldini, N.,Fini, M.,Guzzardella, G.,Tschon, M.,Giardino, R. In vivo experimental study on bone regeneration in critical bone defects using an injectable biodegradable PLA/PGA copolymer. *Oral surgery, oral medicine, oral pathology, oral radiology, and endodontics* **99**, 148-54 (2005).

54. Guo, X. Kawazoe, N.,Hoshiba, T.,Tateishi, T.,Chen, G.,Zhang, X. Repair of osteochondral defects with biodegradable hydrogel composites encapsulating marrow mesenchymal stem cells in a rabbit model. *Acta biomaterialia* **6**, 39-47 (2010).

55. Schleicher, I. Lips, K.S., Sommer, U.,Schappat, I.,Martin, Alexander P.S., Gabor Hartmann, S., Schnettler, R. Biphasic scaffolds for repair of deep osteochondral defects in a sheep model. *The Journal of surgical research* 1-9 (2012).

56. Bernstein, A., Niemeyer, P.,Salzmann, G.,Südkamp, N P.,Hube, R.,Klehm., Menzel, M.,von Eisenhart-Rothe, R.,Bohner, M.,Görz, L.,Mayr, H O. Microporous calcium phosphate ceramics as tissue engineering scaffolds for the repair of osteochondral defects: Histological results. *Acta biomaterialia* 1-16 (2013).doi:10.1016/j.actbio.2013.03.021

57. Koegler, W.S. & Griffith, L.G. Osteoblast response to PLGA tissue engineering scaffolds with PEO modified surface chemistries and demonstration of patterned cell response. *Biomaterials* **25**, 2819-30 (2004).

Chapter 7: Conclusions

7.1 Conclusions for Plasma modifications on PLGA system

The transfer of surface chemistries using the novel plasma polymer deposition technique was successful.

1) Plasma modifications influence the mesenchymal stem cell fate; hydroxyl modifications push mesenchymal stem cells down a chondrocytic pathway and the amine modifications send mesenchymal stem cells down an osteogenic pathway, the methyl modifications seem to deter any differentiation, while the carboxyl groups also so no significant differentiation.
2) Mesenchymal stem cells are influenced by the surface chemistries even in the presence of conflicting signals, and two separate populations of cells can be created by differing surface modifications alone.

7.2 Conclusions silane modifications on glass

1) The silane modifications were transferred successfully using a wet chemical technique onto glass
2) The nanotopography of the materials revealed significant differences between the longest and shortest chain lengths.
3) The water contact angle showed significant differences.
4) The longer chain lengths increased the expression of osteogenic markers from the mesenchymal stem cells.

5) The shorter chain lengths allowed the formation of calcified nodules by primary human osteoblasts, pushing osteoblasts further down the osteogenic lineage towards embedded osteocytes.

7.3 Conclusions for silanes on PLGA films

1) The surface modification induces a nanotopography on PLGA film that is detectable by AFM microscopy
2) The concentration of amine is higher on the CL11 than the other modifications ($p=<0.95$) demonstrating the efficiency of this modification.
3) The dynamic water contact angle measurements showed a significant difference between some of the modifications, this highlighted a correlation between the chain length and the dynamic water contact angle.
4) Human mesenchymal stem cells showed evidence of significant differentiation when incubated on CL11 modified PLGA surface.

7.4 Conclusions for silanes on PLGA injectable system

1) The amine group concentration on the spheres was significantly higher than the concentration of amine groups on the flat PLGA surfaces. This is likely to be responsible for the absence of differentiation seen in the scaffolds.
2) There was no significant differentiation seen on any of the scaffolds, but the further optimisation of this technique will lead to this.

Appendix 1 Ninhydrin assay standard curves

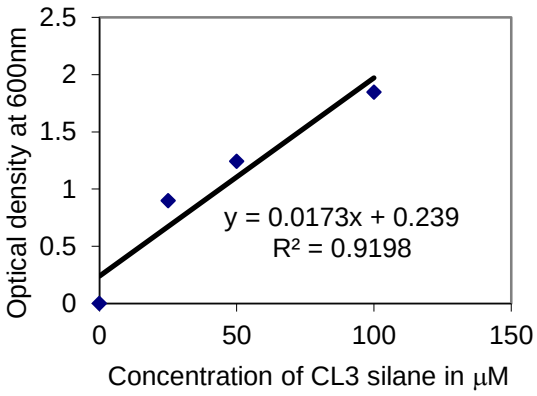

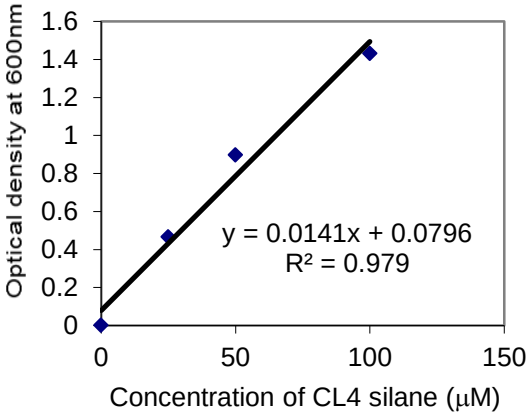

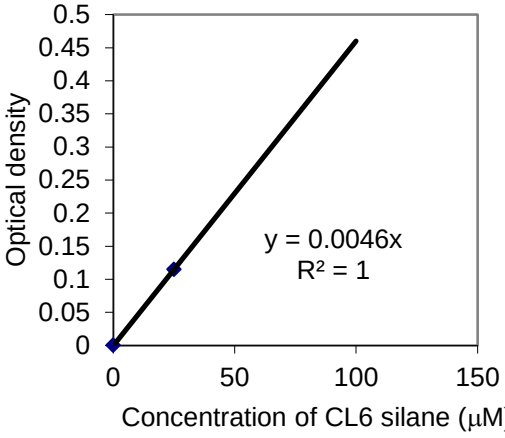

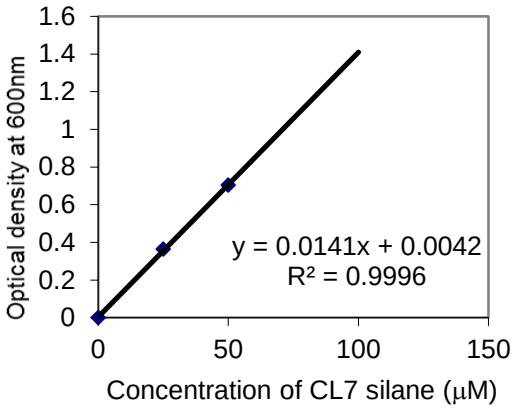

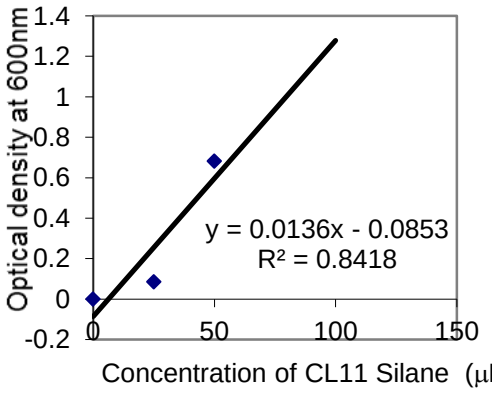

Appendix 1:**Standard curves for individual silanes.** Standard curves used to calculate unknown concentrations of silanes, showing linear regression lines, calculations and r values for each of the silanes used. (a) CL3, (b)CL4, (c) CL6, (d) CL7, and (e)CL11.

Appendix 2 LDH assay standard curves

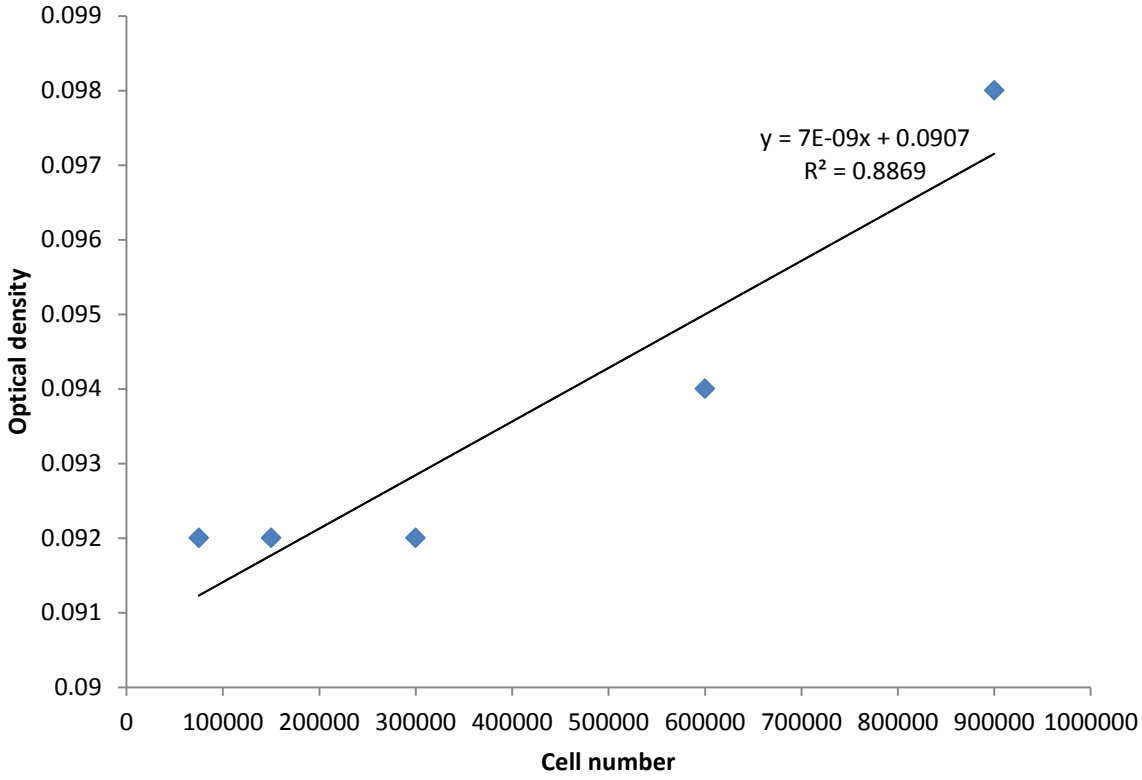

Appendix 2: LDH assay standard curve. Optical density plotted against a known number of cells.